UNIVERSITÀ DEGLI STUDI DI PADOVA

DIPARTIMENTO DI GEOSCIENZE

Direttore Prof.ssa Cristina Stefani

TESI DI LAUREA MAGISTRALE IN
GEOLOGIA E GEOLOGIA TECNICA

TERTIARY PEGMATITE DIKES IN THE CODERA AND BODENGO AREAS OF THE CENTRAL ALPS

Relatore: Prof. Giorgio Pennacchioni

Correlatori: Dott. Alessandro Guastoni

Dott. Anna Maria Fioretti

Laureando: Giacomo Pozzi

ANNO ACCADEMICO 2013 / 2014

Previous page: the “Altare”, upper Codera valley

Abstract

The tertiary pegmatite field of the Central Alps extends for about 100 km in an E–W direction from the Bergell pluton (to the east) to the Ossola valley (to the west). It intrudes the steepened roots of the Alpine nappes (Souther Steep Belt) north of the Periadriatic Fault and gradually fades within 15 km toward north. The pegmatite field geographically overlaps (1) the highest temperature domain of the Lepontine Barrovian metamorphic dome and (2) the zone of Alpine migmatization. In this thesis is attempted a first multisciplinary study on these pegmatites over a limited surface of the whole extension of the pegmatite field. Pegmatites were studied in two different areas: (1) the Codera area, located on the western border of the Bergell Pluton, and (2) the Bodengo area, located between the Mera and the Mesolcina valleys. Results show that Codera and Bodengo pegmatites differ under many aspects including structural, geochemical and radiometric data. The main set of pegmatite dikes of Codera area is steeply dipping and strikes WSW-ENE. Crosscutting relationships suggest the presence of at least two generations. All dikes were involved in ductile deformation and in some cases localize mylonitic shear zones. Codera pegmatites were emplaced at relatively high temperature of at least 500°C, which is constrained by the mineral assemblage along the mylonites and the strong CPO of recrystallized quartz (with c-axis maximum in the direction of the Y kinematic axis of the mylonite). The main set of pegmatites of Bodengo area trends approximately N-S to NNE-SSW and crosscuts the ductile deformation structures of the SSB. Most of these dikes are undeformed but some show ductile reactivation at the borders. Bodengo area also includes an earlier generation of boudinaged and folded pegmatite dikes oriented at a small angle to the host rock foliation. Miarolitic pockets are contained only in some undeformed dikes of Bodengo area. The mineralogical content of pegmatites of the two areas does not differ substantially. Most pegmatites have a simple mineral assemblage consisting of K-feldspar, quartz, and muscovite ± biotite, and only a minor percentage of the dikes contain rare accessories including almandine-spessartine garnet, pale blue beryl and schorl tourmaline. On the other hand chemical analyses on minerals, especially on garnets, allow distinguishing further the two selected areas. Codera garnets are systematically richer in spessartine than Bodengo ones and some Codera tourmalines show higher degrees of evolution (toward elbaite compositions) than Bodengo schorls. Radiometric data of monazite crystals yielded different $^{208}Pb/^{232}Th$ ages for Codera and Bodengo pegmatites, which do not overlap and are respectively older and younger than 24 Ma. We concluded that pegmatites of Codera area and Bodengo area belong to different intrusion events.

Table of contents

1. Introduction

The Central Alps host the largest field of Oligocene-Miocene pegmatite dikes, which intrude the stack of the Alpine nappes (Guastoni *et al*., 2014). Previous studies on pegmatites have mainly dealt with specific characteristics of pegmatite dikes, e.g. their mineralogy and geochronology (e.g. Guastoni, 2012; Romer *et al*., 1996; Rubatto *et al*., 2009) but a comprehensive multidisciplinary study integrating the mineralogical, petrographic, structural and geological data is still missing. This multidisciplinary study is attempted in the current thesis for two selected areas in the central part of the Tertiary pegmatite field: namely the Codera area and the Bodengo area. The first area is located at the western contact between the Bergell intrusion and the Gruf complex migmatitic host rock, and includes two main study localities in the upper Codera Valley (COD) and in the Rossaccio (ROS) alp (*fig. 1*). The second area extends over a wider region between the Mera and the Mesolcina valleys within the heterogeneous metamorphic rocks of the southern Adula nappe. It includes the upper portions of several valleys: Garzelli valley (VG), Leggia valley (VLG), Del Dosso valley (VDD) and Darengo valley (VLD). As will be shown in this thesis, these two areas are dominated by different sets of pegmatites that record two main distinct phases of pegmatite intrusion in the Central Alps. Localities are reported with their codes in *fig. 1*.

2. Overview on the Central Alps in the area of study

2.1. Tectono-metamorphic history of the Central Alps

Central Alps are a subject that boasts of many years of study, which led to the formulation of a complex polyphasic tectono-metamorphic history. For this brief summary I manly refer to recent works of several authors that provided nice

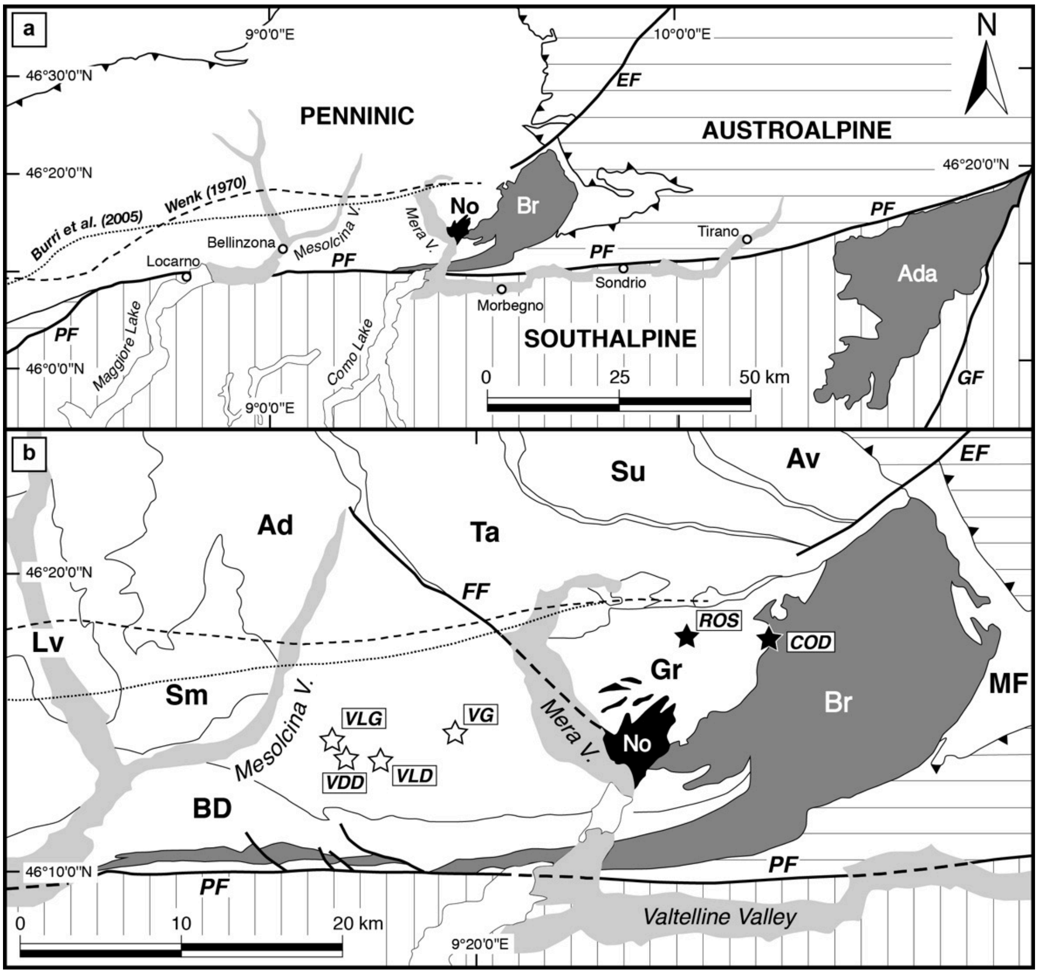

<u>Figure 1</u> ***(a)*** *Simplified structural map of the Central Alps with the field of the Alpine (Oligocene–Miocene?) pegmatites as reported by Wenk (1970) and Burri et al. (2005) outlined by dashed and dotted lines, respectively. The map also shows the two major Tertiary batholiths of Adamello (Ada) and Bergell (Br), in grey, and the smaller and younger Novate stockwork intrusion, in black. The thick black lines represent the Periadriatic Fault (PF), the Giudicarie Fault (GF), and the Engadine Fault (EF). The light grey areas represent quaternary deposits along major valleys. (****b****) Structural map of the Bergell batholith and the region on the west showing the locations of the Codera and the Bodengo areas. The Codera area includes the upper Codera valley (COD) and the Rossaccio locality (ROS) indicated with black stars. The Bodengo area includes the Garzelli valley (VG), the Darengo valley (VLD), the Del Dosso valley (VDD), and the Leggia valley (VLG) indicated by empty stars. The map also shows the main boundaries (thin black lines) of the Penninic tectonic units: **Lv** = Leventina; **Sm** = Simano; **Ad** = Adula; **Ta** = Tambò; **Su** = Suretta; **Av** = Avers; **BD** = Bellinzona-Dascio; **MF** = Malenco-Forno. The thick black line labeled **FF** is the Forcola Fault. Figure by Guastoni et al. (2014).*

reviews concerning our area of interest (see Nagel, 2008; Beltrando *et al*., 2010; Galli *et al*., 2013).

The building of the Alpine orogen starts with the closure of the Piedmont-Ligurian and Valais oceanic basins due to the convergence between the Europe and the Adria microplate paleo-margins (Schmid *et al*., 1996). During this phase, south-dipping consumption by subduction of the oceanic lithosphere beneath the Adriatic margin induced an early staking of the Alpine nappes in an accretionary wedge and finally led to continent-continent collision.

The Central Alps mainly expose tectonic units referred to the lower Penninic domain which includes: (1) the Middle Penninic Zone (composed of the Maggia, Tambo, Suretta and Schams nappes), (2) the Lower Penninic Zone (Antigorio, Lebendun, Monte Leone and Adula nappes) and (3) the Sub-Penninic Zone (Lucomagno, Leventina and Simano nappes) (*fig. 1*). The Middle Penninic Zone has been interpreted as a domain restored in the Jurassic paleogeography between the Valais and the Piedmont oceans. During subduction, the nappe stacking within the accretion wedge occurred under high to ultra-high pressure (3 GPa in the southern part of Adula nappe) metamorphic conditions. This stage has been dated between 38 and 34 Ma. The age of the high-P metamorphism becomes progressively younger from top to the base of the nappe pile suggesting a sequential accretion during the closure of the ocean (Beltrando *et al*., 2010). According to Nagel *et al*. (2002) and Nagel (2008) in the the Adula nappe the oldest pervasive D1 deformation phase of the Central Alps postdates the eclogitic event and is referred as the local Zapport phase (<40Ma). The main foliation S1 is associated to top to N shearing and isoclinal folding. During D1 phase the Adula nappe was thrusted onto the Simano nappe with a substantial exhumation from eclogite to amphibolite facies conditions.

The D2 phase (local Claro for the Adula nappe and Niemet Beverin for the Tambo and Suretta nappes) followed D1 phase with a brief episode of E-W extension between 34 and 30 Ma. Top to SE shearing and folding developed a foliation parallel to the orientation of the fold axes. Extension may have been achieved in different ways: passive re-equilibration after slab breakoff (45 Ma according to Von Blanckenburg and Davies, 1995) or episodic retreat of the subduction zone hinge by slab rollback (Beltrando *et al*., 2010). According to Beltrando *et al*. (2010) D2 deformation of the Central Alps, which formed during E-W extension, is well explained by the rollback of one of the oceanic slabs located west or south-west of the Alps. The collapse of the orogen led to rapid exhumation of the nappes and episodic magmatism such as the Bergell intrusion (Beltrando *et al*., 2010). The instauration of a medium-P and high-T Barrovian metamorphism in the Central Alps is coeval with the D2 ductile deformation phase (i.e. the Lepontine Dome). Peak conditions of 720–740 °C at 6.5–7.5 kbar produced sapphirine-bearing granulites in the Gruf Complex (Galli *et al*. 2011). The dominant phase of the associated migmatisation in the Gruf Complex occurred between 34 and 29 Ma with the highest grade at about 32.7 Ma (Liati and Gebauer, 2003). According to Galli et al. (2012), the intrusion of the Bergell pluton is coupled with the ductile deformation of the migmatitic Gruf Complex (see also Davidson *et al*. 1996 and Berger *et al*. 1996) and their contemporaneous emplacement at higher structural levels was promoted by isostatic uplift due to slab breakoff.

The re-instauration of shortening and crustal thickening took place while the Bergell granodiorite was not completely crystallized (Davidson *et al*., 1996). D3 ductile deformation phase (local Cressim, 30-25 Ma) is associated to dextral backthrusting and backfolding by up to 20 km relative vertical displacement along the Insubric mylonites (Rosenberg *et al*. 1995, Schmid *et al*. 1996). It led to the formation of large antiforms, like the Cressim antiform (which folded the base of the Bergell pluton) and the Paglia antiform, and the formation of the Southern Steep Belt (SSB) in the south. The SSB developed high-temperature mylonites (~700°C and 6-7 kbar, Burri *et al*., 2005) with subvertical stretching lineations and common migmatisation due to white-mica breakdown (water-assisted Alpine migmatisation continued up to 22 Ma, Burri et al. 2005). Some authors (Nagel *et al*. 2002, Maxelon & Mancktelow 2005) suggest that the SSB might be an older south-dipping shear zone with normal sense related to the Claro phase and refolded during the Cressim phase. First Alpine pegmatite and aplite dikes are dated by Romer et al. (1996) who individuated two generations of pegmatites intruding the Symplon ductile shear zone between 29 and 26 Ma. The former is slightly deformed thus concordant to the syn-kinematic emplacement while the latter is undeformed. According to Romer *et al.* (1996) this would provide a minimum age to the backthrusting along the Simplon shear zone (see also Gebauer, 1996).

The D4 deformation phase is related to late continental collision and associated magmatism. Dextral backthrusting was replaced by a pure dextral strike-slip regime. Sin-collisional orogen-parallel extension at the Forcola mylonites drove the emplacement of the Novate granite (~24.2 Ma, Liati et al. 2000), which intrudes discordantly the D3-related structures as well as the associated leucocratic dikes (Ciancaleoni and Marquer 2006). Maxelon and Mancktelow (2005) individuated a late stage of ductile deformation that produced similar structures to those of D3, but prominent only in the Northern and Southern Steep Belts. These folds deep toward the NNW with fold axes oriented (E)NE-(W)SW. Chevron type and kink folds are the most common geometries.

2.2. Pegmatites of the Central Alps

The Tertiary pegmatite field of the Central Alps extends in an E-W direction for about 100 km from the Bergell (East) pluton to the Ossola valley (West) and for about 15 km north of the Periadriatic Fault. Pegmatites are abundant in the steepened roots of the Alpine nappes (Southern Steep Belt) and progressively decrease in number towards north, where the nappes are flat-lying (Burri et al., 2005). The area, mapped by Wenk (1970), Burri *et al*. (2005) and Ghizzoni and Mazzoleni (2005), geographically coincides with the domain of the highest metamorphic grade of the Alpine metamorphism (the Lepontine Barrovian metamorphic dome) and with the zone of Alpine migmatization (Guastoni *et al*., 2014). Burri et al. (2005) observed that only a minor part of the pegmatite dikes developed rare accessory minerals such as beryl and tourmaline. Given the low degree of differentiation of the pegmatites and their depletion in RRE-elements, Von Blanckenburg (1992) referred the pegmatites of the Central Alps to partial melting of the host rocks. However, pegmatites commonly cut and are therefore younger than the hosting migmatites (Wenk, 1973). Radiometric dating of pegmatites by several authors indicate a protracted time of intrusion. These geochronological data also indicate the occurrence of pre-alpine leucocratic dikes within the Central Alps (Romer et al. 1996, Galli et al. 2012, 2013). U-Pb dating of xenotime and monazite from pegmatites intruding the SSB at Malesco indicates the presence of two distinct generations of dikes with ages ranging from 29.2±0.2 and 25.5-±0.2 Ma (Romer *et al*., 1996). An exception is the aplite dike at Lavertezzo yielding an age of ~ 20 Ma. The oldest dikes are deformed and are characterized by high initial $^{87}Sr/^{86}Sr$ ratio (>0.71); the geochemistry suggests an origin by melting of old crustal rocks. The youngest dikes are mainly undeformed and have lower initial $^{87}Sr/^{86}Sr$ ratio (<0.71) suggesting a derivation from melting of a depleted crust. Despite the overlapping of ages of pegmatites from the two sets, in the field there is a clear overprinting relationship with the younger dikes always crosscutting the older. The youngest dike at Malesco has a consistent age to the one (25.1 ± 0.6 Ma) dated by Gebauer *et al*. (1996) north of San Vittore in the SSB, which is more than 50 km far away. Liati *et al*. (2000) highlighted the similar age of intrusion of leucocratic dikes and the Novate granite as well as the similarity in the geochemical signature.

2.3. The Lepontine Dome

Wenk (1970) gave the name of "Lepontine Dome" to the area of the Central Alps affected by the Tertiary Barrovian metamorphism (*fig. 2*). The metamorphic conditions within the Lepontine Dome range from greenschist to the upper amphibolite facies. The dome is asymmetric and extends from the Simplon Line in the west to the Bergell area in the east, confined between the Northern Steep Belt (south of the Gotthard massif) and the Southern Steep Belt, where it is truncated by the Insubric Line. The mineral isograds indicate an increase in

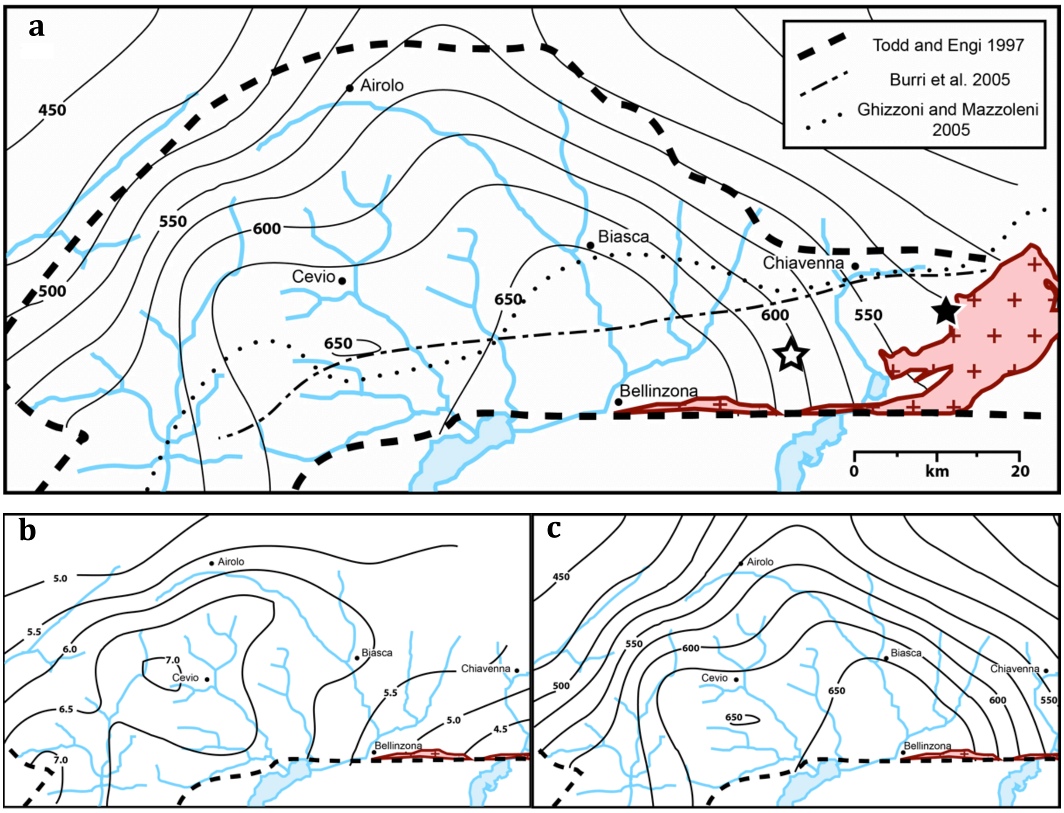

Figure 2 *(**a**) Map of the isotherms (values in °C) of the Lepontine Dome confronted with the distribution of pegmatites reported by Burri et al. (2005) and Ghizzoni and Mazzoleni (2005), the black and the white stars indicate the approximate position of respectively the Codera and the Bodengo areas, the thick dashed line indicates the limit of the amphibolite grade metamorphism overprint. On figure 2 (**b**) and (**c**) are confronted the distribution of isobars (values in kbar) and isotherms (°C), which peaks do not regionally overlap. Peak temperature and pressure data were contoured for an elevation of 1000m and are diachronous. Note that the Gruf complex seems to have no influence on the contouring: no samples used for this study come from the Gruf complex. Redrawn after Todd and Engi (1997).*

temperature from north to south with a peak of 675°C near Bellinzona (fig. 2, Todd and Engi, 1997). Temperature and pressure isograds indicate the maximum metamorphic conditions experienced during the whole tectonometamorphic history of the Central Alps, which means that contour patterns represent a diachronous field (also note the absence of the peak metamorphism recorded in the Gruf complex due to lack of data). Todd and Engi (1997) observed that pressure and temperature maximum do not geographically overlap (fig. 2 a and b). This is in contrast with a single event of crustal thickening and thermal relaxation and request at least two major events: the first affecting the northern part and the second affecting only the south-eastern part, at lower pressure conditions. A support to this interpretation is given by the radiometric ages that suggest differential uplift rates i.e. different peak metamorphism ages.

Several authors speculated about the origin of the high temperature Barrovian metamorphism of the Lepontine Dome. Hypothesis range from the classical radiogenic heating in thickened lithospheric crust to the more recent models of tectonic accretion channel (Engi *et al*., 2001) or viscous shear heating (Burg et al., 2005). According to Beltrando *et al*. (2010) the models that involve continuous shortening and lithospheric thickening are incompatible with the Central Alps scenario. Well-documented extension along regional scale shear zones with generalized E-W stretching is consistent with the fast nappe exhumation and lithospheric thinning. Consequent relaxation of isotherms produced steep geothermal gradients resulted in Barrovian metamorphism and migmatisation while the short-lived generation of mantle melts is related to the rapid advection of mantle material to shallower levels.

2.4. Adula and Simano nappes

Adula and Simano nappes belong to the lower Penninic units of the Central Alps. These rocks represent the distal portion of the European continental margin subducted beneath the Adria microplate between Palaeogene and late Eocene (Schmid *et al*., 1996).

The Adula nappe, in contrast with the other Pennic basement nappes, is generally referred to as a lithospheric melange, formed within a tectonic accretion channel (Engi *et al*. 2001), consisting of Varisican metagranitoids and paragneisses, and Mesozoic sediments. Small to large (up to 2 km of the Arami body) ultramafic bodies are scattered within the nappe. In contrast to the Adula nappe, the Simano nappe is a rather coherent thrust sheet, mainly composed by pre-Alpine metagranitoids.

Nagel *et al*. (2002) distinguished two main metamorphic events during the Alpine metamorphism of the Adula nappe: (1) an early stage of eclogite facies metamorphism during the nappe stacking, and (2) a later Barrovian overprint coeval with the D2 deformation and with the backfolding stage. More or less retrocessed eclogites are found mainly in boudins within metapelitic rocks and yielded peak conditions of 12 kbar (and 500–600°C) in the north and 25–30 kbar (and 750–850°C) in the south. Adula recorded decompression to amphibolite facies conditions during top-to-N thrusting on the lower units (D1 phase), which consequently yield younger ages for the H-P peak. The high-T event reaches in the southwestern part the peak of 10 kbar/700-650°C. The D3 phase of backfolding, well developed in the southern part of Adula nappe, is associated to the high-T thermal event and migmatisation.

2.5. Gruf complex

The Gruf complex is a composite unit mainly represented by amphibolite facies ortho-gneisses and migmatitic metasediments (Galli *et al*., 2012), which are isoclinally folded. Metagranitoids have Permian age (290-260 Ma) and formed during post-Variscan extension and break-up of Pangea. This complex also contains Permian granulite-charnockite rocks (Galli *et al*. 2013) and ultramafics similar to the ophiolites of the Chiavenna unit and Bellinzona-Dascio zone. Though several authors referred the Gruf complex to the SE continuation of the Adula nappe, Galli *et al*. (2013) pointed out important differences. High-pressure metamorphism, typical of the Adula nappe, is not found in the Gruf complex and the granulite-charnockite associations of the Gruf complex are not present in the Adula nappe. These characteristics, along with other structural and lithological evidences (Berger *et al*. 1996; Davidson *et al*. 1996; Schmid *et al*. 1996), distinguish the Gruf complex from the other Penninic units.

Metamorphic peak conditions in the Gruf Complex are referable to two main events: (1) an ultrahigh-temperature Permian event (282-260 Ma, Galli *et al*., 2012) and (2) the Alpine Barrovian metamorphism of the Lepontine Dome. Charnockitic magmatism and sapphirine-bearing granulites are the product of the former event. Metamorphic conditions in excess of 900 °C and pressures of 8.5–9.5 kbar were estimated for the Permian event. Due to the extremely refractory bulk-rock composition of the Gruf granulites, the Alpine upper-amphibolite facies re-equilibration (720–740°C and 7– 7.5 kbar) was only partial (Galli *et al*., 2011). Oligocene Barrovian metamorphism produced widespread migmatisation (the dominant phase was between 34 and 29 Ma) with production of a 10-30% volume of anatectic melt.

2.6. The Bergell Pluton

The Bergell pluton is one of the most studied among the Tertiary Periadriatic intrusions. The Bergell intrusive rocks belong to a calc-alcaline suite and mainly include (1) tonalite forming the outer rim of the pluton ("Serizzo" Auct.) and the "root zone" ("Iorio tonalite"), and (2) granodiorite ("Ghiandone"), forming the main body of the batholith, characterized by pluricentimetric megacrysts of K-feldspar. The shape of the pluton resembles that of a nappe (Wenk, 1973). The main body of the batholith is emplaced at the same structural level of the Suretta and Tambo nappes (Rosenberg *et al*. 1995, Davidson *et al*. 1996, Schmid *et al*. 1996) and extends into an elongated and relatively thin "root" concordant in the main foliation of the SSB mylonites. North of the SSB the Bergell pluton overlap the Gruf complex and the Adula nappe, divided by the remnant of the "North-Penninic suture zone", strictly related to the Misox zone, the Chiavenna ophiolite and the Bellinzona-Däscio zone (Davidson *et al*., 1996). In an E-W profile the Bergell pluton is assumed to expose a fossil crustal section of approximately 20 km of thickness from the deepest portions deformed ductilely (to the west and along the root zone) to the shallowest portions intruded into the brittle crust.

The calc-alcaline rocks of the bergell are referred to low degrees of partial melting of the continental lithosphere, caused by astenospheric counterflow (Von Blanckenburg and Davies, 1995; Beltrando *et al*., 2010). The Bergell tonalite and granodiorite have been dated at 31.88 ± 0.09 Ma and 30.03 ± 0.17, respectivly (Von Blanckenburg *et al*. 1992). The emplacement of the Bergell pluton took place between the final stages of the mesoalpine tectonic extension at the end of the Niemet Beverin deformation phase of Berger *et al*. (1996) and the initial stages of backthrusting. The N-S shortening during the Cressim (D3) phase produced synmagmatic folding at the base of the intrusion (Rosenberg *et al*., 1994; Davidson *et al*., 1996). According to Rosenberg *et al*. (1994, 1995) the shortening along the feeder root zone is responsible for the upward extrusion and final emplacement of the Bergell pluton. This induced ballooning in the country rocks along the eastern border. In the east, the intrusion of tonalite produced a contact metamorphic aureole, within country rocks originally at a temperature 350°C. The temperature rise due to contact metamorphism was in the order of 450°C after 0.5 Ma from tonalite emplacement (Trommsdorff and Connolly, 1996). The Bergell pluton intruded at a considerable depth with respect to other Periadriatic intrusions (Adaamello, Biella and Traversella). Emplacement pressures of 6-7 kbar have been estimated for the main body (hornblende geobarometry on samples from Val Dei Ratti and upper Codera valley). Davidson *et al*. (1996) suggested that the intrusion and cooling of the tonalite occurred at about the same depth of 22-26 km. The pressure increase from northeast to southwest suggests a regional tilting due to differential uplift during backthrusting along the Insubric Line (Davidson *et al*. 1996). Assuming a simple model with a N-S axis perpendicular to the SSB mylonites, the estimated tilt angle of the pluton is between 7° (root zone) and 11° (main body). The real total tilt angle is more likely to be of about 20° considering that part of the rotation was accomplished before the complete solidification of the pluton (Davidson *et al*. 1996).

2.7. The Novate granite

The Novate granite (San Fedelino) is a S-type leucocratic two-mica and locally garnet-bearing granite. The Novate intrusion intrudes discordantly the base of the Bergell batholith (Wenk 1973, Von Blanckenburg *et al*. 1992, Liati *et al*. 2000). Geochemical data indicate that the Novate and the Bergell batholith are not co-genetic. The Novate granite is exposed at the Monte Peschiera in the western side of the lower Val Mera where it intrudes the D3 structures of the Cressim antiform (Berger *et al*., 1996, and references therein). Ciancaleoni and Marquer (2006) proposed that the emplacement of the Novate granite occurred during syn-collisional extension along the Forcola shear zone. Space for magma ascent was provided by opening of an extensional jog along the shear zone. Host rock structures are essentially not deflected by the intrusion and local stoping occurrs at the southern intrusive contact (Ciancaleoni and Marquer, 2006). U-Pb dating of magmatic zircons form the Novate yielded an age of 24.0 ± 1.2 Ma (Liati *et al*., 2000). Syn-intrusive fast isobaric cooling occurred at the host rock conditions of 0.2 GPa and 400 °C (Ciancaleoni and Marquer, 2006). A stockwork of leucocratic dikes (micrograntes, pegmatites and aplites) radiate from and cut through the intrusion. Liati *et al*. (2000) suggested that these dikes may be genetically related to the Novate granite and possibly to other non-outcropping associated intrusive bodies. This conclusion is supported by the 25.1 ± 0.6 Ma age obtained for pegmatites of the SSB (Gebauer, 1996). Both the Novate intrusion and the pegmatites also share a similar geochemistry with a strongly depleted RRE-pattern and a large Eu anomaly with respect to the Bergell tonalites (Von Blanckenburg *et al*., 1992).

3. <u>Field Data</u>

3.1. Areas and localities

The Codera domain is located at the eastern contact of the Bergell pluton. Two areas from this domain were studied: the Upper Codera valley (COD) and the Rossaccio (ROS) (*fig. 1*). The COD area is located in the eastern side of the upper part of the Codera valley at about 2500-2700 m. The area extends between the Pedroni Dal Prà hut and the crest (named “Altare”) at the Italian–Switzerland border, and includes the glacial cirque south of Pizzo Trubinasca. The outcrops include the contact between the intrusives of the Bergell batholith (including the “Ghiandone” granodiorite and the peripheral “Serizzo” tonalite) and the host rock migmatites of the Gruf Complex. The ROS area is located west of the Cima Codera, east of the Aurosina valley and northeast of the Val Piana line. This locality is a few kilometers west from the COD area and is within the Gruf unit. The Bodengo area extends over a wide region between the Mesolcina (in the west) and the Mera (in the east) valleys. The sudy of this area was conducted in different localities in the upper parts of the valleys cutting through the region: Garzelli valley (VG), Leggia valley (VLG), Del Dosso valley (VDD) and Darengo valley (VLD) (*fig. 1*).

3.2. Codera area

Leucocratic dikes and quartz veins are abundant in the Codera area. The dikes are present within both the Gruf migmatites and the Bergell pluton crosscutting the intrusive contact. Within the Bergell, the pegmatites intrude both the tonalite rim (which in the study area is up to 200 m in width) and the granodiorite core (*fig. 3 and 4a*). The leucocratic dikes include pegmatites (barren-type or differentiated dikes with garnet, beryl and tourmaline), aplites and microgranitic dikes. The latter are lithologically very similar to the Novate microgranites.

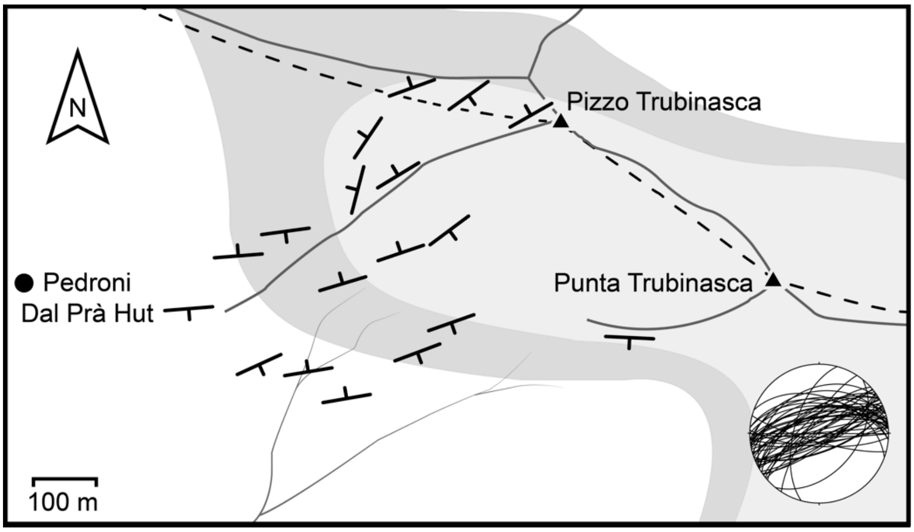

Fig. 3 *Structural map of the upper Codera valley. Markers indicate the dip direction and strike of pegmatite dikes, which are also reported in the attached steroplot. The dark grey and light grey areas indicate respectively the outcropping tonalite and granodiorite rocks of the Bergell intrusion. The dashed line indicates the geographical boundary between Italy and Switzerland.*

These dikes are generally up to 1 m thick with the noteworthy exception one of the large dike outcropping just north of the Pedroni Dal Prà hut (*fig. 4f*). This dike reaches 6-7 m in width and consists of a dominant microgranite at the dike core, rimmed by selvages of pegmatite. The microgranite contains scattered phoenocrystals of K-feldspar. This dike outcrops for several hundred meters, cutting across the contact between the Gruf and the Bergell pluton.

The microgranitic dikes cut and locally even exploit the main set of pegmatite dikes intruding their cores or salbands and achieving the pegmatite orientation (*fig. 4c and 7a*). The large dike described in upper Codera valley is a striking example. In *fig. 4g* large K-feldspar crystals and fragments of graphic texture are deflected by the ascent of microgranite intruding the core of a pegmatite. The main set of pegmatite dikes has an average strike of 70°N and dips steeply (75° mean) both toward north and south (as visible in the upper Codera valley structural map, Fig. 3, and stereoplots on figure 8). From the orientation it is possible to distinguish two different sets: (1) a set (less common) striking E-W, and (2) a set striking ENE-WSW. Pegmatites locally show crosscutting relationships (*fig. 4b*) suggesting poliphasic intrusion. Most pegmatites are less than a meter in thickness and are barren (for a definition see the "Pegmatites" chapter) while only a minor number of dikes show a more "evolved" mineralogy with abundant local garnet, tourmaline and beryl. Although dikes commonly preserve their pristine texture (including graphic K-feldspar and quartz intergrowth and comb texture) it is present an incipient ductile overprint locally evidenced by microboudinage of tourmalines and beryl or healed bent crystals. A weak tilting of feldspar comb texture also locally indicate a shear overprint. Locally the ductile deformation becomes pervasive even in pegmatite dikes and localizes in discrete shear zones (*fig. 4d and 11e*). In the Bergell intrusive rocks, ductile shear zones exploited high-temperature joints and compositional boundaries including pegmatite dikes (*fig. 4d*). Some dikes were simply dragged along crosscutting shear zones but more commonly leucocratic dikes localize deformation and develop mylonites at their boundaries or internally (especially the quartz-rich cores) with transpressive kinematic. Ductile deformation is also pervasive in the quartz veins oriented parallel to the main set of pegmatites. A strong mylonitic overprint is also observed in the pegmatite dikes within the Gruf units of the Rossaccio locality (*fig. 4e*).

3.3. Bodengo area

The country rocks of this area are the high-grade heterogeneous and migmatitic rocks of the Adula and Simano nappes. These units host an extensive swarm of sub-parallel pegmatite dikes, spaced on the order of tens of meters. These dikes generally do not reach one meter in thickness. As in the case of the Codera area, most dikes are barren and consist basically of quartz, feldspar and muscovite (with minor biotite). The dominant set of pegmatites intrudes discordantly the D3 structures and the steepened regional foliation of the SSB and are basically undeformed.

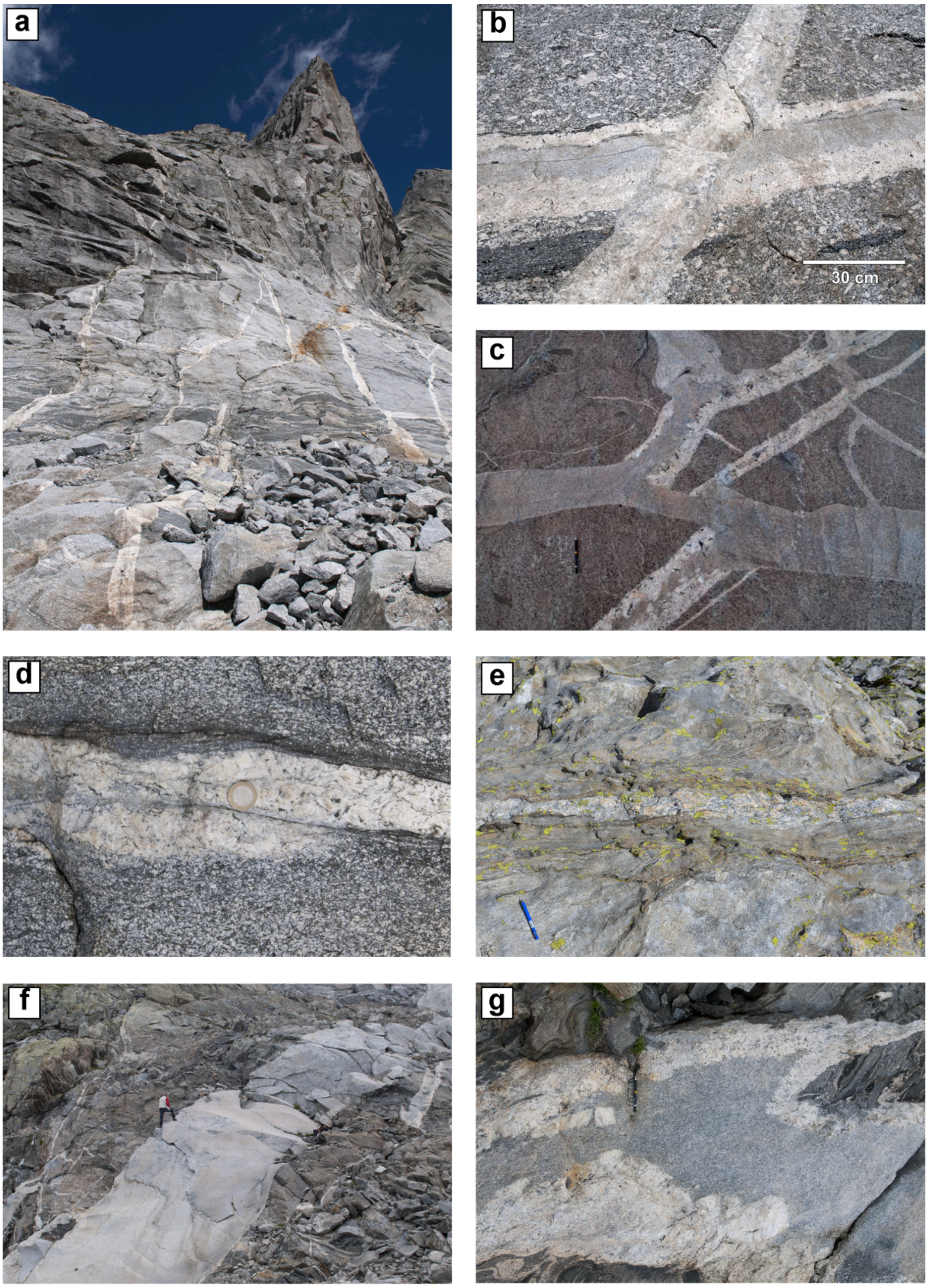
a
b
30 cm
c
d
e
f
g

*<u>Figure 4</u> Outcropping dikes of the Codera area. (**a**) Pegmatite dikes cutting discordantly the transition zone (swarm of mafic inclusions) between the tonalite and the granodiorite of the Bergell pluton south of Pizzo Trubinasca. (**b**) Crosscutting pegmatites in the Bergell granodiorite. The younger dike is oriented at higher angle than the older to the foliation of the granodiorite, which is marked by isoorientation of large K-feldspar phoenocrystals. Upper Codera valley. (**c**) Leucocratic microgranite dike crosscutting and exploiting precursor pegmatite dikes. Pencil (14.5 cm) for scale, upper Codera valley. (**d**) Pegmatite dike exploited by a mylonitic shear zone at the core and one flank. The original texture of the dike (on the right) is lost where the mylonite enters the core (on the centre and left). 1 euro for scale, upper Codera valley. (**e**) Deformed pegmatite dike producing drag folding of the host rock foliation with dextral sense of shear. Pencil (14.5 cm), Rossaccio locality. (**f**) Large microgranite dike outcropping in the upper Codera valley. G. Pennacchioni as scale. (**g**) Close up of the pegmatite dike outcropping on the right of the large microgranite in figure 4 e. The pegmatite is exploited by the microgranitic rock at its core and shows bended texture in the direction of the flow, which is suggested by the large fragments of K-feldspar pointing to the right. Pencil (14.5 cm) for scale.*

In rare cases sheared boundaries of the dikes (with strike-slip kinematic) were observed with the development of S-C foliations delineated by white mica (Garzelli valley, *fig. 6e and 11d*). In the Garzelli valley some deformed dikes of the main set show a sharp internal plane at the dike centre (roughly parallel to the C-planes), which appear to have been formed by reactivation of the dike under brittle conditions. This plane is in some cases weakly reactivated under brittle conditions, allowing late hydrotermal quartz to crystallize within small opened fractures. Pegmatites dip mainly toward W or WNW with an average inclination of 45°-50° (*fig. 4 and 7*). In Garzelli valley they are steeper with an average dip of 70°. This main set of pegmatite crosscuts an earlier one striking NW-SE (*fig. 6b*), which is sub parallel to the host-rock foliation (but still discordant). These earlier dikes show are boudinaged, buckled and sheared (*fig. 6c and d*). They steeply dip toward NE with a mean orientation of 44°N/68°. Most pegmatites exposed in the eastern flank of Garzelli valley belong to this older set.

Except for the degree of ductile overprint the pegmatites of the Bodengo area have the same mineralogy and textures of those of Codera area.

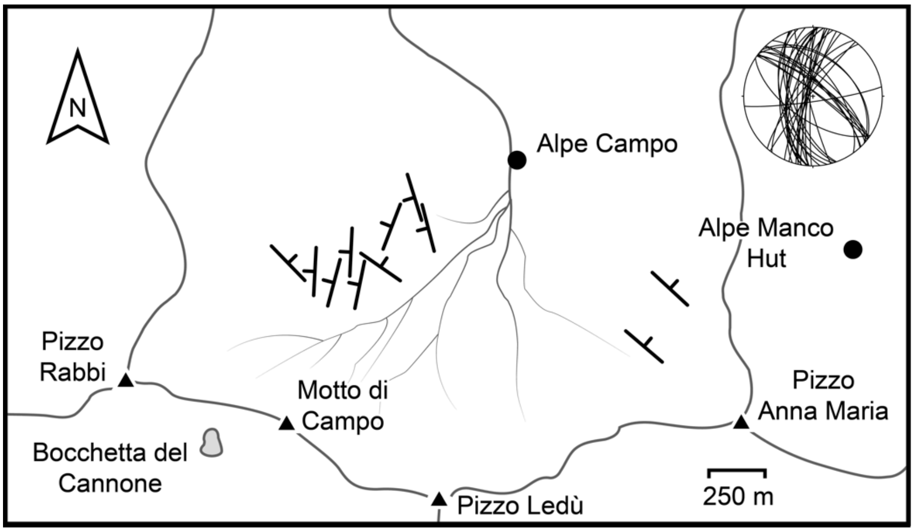

Figure 5 *Structural map of the upper Garzelli valley. Markers indicate the dip direction and strike of pegmatite dikes, which are also reported in the attached steroplot.*

Locally dikes developed a layered structure that can be symmetric (most common) or asymmetric (with a fine-grained layer at the bottom wall zone). Rare miarolitic cavities (*fig 6g)* occur in the upper part of the core zone as isolated large pockets (up to 1m in size) or smaller pockets (pluridecimetric). Usually they contain brownish to smoky vitreous quartz, aquamarine beryl, schorl tourmaline, garnet and rare accessories. Miarolitic dikes do not develop comb textures.

In Garzelli valley a large pull-apart structure filled with foliated aplite was found. Foliation, which is marked by thin trails of garnet (up to 10 cm in length, *fig. 10f*) developed parallel to the feeders, which are roughly parallel to the foliation of the host rock. Aplite texture and foliation is probably genetically linked to the syn-intrusion opening of the pull-apart structure.

Quartz veins discordant to the main set of pegmatites are also common in the area. Most of these veins predate the pegmatite intrusion and are affected by the D3 deformation event. However, some undeformed quartz veins are oriented parallel to the pegmatite dikes and could belong to the same event of intrusion. The largest undeformed quartz vein (up to a few meters thick) was found in the Del Dosso valley.

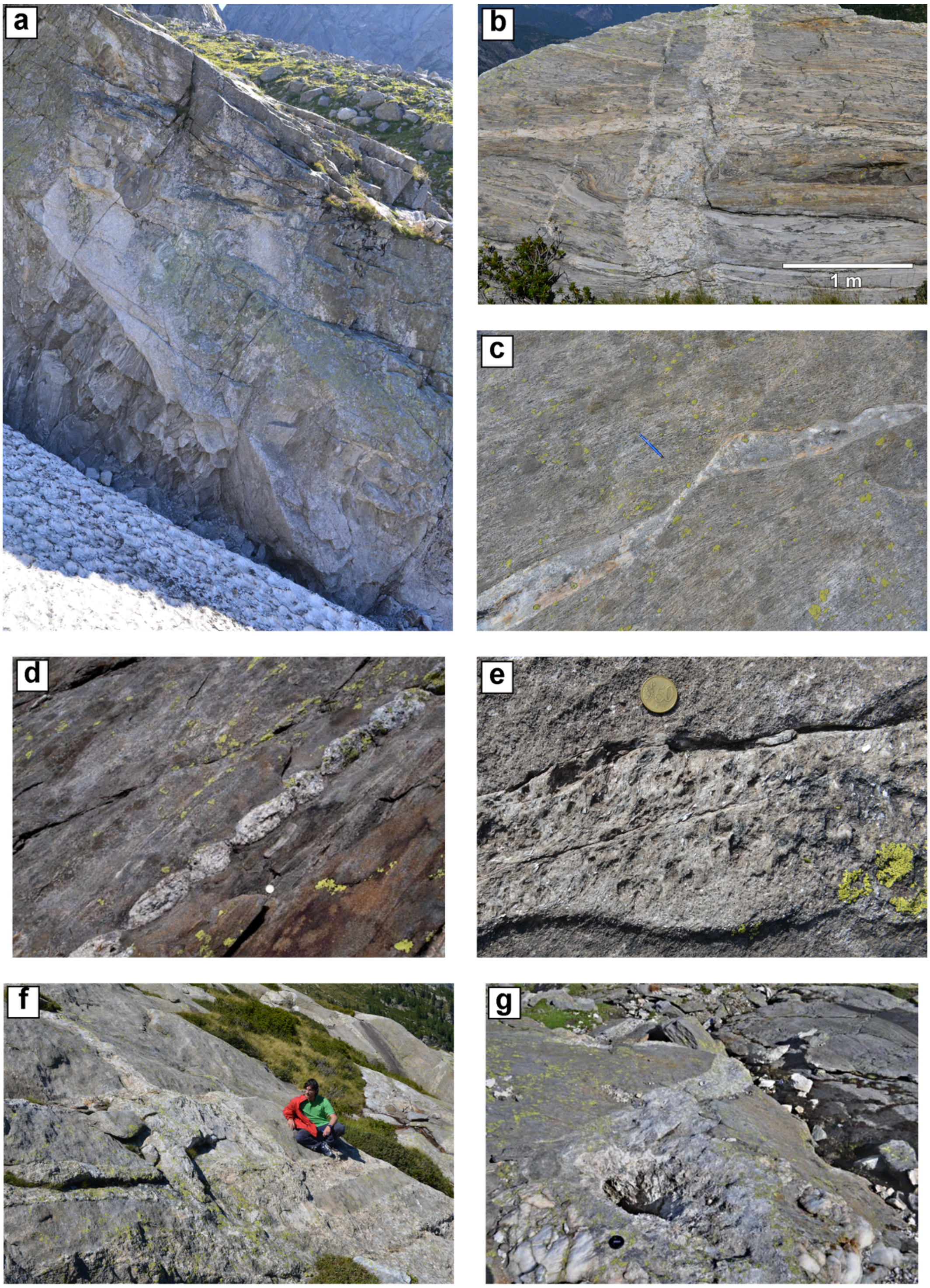
a
b
1 m
c
d
e
f
g

*<u>Figure 6</u> (Page 19) Outcropping dikes of the Bodengo area. **(a)** Gorge set on a NW-SE striking subvertical pegmatite dike on the eastern flank of upper Garzelli valley. **(b)** Block of migmatitic gneisses intruded by two pegmatite dikes showing crosscutting relationship. The older dike (horizontal one in the photo) is sub-parallel to the host rock foliation and cuts a discordant dike (vertical) showing a more preserved internal texture. Codera valley. **(c)** Pegmatite dike displaced left-laterally and thinned along a crosscutting ductile shear zone discordant to the foliation. Pencil (14.5 cm) for scale. **(d)** Pinch-and-swell boudinage of a pegmatite oriented at a small angle to the main foliation of the SSB. Del Dosso valley, 1 euro for scale. **(e)** Ductilely deformed dike of the younger set showing internal S-C foliation. Garzelli valley, 50 euro cent for scale (24.25 mm). **(f)** Foliated aplite dike intruding a pull apart structure and oriented at a small angle to the host rock foliation. The dike is cut by a younger set of pegmatite dikes. Garzelli valley, G. Caviola for scale. **(g)** Miarolitic cavity in a pegmatite dike. The presence of the cavity is associated with a swelling of the pegmatite dike. Leggia valley; camera lens cap (6 cm in diameter) for scale.*

*<u>Figure 7</u> (Page 21) Photomosaics assembled by photogrammetry of glacier- polished outcrops in the upper Codera valley **(a)** and the Garzelli valley **(b)**.*

***(a)** Codera photomosaic shows a set of pegmatite dikes (p) and a younger set of microgranite dikes (g) within the Bergell granitoids. The microgranite dikes crosscut, and locally exploit, the pegmatite dikes.*

***(b)** Garzelli photomosaic shows two intersecting sets of pegmatites with the older thin dikes (p1) deformed along ductile shear bands (indicated by black arrows in the lower left part of the outcrop); the younger dikes (p2) crosscut at a high angle the host- rock foliation and appear mainly undeformed except for showing locally a ductile overprint (as indicated by the white arrow in the upper right part of the outcrop).*

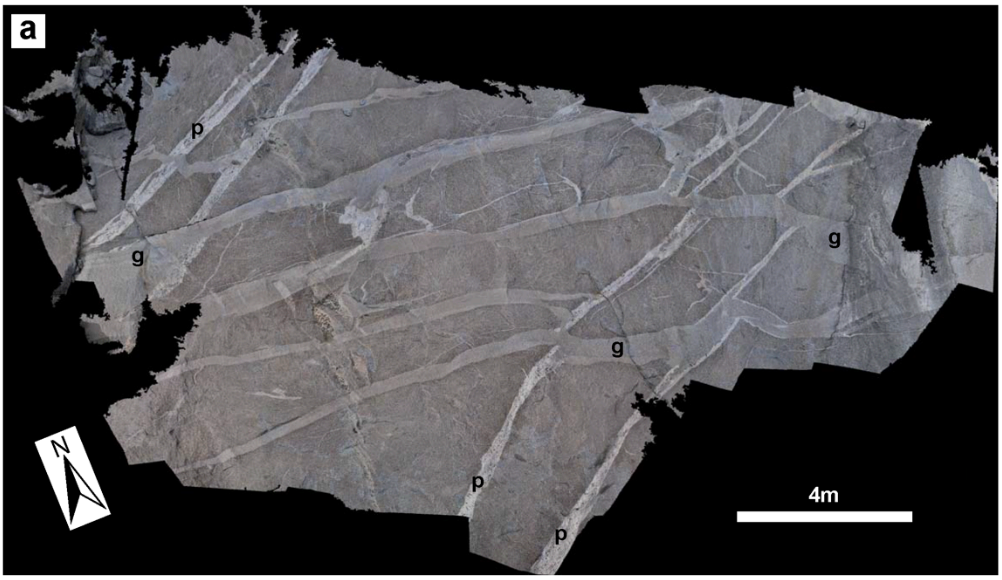
a
p
g
g
g
N
p
4m
p

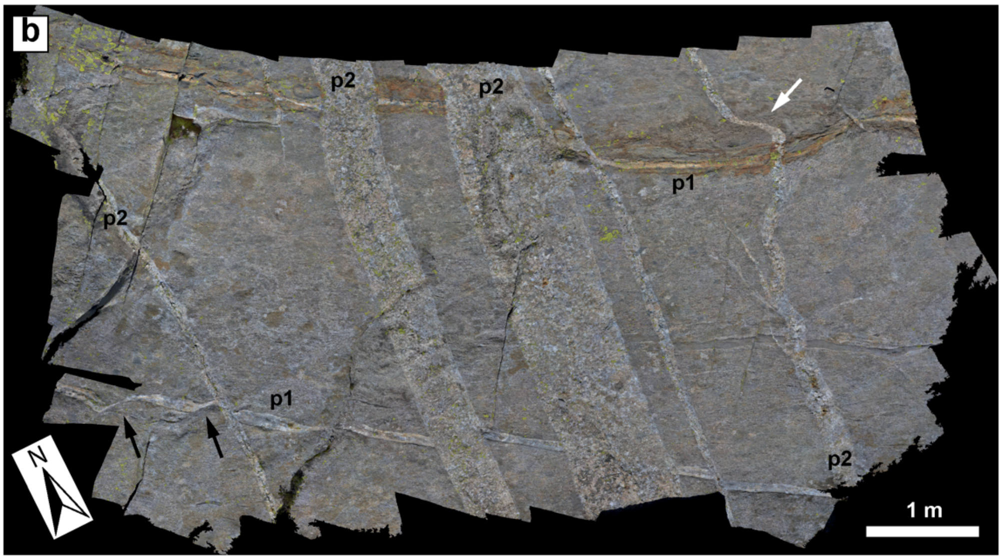
b
p2
p2
p1
p2
p1
N
p2
1 m

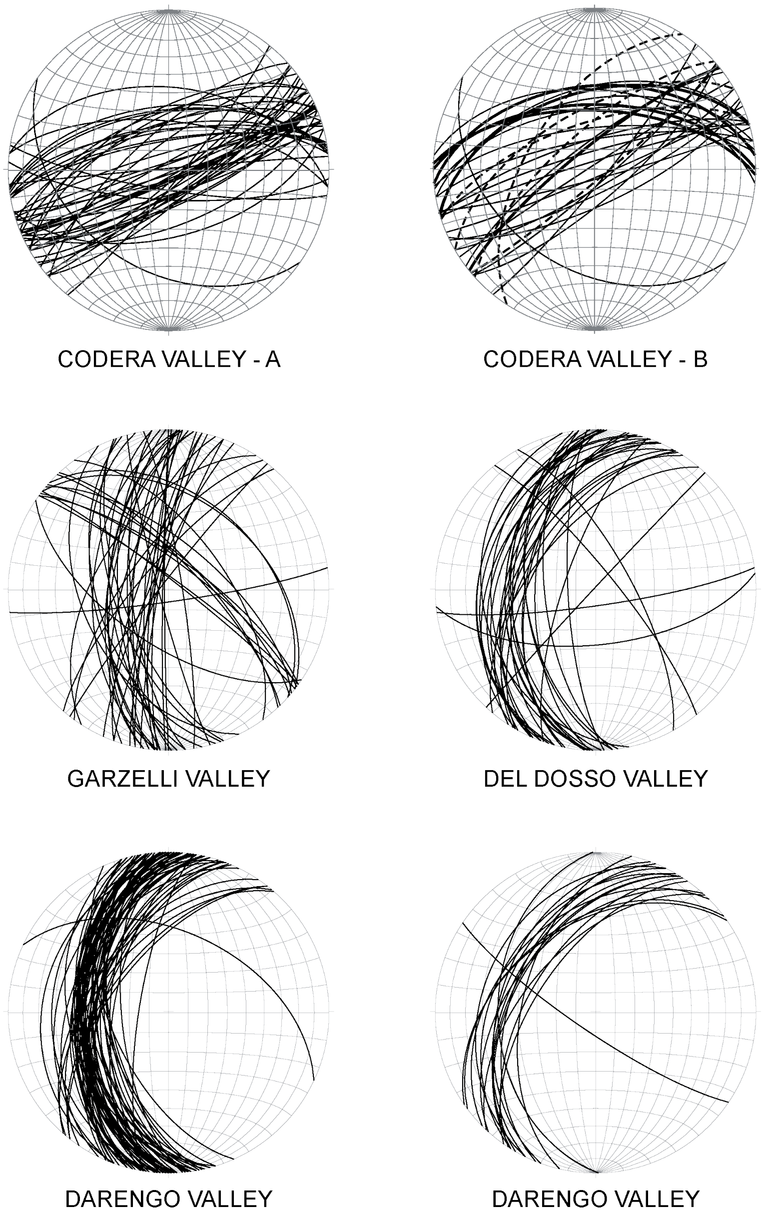

<u>Figure 8</u> *Stereographic plots (lower hemisphere, equal area) of the orientations of pegmatite dikes from different localities (see fig. 1 for location) of the upper eastern Codera and Bodengo area. On Codera valley – A stereoplot are plotted the orientations of pegmatite dikes. On Codera valley – B stereoplot are plotted the orientations of deformed dikes and veins where the thin lines represent pegmatites, thick lines are leucocratic (microgranite) dikes, and dashed lines indicate quartz veins.*

4. Pegmatites

4.1. General appearance of pegmatites

Most pegmatites occur as dikes that to a first approximation have a tabular shape. In some cases the pegmatite terminations pinch out in the host rock and make transition to quartz veins (as observed in Upper Codera and Rossaccio, see also Ghizzoni and Mazzoleni, 2005). In both the Codera and Bodengo areas the pegmatites generally are less than 1 metre thick with a few exceptions of dikes of as much as a few metre thick. Thin dikes commonly thicken at pull-apart structure, at the intersection with other dikes or where miarolitic pockets are developed. Most pegmatites preserve the pristine structure, which include comb structures (*fig. 9b and c*) of K-feldspar, graphic intergrowth between quartz and feldspar or graphic garnet and tourmaline intergrown with quartz (*fig. 9 fand g*). However, to a close inspection the dyke can show a weak ductile overprint and in the Codera area many dikes are clearly mylonitized (*fig. 4d and e*). The pegmatite structure and mineralogy can abruptly change along strike. According to the nomenclature adopted by London (2008), the following structures can be recognized in the layered pegmatites of the study areas: (1) border zone with fine-grained to aplitic texture; (2) wall zone with centimetric K-feldspar, albite, muscovite or biotite and quartz, often with longated crystals arranged in comb structures (*fig. 9b and c*); (3) intermediate zone with coarser (a few cm to dm) graphic quartz and K-feldspar intergrowth, albite, muscovite and local accessory minerals (mm-sized garnets, graphic black schorl and pale blue beryl, *fig. 9g*); (4) core zone developing giant texture (up to metric perthitic K-feldspar) and eventually grey quartz masses; (5) miarolitic cavities in the core zone (only in Bodengo, *fig. 6g*).

4.2. General mineralogy of pegmatites

Most pegmatites have a simple mineral assemblage consisting in K-feldspar, albite, quartz and biotite and/or muscovite (barren pegmatite). A very minor number of dikes locally contain accessory minerals that include: Sn-Nb-Ta-Y-REE-U oxides, Y-REE phosphates, Mn-Fe-phosphates, Ti-Zr-silicates, Be-Y-REE-U-silicates and oxide minerals (beryl, chrysoberyl, bertrandite, bavenite, and milarite), garnet (almandine-spessartine), tourmaline (schorl to rare elbaite), bismutinite, magnetite, and rarely dumortierite and helvite (Guastoni *et al.*, 2014).

Figure 9 ***(a)*** *Thin barren pegmatite dike displaying simple mineralogy (K-feldspar, quartz and biotite flakes). Pluricentimetric K-eldspar crystals point toward the core of the dike and in this rare case achieved a pinkish colour. The colour is probably due to the interaction with the more mafic tonalite host rock. Upper Codera valley, 1 euro for scale.* ***(b)*** *Exposed comb texture on a broken opened barren pegmatite. On the broken surface are visible the K-feldspar crystals and the biotite flakes pointing outward. Upper Codera valley, 1 euro for scale.* ***(c)*** *Pegmatite of the main set of dikes crosscutting the main foliation of the country leucocratic gneisses (lower part of the photograph) showing elongated K-feldspar crystals oriented approximately orthogonal to the dike boundary (comb structure). Garzelli valley; compass for scale.* ***(d)*** *Section of the upper half of an evolved pegmatite dike showing biotite and K-feldspar comb texture, decimetric K-feldspar crystals and an inner zone containing graphic garnets characterised by a finer grained texture and ductile deformation. Rossaccio locality, 1 euro for scale.* ***(e)*** *Large flake of muscovite in the evolved Codera Phosphate dike (CODp). 1 euro for scale.* ***(f)*** *Non-graphic garnet surrounded by graphic intergrowth of garnet and quartz. Upper Codera valley, 2 euros for scale (25,75 mm).* ***(g)*** *Characteristic paragenesis of evolved pockets in pegmatite dikes of the Codera area: graphic black schorl tourmaline, graphic and non-graphic garnet and elongated bent crystals of pale blue beryl. Upper Codera valley, 1 euro for scale.* ***(h)*** *Mn-Fluorelbaite broken crystals of the CODp dike. 1 euro for scale.*

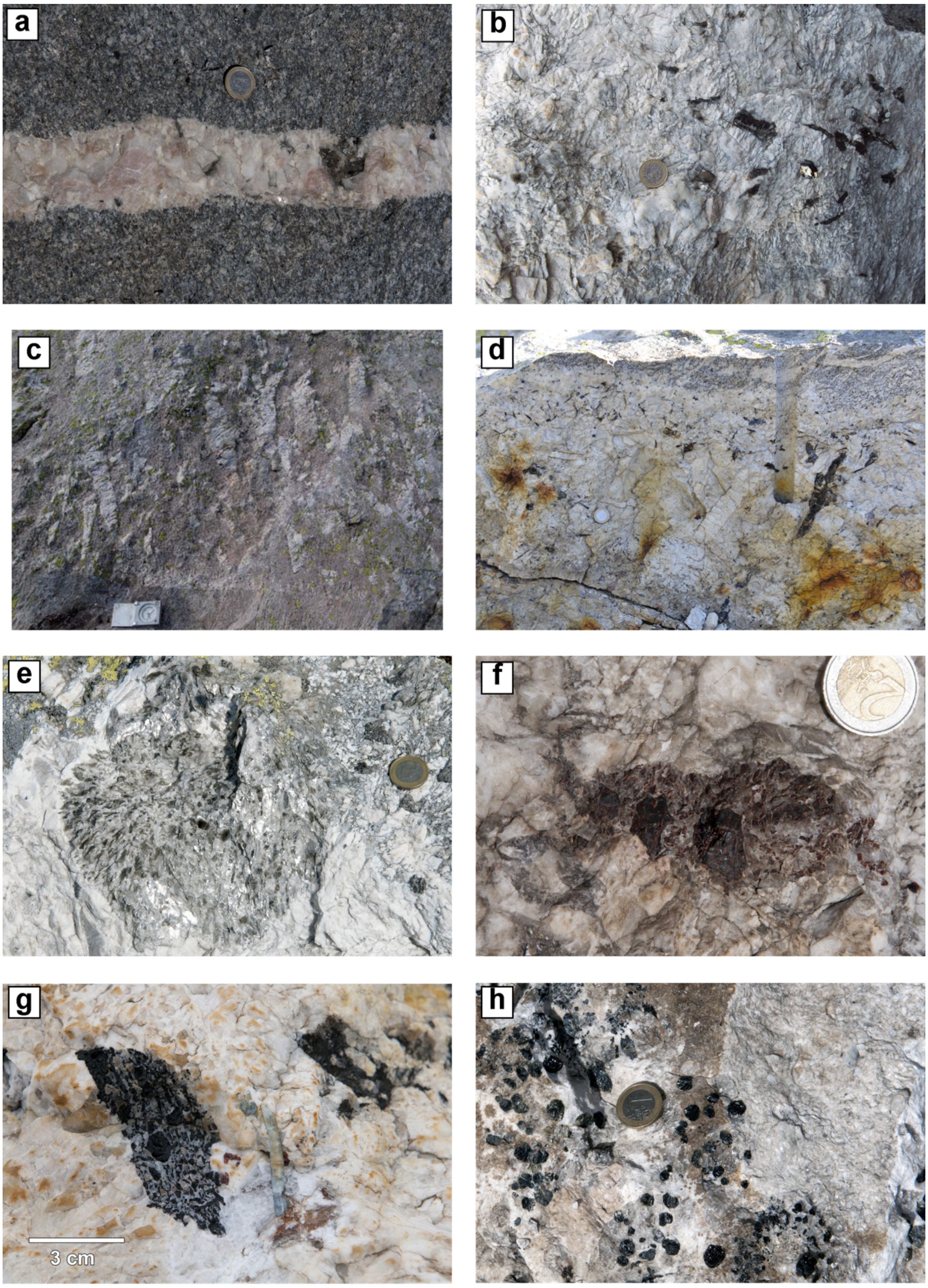
a
b
c
d
e
f
g
3 cm
h

Accessories normally are found only in discrete portions of a pegmatite dike and "mineralized" portion commonly make transition to barren portions. The occurrence of rare accessories is commonly localized to pockets, thin local layers, thickened portions or convergence of multiple dikes. It is possible to correlate the presence of evolved paragenesis to the type of host rock to: for example, in the upper Codera valley, dikes containing garnet, beryl and tourmaline that intrude the Gruf units and the bergell intrusive close to the contact turn to barren types more inside the pluton. For the classification of Codera and Bodengo pegmatites we remand to the work of Guastoni *et al*. (2014).

4.3. Sampled dikes

Pegmatites are heterogeneous rocks both chemically and texturally. Since grain size can exceed the meter and the chemical behaviour can vary substantially in all directions, representative bulk geochemical analyses are difficult to obtain. Geochemical characterization of pegmatites is based on the study of single mineral phases and fine-grained portions (London, 2008), whose composition can be used as a proxy for the pegmatite changing chemistry during crystallisation and for pegmatite classification. Minerals of several evolved dikes were sampled for chemical and isotopical analysis. A brief description of each sampled dike is reported below in the text. Most information comes from the valuable knowledge of the areas and hosted pegmatites of A. Guastoni (2012 and personal communications).

Since rare accessory minerals of pegmatites may occur only as rare scattered occurrences, rarely we can offer a list that includes the whole paragenesis. Nevertheless a list of recognized phases is reported.

CODs zircon sample and VCA monazite and zircon samples were provided by A. Guastoni. CODs (Silvana dike of upper Codera valley) and VCA (dike of Cama valley, ehich is near Leggia valley) dikes will not be described in this section. For information regarding CODs we remand to De Michele and Zezza (1979).

4.3.1. Codera garnet dike – CODg

This dike outcrops for more than 30m in length in the glacial circle of the upper Codera valley. It reaches up to 3m in width in the lower portion where it merges to another pegmatite dike. It is discordant with the foliation of both Bergell tonalite and granodiorite. Ductile deformation of the dike is observed at the dike boundaries where it shows incipient boudinage. The dike is symmetrically layered and includes: (i) border zone of dm-sized K-feldspar, quartz and biotite (arranged in a comb texture); (ii) intermediate zone of K-feldspar; graphic K-feldspar and quartz including layers of millimetric red garnet; (iii) core zone with vitreous smoky quartz and decimetric perthitic K-feldspar. Gemmy aquamarine beryl and trapezohedral red garnet are relatively common. Other subordinate minerals are: schorl tourmaline; rare crystals of columbite-(Fe), euxenite-(Y), monazite-(Ce), xenotime-(Y), uraninite, zircon, magnetite. Monazite crystals were found in the intermediate zone together with garnet. The dike was classified as Rare Elements Pegmatite and belongs to the mixed LCT-NYF family (Guastoni, 2012).

4.3.2. Codera phosphate-bearing dike – CODp

This phosphate-bearing dike outcrops 100 m east of the CODg dike in the upper Codera valley. It cuts discordantly through the foliation and shows a complex internal structure. It is the most evolved dike found in the area as reflected by its peculiar mineralogy. It belongs to the LCT family, rare elements-Li (REL-Li) subclass (Guastoni, 2012). CODp extends for more than for 30 meters in length and reaches up 3 meters in width. As well as the other Codera dikes is deformed and shows lobated boundaries. The sample 12-CODp1 from the dike shows the effect of solid-state ductile deformation at the dike boundary. The dike is texturally and mineralogically zoned and includes: (i) a border zone (30 cm wide) composed by pluricentimetric quartz and albite and containing Mn-rich dark greenish fluorelbaite (*fig 9 h*), black centimetric masses of end-member F-rich triplite, Mn-hydroxides and pale pink prismatic beryl; (ii) a wall zone of medium-coarse grained (up to decimetric) assemblage of graphic K-feldspar and quartz, black schorl and red to orange garnet, triplite masses and colorless to pale pink beryl; (iii) an intermediate zone of medium-coarse grained graphic intergrowth of quartz and K-feldspar, white to yellowish and pale green perthitic Cs-rich K-feldspar, colourless to brownish quartz, large muscovite and biotite flakes. The upper end of the dike developed fine-grained bands of graphic intergrowth of quartz and K-feldspar associated with muscovite flakes. These bands are bordered by a coarse-grained zone (pluridecimetric) of K-feldspar, albite, quartz and muscovite flakes, probably related to the coalescence with a lateral pegmatite dike (Guastoni, 2012).

4.3.3. Codera Mary dike - CODm

This dike occurs within the Gruf migmatites in the eastern flank of the upper Codera valley under the Pizzo Porcellizzo peak. The dike, which reaches 150 cm in thickness, is discordant to the foliation and has similar zoning as the CODg dike including: (i) top wall-border zone with poorly-developed comb texture K-feldspar and muscovite, (ii) intermediate zone with graphic intergrowth of K-feldspar and quartz, biotite and muscovite flakes, (iii) core zone with giant perthitic K-feldspar and smoky masses of quartz at the core. Garnet crystals larger than 1 cm in diameter occur between the graphic layer and the core zone. The presence of pale blue beryl has been reported from this dike.

4.3.4. Codera Trubinasca dike- CODt

The dike outcrops on the north-western flank of the glacial circus under the Pizzo Trubinasca in the upper Codera valley. It is hosted within the Bergell intrusives and cuts discordantly the solid-state foliation. The symmetric zoning of the dike includes: (i) a border zone composed of K-feldspar, quartz and biotite developing minor comb textures; (ii) an intermediate zone with abundant graphic K-feldspar and quartz, and a narrower core of K-feldspar and quartz (which locally occurs as smoky masses). Accessories minerals are garnet, beryl, tourmaline, greenish U-rich monazite-(Ce), zircon and uraninite.

4.3.5. Rossaccio Garnet dike - ROSg

This dike outcrops near the Bocchetta Teggiola within the foliated Gruf mylonitic migmatites. This dike is similar to the CODg dike both texturally and mineralogically. The dike thickness is of as much as 5 m with strong variations along strike. Most segments of the dike are of a barren type, but locally it develops pokets with large garnets (up to 3 cm). At one end this dike transforms makes transition to a massive quartz vein. The dike boundaries are sheared with a mylonitic fabric.

4.3.6. Rossaccio Beryl dike - ROSb

ROSb has a thickness of 2-3 m and outcrops for several tens of meters though partially covered by debris. The internal structure is locally complicated by a strong ductile overprint. The wall zone consists of a medium-grained (up to decimetric) assemblage of K-feldspar, quartz and biotite crystals with a comb texture. The intermediate zone shows a graphic texture of K-feldspar and quartz and contains muscovite and rare zircon. The core zone has pluridecimetric grain size of perthitic K-feldspar, quartz and contain pale blue deformed beryl and graphic to large prismatic (up to 20 cm in lenght) crystals of shorl tourmaline.

4.3.7. Val Garzelli Lower dike - VGb

This dike outcrops in the western side of the upper Garzelli valley near the Alpe Campo, within migmatitic paragneisses. The dike is up to 50 cm in thickness, and cut discordantly across the host rock foliation without showing any deformation structures. It has a simple zoning: (i) medium-fine grained border zone composed of K-feldspar and muscovite; (ii) intermediate zone with graphic intergrowth of

K-feldspar and quartz, muscovite and nice trapezohedral red garnets up to 1-2 cm in diameter; (iii) core zone of coarser perthitic K-feldspar and local masses of dark quartz.

4.3.8. Val Garzelli Upper dike - VGa

VGa is from the same location as VGb but outcrops slightly to the west. The dike is up to 2 m in thickness and has up to decimetric grain size. The border zone is composed by large K-feldspar and muscovite crystals; the intermediate zone has graphic intergrowth of K-feldspar and quartz, muscovite and red garnet crystals with euhedral trapezohedral habit of as much as 1-2 cm in size; the core zone has decimetric perthitic K-feldspar crystals and quartz masses.

4.3.9. Val Del Dosso dike - VDD

This is a quite huge dike (reaching up to 4-5 m in thickness) from the upper part of the Del Dosso valley. VDD has an asymmetric texture including: (i) border zone with giant (up to 50 cm) biotite crystals and K-feldspar forming a comb texture; (ii) intermediate zone with a finer grainsize of K-feldspar, quartz and muscovite; (iii) a layer of garnets (crystals of as much as 2-3 cm in diameter); (iv) core zone with giant (pluridecimetric) texture of K-feldspar, quartz and large silvery mica flakes containing centimetric euhedral garnets. The dike makes transition at the termination to a thick (up to 50 cm) layer of massive quartz of a smoky variety in the core. The dike is intruded by schorl tourmaline-bearing injections that form large hollow pockets within the pegmatite. The dike contains aquamarine, schorl and garnet.

4.3.10. Upper Val Leggia dike - VLGa

This dike extends for a length of ca. 20 m in the upper Leggia valley. It is hosted within the amphibolites and migmatitic gneisses of the Bellinzona-Dascio zone of the SSB, and is concordant to the foliation in its lower end. The dike reaches up to 3-4 m in thickness at this termination where it coalescence with a lateral pegmatite dike. The border zone is coarse-grained (decimetric), composed of idiomorphic white perthitic K-feldspar, albite, large aggregates of muscovite and subordinate brownish-vitreous quartz masses. The intermediate zone contains decimetric euhedral K-feldspar crystals, quartz, albite, black shorl and centimetric trapezohedral crystals of red garnet. The dike contains zircon.

4.3.11. Medium Val Leggia dike - VLGm.

This discordant dike is hosted within the migmatite gneiss of the Southern Steep in the upper Leggia valley. It outcrops for a length of 15 meters and is up to 1.5m in width. The zoned structure is asymmetric including: (i) border zone in the lower part showing a fine-grained layering of K-feldspar, albite, quartz and muscovite; (ii) border zone in the upper part composed of medium coarse grained K-feldspar, albite, quartz and abundant flakes of muscovite; (iii) wall zone composed of centimetric white perthite K-feldspar, albite, flakes of muscovite and quartz; (iv) intermediate with medium to coarse grained texture (pluricentimetric) composed of graphic K-feldspar and quartz, albite, muscovite, red millimetric garnets, centimetric prisms of pale blue beryl and graphic black schorl; core zone developing miarolitic pockets.

One of these pockets reaches one meter in width and hosts brownish-smoky quartz crystals (also with sceptre terminations) up to 15cm in length aquamarine beryl, pluridecimetric idiomorphic white perthite K-feldspars, laminar albite var. clevelandite, rare black schorl and lithiowodginite (Guastoni, 2012). Within the smoky quartz were found several millimetric crystals of yellow subhedral monazite.

4.3.12. Lower Val Leggia (Colonnello) dike - VLGb

VLGb cuts discordantly across the foliation of the migmatitic gneisses of the SSB in the lower part of the Leggia valley. It extends for 15 m in length and reaches up to 1,5m in width. The dike is zoned and includes: (i) a fine-grained lower boundary composed of K-feldspar, albite, quartz and muscovite; (ii) a wall zone of medium grained (centimetric) assemblage of perthitic K-feldspar, albite, muscovite flakes, quartz and millimetric red garnets, centimetric prisms of pale blue beryl and graphic black schorl; (iii) a core zone of coarse grained K-feldspar and quartz with local miarolitic pockets. A large pocket (1 x 0.6 x 0.5 m) provided (Guastoni, 2012): large brownish-smoky quartz crystals (also with sceptre terminations) up to 15 centimeters in length, beryl aquamarine up to 9 x 4 x 4 centimeters, pluridecimetric idiomorphic white perthite K-feldspars, albite var. clevelandite as laminar centimetric crystals, rare black schorl prism up to 5-6 centimeters and lithiowodginite crystals up to 1.6 centimeters in length.

5. Deformation

5.1. Macroscopic evidence of deformation on hand specimens

As described in the chapter 3, pegmatites were locally exploited by ductile deformation especially in the Codera area. Ductile deformation is particularly evident in the quartz veins, associated with the pegmatite swarm, and within the quartz-rich portions of the pegmatite. However, to a close investigation the whole fabric of the pegmatite has been commonly affected even in the case where the pristine pegmatite structure is well preserved (*fig. 9d* and *fig. 10a*). Evidence of this deformation overprint are: (i) the presence of trails of fragmented garnet (see thin section 13-VG-Grt-1 description); (ii) microboudinage and bending of tourmaline and beryl (*fig. 10c and d*). The relatively high temperature condition of the deformation overprint is suggested by the common healing of the fragmented crystals (*fig. 10e* and *fig. 11f*).

Garnets have cubic habit and behave differently from elongated crystals. Euhedral garnets of Codera area commonly show a pervasive net of fractures (*fig. 13a and b, fig. 14e*), which in most case have a preferential trend of sub-parallel planes defining a deformation direction. Although the 12-CODp001 thin section did not intercept garnet crystals, an euhedral one is present on the hand sample surface and displays a short tail of fine-grained garnet (*fig. 11b*).

5.2. Evidence of deformation in thin sections

This session reports the microstructural observations made under the optical microscope of thin sections that include solid-state ductile fabrics of pegmatites. The code of the thin section is reported before each description.

(1) 12-177: (*fig. 11a*) Mylonites of Codera area affect the tonalites and the pegmatites. The tonalite mylonites contain as a synkinematic assemblage: quartz, biotite, plagioclase (oligoclase), epidote, ±K-feldspar. Quartz and biotite underwent dynamic recrystallization. The recrystallized biotite in the mylonitic foliation is lighter coloured than the magmatic biotite, reflecting the decrease in Ti of this relatively lower temperature biotite. K-feldspar is replaced along the boundaries by myrmekites that recrystallized along the foliation to fine (a few microns in size) polygonal aggregates of quartz-oligoclase. Plagioclase and K-feldspar persist up to the mylonitic stage as rounded porphyroclasts immersed in the matrix locally forming d- and s-shaped porphyroclasts systems. These microstructures are similar to those described in granitoid plutons deformed during postmagmatic cooling (Pennacchioni, 2005; Pennacchioni and Zucchi, 2012).

(2) 12-144: (*fig. 11b*) Codera quartz mylonites consist of recrystallized aggregates of small quartz grains (<50μm) of equant or slightly elongated shape, which define a shape preferred orientation oblique to the main foliation.

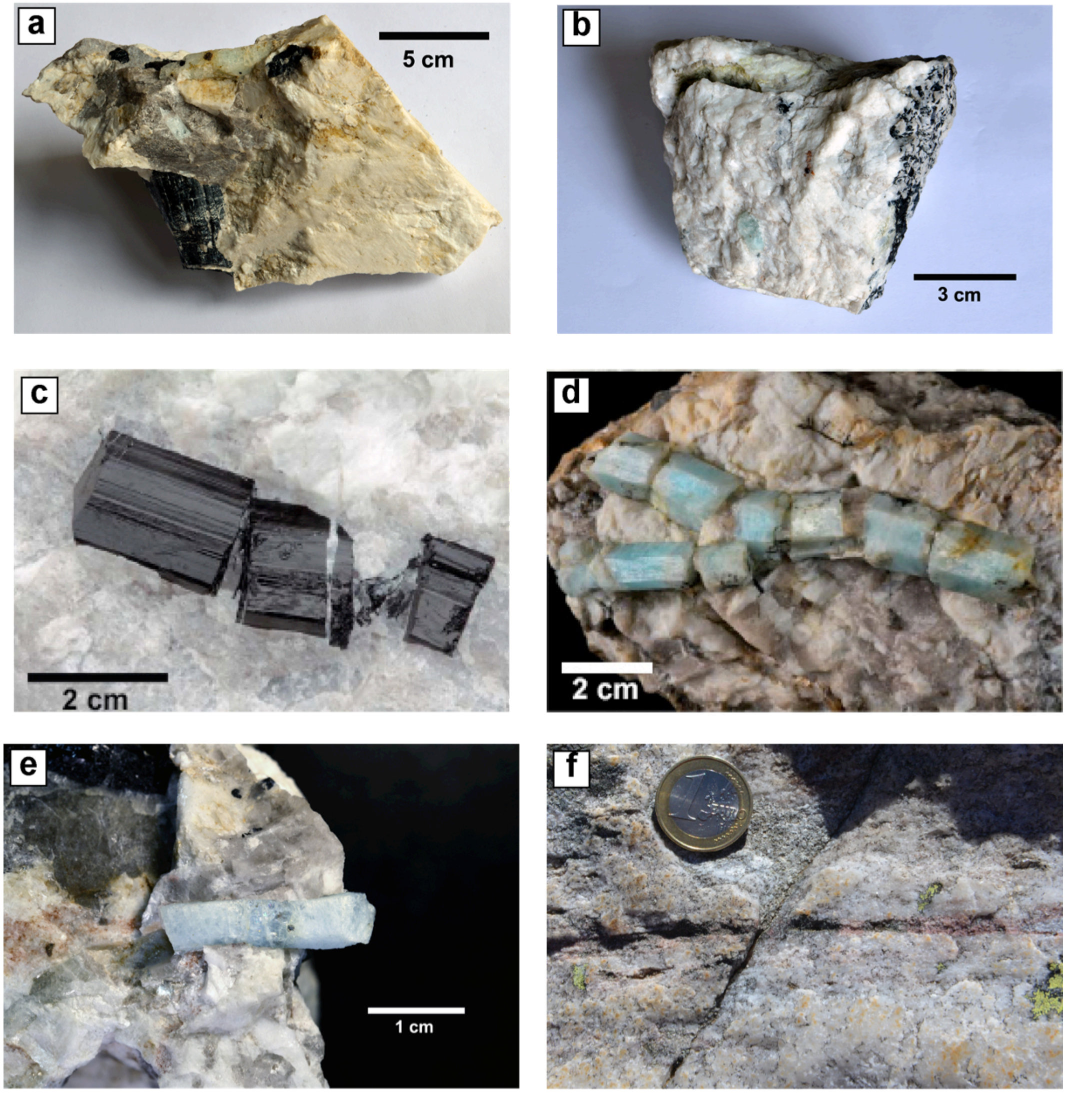

Under crossed polars light the recrystallized aggregates have a dominant dark color or show an extinction banding. The insertion of the gypsum plate under crossed polars indicate a strong crystallographic preferred orientation (CPO) of the recrystallized quartz. The dark overall colour of the recrystallized quartz aggregate under crossed polars suggests a CPO characterized by a c-axis maximum in the direction of the Y kinematic axis of the mylonite (i.e. parallel to the foliation and orthogonal to the lineation). This CPO has been confirmed by x-ray texture goniometry (Guastoni et al., 2014)(*fig. 12*).

<u>Figure 10</u> *(**a**) Large perthitic K-feldspar and smoky quartz in paragenesis with pale blue beryl and boudinaged black schorl tourmaline. The surface of the K-feldspar is decorated with white mica and shows a well developed lineation, which is perpendicular to the beryl prism. The beryl hosts a broken zircon crystal, which caused a yellowish aureola in the beryl. This sample comes from the ROSb dike. (**b**) Handsample of the internal mylonitized zone of CODp dike. From left to right (toward the graphic tourmaline) the graphic structure is gradually obliterated. Are also visible broken pale blue beryl crystal and a small garnet with a recrystallized tail. (**c**) Boudinaged black (schorl) tourmaline within quartz; fractures are sealed with quartz. Rossaccio locality. (**d**) Microboudinaged beryl with the necks filled with quartz. Rossaccio locality. (**e**) Bent crystal of beryl (with small zircon on one prism) showing different deformed areas. The central part seems less pervasively deformed and is more transparent. The sample was found in the CODb dike. (**f**) Thin trails of fine grained garnet in the aplite intruding the pull-apart structure in the western flank of Garzelli valley. 1 euro for scale.*

(3) 12-CODp001: (*fig. 11c*) This sample of CODp dike dike was taken from an internal mylonititized portion. On hand sample the graphic texture of K-feldspar and quartz is gradually deformed toward a discrete surface decorated by white mica and bearing a well-developed lineation. The ductile shearing likely exploited the planar border of graphic schorl. The deformed tourmaline has the c-axis oriented roughly orthogonal to the lineation. Thin section was cut parallel to the lineation of mica and perpendicularly to the shear zone plane. The mono-crystalline quartz of the graphic texture has recrystallized to aggregates of <100μm grainsize by subgrain rotation and high temperature grain boundary migration. K-feldspar crystals are microboudinaged and show elongated optical subgrain with fan-like extinction. The boudin gaps of the K-feldspar are filled with quartz and locally white mica. White mica is dragged in the shear zones eventually producing nice mica-fishes (group-1 mica fish). Maximum reduction of grainsize is achieved near the surface with the graphic schorl, in correspondence of a layer of equant grains of albite and the local complete destruction of the large K-feldspar crystals. Under crossed polars the high strained

zone is dark colored suggesting isoorientation of the quartz with the c-axis perpendicular to the thin section plane (i.e. with a strong Y-maximum of c-axis as described above for the quartz-mylonites). Noteworthy is the orientation of schorl tourmaline whose c-axis is parallel to that of quartz. Fast grain boundary migration and the hypothetical CPO of quartz suggest ductile deformation under high temperature and wet conditions (Vernon, 2004).

(4) GAR-1: (*fig. 11d*) Deformed pegmatites of Garzelli valley display locally a S-C foliation delineated by white mica. Rock in thin section was sampled near the contact with the host rock of a muscovite-rich pegmatite. Deformation mechanism in quartz includes grain boundary migration recrystallization.

(5) 13-VG-Grt-1: (*fig. 11e*) The aplite intruding a pull-apart structure in Garzelli valley was sampled for the study of the garnet trails. The rock is a fine-grained aplite made essentially by equant grains of dominant albite and K-feldspar. Garnets occur as aggregates of rounded (small ones) to angular crystals (large ones) reaching 1-2 mm in size, locally growing close to or in contact with dark brown pleochroic biotite. Aggregates are arranged along parallel trails defining a foliation and, locally, trails seem asymmetrically folded. Despite this the rock

Figure 11 *Thin sections of deformed rocks. (**a**) 12-177: Ultramylonite in tonalite flanking the border of a pegmatite dike of upper Codera valley. Sense of shear is dextral. Plane polarized light. (**b**) 12-144: Dynamically recrystallized aggregate in a quartz mylonite showing extinction banding under crossed polars. Shear sense is dextral. (**c**) 12-CODp001: Trail of small garnet crystal (<2 mm and possibly recrystallized) with pleochroic biotite in aplite matrix. The trail seems asymmetrically folded. Plane polarized light. (**d**) GAR-1: S-C foliation decorated by white mica. The shear sense is dextral. Crossed polars. (**e**) 12-CODp001: Mylonitic shear zone of CODp dike. Well visible the boudinage (vertical cracks) and extinction pattern on K-feldspar. Graphic intergrowth of K-feldspar and quartz is gradually obliterated toward the top of the section where it is the strongest reduction of grainsize of quartz (dark band on the top right). Crossed polars on a thicker thin section (>30µm). (**f**) 13-ROSb001: Different extinction patterns in a bended crystal of beryl under crossed polars. Fragments are partially sutured showing indentation of lobes and cusps boundaries.*

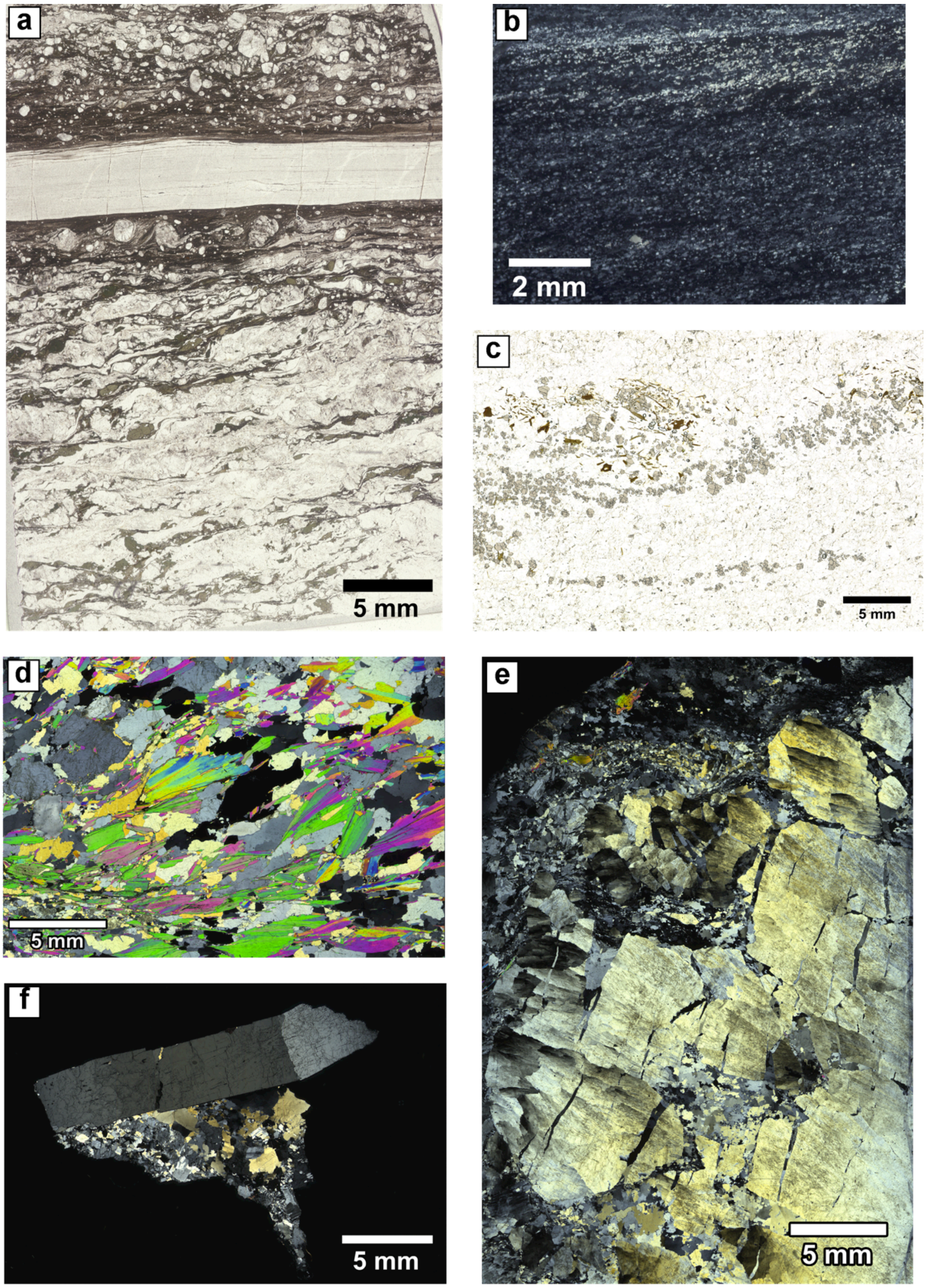
a
5 mm
b
2 mm
c
5 mm
d
5 mm
e
5 mm
f
5 mm

seems to preserve the pristine magmatic texture, with well-defined grain boundaries and no evidence of ductile deformation. Trails of garnet may be generated during syn-intrusion opening of the dextral pull-apart structure. The mechanism of formation however is not yet clear. EMPA analysis might be useful for the study of an eventual compositional zoning developed during growth.

(6) 13-ROSb001: (*fig. 11f*) The pale blue, elongated beryl crystal of *fig. 10e* comes from the ROSb dike of the Rossaccio locality. In the hand specimen the beryl prism is deformed to a faint S-shape with the transparent central part and an "iced" turbid aspect towards the tips. The crystal was cut parallel to the bending plane. Under crossed polars it reveals an internal subtle polygonized extinction pattern, possibly indicating subgrains. The contact between bended fragments of the beryl is sutured (boundaries show indentation of lobes and cusps geometries). The beryl contains widespread healed cracks, decorated by fluid inclusions and forming different sets.

The microstructural observations in the pegmatites and associated mylonites indicate that the dikes were affected by ductile deformation. The mineral assemblage along the mylonites, the type of CPO of recrystallized quartz and the quartz recrystallization mechanisms by subgrain rotation ans GBM are all consistent with deformation temperatures in the order of ≥ 500°C. Similar microstructures are typically developed during postmagmatic cooling of granitoid pluton as described, for example in the Adamello periadriatic pluton (Pennacchioni, 2005).

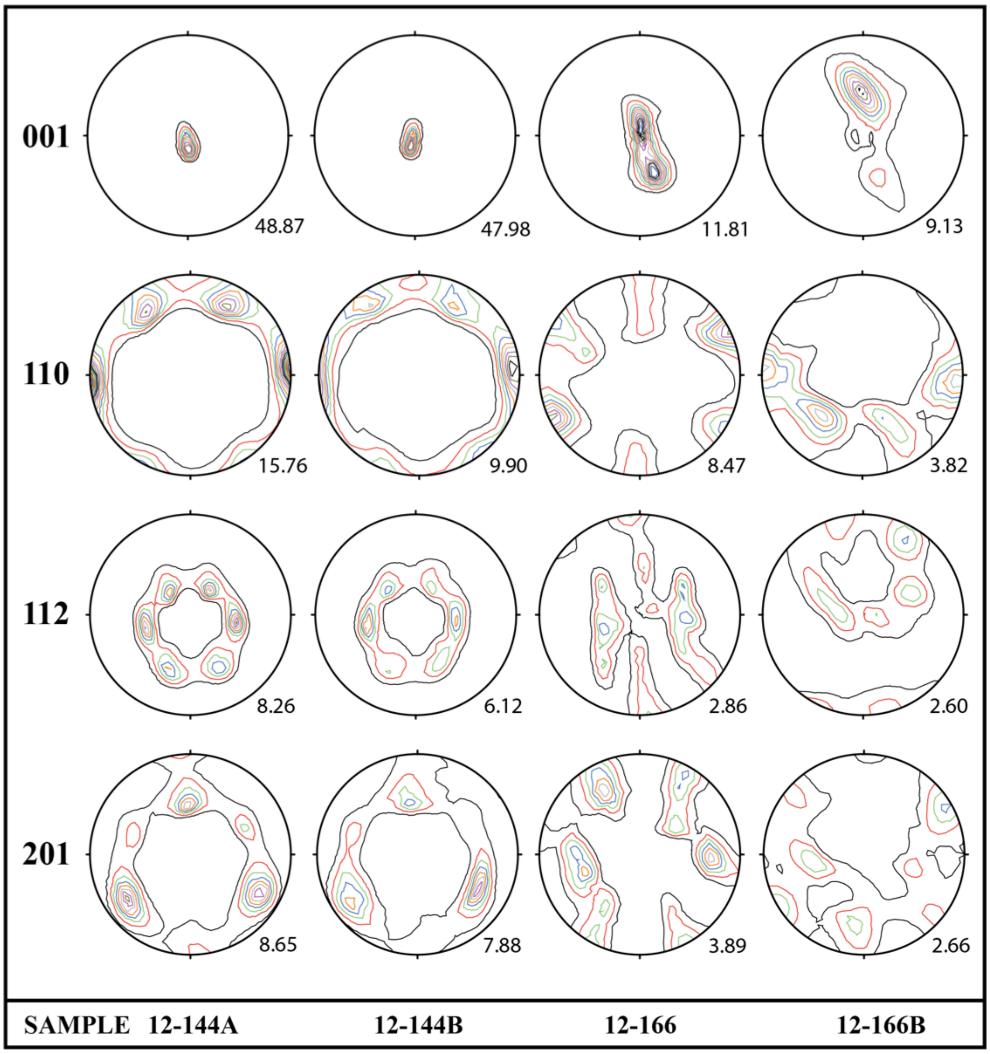

<u>Figure 12</u> *Plots (upper hemisphere, equal area) of (001) (c axis), (110) (<a> axis), (112), and (201) axes of quartz mylonites of the Codera area determined by texture goniometry. The plots are cumulative and the total investigated area in each sample is 2cm. Samples are described by Guastoni et al. (2014).*

6. Mineral samples

6.1. Samples and codes

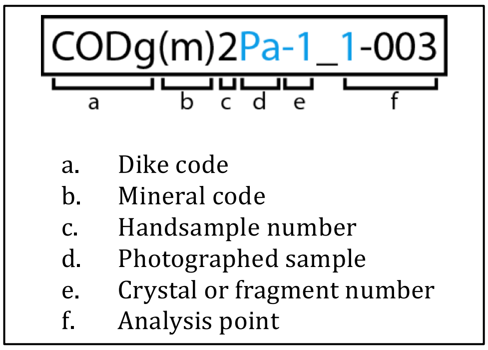

Example of complete code. The first number of "f" field indicate a line of points. This number, "d" and "e" fields are optional.

Minerals sampled for chemical analysis are garnet, tourmaline, monazite and zircon. Main accidental findings include Sn-Nb-Ta-Y-REE-U oxides, xenotime, thorite, REE-bearing epidote and apatite. However significant and systematic analysis made so far, which are presented in this thesis, are limited to garnet, tourmaline and monazite. Anyway zircons were sampled for further future characterizations and here are only described.

In the *tab. 1* are reported the codes of samples for each dike. The identification code is composed by the dike code ("a" field) followed by the mineral code ("b" field with g=garnet, gg=graphic garnet, t=tourmaline, gt=graphic tourmaline, m=monazite, z=zircon, th=thorite) and a number. This number ("c" field) is used to indicate the group of crystals (minimum 1) of the same phase extracted from the same handsample. Single handsamples commonly provided more than one crystal (see monazites and zircons). If there is more than a crystal in a group or the crystal was fragmented for analysis, an additional number ("e" field) is added after a dash to identify the single crystals or fragments. Monazite and zircon codes may contain the "P" letter ("d" field, eventually followed by a letter in case of multiple samples). These "P" samples are representative (selected mainly for the shape) crystals photographed and used for accurate description. The "f" field is used to indicate an analysis point or a profile (e.g. 1-xxx), it is separated from the sample code by an underscore.

6.2. Samples description

For each dike here are reported the descriptions of sampled crystals. Note that the accurate identification of the phase for garnets and tourmaline is omitted since it will be discussed in the following chapter. Dimensions of single crystals are attached to the photographic tables.

	DIKE CODE	SAMPLES			
		Garnet (g)	Tourmaline (t)	Monazite (m)	Zircon (z)
CODERA AREA	CODp	CODp(g)1, CODp(gg)1, CODp(gg)2	CODp(t)1, CODp(gt)1	-	CODg(z)1, CODg(z)2
	CODg	CODg(gg)1, CODg(g)2	-	CODg(m)1, CODg(m)2, CODg(m)3	-
	CODm	-	-	CODm(m)1	-
	CODs	-	-	-	CODs(z)1
	CODt	-	-	CODt(m)1	CODt(z)1, CODt(z)2, CODt(z)3, CODt(z)4
	ROSg	ROSg(g)1, ROSg(g)2	-	-	-
	ROSb	-	ROSb(t)1	-	ROSb(z)1, ROSb(z)2, ROSb(z)3, ROSb(z)4, ROSb(z)5, ROSb(z)6
BODENGO AREA	VGa	VGa(g)1	-	-	-
	VGb	VGb(g)1	-	-	-
	VDD	VDD(g)1, VDD(g)2, VDD(g)3	VDD(t)1	-	-
	VLGa	VLGa(g)1	VLGa(t)1	-	-
	VLGm	VLGm(g)1	-	VLGm(m)1, VLGm(m)2	-
	VLGb	-	VLGb(t)1	-	-
	VCA	-	-	VCA(m)1	VCA(z)1

Table 1 *Handsample codes*

6.2.1. Garnets

Garnets of pegmatite dikes of the Central Alps are already described by Guastoni (2012) as solid solutions of almandine-spessartine. Samples collected display the same described morphology with dominant {211} trapezohedron (*fig. 14e, g and h*). Crystals with dominant romb-dodecahedron {110} faces (*fig. 14f and i*) are far subordinate. Crystals with different habit can be found in the same dike as well as graphical intergrowth of garnet and quartz (*fig. 14a*). Garnets are commonly broken by brittle deformation and Codera area ones seem to develop a preferential set of sub-parallel cracks (*fig.13 a and b*). Following descriptions refer to *fig. 14*.

(CODp, CODg) Sampled garnets from both dikes of Codera area are anhedral to subhedral, also with graphic texture, embedded in white perthitic and graphic K-feldspar along with muscovite flakes. Although nice trapezohedral, centimetric dark red garnets in CODg dike are not rare. Euhedral ones are up to 2-3 cm large while graphic aggregates reach several centimetres in width. Generally garnets are dark red coloured and non-graphic ones are opaque. An exception are the CODp(g)2 crystals, which have a light red to orange colour and are translucent. Commonly garnet crystals are found with a hybrid habit, composed by a single anhedral large crystal surrounded by graphic intergrowth with quartz. All garnet crystals from COD dikes are pervasively fractured with a distinguishable dominant set of subparallel fractures (*fig. 13a and b*).

(ROSg) Similarly to CODg, the Rossaccio garnet dike provided nice euhedral garnet crystals of up to 2-3 cm. They have trapezohedral habit and a dark red colour, poorly translucent. It is pervasively fractured and displays a dominant set of parallel fractures. Fine-grained white mica grows within the gaps. Crystals are embedded within perthitic white K-feldspar.

(ROSb) Garnets of this dike are less developed and do not reach 1 cm in width. Sampled ones exhibit euhedral romb-dodecahedron habit and are dark red coloured. Crystals are embedded in white perthitic K-feldspar.

(VGa, VGb) Both dikes of Garzelli valley provided nice centimetric euhedral granets, which have trapezohedral habit, bright to dark red colour and are translucent. Best crystals for shape, which reach 1-2 cm in width, are found embedded within large muscovite flakes and quartz.

(VDD) This dike provided two types of garnet that come respectively from the giant-textured core (VDD(g)1 and 2) and from the miarolitic pockets (VDD(g)3). Crystals of the first type grow with large flakes of muscovite and quartz. They exhibit euhedral trapezohedral habit and a bright red to dark red translucent colour. VDD(g)1 hosts a zircon crystal visible in thin section (*fig. 13c)*. Volume expansion of zircon caused radial cracks in the garnet (*fig. 13d)*. The second type of garnet grows on the free surface of K-feldspar crystals. They are bright red and gemmy, with a good trapezohedral habit.

(VLGa) These garnets are found growing with muscovite on large prisms of black schorl. The habit is euhedral trapezohedral and partially rounded. The colour is dark opaque red.

(VLGm) The crystal sampled in this dike differs substantially from the other ones described so far. It has a dark red colour, almost black, and shows locally pristine faces interrupted by irregular areas. Since it is possible to recognize discrete faces in those parts, it reasonable to impute the garnet shape to competitive growth against other crystals, maybe complicated by a latter stage of corrosion (rough and rounded surfaces).

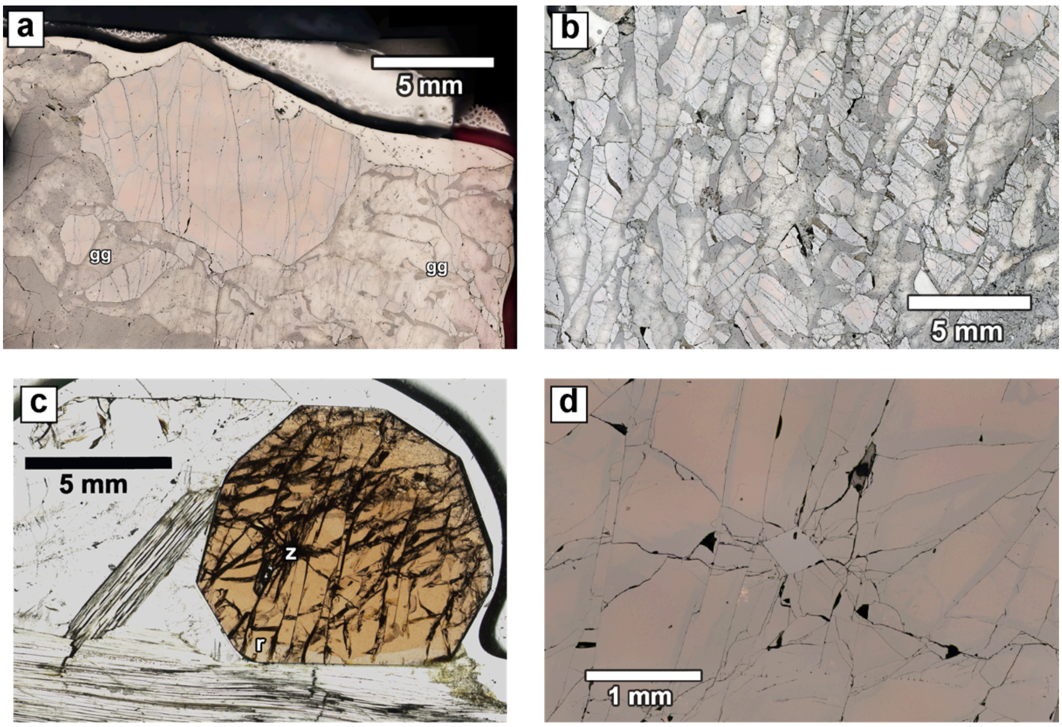

Figure 13 *Garnet sections. (**a**) CODp(g)1: Non-graphic garnet surrounded by a graphic aggregate (gg). The crystal shows a set of vertical fractures. (**b**) CODg(gg)1: Graphic garnet with a pervasive set of subparallel fractures trending NW-SE in the photo. (**c**) VDD(g)1: Zoned garnet with lighter thin rim (r) and included zircon. (d) Zircon crystal included in VDD(g)1 that caused radial cracks in the host due to volume expansion.*

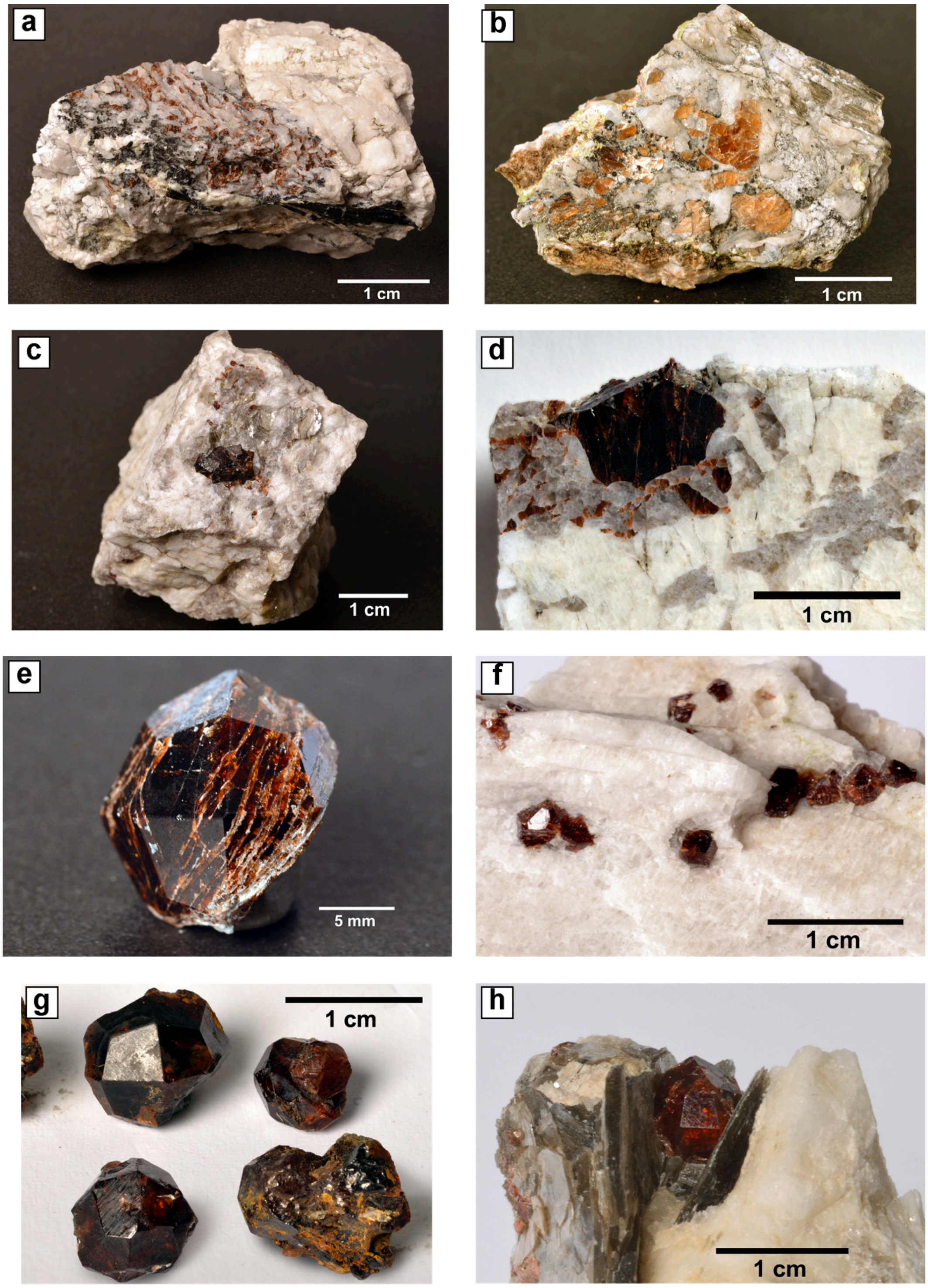
a
1 cm
b
1 cm
c
1 cm
d
1 cm
e
5 mm
f
1 cm
g
1 cm
h
1 cm

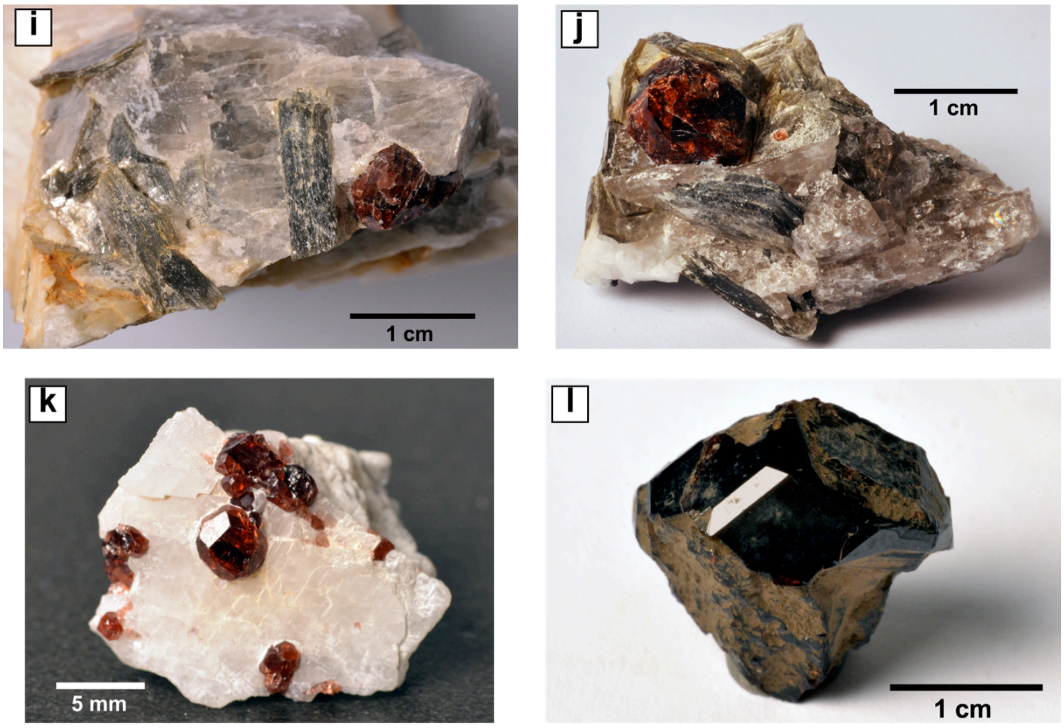

Figure 14 *Analysed garnets. (**a**) CODg(gg)1. (**b**) CODp(g)2. (**c**) CODg(**g**)2. (**d**) CODp(**g**)1. (**e**) ROSg(g)1. (**f**) ROSb(g)1. (**g**) VGa(g)1. (**h**) VGb(g)1. (**i**) VDD(g)1. (**j**) VDD(g)2. (**k**) VDD(g)3. (**l**) VLGm(g)1.*

Despite this it is possible to determine the habit by the visible faces that are the rombododecahedron, which is dominant, and the trapezohedron. Note that almost all Bodengo area garnets show a dominant trapezohedral habit.

6.2.2. Tourmalines

All tourmalines are black schorl with very rare exceptions. They occur as elongated prisms with common parallel growth. Tourmalines of deformed dikes show pervasive microboudinage perpendicular to the c-axis and some are bended. Greenish Mn-rich fluorelbaite with schorl core is described by Guastoni (2012) in the CODp dike (*fig. 9 h*).

(CODp) Graphic tourmalines are typical evolved parts of Codera pegmatites and commonly occur with beryl. The black schorl tourmaline sampled in the CODp dike is a composite one, made of an inner prismatic crystal surrounded by a graphic intergrowth with mainly quartz. The aggregate is 4 cm in width.

(ROSb) 5 cm long, black prismatic schorl tourmaline found in an aggregate of deformed quartz. As for the other tourmalines from the Codera area, the crystal was extracted broken, without termination, and showed an evident microboudinage with cracks perpendicular to the c-axis. These planes act as a pseudo-cleavage since microboudinaged crystals are easily broken into small slices. Some fragments are dislocated and separated by the same recrystallized quartz matrix.

(VDD) 3 cm, black prismatic schorl crystal grown with K-feldspar, muscovite and quartz.

(VLGa) Black prismatic schorl crystal of 2 cm in width and 6 cm in length associated to red garnet crystals, which grew on the prismatic faces, muscovite, K-feldspar and quartz.

(VLGb) Small prismatic, terminated crystals of dark olive green tourmaline up to 6 mm in width. These crystals were found within a miarolitic pocket, growing with large quartz crystals, albite var. clevelandite and K-feldspar perthitic crystals.

6.2.3. Monazites

Monazite crystals were sampled in three different dikes of Codera area (CODg, CODt and CODm) and two different dikes of Bodengo area (VLGm and VCA). Morphology of sampled crystals reflects that described by Catlos (2013) for Th-rich monazites: most crystals are flattened on {100} and show small or absent {101} faces. Most crystals are stubby while elongation occur commonly on the c-direction, with the exception of CODm(m) samples that is probably strongly elongated on the b-direction (*fig. 15j*). The non-conventional habit of CODg(m)3 might be an example of competitive growth in pegmatites that imposed the form of adjacent growing crystals (*fig 16d and 16b*). Following descriptions mainly refer to samples in fig. 15 and 16.

Dike	H. Sample	Tot.	P Crystals
CODg	CODg(m)1	12	CODg(m)1P
	CODg(m)2	11	CODg(m)2Pa, CODg(m)2Pb
	CODg(m)3	1	CODg(m)3P
CODt	CODt(m)1	3	CODt(m)1P
CODm	CODm(m)1	8	CODm(m)1P
VLGm	VLGm(m)1	21	VLGm(m)1P
	VLGm(m)2	15	VLGm(m)2P
VCA	VCA(m)1	11	VCA(m)1Pa, VCA(m)1Pb

Table 2 *Analysed monazites.*

Tot. indicates the number of extracted crystals and fragments. P crystals are the codes of samples that were photographed and described.

(CODg) Yellow prismatic crystals found in paragenesis with K-feldspar, quartz and Nb-Ta-REE oxides. Most of them are translucent but appear turbid under the stereoscope. Crystals are elongated on the c-direction with a euhedral to subhedral shape. Prismatic and pinacoidal faces are well developed and some crystals are twinned. Some of these crystals are the largest found among sampled monazites, exceeding 5 mm in length (CODg(m)3P, *fig. 15d and 16d*). Each crystal shows a well-developed parting on {001}. CODg(m)1 hosted at its nucleus small green prismatic crystals of thorite (*fig. 15a)*, surrounded by black lamellar Nb-Ta-U elements-oxide. This crystal contains numerous small inclusions of monazite (<10µm, *fig. 18i*).

(CODm) These crystals are the clearest monazites among all samples. Crystals are gemmy, euhedral and strongly elongated, showing well developed sharp faces. They reach several millimetres in length and less than 1 mm in width. Parting on {001} is not macroscopically visible, though BSE imaging shows sector zoning parallel to elongation that suggests b-direction elongation. These monazite crystals are hosted in massive white cloudy quartz, in association with black euhedral crystals of euxenite.

(CODt) Single crystal of green monazite. This specimen was found at the core of a deformed (microboudinaged) and recrystallized yellow beryl embedded in quartz. On the same sample two crystals of pale brown zircon and one crystal of

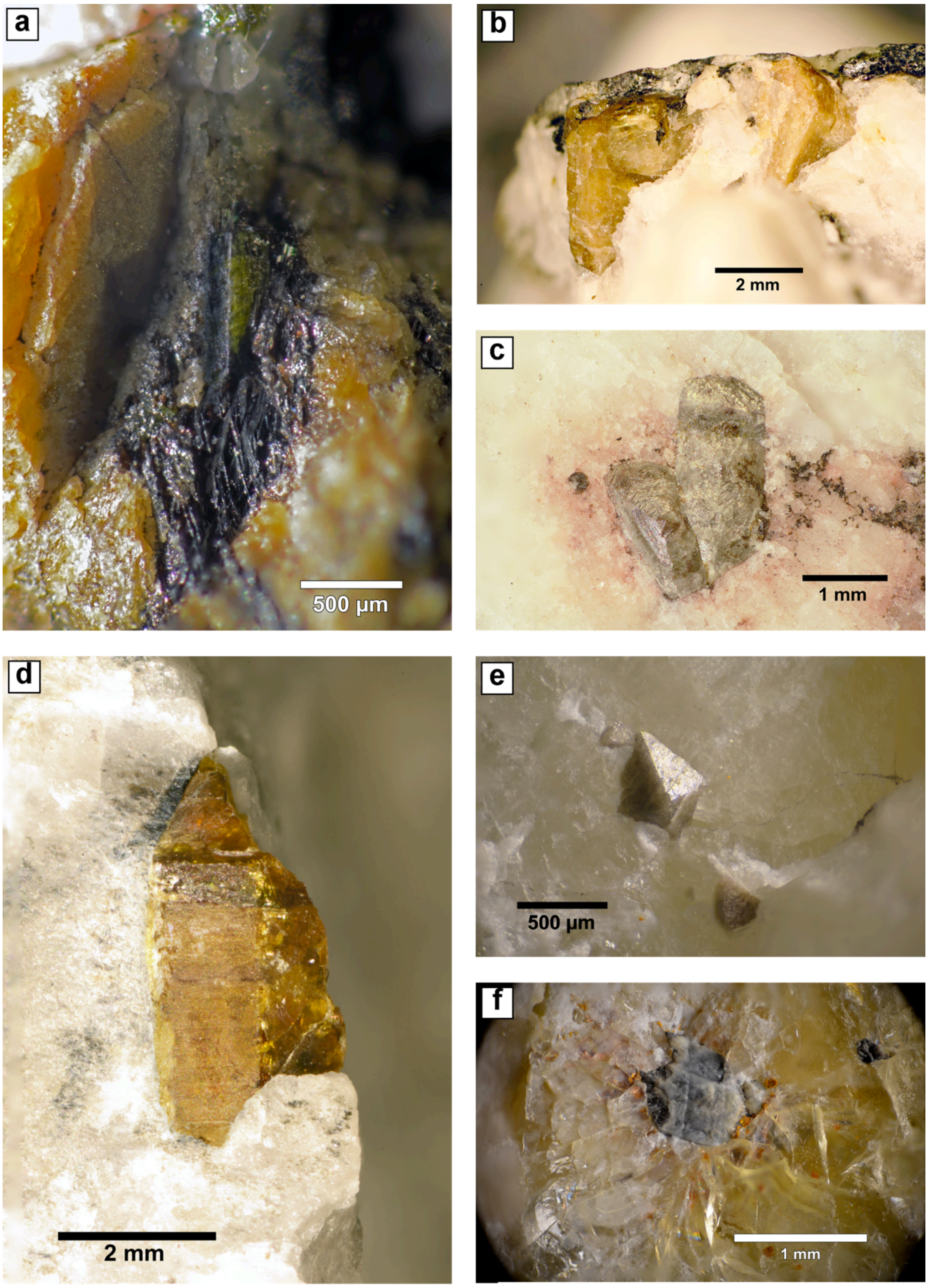
a
500 µm
b
2 mm
c
1 mm
d
2 mm
e
500 µm
f
1 mm

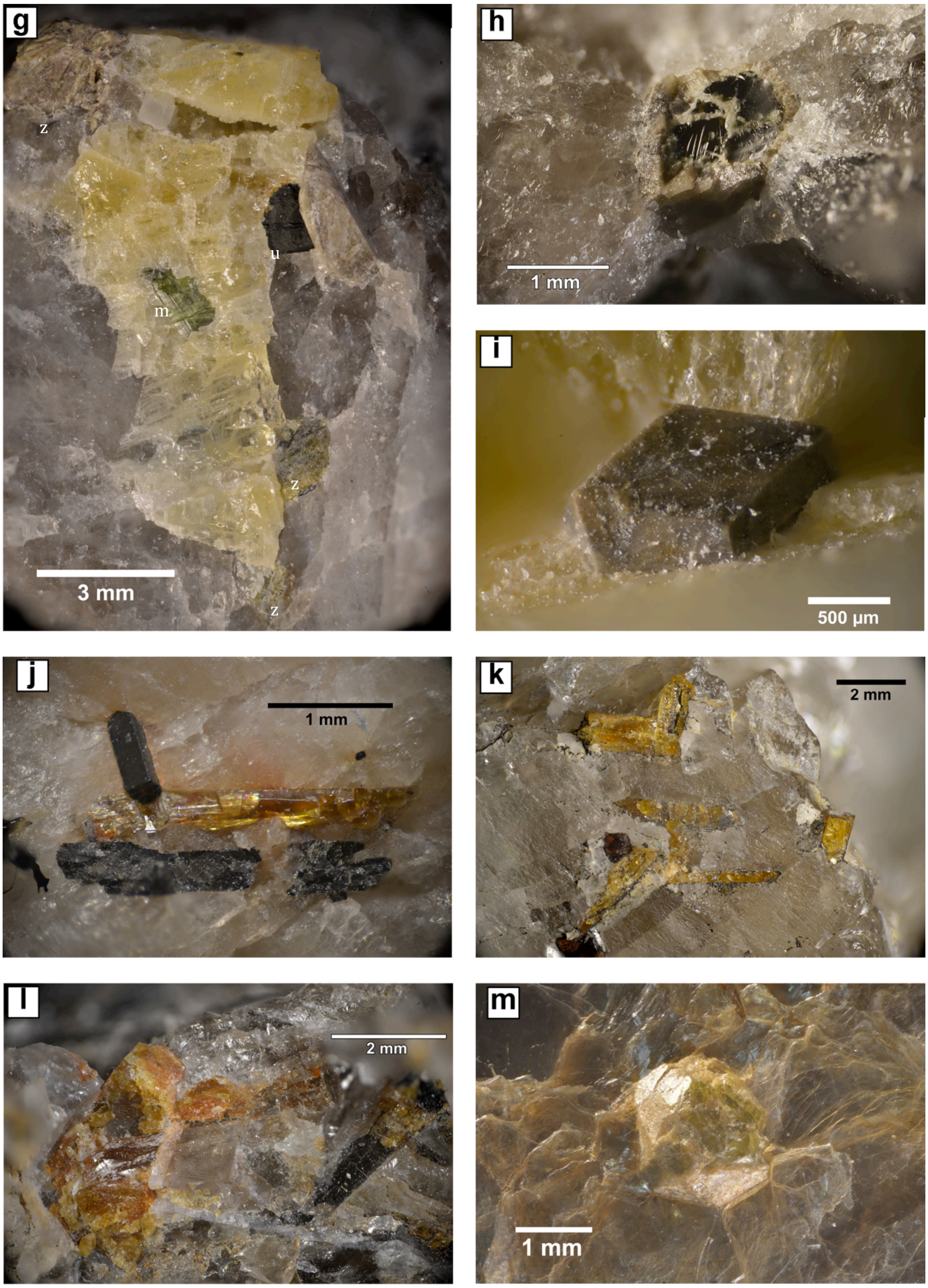
g
z
u
m
z
3 mm
z
h
1 mm
i
500 µm
j
1 mm
k
2 mm
l
2 mm
m
1 mm

<u>Figure 15</u> *(Pages 48 and 49) Monazite and zircon hand samples. (**a**) CODg(m)1: Close up of the monazite crystal (yellow) hosting black lamellar Nb-Ta-REE oxides and a prismatic bottle-green crystal of thorite. (**b**) CODg(m)2: Yellow geminated crystals of monazite with black Nb-Ta-REE oxides hosted in K-feldspar. (**c**) CODg(z)1: Crystals of zircon hosted in K-feldspar displaying a pink aureole. The particular habit may be interpreted as a consequence of competitive growth. (**d**) CODg(m)3: The largest monazite crystal among sampled ones. It is hosted in a greyish quartz mass. (**e**) CODt(z)1: Bipiramidal crystal of zircon growing on yellow beryl. (**f**) CODt(z)2: Zircon hoste in yellow beryl, which displays radial cracking. (**g**) CODt(m)1: Green U-rich monazite (m) hosted in recrystallized yellow beryl with three light brown zircons (z) and a black crystal of uraninite (u). (**h**) CODt(z)4: Zircon with light brown rim and black vitrified core hosted in quartz. (**i**) CODs(z)1: Light brown zircon with particular shape included in a yellow beryl.. (**j**) CODm(m)1: Gemmy euhedral crystal of monazite strongly elongated on the b-direction, growing with Nb-Ta-REE oxides o quartz. (**k**) VLGm(m)1: Clear miarolitic monazites growing on quartz. (**l**) VLGm(m)2: Yellow-orange monazite and Nb-Ta-REE oxides growing on quartz from a miarolitic pocket. (**m**) VCA(m)1: Rounded crystal of greenish and pink monazite growing on muscovite.*

black uraninite are growing in contact with the beryl. Beryl colour is commonly turned to yellow by the local presence of metamictic minerals, which sometimes are hosted or grow in contact with the former. In this case the whole crystal achieved a uniform bright yellow colour. The green monazite crystal was pre-fractured and post-extraction was impossible to determine the habit. Anyway the crystal appear euhedral and with no appreciable elongation. C. M. Gramaccioli (1986) reports the finding of green U-rich monazites in the Piona pegmatites of the Como Lake.

(VLGm) Clear, yellow, millimetric crystals of monazite hosted in smoky quartz. This samples come from the central large pocket of the VLGm dyke. VLGm(m)1 crystals are scattered on a clear surface of a fragment of quartz, probably a face, with small red crystals of garnet (*fig. 15k)*. VLGm(m)2 appear as a group of broken orange-yellow crystals in association with flat wodginite crystals, hosted in massive quartz (*fig. 15l*).

(VCA) This specimen was a large flake of silvery muscovite hosting several crystals of greenish monazites and a group of twinned zircons. The latter have rounded anhedral shape with a greenish core and a partial brown to pinkish coating with cribrous aspect. These crystals are composed by a green monazite core and a rim of riprecipitated poikilitic monazite, which contains small uraninites (*fig. 18e*), or xenotime (containing also zircon crystals, *fig. 18f*) on VCA(m)1Pa and VCA(m)1Pb, respectively.

6.2.4. Zircons

All zircons sampled display the same morphology of those described by Corfu et al. (2003) from pegmatite rocks and compared on the "Pupin diagram". Dominant faces are the {110} prism and the {101} tetragonal bipiramid. Some samples developed flattening and curious pseudo-symmetries probably due to competitive growth in pegmatite.

(CODg) Zircons found are CODg(z)1 and CODg(z)2. The latter is a subhedral partially altered crystal, little elongated on c-direction. The color varies from light brown to greenish where it is compenetrated by black lamellae of Nb-Ta-U oxides. CODg(z)1 is composed by two flat, light brown coloured, crystals elongated on the c-direction. The hypothetical prism face displays a peculiar, flat pyramidal shape, with concentric stripes (we remand to the CODs(z) for an hypothesis). Crystals produced pink halo in the hosting feldspar.

(CODs) These two crystals are the largest and most intriguing samples among zircons. Both were found within a parallel growth of light blue beryl. The small one CODs(z)1Pb is flat with a hexagonal shape. It displays a curious pseudo-hexagonal (six faces) symmetry on one side (*fig. 16n*) and a pseudo-ternary (three faces) symmetry on the other side (*fig. 16o*). The large one CODs(z)1Pa, which is 5,2 mm in length, has a deformed euhedral prismatic habit with one nice termination (four bipyramid faces) and the other pinching out as a wedge. It also displays the pseudo-exagonal symmetry, but less evident, on both two of opposite hypothetical faces of the prism, which are inclined at a small angle. The other two hypothetical prisms have a little pronounced wedge shape. Each irregular face has a sort of resonant striped texture, which is concentric on the pseudo-hexagonal side. Since all these crystals were found growing at the interface between the beryl prisms, an explanation for the strange habit may come from the competitive growth between the beryl crystal and the zircon crystal. Commonly in pegmatites crystals grow against each other competing for space (London 2008), an example is the graphic intergrowth of quartz and K-feldspar. London (2008) reported the image of a columbite-tantalite that competed successfully against another crystal. Accessories that compete for space are forced to assume a particular shape depending on the surrounding crystals (see also the description of monazite CODg(m)3). If we assume that zircon nucleated on the prism of one beryl crystal, the successive steps of growth may have forced the crystal to assume a complex habit related to the geometry of beryl. A hint comes from the evidence of steps on such surfaces, which represent discrete phases of growth (grow-steps are evident in quartz, feldspars, beryl and in some cases other minerals in pegmatites; London 2008). The free surface pointing out of the beryl was allowed to develop the real habit of zircon (see the termination with bipyramid faces on CODs(z)1Pa). In the case of CODs(z)1Pb, the free surface might be the pseudo-trigonal one. Assuming that the crystal nucleated with the c-axis emerging at a small angle to the beryl c-axis and one prism of the zircon facing the beryl, the pseudo-trigonal arrangement may be the area of the confluence of two bipyramids and a prism (for example (101), (010) and (110)). The crystallographical angles on the faces of bipyramid-prism-bipyramid and prism-bipiramid-bipiramid are respectively 95,63° and 116,80°. Accurate measuring on the existing sample is yet to be done but this hypothesis seems reasonable. CODs(z)1Pa crystal has two opposite surfaces displaying pseudo-hexagonal symmetry and has one regular termination with the {101} bipyramids (*fig. 16p*). This may be explained with the growth against two flanked beryl crystals. Further analysis are needed to confirm this hypothesis.

CODs(z)1Pa after cutting revealed a dominant black core surrounded by a thin light brown rim (*fig. 16w*), which gives the exterior aspect of the crystal. The rim shows radial cracks suggesting a major content in radioactive elements of the internal one that caused differential volume expansion (Corfu *et al.*, 2003). The black core seems vitrified and shows (1) an internal oblique band (which follows probably a crack) of a feather-shaped recrystallized phase, similar to the rim one, and (2) needle-like light-coloured longitudinal bands. It is likely that CODs(z)1Pb posses the same core-rim structure.

(CODt) Four different samples come from the Trubinasca Codera dike: CODt(z)1, 2, 3 and 4. CODt(z)1 includes many little, light brown crystals (up to 640 μm) growing on a yellow altered beryl crystal. They developed a bipyramidal habit with no prism faces. CODt(z)2 is an altered subhedral crystal with colours ranging from bluish to greenish and brown, grown within a beryl crystal. The habit is complex and it is probably twinned. It is associated to a dark crystal of probably a Nb-Ta-REE oxide. The beryl crystal colour is altered to yellow and show radial cracks surrounding the zircon (*fig. 15f*). CODt(z)3 crystals are euhedral light brown colored. They grew at the contact of a yellow beril (see CODt monazite description) with uraninite and monazite. CODt(z)4 zircons are light brown, perfectly euhedral, prismatic and with c-elongation. They grew both in contact with yellow beryl and quartz. The CODt(z)Pb broken crystal displays a black dominant core with conchoidal fracture (*fig. 16t*).

(ROSb) Several samples were collected from this dike within the intermediate and core zones of the dike. ROSb(z)1 zircons found on muscovite are light brown coloured and developed faces only on the side not in contact with muscovite ROSb(z)2 is a single subhedral, light brown elongated crystal. It grew on a muscovite flake within K-feldspar, which developed a pink halo surrounding the zircon. ROSb(z)3 is an aggregate of several twinned crystals surrounding a black uraninite core. Differently from all other specimens these are translucent and dark orange coloured (*fig. 16u*). Although they seem perfectly euhedral is not easy to recognize a definite habit due to the intergrowth of several individuals. ROSb(z)4 is an euhedral, light brown crystal grown within quartz and K-feldspar. It is flattened perpendicularly to two of the prisms. ROSb(z)5 was lost during extraction.

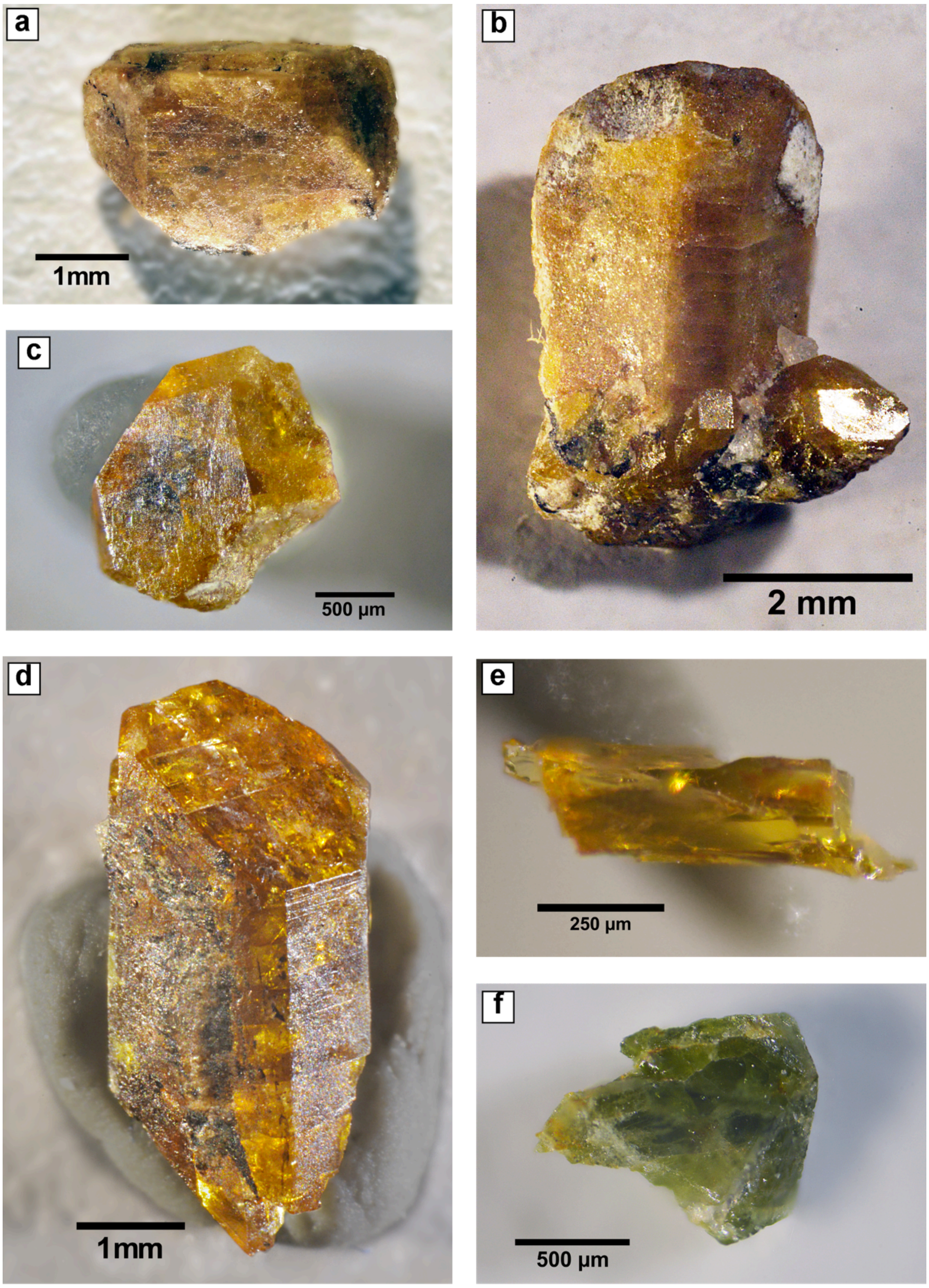
a
1mm
b
2 mm
c
500 µm
d
1mm
e
250 µm
f
500 µm

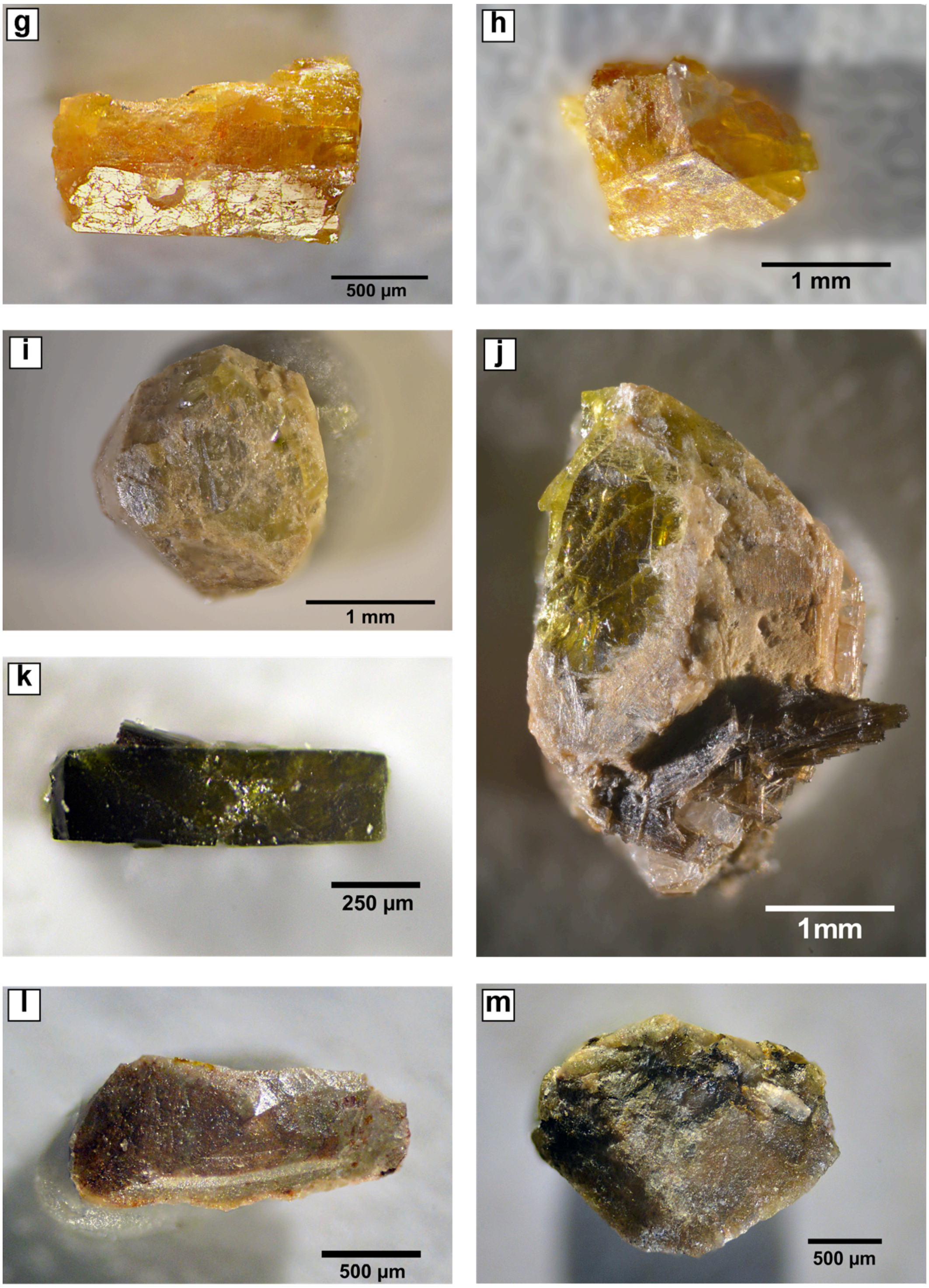
g
500 µm
h
1 mm
i
1 mm
j
1mm
k
250 µm
l
500 µm
m
500 µm

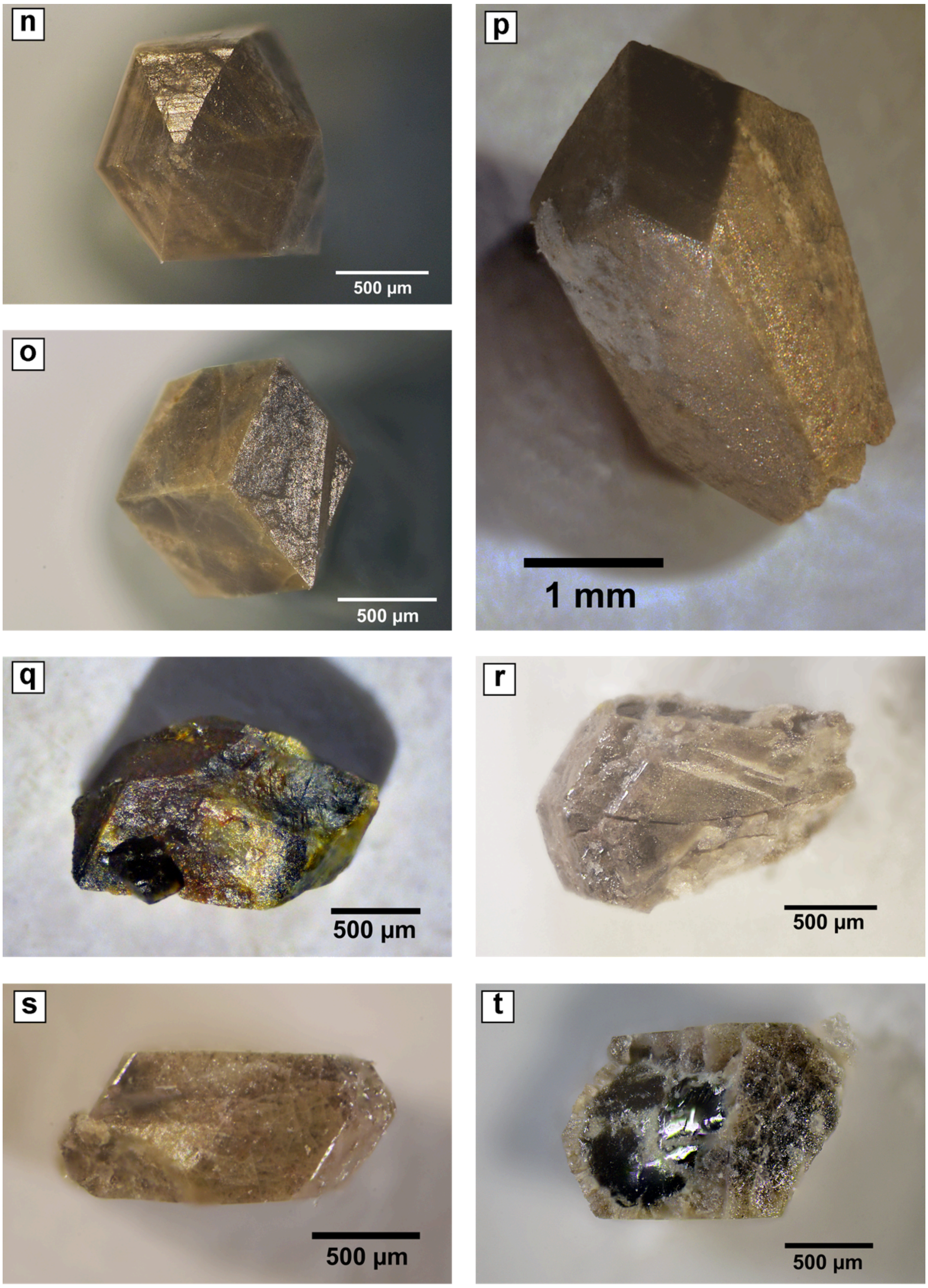
n
500 µm
o
500 µm
p
1 mm
q
500 µm
r
500 µm
s
500 µm
t
500 µm

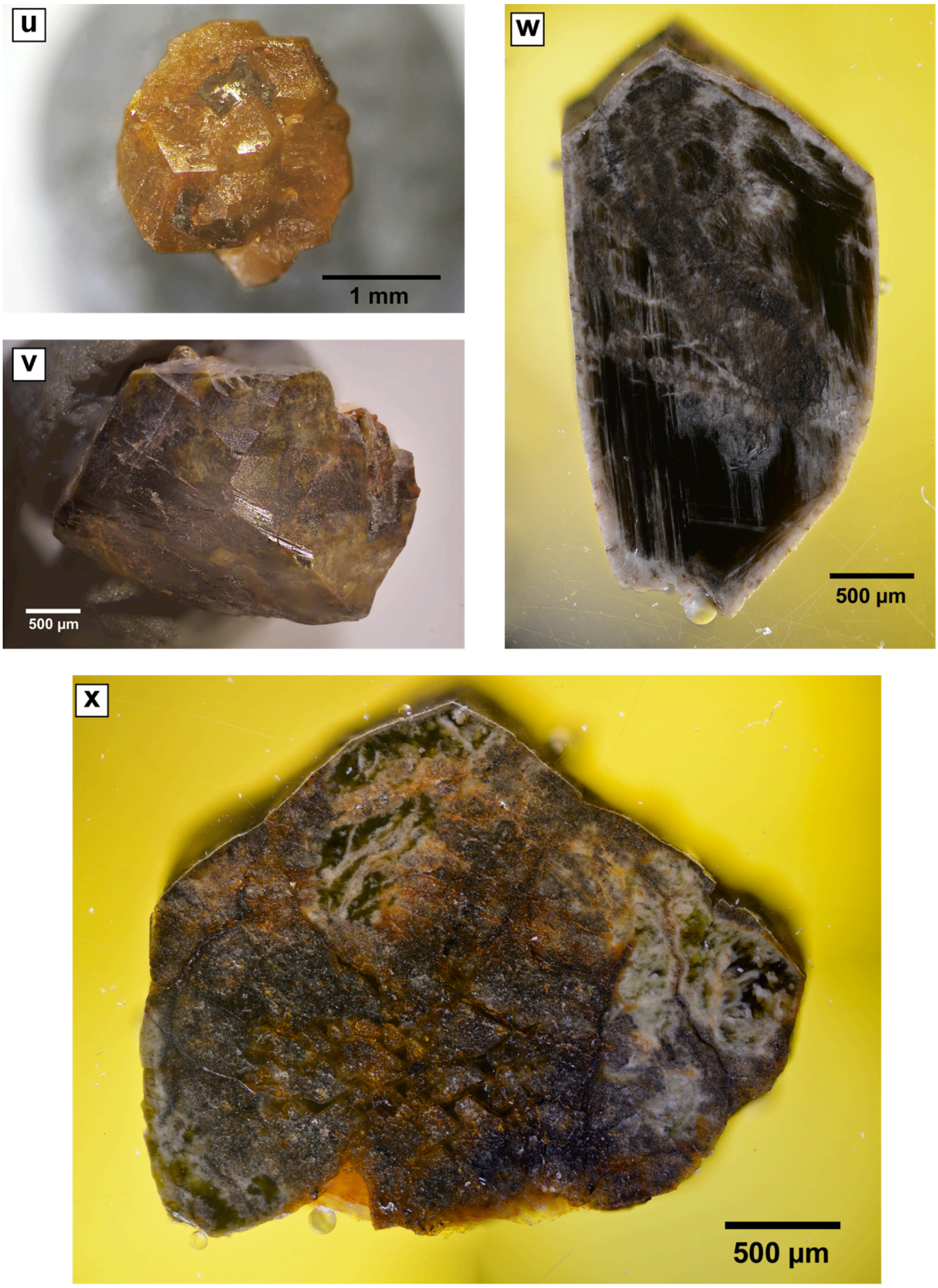
u
1 mm
v
500 µm
w
500 µm
x
500 µm

<u>Figure 16</u> *(Pages 54-57) Monazite, thorite and zircon crystals.*

Monazite crystals description:

***(a)** CODg(m)1P: Stubby prismatic sub-euhedral crystal of honey yellow monazite. Figure was taken with the crystal c-axis oriented N-S and the binary axis of monocline symmetry E-W. Parting on {001} is visible on the E-W direction. **(b)** CODg(m)2Pa: Prismatic euhedral crystal of monazite. It displays c-direction elongation and flattening on {100}. Other smaller crystals grow at the contact with the matrix. Visible the parting {001}, the prism {110} and the pinacoid {100}. The termination faces are not well preserved but is is possible to recognise the small (10-1) pinacoidal face. See fig. 17a. **(c)** CODg(m)2Pb: Stubby prismatic, euhedral crystal of monazite. Traces of parting and cleavage are clearly visible on the fractured surfaces. **(d)** CODg(m)3P: Euhedral prismatic crystal of clear yellow monazite. The habit is curious since it developed large faces apparently corresponding to the {100}, {010} and {001} pinacoids (see model). This may be imputed to competitive growth against other crystals, which impose the shape. Parting {001} parallel to the termination face and the cleavage {100} are clearly visible. See fig. 17b. **(e)** CODm(m)1P: Fragment of monazite showing conchoidal fracture. The colour is clear yellow with local orange inclusions. **(f)** CODt(m)1P: Largest fragment of the green U-rich monazite crystal of CODt dike. Parting and faces are not easily distinguishable so the habit couldn't be described. **(g)** VLGm(m)1P: Elongated (c-direction) crystal of clear yellow monazite. Parting {100} is visible on the prism face along the N-S direction of the picture. **(h)** VLGm(m)2P: Fragment of euhedral prismatic crystal of clear yellow monazite. The parting is clear and faces of the crystal resembles those of CODg(m)3P. **(i)** VCA(m)1Pa: Rounded subhedral crystal of greenish and pinkish monazite. A tentative to recognise some faces is made with the drawing (fig. 17c). This seem to find some resemblance with the model Monazite no.1 by Goldschmid (1913-1926) of fig. 17d (source: www.mindat.org). **(j)** VCA(m)1Pb: Large anhedral complex crystal of greenish monazite and pinkish xenotime growing with REE-bearing epidote and prismatic apatite.*

Thorite and Zircon crystals (single zircon crystals are already described in the text):

***(k)** CODg(th)1P: Fragment of prismatic euhedral crystal of dark green thorite. It is twinned with another smaller crystal on a prism face. **(l)** CODg(z)1P. **(m)** CODg(z)2P. **(n** and **o)** CODs(z)2Pb both sides. **(p)** CODs(z)1Pa. **(q)** CODt(z)2. **(r)** CODt(z)3P. **(s)** CODt(z)4Pa. **(t)** CODt(z)4Pb. **(u)** ROSb(z)3P. **(v)** ROSb(z)6P.*

Polished sections of zircons:

***(w)** Polished section of CODs(z)1Pa. **(x)** Polished section of ROSb(z)6P.*

ROSb(z)6 is an aggregate of small zircons and a large one (420 μm) growing on feldspar. These crystals are dark coloured displaying an altered surface, the habit is prismatic euhedral but complicated by the coalescence. The internal structure of the largest one (ROSb(z)6P) is complex, composed by a thin outer rim and a large complex core (*fig. 16x*). It resembles that of CODs(z)1Pa and is composed by a glassy internal mass, which in this case is dark green, fractured and pervasively replaced by vermicular riprecipited rusty to light-coloured zircon. Another feature of the core is the presence of a (scheletal?) swarm of small isooriented bipyramidal crystals. It was proofed that all these phases are zircon with some rapid EMP analysis not reported in this thesis.

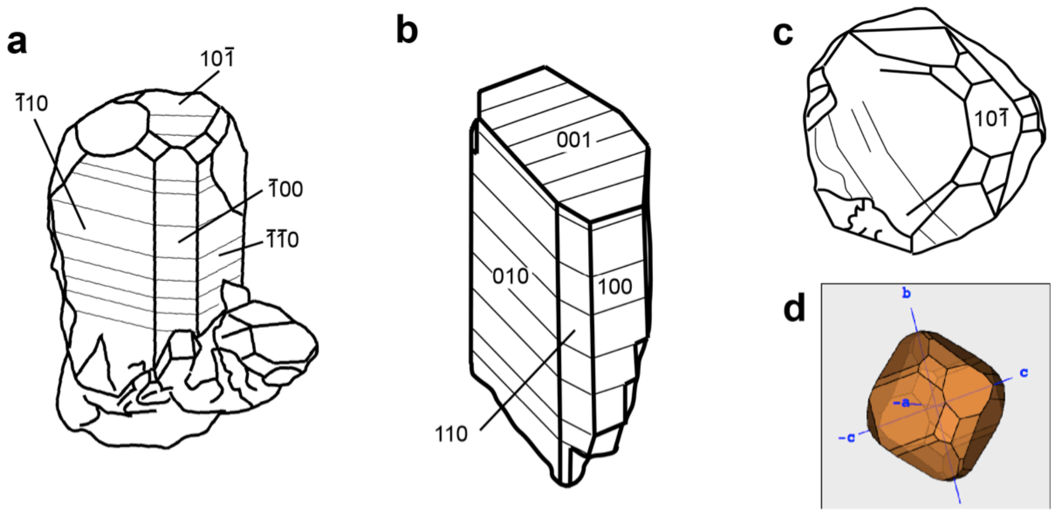

Figure 17 *Graphic study on monazite crystals:*
Recognizable faces are confronted with Goldschmidt models (1913-1926) and indicized. (a) Drawing of sample CODg(m)2Pa. (b) Drawing of sample CODg(m)3P. (c) Drawing of sample VCA(m)1Pa and (d) model no.1 by Goldschmid (1913-1926) confronted (source: www.mindat.org).

(VCA) As described for the monazite samples, this pale brown zircon was found within a large flake of muscovite. It is a spray-like aggregate of twinned individuals, which have euhedral prismatic habit. The whole aggregate measures 1,4 mm in length.

6.2.5. Thorite

Dark green thorite crystals (*fig. 15a and 16k*) were found at the core of one monazite crystal of the CODg(m)1 sample, embedded in lamellar Nb-Ta-REE oxides. The crystals have elongated prismatic habit with flat pinacoidal termination and some are twinned. The largest one reaches 1,5 mm in length.

7. Chemical Analyses

7.1. SEM BSE imaging

Backscattered electrons (BSE) images of polished monazite, xenotime and thorite were taken in order to have a qualitative control on internal chemical variation. These images were useful to plan the successive EMPA and LA-ICP-MS analyses. Since dating was planned for monazite samples it was of primary importance to discriminate different chemical internal domains: growth and sector zoning, riprecipited or different phases like inclusions and alteration. Rapid qualitative analyses on chemistry allowed a first qualitative identification of the included phases. Images were acquired with the scanning electron microscope (SEM) at the SEM laboratory of Dipartimento di Geoscienze of Padova. Analytic conditions and further information are reported in the appendix I.A.

Most of sampled monazites are chemically quite homogeneous and only highly contrasted BSE images help to recognize the faint primary zoning. Among zoned fragments of sampled monazites two types of zoning are recognisable: primary zoning and secondary zoning. Primary sector zoning is imputed to: (1) selective adsorption on the crystal surface, or (2) different attachment kinetics on different facets (Catlos, 2013, and references therein). It can be distinguished from secondary zoning by the regular geometries of the chemical variations, which follow precise crystallographic directions. The spectacular concentric zoning on CODg(m)3 (*fig. 18b*) clearly highlights the growth steps of the crystal.

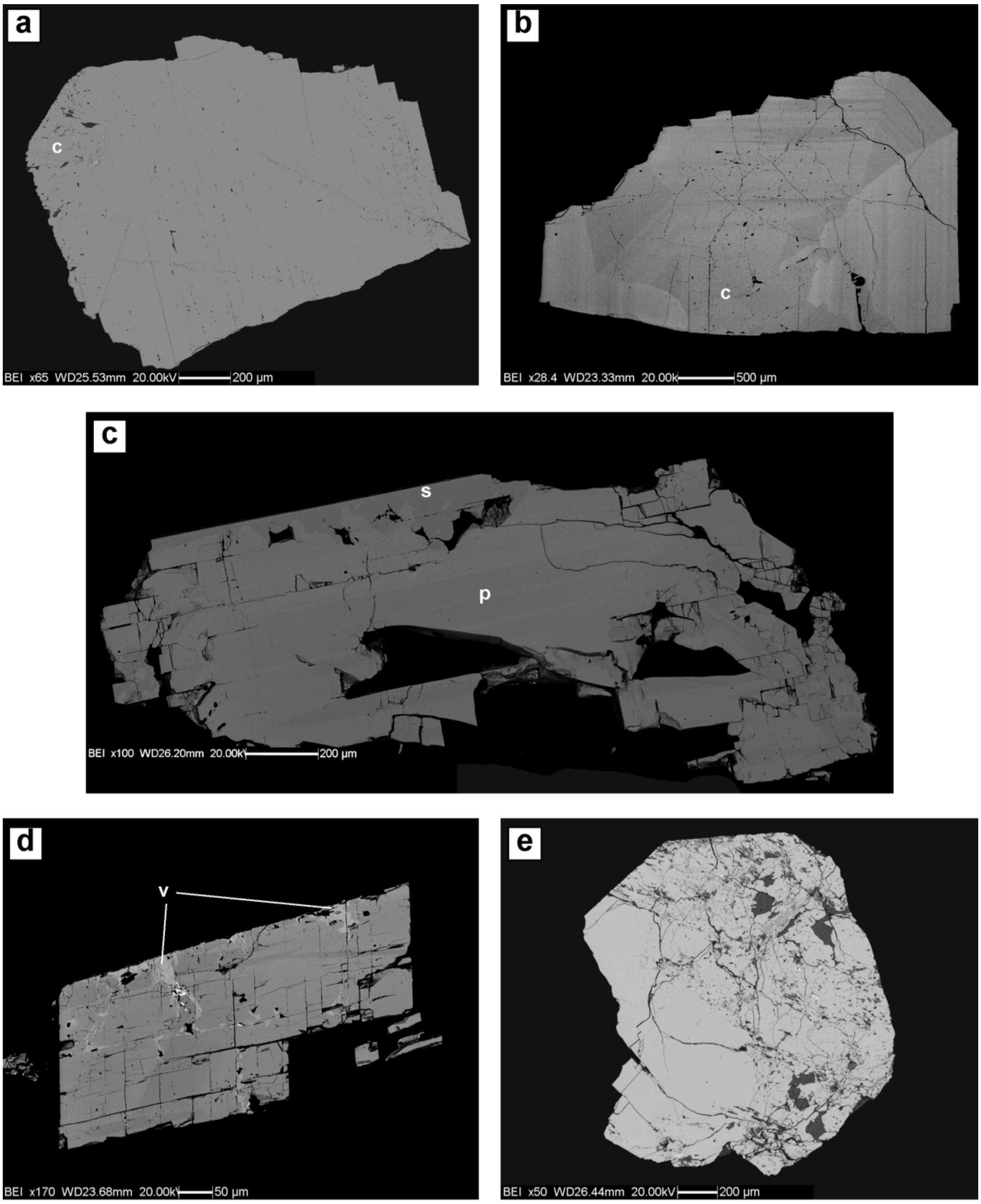

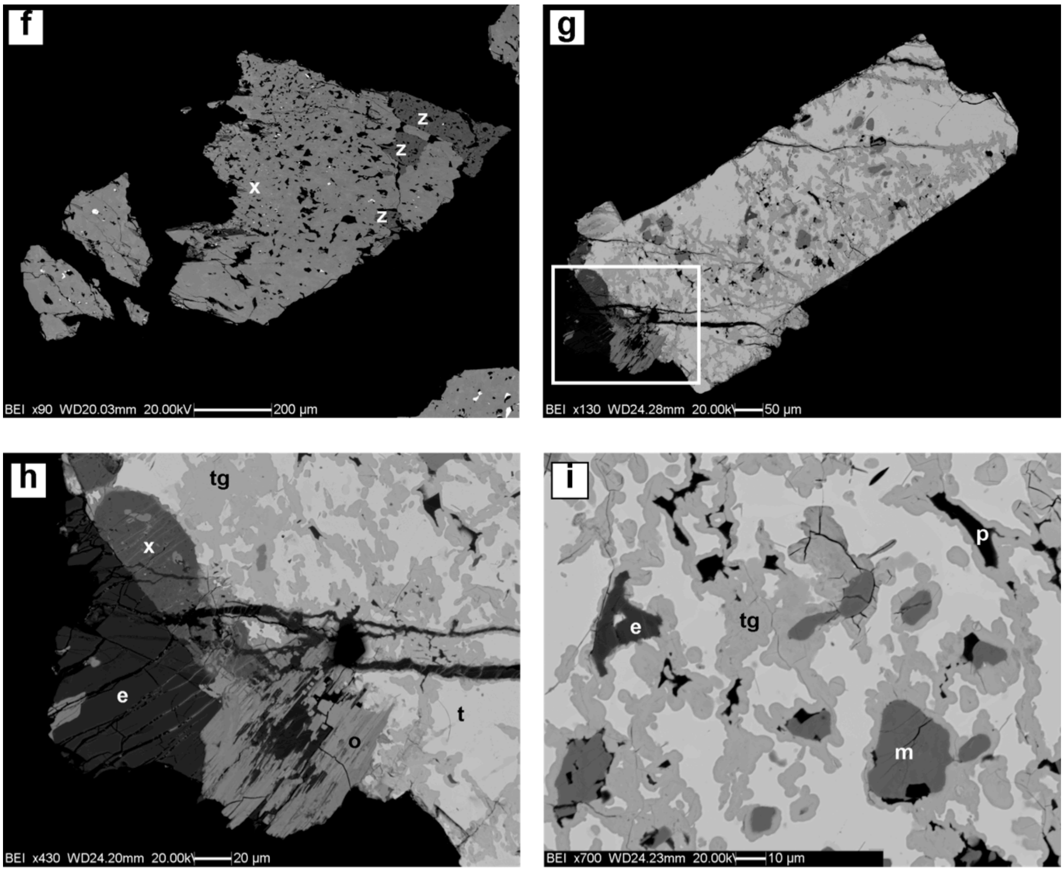

<u>Figure 18</u> *Higly contrasted BSE images of monazits, xenotime and thorite:*

***(a)** CODg(m)1P: Large unzoned crystal with cribriform (c) areas. Bright spots are small uraninite grains. **(b)** CODg(m)3P: Spectatular concentric zoning showing asymmetrical growth of the crystal (c=core of the crystal). **(c)** VLGm(m)2-8: Fragment displaying primary sector zoning (p) parallel to the parting and secondary less brighter patchy zoning (s) at the border. **(d)** CODm(m)1-5: Fragment showing secondary brighter vein zoning (v). **(e)** VCA(m)1Pa: This monazite crystal is composed by a cribrous, poikiloblastic phase and a omogeneous one (bottom left). The cribrous phase is probably reprecipited. **(f)** VCA(m)1Pb-3: Cribrous xenotime including zircon crystals. **(g)** CODg(th)1-2: Thorite fragment displaying the pervasive alteration to thorogummite and numerous inclusions. **(h)** Close up of the white frame of fig. 18g. Crystals growing in contact with thorite (t), which is partially altered to thorogummite (tg), are: xenotime (x), REE-epidote (e) and Nb-Ta-REE oxides, probably euxenite (o). **(i)** Close up of monazites (m), allotriomorphic phosphates (dark areas signed with p) and REE-epidote (e) included in CODg(th)1. The alteration to thorogummite is signed with tg.*

As it is evident in the image, the monazite nucleated against another crystal since zoning is strongly asymmetrical. On VLGm(m)2-8 it is visible another type of sector zoning, probably oscillatory zoning, consisting in bands with different brightness parallel to the parting (*fig. 18c*). Secondary, irregular zoning includes patchy (regions marked by smaller, irregular regions of different brightness and composition) (*fig. 18c,* signed with s*)* and vein (differences in composition or brightness near cracks or veins) zoning (*fig. 18d*). Secondary zoning is common in sampled crystals and in most cases develops in correspondence of cracks or other discontinuities. Most secondary chemical variations in monazites occur with reduction of brightness in BSE images, which suggests depletion in heavy elements. An exception is CODm(m)1 samples that are locally penetrated by brighter thin veins with cloudy aspect (*fig. 18d*). CODg(m)1 samples don't show primary zoning but have broad volumes with cribriform aspect (*fig. 18a*). Polished areas show swarms of small irregular holes (most are less than 10 μm in length) gathered especially near the borders. Those are filled with allotriomorphic phosphates (including REE-phosphates and apatite), quartz and commonly contain rounded grains of xenotime, uraninite, REE-bearing epidote and Nb-Ta-REE oxides. Less bright patchy zoning is visible in these areas.

VCA(m)1Pa and Pb polished crystals confirm their complexity with BSE imaging. VCA(m)1Pa is composed of two different monazite phases: one is clear and homogeneous, the other is cribriform and hosts numerous grains (cribriform themselves) of REE-phosphates and uraninite. VCA(m)1Pb monazite is similar to the clear one of VCA(m)1Pa, but it is intergrown with a large crystal of xenotime and spongiform crystals of zircon. Xenotime locally displays cribriform zones. Areas not affected by cribriform zones display sector zoning (following crystallographical directions) and altered areas with irregular borders. Cribriform areas in xenotime and zircons show patchy zoning suggesting pervasive alteration. The irregular cavities contain the same phases seen in VCA(m)1Pa. Cribriform aspect of inclusions-rich monazite are associated to mottled zoning (Catlos, 2013, and reference therein), which is typical of dissolution and riprecipitation processes on monazite. Similar processes are likely to have been affecting xenotime and zircon crystals too.

CODg(th) thorite samples display a pervasive internal alteration to thorogummite (*fig. 8g*). It appear as less bright vermicular to dendritic volumes that follow major fractures and penetrate in the crystal. Thorite contains numerous inclusions: rounded monazite and REE-rich epidote grains, xenotime and Nb-Ta-REE oxides (*fig. 18h and i*). Fractures and related alteration commonly exploit grain boundaries of inclusions like monazites. Dark phases filling the fractures are mainly REE-phosphates and apatite.

7.2. EMP analysis

Electron-microprobe analysis (EMPA) was performed on garnet, tourmaline, monazite, thorite and xenotime samples (also for some inclusions) at the laboratory of microanalysis of the Istituto di Geoscienze e Georisorse - CNR (Padova). Complete tables with chemical analysis results are attached in the appendix II, including those of thorite, thorogummite, xenotime and inclusions. Since analysis on inclusions are insufficient for a complete characterization and EMP- was calibrated only for elements expected in monazites, they won't be discussed in this thesis. Analytic conditions and further information are reported in the appendix I.A.

7.2.1. Garnet

Garnet is used as a useful indicator of fractionation trends in pegmatites (London, 2008). Core-rim or rim-rim chemical profiles were provided with punctual measures, separated by 50 to 200 μm steps depending on chemical variation and size of the crystal, on each garnet. Spessartine (mole %) vs distance (core = 0 μm) profiles of representative samples are reported in *fig. 19*. Crystal Sps-content profiles of each garnet were plotted on the same diagram and showed that samples separate in two different groups with strong concordance of core composition and few exceptions. Representative garnets profiles are plotted in *fig. 19*.

The first group includes all garnets characterised by dominant spessartine content at the core with values ranging between Sps_{61} and Sps_{65}. CODp(g)1 garnet is fairly homogeneous with compositions ranging from $Alm_{32}Sps_{64}Pyr_{2}$ (core) to $Alm_{36}Sps_{61}Pyr_{2}$ (rim). CODp dike also hosts nearly pure spessartine garnet with composition $Alm_{7–17}Sps_{92–82}Pyr_{05–0.3}$ (CODp(g)2). CODg(g)1 is moderately zoned with core composition similar to CODp(g)1 and $Alm_{44}Sps_{53}Pyr_{2}$ rim. ROSg(g)1 has a well-developed bell-shaped zoning with core overlapping COD compositions ($Alm_{31}Sps_{64}Pyr_{3}$) and minimum $Alm_{53}Sps_{39}Pyr_{6}$ rim. ROSb(g)1, which has rhomb-dodecahedron habit, has slightly lesser spessartine component $Alm_{40}Sps_{56}Pyr_{3}$ at the rim, $Alm_{46}Sps_{49}Pyr_{3}$ in the inner rim and a thin outer rim of $Alm_{39}Sps_{59}Pyr_{2}$.

	CODp(g)2		CODp(g)1		CODp(gg)1		CODg(g)1		ROSg(g)1	
Oxide wt.%	core	rim	core	rim	core	rim	core	rim	core	rim
SiO_2	35.90	35.61	35.34	36.14	35.57	35.98	35.77	36.18	35.14	36.38
TiO_2	0.02	0.08	0.11	0.05	0.09	0.06	0.09	0.05	0.12	0.05
Al_2O_3	20.82	20.32	19.96	20.08	20.02	19.94	20.27	20.28	19.79	20.42
Cr_2O_3	0.01	0.00	0.00	0.01	0.01	0.01	0.02	0.02	0.01	0.02
FeO*	3.06	7.23	13.45	15.50	13.40	15.04	13.52	19.03	12.64	22.92
Fe_2O_3*	0.53	0.62	2.54	0.50	2.00	0.69	1.26	0.41	2.36	0.55
MnO	39.11	34.55	27.06	26.05	27.55	26.29	27.67	22.77	27.32	16.91
MgO	0.02	0.06	0.55	0.48	0.45	0.49	0.44	0.51	0.66	1.48
CaO	0.19	0.25	0.40	0.41	0.39	0.42	0.41	0.24	0.50	0.67
Total	99.66	98.73	99.42	99.21	99.48	98.91	99.45	99.49	98.54	99.39
Si	2.968	2.975	2.936	2.999	2.952	2.996	2.965	2.995	2.941	2.991
Ti	0.002	0.005	0.007	0.003	0.006	0.004	0.005	0.003	0.008	0.003
Al	2.028	2.001	1.955	1.964	1.959	1.957	1.980	1.978	1.953	1.978
Cr	0.000	0.000	0.000	0.000	0.001	0.000	0.001	0.001	0.001	0.001
Fe^{3+}	0.033	0.039	0.159	0.031	0.125	0.043	0.079	0.026	0.148	0.034
Fe^{2+}	0.212	0.505	0.935	1.076	0.930	1.047	0.937	1.317	0.884	1.576
Mn	2.739	2.445	1.905	1.831	1.937	1.854	1.943	1.596	1.937	1.177
Mg	0.002	0.008	0.068	0.059	0.056	0.061	0.054	0.063	0.083	0.182
Ca	0.017	0.022	0.036	0.036	0.035	0.038	0.036	0.021	0.045	0.059
Cation Sum	8.000	8.000	8.000	8.000	8.000	8.000	8.000	8.000	8.000	8.000
Py	0.07	0.27	2.25	1.97	1.86	2.02	1.79	2.11	2.74	6.05
Al	8.15	17.64	33.39	35.77	32.65	34.91	32.42	44.00	31.49	52.78
Sp	91.22	81.35	63.17	61.05	64.33	61.81	64.58	53.19	64.29	39.22
Uv	0.02	0.00	0.00	0.02	0.04	0.02	0.06	0.06	0.04	0.06
An	0.00	0.69	4.37	1.70	3.60	2.14	2.05	1.13	4.23	1.29
Gr	0.56	0.74	1.19	1.21	1.15	1.26	1.21	0.71	1.49	1.95

Table 3 *Garnet from the Codera area.*

Renamed after Guastoni et al. (2014). Structural formula based on 12 oxygen atoms. * (Fe3+/Fe2+) calculated (Droop 1987).

Codera graphic garnets, even if the core of the intergrowth is individuated, are unzoned and have group-1 core composition. VLGm(g)1 garnet is the only one from Bodengo area whose core composition overlaps those of Codera. It has $Alm_{29}Sps_{65}Pyr_4$ core and $Alm_{40}Sps_{51}Pyr_5$ rim, but has higher TiO_2 values. It should be noted that unlike other Bodengo area garnets it has an extremely dark red colour and rhomb-dodecahedron habit.

Group-two includes all other garnets, which are exclusively from Bodengo area and all display a well-developed bell-shaped zoning. With the exception of VGa(g)1 and VGb(g)1, all group-two garnets have rather coherent core composition of medium $Alm_{57}Sps_{41}Pyr_1$ (within the range of $Sps_{39\text{-}42}$). VGb(g)1 is richer in Alm with $Alm_{64}Sps_{34}Pyr_2$ core and $Alm_{73}Sps_{23}Pyr_3$ rim while VGa(g)1 has higher Sps with $Alm_{48}Sps_{47}Pyr_4$ core and $Alm_{59}Sps_{32}Pyr_7$ rim. Since VGb(g)1 core composition is lower in Sps but overlaps the compositions range of other Bodengo garnets, the difference can be imputed to different time of nucleation during pegmatite liquid evolution. On the other hand VLGa(g)1 higher Sps core

Oxide wt.%	VLGa(g)1		VLGm(g)1		VDD(g)2		VGb(g)1		VGa(g)1	
	core	rim	core	rim	core	rim	core	rim	core	rim
SiO_2	35.57	36.24	36.15	36.95	35.80	35.99	35.90	36.50	36.16	36.78
TiO_2	0.07	0.02	0.35	0.14	0.05	0.02	0.05	0.01	0.11	0.01
Al_2O_3	20.55	21.02	19.67	20.32	20.61	20.75	20.66	20.92	20.66	20.99
Cr_2O_3	0.01	0.00	0.01	0.01	0.00	0.01	0.01	0.04	0.01	0.02
FeO*	24.24	29.11	13.12	18.16	24.59	31.45	25.08	30.34	20.48	25.35
Fe_2O_3*	1.26	0.52	0.00	0.00	0.83	0.79	0.03	0.00	0.35	0.00
MnO	17.41	11.54	27.25	22.05	17.40	9.75	16.94	10.81	20.14	14.01
MgO	0.27	1.10	0.96	1.33	0.18	0.70	0.20	0.66	1.00	1.72
CaO	0.19	0.47	0.80	0.90	0.26	0.37	0.30	0.37	0.53	0.62
Total	99.57	100.01	98.32	99.86	99.73	99.83	99.16	99.65	99.43	99.49
Si	2.951	2.968	3.013	3.019	2.965	2.966	2.984	3.001	2.979	3.003
Ti	0.004	0.001	0.022	0.009	0.003	0.001	0.003	0.000	0.007	0.000
Al	2.009	2.029	1.932	1.957	2.012	2.015	2.024	2.027	2.006	2.019
Cr	0.001	0.000	0.001	0.001	0.000	0.000	0.001	0.002	0.000	0.001
Fe^{3+}	0.079	0.032	0.000	0.000	0.052	0.049	0.002	0.000	0.021	0.000
Fe^{2+}	1.682	1.994	0.915	1.241	1.703	2.168	1.743	2.087	1.411	1.731
Mn	1.223	0.800	1.924	1.526	1.221	0.681	1.193	0.753	1.405	0.969
Mg	0.033	0.134	0.120	0.162	0.022	0.086	0.024	0.081	0.123	0.209
Ca	0.017	0.041	0.072	0.078	0.023	0.033	0.026	0.033	0.047	0.055
Cation Sum	8.000	8.000	7.998	7.993	8.000	8.000	8.000	7.984	8.000	7.987
Py	1.10	4.46	4.02	5.46	0.73	2.87	0.82	2.73	4.11	7.05
Al	57.72	67.50	29.04	40.53	57.94	73.40	58.39	70.66	47.56	58.41
Sp	40.61	26.67	64.54	51.36	40.57	22.63	39.90	25.50	46.79	32.71
Uv	0.04	0.00	0.03	0.04	0.02	0.02	0.03	0.12	0.02	0.05
An	1.14	0.00	2.48	1.83	0.56	0.41	0.00	0.00	0.21	0.00
Gr	0.57	1.37	2.41	2.64	0.76	1.10	0.89	1.11	1.55	1.84

Table 4 *Garnet from the Bodengo area.*

Renamed after Guastoni et al. (2014). Structural formula based on 12 oxygen atoms. * (Fe3+/Fe2+) calculated (Droop 1987).

values exceed the mean value of group-2 (Bodengo) core compositions and represents an exception.

Results show that Codera and Bodengo garnets (with the exception of VLGm(g)1) form two separate groups with different Sps content. However all non-graphic garnets show the same trend of inverse zoning with Sps-rich core and Alm-rich rim. Pyr (Mg end member) component generally is less than 3 mol % but dark red VLGm(g)1, VGa(g)1 and ROSg(g)1 garnets exceed Pyr_6 values at the rim. Grossular, andradite, and uvarovite components sumalways less than 5 mol.%. Despite the relative variance in Sps content, all non-graphic samples display the same trend, more or less pronounced, of depletion in spessartine (Sps) component toward the rim and coupled enrichment in almandine (Alm).

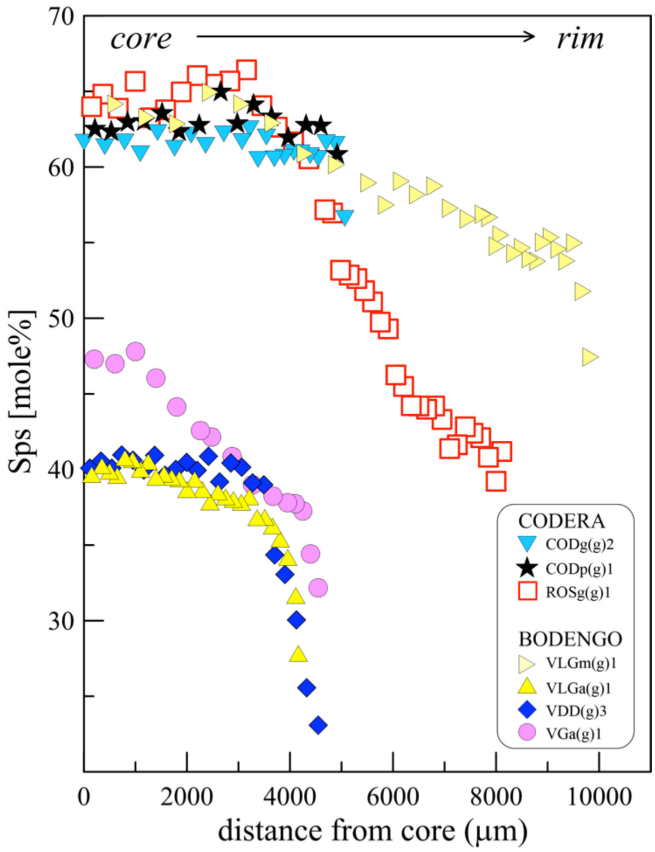

Figure 19 *Zoning patterns of Sps content in selected garnets from Codera and Bodengo areas. Renamed after Guastoni et al. (2014).*

7.2.2. Tourmaline

Like garnets, tourmalines are important minerals for the mineral-based classification and study fractionation trend of pegmatites. All analysed tourmalines are prismatic and were cut perpendicular to the c-axis. On most crystals composition was measured along core-rim profiles.

All Bodengo tourmalines are schorl with rather low variation in Li content and $2Li/(2Li+Mg+Fe^{2+})$ ratio ranging between 0.05 and 0.25 (*fig. 20c)*. The most homogeneous one is the miarolitic VLGb(t)1 tourmaline, which, despite the greenish colour, is a schorl and has the lowest Mg number ($Mg/(Mg+Fe^{2+})<0.1$). Other Bodengo tourmalines show rim-core variations in Mg content. VDD(t)1 miarolitic tourmaline has similar Mg number (~0.1) to VLGb(t)1 but has a thin rim (60µm) showing enrichment in Mg (up to 0.25). VLGa(t)1 shows internal zoning with (1) a foititic (vacant X site >0.5) core with rather constant Mg number of 0.21, (2) a thin transition non-foititic zone with lower Mg number and (3) a non-foititic thicker rim with gradual increase in Mg number (up to 0.35). Both VLGa and VDD dikes intrude amphibolites, which may explain the relatively higher Mg number of hosted tourmalines (Guastoni et al. 2014).

Most Codera tourmalines are prismatic and graphic schorls with composition similar to the cores of Bodengo ones. They don't show comparable Mg-number variations but some have higher grade of evolution with local enrichment in Li (*fig 20 a)*. The most fractionated dike of Codera CODp hosts tourmaline crystals with yellow-green Mn-rich fluorelbaite rim (CODp Elb. in *fig. 20a,* Guastoni, 2012, and references therein). CODp(gt)1 portion of graphic tourmaline has thin rims evolving toward elbaite. Guastoni *et al*. (2014) report the composition of a tourmaline grown in the host rock gneiss of a pegmatite (sample PP), which is identical to that of tourmaline from the VLGb sample.

Table 5 *Tourmaline from the Codera area (**a**) and from the Bodengo area (**b**). Renamed after Guastoni et al. (2014).* Structural formula based on 31 anions (O, OH, F), calculated using the program by Julie Selway (Ontario Geological Survey).

a

Oxide wt.%	ROSb(t)1 pr Schorl	# 45 st.dev	CODp(t)1 pr Schorl	# 60 st.dev	CODp(gt)1 graph Schorl	# 65 st.dev	CODp Elbaite pr rim Elbaite	# 4 st.dev	CODp Elbaite pr core Schorl	# 4 st.dev
SiO_2	35.76	*0.20*	35.76	*0.23*	35.26	*0.24*	33.96	*0.78*	32.68	*0.47*
TiO_2	0.13	*0.03*	0.16	*0.05*	0.21	*0.04*	0.22	*0.06*	0.18	*0.07*
Al_2O_3	33.65	*0.28*	33.22	*0.71*	33.80	*0.65*	39.88	*1.13*	38.61	*0.48*
FeO	13.54	*0.22*	13.12	*0.69*	13.16	*0.30*	1.95	*0.35*	6.42	*0.35*
MgO	1.59	*0.11*	2.09	*0.16*	1.28	*0.53*	0.13	*0.07*	0.20	*0.02*
CaO	0.07	*0.02*	0.09	*0.03*	0.09	*0.03*	0.07	*0.07*	0.10	*0.04*
MnO	0.49	*0.05*	0.59	*0.11*	0.95	*0.20*	4.75	*0.26*	3.49	*0.23*
ZnO	0.32	*0.04*	0.32	*0.06*	0.43	*0.13*	0.00	*0.00*	0.00	*0.00*
Na_2O	1.96	*0.12*	2.04	*0.12*	2.02	*0.13*	2.52	*0.29*	2.05	*0.11*
K_2O	0.04	*0.01*	0.05	*0.01*	0.05	*0.01*	0.00	*0.00*	0.00	*0.00*
F	0.33	*0.15*	0.28	*0.15*	0.40	*0.18*	1.20	*0.27*	0.69	*0.06*
H2O*	3.47		3.48		3.41		3.09		3.24	
B_2O_3*	10.49		10.48		10.44		10.59		10.34	
Li_2O*	0.17		0.15		0.19		1.11		0.57	
Total	101.87		101.72		101.54		98.96		98.27	
Si	5.923		5.931		5.872		5.572		5.494	
Al	0.077		0.070		0.128		0.428		0.506	
Sum T site	*6.000*		*6.001*		*6.000*		*6.000*		*6.000*	
Al	6.000		6.000		6.000		6.000		6.000	
Mg	0.000		0.000		0.000		0.000		0.000	
Fe^{3+}	0.000		0.000		0.000		0.000		0.000	
Sum Z site	*6.000*		*6.000*		*6.000*		*6.000*		*6.000*	
Al	0.493		0.423		0.506		1.282		1.143	
Ti	0.016		0.020		0.027		0.027		0.023	
Fe^{3+}	0.000		0.000		0.000		0.000		0.000	
Mg	0.392		0.516		0.318		0.031		0.050	
Mn	0.069		0.083		0.134		0.660		0.496	
Fe^{2+}	1.875		1.820		1.833		0.267		0.902	
Zn	0.039		0.040		0.053		0.000		0.000	
Li*	0.115		0.098		0.129		0.733		0.385	
Sum Y site	*3.000*		*3.000*		*3.000*		*3.000*		*3.000*	
Ca	0.012		0.016		0.016		0.012		0.018	
Na	0.631		0.657		0.654		0.801		0.668	
K	0.008		0.011		0.011		0.000		0.000	
□	0.348		0.317		0.320		0.187		0.315	
Sum X site	*1.000*		*1.000*		*1.000*		*1.000*		*1.000*	
B	3.000		3.000		3.000		3.000		3.000	
OH	3.829		3.851		3.789		3.378		3.636	
F	0.171		0.149		0.211		0.622		0.364	
Sum W site	*4.000*		*4.000*		*4.000*		*4.000*		*4.000*	
$Mg/Mg+Fe^{2+})$	0.17		0.22		0.15		0.10		0.05	
$2Li/(2Li+Mg+Fe^{2+})$	0.09		0.08		0.11		0.83		0.45	

b

Oxide wt.%	VLGa(t)1 Pr core Foitite	# 40 st.dev	VLGa(t)1 Pr int Schorl	# 61 st.dev	VLGa(t)1 Pr rim Schorl	# 18 st.dev	VLGb(t)1 pr Schorl	# 68 st.dev	VDD(t)1 pr Schorl	# 59 st.dev	PP bulk Schorl
SiO_2	36.26	*0.35*	35.84	*0.31*	35.80	*0.40*	35.01	*0.23*	35.34	*0.32*	35.62
TiO_2	0.17	*0.11*	0.37	*0.10*	0.67	*0.06*	0.50	*0.03*	0.14	*0.11*	0.11
Al_2O_3	35.09	*0.32*	34.56	*0.33*	33.95	*0.35*	34.28	*0.18*	34.16	*0.41*	34.34
FeO	12.13	*0.56*	12.67	*0.58*	11.34	*0.65*	14.18	*0.24*	13.97	*0.23*	14.3
MgO	1.84	*0.30*	1.66	*0.38*	2.85	*0.19*	0.40	*0.09*	0.96	*0.16*	0.44
CaO	0.07	*0.02*	0.08	*0.04*	0.14	*0.03*	0.02	*0.01*	0.06	*0.02*	0.11
MnO	0.22	*0.03*	0.21	*0.04*	0.09	*0.03*	0.24	*0.03*	0.23	*0.03*	0.15
ZnO	0.09	*0.04*	0.13	*0.05*	0.09	*0.03*	0.62	*0.10*	0.12	*0.04*	n.a.
Na_2O	1.42	*0.06*	1.74	*0.10*	1.93	*0.05*	2.19	*0.06*	1.82	*0.17*	1.83
K_2O	0.03	*0.01*	0.04	*0.01*	0.04	*0.01*	0.04	*0.01*	0.04	*0.01*	n.a.
F	0.09	*0.10*	0.15	*0.10*	0.24	*0.10*	0.94	*0.16*	0.33	*0.16*	n.a.
H2O*	3.62		3.58		3.54		3.16		3.44		3.61
B_2O_3*	10.63		10.57		10.58		10.45		10.43		10.46
Li_2O*	0.22		0.25		0.27		0.32		0.22		0.33
Total	101.85		101.79		101.45		101.95		101.12		101.30
Si	5.928		5.893		5.882		5.823		5.891		5.920
Al	0.072		0.107		0.118		0.177		0.109		0.080
Sum T site	*6.000*		*6.000*		*6.000*		*6.000*		*6.000*		*6.000*
Al	6.000		6.000		6.000		6.000		6.000		6.000
Mg	0.000		0.000		0.000		0.000		0.000		0.000
Fe^{3+}	0.000		0.000		0.000		0.000		0.000		0.000
Sum Z site	*6.000*		*6.000*		*6.000*		*6.000*		*6.000*		*6.000*
Al	0.689		0.590		0.455		0.542		0.602		0.646
Ti	0.021		0.046		0.083		0.062		0.018		0.014
Fe^{3+}	0.000		0.000		0.000		0.000		0.000		0.000
Mg	0.448		0.407		0.699		0.099		0.238		0.109
Mn	0.030		0.029		0.012		0.034		0.033		0.021
Fe^{2+}	1.659		1.743		1.559		1.972		1.947		1.988
Zn	0.011		0.015		0.011		0.076		0.015		0.000
Li*	0.142		0.168		0.181		0.213		0.147		0.222
Sum Y site	*3.000*		*3.000*		*3.002*		*3.000*		*3.000*		*3.000*
Ca	0.012		0.014		0.025		0.003		0.011		0.020
Na	0.452		0.553		0.615		0.707		0.587		0.590
K	0.007		0.009		0.009		0.009		0.008		0.000
□	0.529		0.423		0.352		0.282		0.394		0.391
Sum X site	*1.000*		*1.000*		*1.000*		*1.000*		*1.000*		*1.000*
B	3.000		3.000		3.000		3.000		3.000		3.000
OH	3.951		3.922		3.877		3.507		3.826		4.000
F	0.049		0.078		0.123		0.493		0.174		0.000
Sum W site	*4.000*		*4.000*		*4.000*		*4.000*		*4.000*		*4.00*
$Mg/Mg+Fe^{2+})$	0.21		0.19		0.31		0.05		0.11		0.05
$2Li/(2Li+Mg+Fe^{2+})$	0.12		0.14		0.14		0.17		0.12		0.18

7.2.3. Monazite

Monazites were preliminary chemically analysed before LA-ICP-MS U-Th–Pb dating. The composition is typical of pegmatitic Th-rich monazite-(Ce), with an average Ce_2O_3 of 27.5 mol. % for Codera crystals and 25 mol. % for Bodengo ones. Monazites have medium-high ThO_2 content (6-7 mol. %), which is coherent with the habit of most crystals (Catlos, 2013), and subordinate UO_2 (<1 mol.%). Other components (REE elements oxides) exceeding the 1 mol. % are (with decreasing relevance) Nd_2O_3, La_2O_3, Pr_2O_3, Sm_2O_3 and Y_2O_3, which sum up to

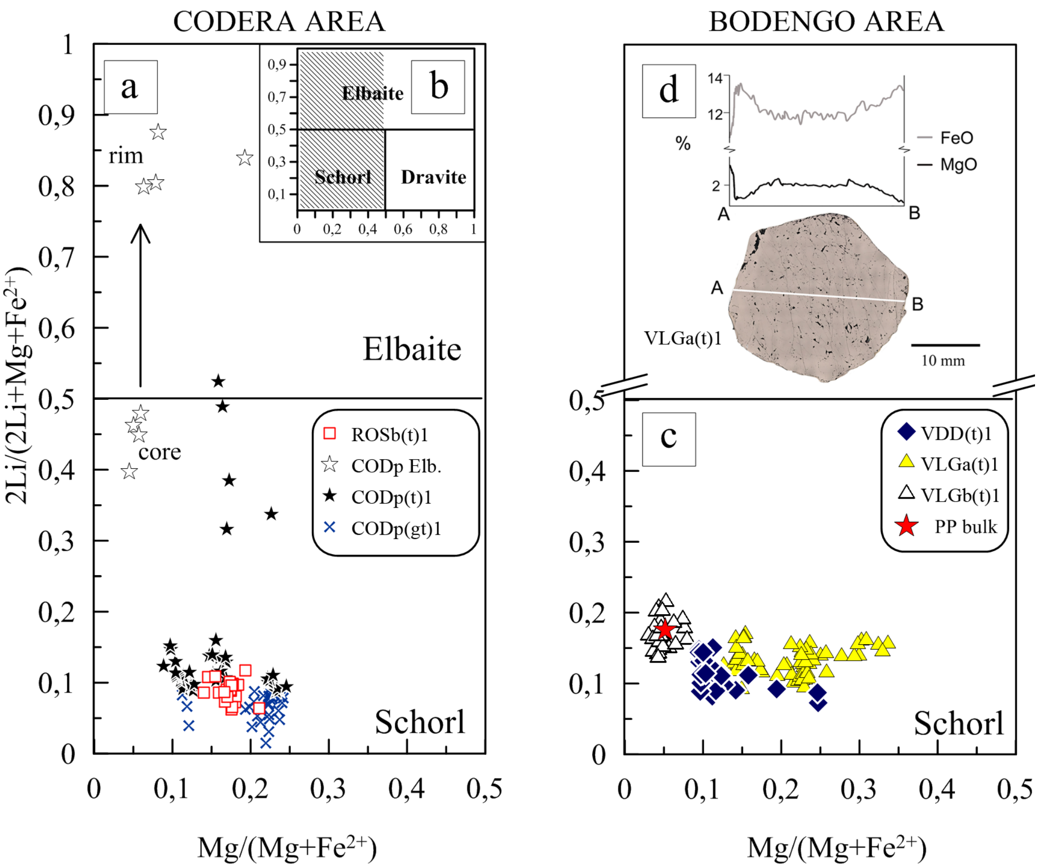

<u>Figure 20</u> *Classification diagram of tourmaline from the Codera (**a**) and the Bodengo (**c**) areas. The complete classification scheme is reported in the inset (**b**). The compositional profile of a zoned tourmaline crystal from the VLGa dike is shown in (**d**). Renamed after Guastoni et al. (2014).*

an average of 30.5 mol. %. Exceptions are the green monazites from both Codera and Bodengo areas. One is a dark green monazite from CODt dyke of the upper Codera valley that has lower Ce_2O_3 (~22.7 mol. %) and very high UO_2 (~10.5 mol. %). VCA(m)1 greenish monazites have higher ThO_2 (10-11 mol. %), slightly higher UO_2 (1-2 mol. %) and lower Ce_2O_3 (~25 mol. %), Pr_2O_3 and Nd_2O_3. Greenish U-rich monazites have higher CaO content. CaO values of 3.5 and 2.1 mol. % are measured respectively on CODt(m)1 and VCA(m)1.

VLGm(m) monazites have higher Nd_2O_3 (as much as 17.5 mol. %), Sm_2O_3 (as much as 11 mol. %) and lower Y_2O_3 (<2 mol. %).

Primary zoning of monazites reflect low oscillation of mainly U, Th and Ce content. Secondary zoning occurs generally as darker irregular zones depleted in Th, Pb and U (*fig. 18c*). In these areas the UO_2 value is more than halved. Vein zoning found in CODm(m) samples has higher content in REE and appear as brighter veins in BSE images (*fig. 18d*). Veins are filled by a secondary monazite phase with higher Ce_2O_3 (as much as 30 mol. %), high ThO_2 (as much as 11 mol. %) and low UO_2 (<0.2 mol. %). The high Th phase seems more suitable with chemical instability during magmatism since hydrothermal monazite commonly has lower Th content than magmatic monazite (Catlos, 2013).

Monazites included in the CODg(th)1 thorite crystal are similar to Codera ones but have higher Ce_2O_3 (30 mol. %) and slightly lower ThO_2 (5.5 mol. %).

7.3. LA-ICP-MS U-Th–Pb Monazite dating

Isotopic analyses on monazite were obtained with the Laser Ablation and Induced Coupled Plasma Mass Spectrometry (LA-ICP-MS) technique performed at the Istituto di Geoscienze e Georisorse (IGG) of CNR (Pavia). Technique description and analytical conditions are reported in the appendix I.A.

Ages are obtained from monazite samples from three dikes of Codera area (CODg, CODt CODm) and two dikes of Bodengo area (VLGm, VCA). Virtually the three obtained isotope ratios ($^{206}Pb/^{238}U$, $^{207}Pb/^{235}U$ and $^{208}Pb/^{232}Th$) would yield the same age if the crystal system is considered close. However analysis results show a drastic systematic difference in age between the Pb/U ratios and the Pb/Th ratio. This can be explained by the decoupling of the systems caused by alteration. It is noteworthy that monazites sampled show both altered and riprecipited areas. Major age discordance between Pb/U and Pb/Th ratios are found in the analysis spots of monazites from the VLGm dike of Bodengo area: VLGm(m)1-12_036, VLGm(m)2-4_014, VLGm(m)2-8_019, VLGm(m)2-12_027 and _030 (see age table for correct spots). Each of these analyses comes from darker areas (on SEM BSE images) with irregular borders (e.g. *fig. 18c*). Correspondent EMPA analyses highlight that those areas are depleted in Th, Pb and U. However ages obtained with the $^{208}Pb/^{232}Th$ ratio on the same crystal are comparable both in the altered volume and in the pristine one. Therefore, as for the work of Bosse *et al*. (2009), accepted ages are those of the $^{208}Pb/^{232}Th$ ratio since:

- Monazites contain more Th than U thus the signal of $^{208}Pb/^{232}Th$ is better in accuracy.
- ^{208}Pb originating from common Pb is negligible thanks to the abundance of Th.
- Ages obtained with the Pb/U ratios for Codera samples yielded unrealistic older ages than those of emplacement of the Bergell tonalite.
- Altered areas show a strong decrease in U and lesser for Th suggesting circulation of U-aggressive fluids. Loss of U results in age sovrastimation (M. Tiepolo personal communication).

$^{208}Pb/^{232}Th$ ages yielded by monazites show significant variations even in the same crystal (>2 Ma on different analysis spots). Since dating work is yet preliminary and lacks of more accurate data discussion it won't be examined in depth in this thesis and only rough data are presented. Even though dating of dikes actually wouldn't provide a representative mean age, ages of Codera and Bodengo dikes plot in two rather distinguishable groups of points (including the 2σ error bars, *fig. 21*).

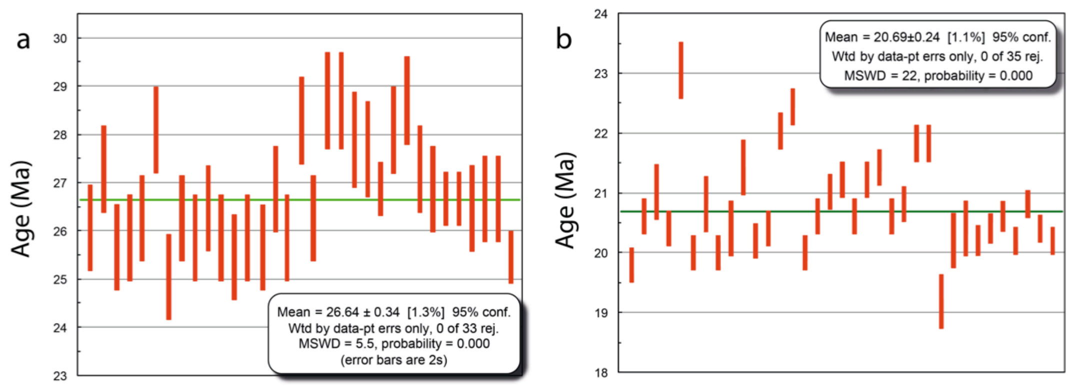

Figure 21 *Plot of ages obtained from analysis spots on the Codera (**a**) and the Bodengo (**b**) monazites. Box heights are 2σ.*

Codera monazites yielded ages ranging from 28 and 25 Ma. Bodengo monazites are younger and ages range from 23 and 19 Ma. Even if the higher and lower ages of each group are included, pegmatites from Codera area are all older than 24 Ma and vice versa for the Bodengo pegmatites.

Only one fragment included in the VLGm(m) samples yielded discordant age of ~26 Ma. EMP analysis on this fragment plot on those of CODm(m)1, whose fragments also share similar appearance and age. Since it is reasonable to consider this as a case of contamination, it was renamed temporarily CODm(m)1-C and added to Codera monazites but not included in the plot.

The same dating was carried on the thorite sample CODg(th) and the xenotime intergrown with VCAm(m)1Pb monazite. Thorite ages are concordant for each ratio but are 5 to 6 Ma older than those of hosting monazite. On the other hand $^{206}Pb/^{238}U$ and $^{207}Pb/^{235}U$ ages of xenotime are only 2 and 1 Ma respectively older of the intergrown monazite VCA(m)1Pb ages.

The two age groups of Codera and Bodengo pegmatites are respectively older and younger than 24 Ma. According to Liati *et al*. (2000) who dated the Novate granite at 24.0 ± 1.2 Ma, the Codera monazite ages of pegmatites would be consistent with the field evidence of younger microgranite dikes crosscutting the main set of pegmatite dikes in the upper Codera valley. Codera pegmatite intrusion would be coeval with the late D3 (Cressim) ductile deformation stage, which is consistent with the higher degree of deformation of dikes than the Bodengo ones. On the other hand Bodengo deformed pegmatites would be emplaced during the waning stage of ductile deformation in the southern Adula nappe.

8. Discussion and Conclusions

In this work only a minor portion of the large Tertiary pegmatitic field of the Central Alps was investigated in Codera and Bodengo areas. Pegmatites of both areas seem comparable by the similar grade of evolution, since evolved dikes display more or less the same mineralogy. On the other hand structural, textural, chemical and radiometric results tell a more complicated story that allows individuating at least two different intrusion events.

8.1. Stuctural data

Codera pegmatites occur with two main groups with different orientations. The main set strikes WSW-ENE, other dikes are oriented E-W. Crosscutting relationships suggest the existence of at least two different generations.

Pegmatites clearly postdate the emplacement of the Bergell pluton since they cut discordantly (1) the base of the intrusion and (2) its parallel pervasive solid-state foliation, and (3) the main fabric of the Gruf complex. Dikes crosscut migmatitic structures thus syn-intrusion peak conditions of 720–740°C and 6–7 kbar (Galli *et al*., 2011) clearly exceed those of emplacement of pegmatites.

Microgranitic dikes related to the intrusion of the Novate granite (24.0 ± 1.2 Ma, Liati *et al*., 2000) seem to postdate pegmatites by crosscutting relationships and radiometric results on monazites. Therefore assumed country rock conditions of 0.2 GPa and 400 °C (Ciancaleoni and Marquer, 2006) represent the lower limit.

All pegmatites from Codera area show solid-state deformation and locally localize well-developed mylonites with transpressive kinematics. On two of the sampled quartz-mylonites (nucleated at the wall of deformed pegmatites) the measured crystallographic preferred orientation shows a strong, single c-axis maximum parallel to the Y-axis of the mylonite (perpendicular to the lineation and parallel to the foliation). This quartz CPO pattern suggest syn-deformation temperatures of ~500°C and is similar to those studied in Adamello quartz-mylonites (Pennacchioni *et al.*, 2010; Guastoni *et al.*, 2014 and references therein). Temperature is consistent with recrystallized stable biotite and k-feldspar in the foliation.

D3 peak conditions of migmatisation in southern Adula nappe (650–750 °C and 0.4–0.6 GPa, Nagel *et al.*, 2002) are similar to those of Codera and can be used as upper limit to the pegmatite intrusion in the Bodengo area. The main set of Bodengo pegmatites is generally undeformed and cuts discordantly the D3 structures. However some dikes show ductile deformation on boundaries (with an annealed quartz fabric typical of a temperature >500 °C) with strike-slip kinematic. Also in Bodengo area there is evidence of at least two generations of pegmatites: the main set dips toward W and NW and crosscuts a former set of strongly deformed pegmatites striking NW-SE. These may represent the ductile deformed set with Codera affinity that predate the main set.

8.2. Chemical data

Pegmatites of Codera and Bodengo areas show a similar grade of evolution and mineralogy. On the other hand some minerals show a chemical signature that is typical of all crystals of the same phase of the same area.

Garnet is the most evident one with Codera ones displaying Sps-rich cores and Bodengo ones Alm-rich cores. With few exceptions all garnet cores of the same area plot coherently on the same Sps content.

Chemical signature of tourmalines are less evident but Codera ones show the highest grade in fractionation, reaching F-elbaite compositions in the Phosphate dike in the Upper val Codera. Bodengo schorls display minor fractionation but higher grade of variance in Mg content. This is probably due to interaction with the host rock (Guastoni *et al*. 2014).

Monazite samples of Codera area display an higher content in Ce (27.5 mol. %) than those of Bodengo (25 mol. %). However this last datum is based only on two dikes from Bodengo area and should be treated critically.

8.3. Radiometric data

As Guastoni et al. (2014) assumed, Pb/Th dating on monazite yielded two different age groups for pegmatite dikes of the two different areas. Codera pegmatites are older than 24 Ma, with monazite $^{208}Pb/^{232}Th$ ages ranging from 28 to 25 Ma, and Bodengo ones are younger with monazite $^{208}Pb/^{232}Th$ ages ranging from 23 and 19 Ma. Error bars (2σ) of single age measures of monazites from the same area do not overlap sufficiently to give an acceptable average age. On the other hand, the virtual medium age of 20,69±0.24 Ma (2σ) for Bodengo pegmatites is coherent with observation of some authors that pegmatite emplacement was associated with a protracted magmatic activity over a time range from 32 to 20 Ma (Romer *et al*. 1996, Schärer *et al*. 1996, Rubatto et al. 2009).

8.4. Conclusions

- Codera and Bodengo areas represent two small portions of the large tertiary pegmatite field of the Central Alps. Despite a similar grade of evolution of the dikes and mineralogy, these two areas show systematic differences after structural, chemical and radiometric study.

Codera pegmatites are older than 24 Ma (monazite ages) and locally show the major grade of evolution among all sampled dikes (e.g. CODp dike). The main set trends WSW-ENE and is affected by solid-state pervasive deformation, which locally produces high-temperature mylonites, developed under transpressive conditions. Bodengo Pegmatites are younger than 24 Ma and thus than Codera ones. The main set is oriented N-S and dikes are mainly undeformed but locally show ductile reactivation of borders with strike slip kinematic. Codera garnets are richer in spessartine than Bodengo ones and Codera schorl tourmalines show locally highest grade of evolution.

Since pegmatites of the two areas have (i) different orientations, (ii) different grade of deformation and (iii) different chemical signature of minerals it is reasonable to individuate two separate intrusion events. This is supported by radiometric dating on monazite, which shows no overlap between the Codera and Bodengo pegmatite ages.

- Pegmatites of Codera area emplaced the host rock at a temperature of at least 500°C, which is constrained by the presence of high-temperature quartz mylonites at their boundaries. Dating of pegmatites well concords with the progressive younging of the radiometric ages of peak metamorphism from E to W along the SSB (Todd and Engi, 1997). It is reasonable that Bodengo pegmatites occurred later at similar T conditions during differential uplift rates along the SSB. The time span of emplacement of pegmatites also overlaps the protracted stage of fluid-assisted migmatisation in the SSB, which occurred up to 20 Ma (Romer *et al*. 1996, Schärer *et al*. 1996, Rubatto et al. 2009). However pegmatites and migmatites seem genetically unrelated since pegmatite intrusion always postdates the local leucosomes.

- Many authors individuated different pegmatite generations in the Central Alps with young pegmatites treated as post-kinematic intrusions (e.g. Romer *et al.* 1996). However monazite ages of pegmatite dikes of Bodengo area, which show sometimes ductile reactivation of the margins, indicate that ductile deformation was still active in the southern Adula nappe after 24 Ma and possibly even up to ~20 Ma if the average age is considered. Waning of such conditions is witnessed by the elder set of Bodengo, which is strongly deformed than the crosscutting younger ones.

REFERENCES

Beltrando, M., Lister, G. S., Rosenbaum, G., Richards, S., & Forster, M. A. (2010). Recognizing episodic lithospheric thinning along a convergent plate margin: The example of the Early Oligocene Alps. *Earth-Science Reviews*, *103*(3), 81-98.

Berger, A., Rosenberg, C., & Schmid, S. M. (1996). Ascent, emplacement and exhumation of the Bergell pluton within the Southern Steep Belt of the Central Alps. *Schweizerische mineralogische und petrographische Mitteilungen*, *76*, 357-382.

Bosse, V., Boulvais, P., Gautier, P., Tiepolo, M., Ruffet, G., Devidal, J. L., ... & Paquette, J. L. (2009). Fluid-induced disturbance of the monazite Th–Pb chronometer: in situ dating and element mapping in pegmatites from the Rhodope (Greece, Bulgaria). *Chemical Geology*, *261*(3), 286-302.

Burg, J. P., & Gerya, T. V. (2005). The role of viscous heating in Barrovian metamorphism of collisional orogens: thermomechanical models and application to the Lepontine Dome in the Central Alps. *Journal of Metamorphic Geology*, *23*(2), 75-95.

Burri, T., & Berger, A. (2005). Tertiary migmatites in the Central Alps: Regionaldistribution, field relations, conditions of formation and tectonic implications. *Schweizerische Mineralogische und Petrographische Mitteilungen*, *83*, 215-235.

Catlos, E. J. (2013). Generalizations about monazite: Implications for geochronologic studies. *American Mineralogist*, *98*, 819-832.

Ciancaleoni, L., & Marquer, D. (2006). Syn-extension leucogranite deformation during convergence in the Eastern Central Alps: example of the Novate intrusion. *Terra Nova*, *18*(3), 170-180.

Corfu, F., Hanchar, J. M., Hoskin, P. W., & Kinny, P. (2003). Atlas of zircon textures. *Reviews in mineralogy and geochemistry*, *53*(1), 469-500.

Davidson, C., Rosenberg, C., & Schmid, S. M. (1996). Synmagmatic folding of the base of the Bergell pluton, Central Alps. *Tectonophysics*, *265*(3), 213-238.

Engi, M., Berger, A., & Roselle, G. T. (2001). Role of the tectonic accretion channel in collisional orogeny. *Geology*, *29*(12), 1143-1146.

Galli, A., Le Bayon, B., Schmidt, M. W., Burg, J. P., Caddick, M. J., & Reusser, E. (2011). Granulites and charnockites of the Gruf Complex: Evidence for

Permian ultra-high temperature metamorphism in the Central Alps. *Lithos*, *124*(1), 17-45.

Galli, A., Le Bayon, B., Schmidt, M. W., Burg, J. P., Reusser, E., Sergeev, S. A., & Larionov, A. (2012). U–Pb zircon dating of the Gruf Complex: disclosing the late Variscan granulitic lower crust of Europe stranded in the Central Alps. *Contributions to Mineralogy and Petrology*, *163*(2), 353-378.

Galli, A., Le Bayon, B., Schmidt, M. W., Burg, J. P., & Reusser, E. (2013). Tectonometamorphic history of the Gruf complex (Central Alps): exhumation of a granulite–migmatite complex with the Bergell pluton. *Swiss Journal of Geosciences*, *106*(1), 33-62.

Gebauer, D. (1996). A P-T-t Path for an (ultra?-) High-Pressure Ultramafic/Mafic Rock-Association and Its Felsic Country-Rocks Based on SHRIMP-Dating of Magmatic And Metamorphic Zircon Domains. Example: Alpe Arami (Central Swiss Alps). *Earth processes: Reading the isotopic code*, 307-329.

Ghizzoni, S., & Mazzoleni, G. (2005). *Itinerari mineralogici in Val Codera*. Geologia Insubrica.

Gramaccioli C. M. (1986). Conoscere i minerali, i fosfati. Istituto Geografico De Agostini.

Guastoni, A. (2012). LCT (lithium, cesium, tantalum) and NYF (niobium, yttrium, fluorine) pegmatites in the Central Alps. Exhumation history, mineralogy and geochemistry. Ph.D. Thesis, XIV° cycle, Department of Geoscience, University of Padova.

Guastoni, A., Pennacchioni, G., Pozzi, G., Fioretti, A. M., & Walter, J. M. (2014). Tertiary pegmatite dikes of the Central Alps. *The Canadian Mineralogist*, *52*(2), 191-219.

Liati, A., Gebauer, D., & Fanning, M. (2000). U-PbSHRIMP dating of zircon from the Novate granite (Bergell, Central Alps): evidence for Oligocene-Miocene magmatism, Jurassic/Cretaceous continental rifting and opening of the Valais trough. *Schweizerische mineralogische und petrographische Mitteilungen*, *80*(3), 305-316.

Liati, A., & Gebauer, D. (2003). Geochronological constraints for the time of metamorphism in the Gruf Complex (Central Alps) and implications for the Adula-Cima Lunga nappe system. *Swiss Bulletin of Mineralogy and Petrology*, *83*(2), 159-172.

London, D. (2008). *Pegmatites* (Vol. 10). Ottawa, Canada: Mineralogical Association of Canada.

Maxelon, M., & Mancktelow, N. S. (2005). Three-dimensional geometry and tectonostratigraphy of the Pennine zone, Central Alps, Switzerland and Northern Italy. *Earth-Science Reviews*, *71*(3), 171-227.

Nagel, T., De Capitani, C., Frey, M., Froitzheim, N., Stunitz, H., & Schmid, S. M. (2002). Structural and metamorphic evolution during rapid exhumation in the Lepontine dome (southern Simano and Adula nappes, Central Alps, Switzerland). *Eclogae Geologicae Helvetiae*, *95*(3), 301-321.

Nagel, T. J. (2008). Tertiary subduction, collision and exhumation recorded in the Adula nappe, central Alps. *Geological Society, London, Special Publications*, *298*(1), 365-392.

Paquette, J. L., & Tiepolo, M. (2007). High resolution (5 μm) U–Th–Pb isotope dating of monazite with excimer laser ablation (ELA)-ICPMS. *Chemical Geology*, *240*(3), 222-237.

Pennacchioni, G. (2005). Control of the geometry of precursor brittle structures on the type of ductile shear zone in the Adamello tonalites, Southern Alps (Italy). *Journal of Structural Geology*, *27*(4), 627-644.

Pennacchioni, G., Menegon, L., Leiss, B., Nestola, F., & Bromiley, G. (2010). Development of crystallographic preferred orientation and microstructure during plastic deformation of natural coarse-grained quartz veins. *Journal of Geophysical Research: Solid Earth (1978–2012)*, *115*(B12).

Pennacchioni, G., & Zucchi, E. (2013). High temperature fracturing and ductile deformation during cooling of a pluton: The Lake Edison granodiorite (Sierra Nevada batholith, California). *Journal of Structural Geology*, *50*, 54-81.

Romer, R. L., Schärer, U., & Steck, A. (1996). Alpine and pre-Alpine magmatism in the root-zone of the western Central Alps. *Contributions to Mineralogy and Petrology*, *123*(2), 138-158.

Rosenberg, C., Berger, A., Davidson, C., & Schmid, S. M. (1994). Messa in posto del plutone di Masino-Bregaglia, Alpi Centrali. *Atti Ticinensi Sci. Terra Ser. spec*, *1*, 31-39.

Rosenberg, C. L., Berger, A., & Schmid, S. M. (1995). Observations from the floor of a granitoid pluton: inferences on the driving force of final emplacement. *Geology*, *23*(5), 443-446.

Rubatto, D., Hermann, J., Berger, A., & Engi, M. (2009). Protracted fluid-induced melting during Barrovian metamorphism in the Central Alps. *Contributions to Mineralogy and Petrology*, *158*(6), 703-722.

Schärer, U., Cosca, M., Steck, A., & Hunziker, J. (1996). Termination of major ductile strike-slip shear and differential cooling along the Insubric line (Central Alps): U□ Pb, Rb□ Sr and 40Ar39Ar ages of cross-cutting pegmatites. *Earth and planetary science letters*, *142*(3), 331-351.

Schmid, S. M., Pfiffner, O. A., Froitzheim, N., Schönborn, G., & Kissling, E. (1996). Geophysical-geological transect and tectonic evolution of the Swiss-Italian Alps. *Tectonics*, *15*(5), 1036-1064.

Todd C. S., & Engi, M. (1997). Metamorphic field gradients in the Central Alps. *Journal of Metamorphic Geology*, *15*(4), 513-530.

Trommsdorff, V., & Connolly, J. A. (1996). The ultramafic contact aureole about the Bregaglia (Bergell) tonalite: isograds and a thermal model. *Schweizerische Mineralogische und Petrographische Mitteilungen*, *76*, 537-547.

Vernon, R. H. (2004). *A practical guide to rock microstructure*. Cambridge university press.

Von Blackenburg, F. (1992). Combined high-precision chronometry and geochemical tracing using accessory minerals: applied to the Central-Alpine Bergell intrusion (central Europe). *Chemical Geology*, *100*(1), 19-40.

Von Blanckenburg, F., & Davies, J. H. (1995). Slab breakoff: a model for syncollisional magmatism and tectonics in the Alps. *Tectonics*, *14*(1), 120-131.

Wenk, E. (1970). Zur regionalmetamorphose und Ultrametamorphose im Lepontin. *Fortschr. Mineral*, *47*, 34-51.

Wenk, H. R. (1973). The structure of the Bergell Alps. *Eclogae Geol. Helv*, *66*, 255-291.

APPENDICES

I. Analytical methods

8.5. Scanning Electron Microscope Backscattered Electrons imaging

The electronic microscope used for BSE imaging is the CamScan MX3000 at the SEM laboratory of the Dipartimento di Geoscienze of Padova. The electron beam source is a LaB6 crystal working at standard conditions of 15-20 kV and a current of ~1 nA on the sample. It is equipped with a solid-state semiconductor BSE detector which has 4 indipendent sectors. At optimum working conditions (10 mm working distance) the resolution is better than 50 nm for silicates.

8.6. Electron Microprobe Analysis (EMPA)

Electron-microprobe analyses were performed on garnet, tourmaline, monazite, thorite and xenotime samples (also for some inclusions) at the laboratory of microanalysis of the Istituto di Geoscienze e Georisorse (IGG) of CNR (Padova). The instrument used is a CAMECA SX-50 electron microprobe, equipped with four Wavelength Dispersive Spectrometers (WDS) and one Energy Dispersive Spectrometer (EDS). The operating conditions were 20 kV accelerating voltage and 20 nA beam current. Counting times were 10 s at the peak and 5 s at the background for major elements and 20 to 100 s at peak and background for minor elements. X-ray counts were converted into oxide weight percentages using the PAP correction program. Analyses are precise to within 1% for major elements and 3–5% for minor elements. Calibration was carried using natural and synthetic international standards in part supplied by Cameca and in part kindly provided by the Smithsonian National Museum of Natural History (Smithsonian Microbeam Standards).

8.7. Laser Ablation and Induced Coupled Plasma Mass Spectrometry (LA-ICP-MS)

Isotopic analyses on monazite were obtained with the LA-ICP-MS technique at the Istituto di Geoscienze e Georisorse (IGG) of CNR (Pavia). The instrument consists in a laser apparatus coupled with a mass spectrometer. The former is the commercial GeoLas102 from MicroLas (Göttingen, Germany), which works with a wavelength of 193 nm and a maximum output energy of 200 mJ per pulse. Spot size depends on focusing and can be varied from 5 to 120 µm. For monazite samples the spot size choice depends on the concentration of U and Th. In order to increase the signal vs. background ratio in high-U/Th monazites a small spot size is recommended. Highly focused beam can be even used to resolve age domains in zoned crystals. The mass spectrometer consists in a single collector double-focusing sector field ICPMS with reverse geometry (type Element I from ThermoFinnigan, Bremen, Germany).

Isotope dating of monazite with laser ablation ICPMS is operated with an analytical method basically similar to that developed for zircon (Paquette and Tiepolo, 2007). The signal of ^{202}Hg, ^{204}(Pb+Hg), ^{206}Pb, ^{207}Pb, ^{208}Pb, ^{232}Th and ^{238}U masses are acquired, where ^{202}Hg is used to correct the isobaric interference of ^{204}Hg on ^{204}Pb by peak stripping. This allows to monitor the presence of common Pb in the sample. The ^{235}U signal is calculated from ^{238}U on the basis of the ratio $^{238}U/^{235}U = 137.88$. The high sensitivity and low background allows extremely low limits of detection (down to the ppb level) for the heaviest elements, and between 10 and 100 ppb for the lighter masses. Precision and accuracy in age determinations to better than ~2% were attained on the zircon standard 91500 (Paquette and Tiepolo 2007). Analytical conditions used for monazites are the same reported by Paquette and Tiepolo (2007). Thanks to the large size and quality of monazites a 10 µm spot size was used to get more accurate data. The standard used for monazite dating is the Moacir sample described by Paquette and Tiepolo (2007).

II. <u>EMP and LA-ICP-MS analyses results</u>

Following tables include all EMP and LA-ICP-MS results for each analysis spot (An. Pt.) on sampled crystals. The positions of the spots are reported on photographic tables in the attached CD.

- Pages 86-94 Garnet EMPA
- Pages 95-99 Tourmaline EMPA
- Page 99 Inclusions EMPA
- Pages 100-101 Monazite EMPA
- Page 102 Monazite, Thorite and Xenotime LA-ICP-MS

Sample code	Crystal	An. Pt.	SiO_2	TiO_2	Al_2O_3	Cr_2O_3	$FeO+Fe_2O_3$	MnO	MgO	CaO	Sum	Alm	Sps	Pyr
Codera Garnet dike														
CODg(gg)1	-	1-001	35,5370	0,0735	20,0812	0,0000	14,7549	27,2978	0,4728	0,3628	98,5800	31,9659	64,9616	1,9803
CODg(gg)1	-	1-002	35,7828	0,0809	20,1736	0,0000	14,8627	27,2213	0,4628	0,4134	98,9975	32,5141	64,3253	1,9248
CODg(gg)1	-	1-003	36,0087	0,0915	20,1208	0,0000	14,6876	27,7586	0,4202	0,3833	99,4707	31,9556	65,1697	1,7363
CODg(gg)1	-	1-004	35,7039	0,0584	20,4814	0,0000	14,5763	27,4586	0,4733	0,3863	99,1382	31,8084	65,0600	1,9738
CODg(gg)1	-	1-005	35,8657	0,0629	20,0935	0,0000	14,8650	27,5825	0,4859	0,4116	99,3671	31,7021	65,0529	2,0170
CODg(gg)1	-	1-006	35,9201	0,1005	20,1178	0,0262	14,8061	27,3805	0,4791	0,4367	99,2670	32,2877	64,4282	1,9842
CODg(gg)1	-	1-007	35,9510	0,0949	20,1596	0,0240	14,9680	27,3711	0,4669	0,3750	99,4105	32,5940	64,3584	1,9322
CODg(gg)1	-	1-008	35,7576	0,1078	20,4026	0,0000	15,1710	27,1823	0,4713	0,3684	99,4610	32,6961	64,2420	1,9604
CODg(gg)1	-	1-009	35,7291	0,1049	20,2359	0,0306	14,8641	27,6053	0,4569	0,4215	99,4483	31,5390	65,2976	1,9022
CODg(gg)1	-	1-010	35,7420	0,1067	20,2779	0,0000	15,1713	27,2450	0,4930	0,4189	99,4548	32,2757	64,4197	2,0516
CODg(gg)1	-	1-011	35,7570	0,0932	20,2643	0,0000	14,9060	27,4894	0,5077	0,3911	99,4087	31,7290	64,9888	2,1125
CODg(gg)1	-	1-012	36,0181	0,0848	20,2155	0,0175	15,3102	26,9609	0,4928	0,4029	99,5027	33,4782	63,2893	2,0361
CODg(gg)1	-	1-013	35,9144	0,0892	20,2443	0,0000	14,6967	27,7710	0,4441	0,4283	99,5880	31,5118	65,3729	1,8400
CODg(gg)1	-	1-014	35,6787	0,0634	20,3270	0,0284	14,4186	27,6435	0,4070	0,3811	98,9477	31,6214	65,5374	1,6983
CODg(gg)1	-	1-015	35,9380	0,0803	20,2986	0,0000	15,4647	26,9811	0,5392	0,4279	99,7298	33,0099	63,4836	2,2329
CODg(gg)1	-	1-016	35,8064	0,1061	20,0249	0,0546	15,1255	27,2388	0,5016	0,4010	99,2589	32,4287	64,2903	2,0837
CODg(gg)1	-	1-017	35,8812	0,0831	20,1968	0,0000	14,9886	27,0084	0,4735	0,4306	99,0622	33,1080	63,6445	1,9638
CODg(gg)1	-	1-018	35,7710	0,1246	19,8056	0,0240	15,0774	27,3905	0,4451	0,4353	99,0735	32,1623	64,6871	1,8501
CODg(gg)1	-	1-019	36,1358	0,0410	20,2652	0,0000	15,2605	26,8973	0,5050	0,3642	99,4690	33,8474	62,9920	2,0816
CODg(gg)1	-	1-020	35,6834	0,0719	19,9979	0,0371	15,0236	27,1767	0,5388	0,4083	98,9377	32,1176	64,4107	2,2476
CODg(gg)1	-	1-021	36,1796	0,0629	20,1419	0,0000	15,2757	27,1070	0,4842	0,4402	99,6915	33,3280	63,3775	1,9925
CODg(gg)1	-	1-022	35,9021	0,1213	20,1187	0,0000	15,5743	26,8125	0,4983	0,3962	99,4234	33,6610	63,0958	2,0638
CODg(gg)1	-	1-023	36,0224	0,1168	19,8626	0,0000	15,4934	26,9346	0,4708	0,4511	99,3517	33,5400	63,1779	1,9436
CODg(gg)1	-	1-024	35,7153	0,1067	20,0640	0,0414	15,6113	26,7157	0,5029	0,4450	99,2023	33,3582	63,2153	2,0944
CODg(g)2	-	1-001	36,1854	0,0084	20,6882	0,0239	17,6463	24,1825	0,3977	0,2641	99,3965	40,9851	56,5949	1,6382
CODg(g)2	-	1-002	35,8174	0,0809	20,0482	0,0065	16,4428	25,8625	0,3934	0,2896	98,9413	36,4451	61,0554	1,6346
CODg(g)2	-	1-003	35,6420	0,1000	20,1045	0,0022	16,2595	25,9262	0,4030	0,2891	98,7265	35,9689	61,4818	1,6820
CODg(g)2	-	1-004	35,8479	0,0775	20,0985	0,0109	16,2426	26,2438	0,4313	0,3024	99,2549	35,3996	61,9074	1,7907
CODg(g)2	-	1-005	35,9213	0,1101	20,2968	0,0000	16,5974	26,1936	0,4274	0,3118	99,8584	35,6815	61,6209	1,7697
CODg(g)2	-	1-006	35,8198	0,1107	20,3156	0,0152	16,3466	26,0862	0,3862	0,2630	99,3433	36,0706	61,5410	1,6036
CODg(g)2	-	1-007	35,9042	0,1034	19,9583	0,0044	16,2538	25,7241	0,3614	0,2964	98,6060	37,0664	60,5536	1,4973
CODg(g)2	-	1-008	35,6417	0,0893	20,3035	0,0000	16,5564	25,8091	0,4579	0,2980	99,1559	35,9758	61,2184	1,9116
CODg(g)2	-	1-009	35,8994	0,1107	20,0968	0,0000	16,4380	25,8122	0,4542	0,3125	99,1238	36,4279	60,7599	1,8818
CODg(g)2	-	1-010	35,7291	0,0914	19,9844	0,0239	16,4119	26,4227	0,4873	0,2588	99,4095	34,6780	62,5180	2,0293
CODg(g)2	-	1-011	35,8564	0,0843	19,9924	0,0000	16,4603	25,8467	0,3807	0,2713	98,8921	36,6632	60,9475	1,5800
CODg(g)2	-	1-012	36,0366	0,0669	20,1159	0,0022	16,2826	26,0584	0,4516	0,2814	99,2956	36,1367	61,1622	1,8656
CODg(g)2	-	1-013	35,5575	0,1085	20,2545	0,0196	16,2793	25,6550	0,4191	0,2931	98,5866	36,3938	60,9720	1,7531
CODg(g)2	-	1-014	35,4124	0,0876	20,1290	0,0000	15,8703	26,1958	0,4173	0,3129	98,4253	34,7621	62,5395	1,7535
CODg(g)2	-	1-015	35,9737	0,0905	20,0895	0,0174	16,5363	25,8060	0,4163	0,3025	99,2322	36,7332	60,6457	1,7219
CODg(g)2	-	1-016	35,4666	0,0757	20,1647	0,0000	16,6094	26,1015	0,4148	0,2683	99,1010	35,2151	62,2349	1,7407
CODg(g)2	-	1-017	36,0241	0,0911	20,0525	0,0000	16,1747	25,7941	0,4306	0,3037	98,8708	36,7876	60,5323	1,7785
CODg(g)2	-	1-018	35,8912	0,0972	20,0648	0,0000	16,2292	25,8634	0,4228	0,2864	98,8550	36,4827	60,9115	1,7526
CODg(g)2	-	1-019	35,6779	0,0876	20,1276	0,0653	16,3275	26,1593	0,4066	0,2923	99,1441	35,4396	61,9884	1,6958
CODg(g)2	-	1-020	35,3350	0,0803	20,1243	0,0044	16,2924	25,9171	0,4718	0,2901	98,5154	35,1157	62,0190	1,9871
CODg(g)2	-	1-021	35,9885	0,0827	20,4985	0,0000	16,4135	25,7461	0,4412	0,2893	99,4598	36,8258	60,4899	1,8244
CODg(g)2	-	1-022	35,4860	0,1016	20,0676	0,0000	16,2862	26,2332	0,4263	0,3122	98,9131	34,7918	62,4806	1,7870
CODg(g)2	-	1-023	35,8190	0,1246	20,1870	0,0000	16,4351	26,5109	0,3973	0,2666	99,7405	35,0293	62,5261	1,6492
CODg(g)2	-	1-024	35,6617	0,0781	20,2255	0,0000	16,5362	25,8359	0,3955	0,3024	99,0353	36,1803	61,2621	1,6506
CODg(g)2	-	1-025	35,7365	0,1168	20,2215	0,0087	16,7342	26,0926	0,4435	0,3067	99,6605	35,5458	61,6913	1,8455
CODg(g)2	-	1-026	35,8924	0,1011	20,1696	0,0305	16,5655	25,9076	0,4565	0,3325	99,4557	36,1090	61,0085	1,8920
CODg(g)2	-	1-027	35,7248	0,1134	20,0022	0,0000	16,4898	26,2901	0,3708	0,3172	99,3083	35,3243	62,1830	1,5436
CODg(g)2	-	1-028	36,0445	0,0573	20,0513	0,0000	16,7510	25,7162	0,3733	0,3264	99,3200	37,1310	60,3579	1,5421
CODg(g)2	-	1-029	35,6345	0,0449	20,1626	0,0152	16,4911	25,8714	0,3708	0,3202	98,9107	36,0524	61,4360	1,5498
CODg(g)2	-	1-030	36,0575	0,0640	20,1904	0,0000	16,5211	25,9800	0,4313	0,2941	99,5384	36,3999	60,9466	1,7808
CODg(g)2	-	1-031	35,6673	0,0898	20,1456	0,0000	16,3700	26,2015	0,4189	0,2651	99,1582	35,3536	62,1040	1,7475
CODg(g)2	-	1-032	35,7087	0,1235	20,2455	0,0044	16,5581	26,0311	0,4378	0,3023	99,4114	35,6873	61,5850	1,8230
CODg(g)2	-	1-033	35,8213	0,1011	20,2148	0,0000	16,7309	25,9534	0,4333	0,2873	99,5421	36,1056	61,2374	1,7994
CODg(g)2	-	1-034	35,8300	0,1382	20,0456	0,0044	16,2728	26,1237	0,4278	0,3463	99,1888	35,6162	61,5765	1,7748
CODg(g)2	-	1-035	35,5937	0,0690	20,0993	0,0239	16,5604	26,2089	0,4246	0,3067	99,2865	35,0253	62,2770	1,7758
CODg(g)2	-	1-036	36,0006	0,0781	20,3266	0,0327	16,4410	26,1144	0,3718	0,2763	99,6415	36,3014	61,3405	1,5371
CODg(g)2	-	1-037	36,0095	0,0483	20,1216	0,0000	16,2714	25,9115	0,4457	0,2853	99,0933	36,4219	60,8867	1,8433
CODg(g)2	-	1-038	35,8146	0,0859	20,2891	0,0000	16,6110	25,9736	0,4181	0,2991	99,4914	36,0535	61,3161	1,7372
CODg(g)2	-	1-039	35,7664	0,0937	20,2275	0,0022	16,7339	26,0880	0,3962	0,3089	99,6168	35,7694	61,6589	1,6481
CODg(g)2	-	1-040	35,5017	0,1005	20,1178	0,0218	16,4492	25,9642	0,4283	0,3101	98,8936	35,4574	61,8140	1,7947
CODg(g)2	-	1-041	36,0697	0,0646	20,2177	0,0022	16,6173	26,1546	0,3971	0,2935	99,8167	36,1557	61,3347	1,6390
CODg(g)2	-	1-042	35,7306	0,1152	20,2109	0,0174	16,1222	25,8607	0,4873	0,3009	98,8452	35,9165	61,1552	2,0282
CODg(g)2	-	1-043	35,6120	0,1197	20,1590	0,0044	16,0575	25,9828	0,2312	0,3158	98,4824	36,4447	61,6422	0,9654
CODg(gg)2	-	1	35,9612	0,0920	20,0060	0,0611	15,4235	27,3776	0,1796	0,2860	99,3870	34,0471	64,3593	0,7431
CODg(gg)2	-	2	35,5438	0,0966	20,3909	0,0000	16,5834	26,0768	0,3940	0,3467	99,4322	35,2940	62,0138	1,6491
CODg(gg)2	-	3	36,1291	0,0185	20,4871	0,0022	15,0721	26,8245	0,2482	0,2509	99,0326	35,3699	62,8626	1,0237
CODg(gg)2	-	1-001	35,7490	0,0258	20,5310	0,0000	15,2646	27,0280	0,2385	0,2268	99,0637	34,3237	64,0029	0,9940
CODg(gg)2	-	1-002	36,3579	0,0534	20,6768	0,0000	16,9225	25,4610	0,3262	0,2616	100,0594	38,6447	59,2492	1,3360
CODg(gg)2	-	1-003	35,7481	0,0870	20,3398	0,0436	16,1543	26,5603	0,4359	0,2939	99,6629	34,4902	62,8161	1,8145
CODg(gg)2	-	1-004	35,8030	0,0893	20,1064	0,0000	16,2068	26,3011	0,4210	0,2601	99,1877	35,3685	62,1049	1,7497
CODg(gg)2	-	1-005	35,5654	0,0719	20,2180	0,0022	16,5457	25,9759	0,3930	0,2806	99,0527	35,7425	61,7687	1,6448
CODg(gg)2	-	1-006	35,5017	0,1000	20,1020	0,0479	16,1397	26,1663	0,3856	0,3258	98,7690	35,1072	62,2958	1,6158
CODg(gg)2	-	1-007	35,5394	0,1282	20,0799	0,0000	16,0291	25,7145	0,3846	0,3064	98,1821	36,3508	61,1190	1,6089
CODg(gg)2	-	1-008	35,3950	0,1180	20,1271	0,0065	15,8594	26,0722	0,4282	0,2729	98,2793	35,1422	62,2348	1,7990
CODg(gg)2	-	1-009	36,3797	0,0889	20,6786	0,0065	17,6612	24,8835	0,4156	0,2788	100,3928	39,6522	57,8282	1,6999
CODg(gg)2	-	1-010	36,1830	0,0484	20,2788	0,0195	19,4006	22,7672	0,5125	0,2395	99,4495	43,9402	53,2419	2,1094
Codera Phosphate dike														
CODp(g)1	-	1-001	36,3120	0,0135	20,2900	0,0000	15,9652	26,0923	0,4222	0,4141	99,5093	36,2005	60,8451	1,7328
CODp(g)1	-	1-002	35,6111	0,1251	19,7933	0,0000	16,2635	26,0986	0,6089	0,4479	98,9484	34,2022	61,9114	2,5423
CODp(g)1	-	1-003	35,9919	0,0640	20,1222	0,0000	15,4062	26,5602	0,5305	0,4038	99,0788	34,1841	62,4211	2,1944
CODp(g)1	-	1-004	35,9223	0,0634	20,1888	0,0523	15,4305	26,6396	0,5459	0,3627	99,2055	33,9275	62,7296	2,2625
CODp(g)1	-	1-005	35,9611	0,0466	19,7415	0,0000	15,3309	26,3472	0,5546	0,3655	98,3474	34,6192	61,9960	2,2968
CODp(g)1	-	1-006	35,6671	0,0927	20,0003	0,0131	15,3760	26,1690	0,5143	0,4433	98,2758	34,5020	62,0235	2,1454
CODp(g)1	-	1-007	35,8413	0,0589	19,7955	0,0000	15,7312	26,5920	0,5547	0,4218	98,9954	33,6715	62,7648	2,3043
CODp(g)1	-	1-008	36,0073	0,0953	19,7692	0,0000	15,8827	26,6703	0,5050	0,4295	99,3593	34,0257	62,6122	2,0866
CODp(g)1	-	1-009	35,9673	0,0842	19,8697	0,0152	15,9335	26,0092	0,5316	0,4039	98,8146	35,4573	61,1421	2,1995
CODp(g)1	-	1-010	35,9588	0,1353	19,6341	0,0022	15,6109	26,3689	0,5182	0,4048	98,6332	34,7188	61,9362	2,1423
CODp(g)1	-	1-011	35,6018	0,1211	20,0000	0,0000	15,3769	26,8828	0,5338	0,4118	98,9282	32,7406	63,7937	2,2295
CODp(g)1	-	1-012	35,2336	0,0908	19,8944	0,0000	15,7683	26,7911	0,5284	0,3987	98,7053	32,2783	64,2803	2,2314
CODp(g)1	-	1-013	35,8660	0,0841	20,0197	0,0000	15,7276	26,8602	0,5584	0,3957	99,5117	33,1823	63,3208	2,3169
CODp(g)1	-	1-014	35,5943	0,1094	20,0106	0,0000	15,6465	26,7228	0,5647	0,4317	99,0800	32,9009	63,4430	2,3596
CODp(g)1	-	1-015	35,7114	0,0768	19,9032	0,0000	15,5528	26,8164	0,5320	0,3740	98,9666	33,1620	63,5004	2,2172
CODp(g)1	-	1-016	35,6330	0,1260	19,9085	0,0000	16,0574	27,0451	0,5406	0,4047	99,7153	32,4145	64,1162	2,2557
CODp(g)1	-	1-017	36,0531	0,1212	19,8222	0,0087	15,9501	26,5663	0,5423	0,4518	99,5157	34,1686	62,2554	2,2367

Sample code	Crystal	An. Pt.	SiO_2	TiO_2	Al_2O_3	Cr_2O_3	$FeO+Fe_2O_3$	MnO	MgO	CaO	Sum	Alm	Sps	Pyr
CODp(g)1	-	1-018	36,0443	0,0791	19,9305	0,0109	15,9262	26,7508	0,5196	0,4312	99,6926	33,8169	62,7580	2,1455
CODp(g)1	-	1-019	35,8372	0,1452	19,7840	0,0022	15,7249	26,6769	0,4854	0,4101	99,0659	33,9060	62,8586	2,0130
CODp(g)1	-	1-020	35,8000	0,0898	19,8825	0,0087	15,7726	26,5100	0,5319	0,4457	99,0412	33,8551	62,6027	2,2107
CODp(g)1	-	1-021	36,1237	0,0859	20,0312	0,0131	15,3236	27,0448	0,5466	0,4319	99,6008	33,1700	63,2995	2,2517
CODp(g)1	-	1-022	35,0105	0,1132	19,9377	0,0000	15,3826	26,9197	0,5188	0,4153	98,2978	31,5600	64,9684	2,2037
CODp(g)1	-	1-023	35,3754	0,0829	20,0461	0,0000	15,7675	27,2265	0,5847	0,3881	99,4712	31,2924	65,0745	2,4597
CODp(g)1	-	1-024	36,0753	0,0831	19,8947	0,0000	15,7262	26,4371	0,5233	0,4460	99,1857	34,5553	61,9637	2,1587
CODp(g)1	-	1-025	35,9349	0,0808	20,0723	0,0000	15,7871	26,6731	0,4899	0,4558	99,4939	33,8507	62,7637	2,0289
CODp(g)1	-	1-026	35,9136	0,0747	19,7908	0,0109	15,5780	26,0645	0,5317	0,3550	98,3192	35,3632	61,3757	2,2036
CODp(g)1	-	1-027	35,5464	0,0589	19,9117	0,0000	15,4196	26,9632	0,5666	0,3629	98,8293	32,3660	64,1682	2,3733
CODp(g)1	-	1-028	35,7331	0,0988	19,9283	0,0218	15,8315	26,3527	0,5240	0,4447	98,9349	34,1520	62,3358	2,1816
CODp(g)1	-	1-029	35,8984	0,1055	19,9731	0,0087	15,6600	26,6449	0,5268	0,4114	99,2288	33,8634	62,7285	2,1828
CODp(g)1	-	1-030	35,6160	0,0925	19,8417	0,0000	15,5206	26,8785	0,5594	0,4561	98,9648	32,4971	63,7966	2,3369
CODp(g)1	-	1-031	35,7899	0,0712	19,9617	0,0000	15,6482	26,8914	0,5325	0,4256	99,3205	32,9670	63,5461	2,2147
CODp(g)1	-	1-032	35,6796	0,0438	20,2905	0,0022	15,4565	26,4752	0,5596	0,3532	98,8606	33,8125	62,7919	2,3360
CODp(g)1	-	1-033	36,0292	0,0427	20,0166	0,0044	15,5846	26,6096	0,6014	0,3932	99,2817	33,8453	62,5003	2,4862
CODp(g)1	-	1-034	35,9252	0,0842	19,9817	0,0000	15,3898	26,7771	0,5831	0,3620	99,1031	33,4860	63,0209	2,4154
CODp(g)1	-	1-035	35,9233	0,0438	19,8802	0,0000	15,4900	26,6564	0,6147	0,3704	98,9788	33,5545	62,7932	2,5486
CODp(g)1	-	1-036	35,9854	0,0460	19,8781	0,0152	15,7848	26,7647	0,5514	0,3547	99,3803	33,7261	62,9367	2,2821
CODp(g)1	-	1-037	35,8854	0,0628	19,8739	0,0000	15,5924	26,7041	0,5324	0,3880	99,0390	33,6874	62,9468	2,2088
CODp(g)1	-	1-038	36,0412	0,0590	19,9184	0,0153	15,6335	26,1791	0,5435	0,3895	98,7795	35,1504	61,4478	2,2453
CODp(g)1	-	1-039	36,0585	0,0521	20,1231	0,0000	15,8442	26,9778	0,5369	0,3674	99,9600	33,3909	63,3012	2,2173
CODp(g)1	-	1-040	35,7415	0,0803	19,9680	0,0000	15,3131	26,3528	0,5072	0,3911	98,3540	34,3720	62,3456	2,1119
CODp(g)1	-	1-041	36,1878	0,0657	19,7474	0,0152	15,7136	26,3650	0,5517	0,3710	99,0174	35,0082	61,6252	2,2696
CODp(g)1	-	1-042	36,2348	0,0668	19,8853	0,0065	15,5041	26,5442	0,5441	0,3383	99,1241	34,8034	61,9622	2,2354
CODp(g)1	-	1-043	35,7799	0,0926	20,0029	0,0000	15,8692	26,4589	0,5216	0,4169	99,1420	34,0716	62,5134	2,1690
CODp(g)1	-	1-044	35,8004	0,1055	20,1932	0,0153	15,3748	26,6409	0,5725	0,4087	99,1113	33,5104	62,8904	2,3787
CODp(g)1	-	1-045	35,5909	0,0718	19,7611	0,0000	15,5039	26,6884	0,5576	0,4229	98,5966	32,9791	63,4177	2,3320
CODp(gg)1	-	1	36,1029	0,1094	19,9411	0,0153	15,4991	26,9009	0,4527	0,3836	99,4050	34,0309	62,9682	1,8650
CODp(gg)1	-	2	35,7773	0,0987	19,9236	0,0000	15,1485	26,9800	0,4547	0,4657	98,8485	32,9764	63,7411	1,8907
CODp(gg)1	-	3	35,6240	0,1071	19,6546	0,0022	15,3686	26,9838	0,5652	0,4516	98,7571	32,2725	64,0125	2,3599
CODp(gg)1	-	4	35,6456	0,1260	19,7249	0,0000	15,8505	27,0298	0,4133	0,4031	99,1932	33,0103	64,0573	1,7239
CODp(gg)1	-	1-001	35,7265	0,0712	20,0875	0,0174	15,4858	26,9867	0,5155	0,4256	99,3162	32,6934	63,8843	2,1478
CODp(gg)1	-	1-002	35,6670	0,1087	20,0795	0,0000	15,3441	26,8124	0,5333	0,4239	98,9689	32,9784	63,5272	2,2239
CODp(gg)1	-	1-003	35,8394	0,1396	19,8415	0,0000	15,5482	26,9163	0,5546	0,4223	99,2619	33,0148	63,4263	2,3002
CODp(gg)1	-	1-004	35,9888	0,1088	20,0571	0,0000	15,6814	26,7346	0,4999	0,3991	99,4697	33,9708	62,7776	2,0660
CODp(gg)1	-	1-005	36,0215	0,0696	19,8049	0,0087	15,6363	26,3112	0,4948	0,4371	98,7841	34,8790	61,7779	2,0448
CODp(gg)1	-	1-006	35,9514	0,1072	19,9009	0,0240	15,5824	26,6644	0,4990	0,4152	99,1445	34,0210	62,6799	2,0645
CODp(gg)1	-	1-007	35,8753	0,0965	20,0845	0,0000	15,3691	26,7089	0,5082	0,4037	99,0462	33,7578	62,9315	2,1075
CODp(gg)1	-	1-008	35,5592	0,1031	20,0784	0,0196	15,3679	27,2480	0,5150	0,4165	99,3077	31,8312	64,7622	2,1544
CODp(gg)1	-	1-009	35,6939	0,0583	19,7897	0,0261	15,5347	26,7645	0,5382	0,4467	98,8521	32,9824	63,4333	2,2450
CODp(gg)1	-	1-010	35,9386	0,0646	19,7735	0,0000	15,4812	26,3631	0,5161	0,4160	98,5531	34,5747	62,0488	2,1379
CODp(gg)1	-	1-011	35,9210	0,0836	20,0820	0,0065	15,7026	26,6682	0,4884	0,4069	99,3592	33,9923	62,7727	2,0234
CODp(gg)1	-	1-012	35,9780	0,0449	20,2482	0,0109	15,8453	26,2051	0,4521	0,4144	99,1989	35,2606	61,6349	1,8715
CODp(gg)1	-	2-001	35,9011	0,0645	20,1299	0,0022	15,4101	27,1903	0,4199	0,3801	99,4981	33,0632	64,0626	1,7412
CODp(gg)1	-	2-002	35,6904	0,1032	20,0480	0,0284	15,0268	27,3870	0,4731	0,3935	99,1504	31,9958	64,8537	1,9718
CODp(gg)1	-	2-003	35,7899	0,0785	19,8877	0,0174	15,1949	27,0921	0,4374	0,3607	98,8586	33,0925	64,0105	1,8189
CODp(gg)1	-	2-004	35,6273	0,0701	19,6002	0,0000	15,3740	26,6958	0,4535	0,3829	98,2038	33,5826	63,3728	1,8948
CODp(gg)1	-	2-005	35,4218	0,0566	20,2326	0,0000	15,2493	27,0893	0,3927	0,3945	98,8368	32,4594	64,6980	1,6507
CODp(gg)1	-	2-006	35,7478	0,0718	20,0653	0,0000	15,5502	26,7034	0,3874	0,3797	98,9056	34,0753	63,1752	1,6131
CODp(gg)1	-	2-007	35,8233	0,0953	19,9123	0,0305	15,0559	27,0093	0,4736	0,3878	98,7880	33,1425	63,7330	1,9669
CODp(gg)1	-	2-008	35,9143	0,0718	19,9888	0,0000	15,1870	27,2534	0,4644	0,3740	99,2537	32,7832	64,1779	1,9248
CODp(gg)1	-	2-009	35,8109	0,0482	19,8200	0,0065	15,2254	27,6379	0,4928	0,3371	99,3788	31,6397	65,3034	2,0494
CODp(gg)1	-	2-010	35,8502	0,0696	20,0530	0,0131	14,9633	27,3780	0,4512	0,3898	99,1682	32,3738	64,5894	1,8735
CODp(gg)1	-	2-011	35,6661	0,0913	19,6982	0,0392	15,4158	27,0695	0,4789	0,3866	98,8456	32,6815	64,1615	1,9978
CODp(gg)1	-	2-012	35,6520	0,0974	20,0537	0,0022	15,2620	27,6411	0,4454	0,3820	99,5358	31,4620	65,5337	1,8586
CODp(gg)1	-	2-013	35,6732	0,0963	19,9301	0,0000	15,3756	27,5483	0,4460	0,3859	99,4554	31,7068	65,2765	1,8600
CODp(gg)1	-	2-014	35,5699	0,1066	19,9915	0,0000	14,9575	27,0143	0,4096	0,3968	98,4462	32,9119	64,1827	1,7128
CODp(gg)1	-	2-015	35,5296	0,0617	20,3521	0,0000	14,8775	27,3008	0,4991	0,4030	99,0238	31,6964	64,9985	2,0914
CODp(gg)1	-	2-016	35,7247	0,0735	19,9116	0,0000	14,9867	27,0599	0,4180	0,3957	98,5701	33,0158	64,0577	1,7416
CODp(gg)1	-	2-017	35,5524	0,0858	19,9268	0,0153	14,9413	27,0456	0,4530	0,4495	98,4697	32,4348	64,3169	1,8961
CODp(gg)1	-	2-018	35,6591	0,0931	19,7589	0,0000	15,1146	27,1118	0,4315	0,3884	98,5574	32,7630	64,2719	1,8004
CODp(gg)1	-	2-019	35,5232	0,1060	19,8809	0,0000	15,0609	26,8907	0,4537	0,3935	98,3089	32,9424	63,9737	1,8997
CODp(gg)1	-	2-020	35,6610	0,0852	20,1190	0,0000	15,1411	27,6083	0,4770	0,3923	99,4839	31,3767	65,4563	1,9905
CODp(gg)1	-	2-021	35,6717	0,0650	20,0398	0,0654	15,1841	27,5635	0,4871	0,3773	99,4539	31,4771	65,3583	2,0329
CODp(gg)1	-	2-022	35,8483	0,0992	20,0311	0,0218	15,2488	27,2423	0,4453	0,3773	99,3141	32,7938	64,2329	1,8479
CODp(gg)1	-	2-023	35,7804	0,0825	20,1749	0,0283	15,2877	26,8480	0,4761	0,4081	99,0860	33,3546	63,4453	1,9802
CODp(gg)1	-	2-024	35,7227	0,0992	19,9159	0,0109	15,1721	27,0557	0,4516	0,3846	98,8127	32,9515	64,0167	1,8807
CODp(gg)1	-	2-025	35,7388	0,0881	20,2527	0,0000	15,4242	27,1453	0,4931	0,3936	99,5358	32,5543	64,2148	2,0530
CODp(gg)1	-	2-026	35,6099	0,0948	19,8253	0,0284	14,9648	26,7708	0,4488	0,3559	98,0987	33,5075	63,5487	1,8751
CODp(gg)1	-	2-027	35,9613	0,0920	19,8574	0,0000	15,0390	27,1088	0,4417	0,4024	98,9026	33,2486	63,7272	1,8275
CODp(gg)1	-	2-028	35,8022	0,1232	19,8617	0,0457	15,3425	27,4741	0,4383	0,3915	99,4792	32,1810	64,8300	1,8203
CODp(gg)1	-	2-029	35,4641	0,1099	19,9820	0,0000	15,1880	27,1571	0,4115	0,3935	98,7061	32,3786	64,7096	1,7258
CODp(gg)1	-	2-030	35,2731	0,1125	20,0371	0,0000	15,1943	27,7242	0,4933	0,4323	99,2668	30,1961	66,4140	2,0799
CODp(gg)1	-	2-031	35,7878	0,1026	19,8249	0,0218	15,3092	27,1185	0,4467	0,4211	99,0326	32,8410	64,0443	1,8568
CODp(gg)1	-	2-032	35,9363	0,0864	19,7876	0,0000	15,2827	27,1882	0,4656	0,4136	99,1604	32,8753	63,9658	1,9280
CODp(gg)1	-	2-033	35,9970	0,1195	19,8430	0,0371	15,3820	26,7374	0,4864	0,4708	99,0732	33,8369	62,7559	2,0093
CODp(gg)1	-	2-034	35,5836	0,1182	19,9519	0,0370	15,2487	27,4551	0,4445	0,4369	99,2759	31,6411	65,1890	1,8576
CODp(gg)1	-	2-035	35,6167	0,1143	19,9271	0,0153	15,2831	27,1794	0,4476	0,3739	98,9574	32,5291	64,4799	1,8690
CODp(gg)1	-	2-036	35,7518	0,1110	20,0421	0,0196	15,3286	27,1269	0,4587	0,4034	99,2421	32,7685	64,1172	1,9082
CODp(gg)1	-	2-037	35,9921	0,1432	19,9126	0,0087	15,1734	26,8023	0,4516	0,4300	98,9139	33,9731	62,8857	1,8649
CODp(gg)1	-	2-038	36,0868	0,0953	20,0086	0,0000	15,1144	27,6221	0,4258	0,4080	99,7610	32,3314	64,7041	1,7555
CODp(gg)1	-	2-039	35,7140	0,1251	19,8776	0,0000	15,0381	27,2210	0,4173	0,3741	98,7672	32,7549	64,3884	1,7373
CODp(gg)1	-	2-040	35,7047	0,1183	19,9108	0,0000	15,1050	27,3285	0,3757	0,4171	98,9601	32,5179	64,6688	1,5647
CODp(gg)1	-	2-041	35,7149	0,0544	19,9253	0,0284	14,5480	27,2064	0,3871	0,4310	98,2955	32,6465	64,4480	1,6139
CODp(gg)1	-	2-042	35,7714	0,0897	19,9516	0,0196	15,0379	27,2845	0,3937	0,3995	98,9479	32,6848	64,4832	1,6376
CODp(gg)1	-	2-043	35,8662	0,1206	20,1184	0,0065	15,0887	27,2668	0,3279	0,4014	99,1965	33,2146	64,2298	1,3595
CODp(gg)1	-	2-044	35,3453	0,1160	20,0479	0,0087	15,1656	27,3114	0,4034	0,3876	98,7859	31,8437	65,2870	1,6972
CODp(gg)1	-	2-045	35,6840	0,1066	20,1072	0,0196	15,0345	27,2608	0,3958	0,4608	99,0693	32,4079	64,5618	1,6498
CODp(gg)1	-	2-046	35,3063	0,1076	20,1419	0,0000	14,8083	27,3322	0,4430	0,3722	98,5115	31,5864	65,4204	1,8662
CODp(gg)1	-	2-047	35,6745	0,0599	20,0722	0,0022	15,3445	27,6954	0,4050	0,3833	99,6370	31,4870	65,6730	1,6903
CODp(gg)1	-	2-048	35,8104	0,1031	19,9190	0,0087	15,0748	27,5297	0,4349	0,3544	99,2350	32,1616	64,9738	1,8065
CODp(gg)1	-	2-049	35,9534	0,0948	19,9712	0,0284	15,0440	27,2804	0,4025	0,4051	99,1798	32,9886	64,1410	1,6656
CODp(gg)1	-	2-050	35,5072	0,0869	19,9175	0,0000	15,3083	27,1817	0,4377	0,3838	98,8231	32,2885	64,7212	1,8343
CODp(gg)1	-	2-051	35,6666	0,1425	19,9004	0,0000	15,0387	26,8397	0,4649	0,4419	98,4947	33,1917	63,5474	1,9373
CODp(gg)1	-	2-052	35,7010	0,1127	19,9269	0,0000	15,1581	26,9292	0,4041	0,3985	98,6305	33,3855	63,7380	1,6834
CODp(g)2	-	1-001	36,0343	0,0402	20,6028	0,0135	3,2425	38,6567	0,0007	0,1849	98,7756	8,6596	90,7882	0,0029
CODp(g)2	-	1-002	35,6014	0,0485	20,8237	0,0000	3,7318	38,7698	0,0026	0,2262	99,2040	7,1651	92,1439	0,0109
CODp(g)2	-	1-003	35,9580	0,0268	20,5664	0,0000	3,7396	38,7435	0,0086	0,2013	99,2442	8,1543	91,2105	0,0356
CODp(g)2	-	1-004	35,7945	0,0842	20,6242	0,0000	4,3632	38,2127	0,0000	0,1847	99,2635	9,1853	90,2628	0,0000
CODp(g)2	-	1-005	35,0122	0,0858	20,7670	0,0067	3,9560	37,9661	0,0153	0,1880	97,9971	7,6834	91,6773	0,0650

Sample code	Crystal	An. Pt.	SiO_2	TiO_2	Al_2O_3	Cr_2O_3	$FeO+Fe_2O_3$	MnO	MgO	CaO	Sum	Alm	Sps	Pyr
CODp(g)2	-	1-006	35,7565	0,0479	20,4743	0,0022	4,4377	38,1835	0,0000	0,1792	99,0813	9,1052	90,3584	0,0000
CODp(g)2	-	1-007	35,6872	0,0725	20,6438	0,0022	4,5605	37,9952	0,0000	0,1891	99,1505	9,3926	90,0406	0,0000
CODp(g)2	-	1-008	35,6364	0,0820	20,4553	0,0000	4,4179	37,5986	0,0190	0,1903	98,3995	10,1398	89,2097	0,0793
CODp(g)2	-	1-009	35,6486	0,0770	20,5957	0,0000	4,6251	37,5905	0,0000	0,2003	98,7372	10,2296	89,1694	0,0000
CODp(g)2	-	1-011	35,7615	0,0736	20,6903	0,0045	3,9585	38,2250	0,0065	0,2197	98,9396	8,9206	90,3951	0,0271
CODp(g)2	-	1-012	36,2013	0,0000	20,8109	0,0135	3,3494	39,4585	0,0302	0,1549	100,0187	7,0960	92,3212	0,1244
CODp(g)2	-	1-013	35,2917	0,0641	20,4397	0,0000	4,7639	37,4163	0,0053	0,2257	98,2067	9,6165	89,6769	0,0224
CODp(g)2	-	1-014	35,6949	0,0536	20,3464	0,0267	6,1002	35,6290	0,0444	0,2004	98,0956	14,7653	84,4486	0,1852
CODp(g)2	-	1-015	35,2669	0,0870	20,1160	0,0444	7,6676	34,7914	0,0596	0,2462	98,2791	15,5984	83,4036	0,2515
CODp(g)2	-	1-016	35,4331	0,1022	20,1239	0,0022	7,7132	34,5269	0,0806	0,2757	98,2578	16,4743	82,3555	0,3384
CODp(g)2	-	1-017	35,6208	0,0754	20,2213	0,0000	7,7859	34,5222	0,0578	0,2630	98,5464	17,0111	81,9576	0,2415
CODp(g)2	-	1-018	35,6220	0,0670	20,3406	0,0000	7,7086	34,9175	0,0931	0,2386	98,9874	15,9864	82,9079	0,3891
CODp(g)2	-	1-019	35,3899	0,0770	20,2762	0,0067	7,6108	35,1335	0,0630	0,2434	98,8005	15,0501	83,9493	0,2649
CODp(g)2	-	1-020	35,6045	0,0838	20,4203	0,0000	7,7831	34,5797	0,0716	0,2365	98,7795	16,8733	82,1170	0,2993
CODp(g)2	-	1-021	35,3209	0,0899	20,5882	0,0022	7,5753	34,6164	0,0565	0,2265	98,4759	16,2239	82,8523	0,2380
CODp(g)2	-	1-022	35,3686	0,0821	20,2763	0,0067	7,6925	34,5283	0,0857	0,2530	98,2932	16,3304	82,5439	0,3606
CODp(g)2	-	1-023	35,4210	0,0766	20,3621	0,0089	7,6007	34,3495	0,0785	0,2404	98,1377	16,9394	82,0047	0,3298
CODp(g)2	-	1-024	35,3279	0,0519	20,3814	0,0288	7,7983	34,4859	0,0722	0,2132	98,3596	16,4594	82,5903	0,3043
CODp(g)2	-	1-025	35,5062	0,0609	20,4105	0,0000	7,4727	34,0482	0,0569	0,1846	97,7400	18,0875	81,1176	0,2386
CODp(g)2	-	1-026	34,9596	0,0587	20,4515	0,0133	7,6943	34,1208	0,0919	0,2498	97,6399	16,2802	82,5638	0,3914
Rossaccio Garnet dike														
ROSg(g)1	-	1-001	36,0205	0,0096	20,5269	0,0258	23,3134	17,5176	1,4630	0,6689	99,5457	50,7736	41,1835	6,0536
ROSg(g)1	-	1-002	36,1814	0,0357	20,3981	0,0129	23,6942	16,8645	1,5090	0,6442	99,3400	52,4305	39,4504	6,2128
ROSg(g)1	-	1-003	36,5790	0,0596	20,4327	0,0258	23,1435	16,9541	1,4542	0,6873	99,3362	52,8600	39,2099	5,9193
ROSg(g)1	-	1-004	36,0685	0,0578	20,3750	0,0194	22,9193	17,3298	1,4502	0,7158	98,9358	51,2426	40,6469	5,9867
ROSg(g)1	-	1-005	36,1636	0,1014	20,1268	0,0000	22,7706	17,4638	1,3560	0,6670	98,6492	51,6333	40,8166	5,5780
ROSg(g)1	-	1-006	36,1720	0,1030	20,4555	0,0000	23,1303	17,8803	1,4271	0,6581	99,8263	50,4068	41,7790	5,8690
ROSg(g)1	-	1-007	36,5529	0,1030	20,4438	0,0065	22,6901	18,2100	1,4216	0,6399	100,0678	50,2358	42,1069	5,7855
ROSg(g)1	-	1-008	36,3174	0,1042	20,2738	0,0151	22,7670	17,8679	1,3623	0,6620	99,3697	50,8890	41,5822	5,5799
ROSg(g)1	-	1-009	36,6972	0,0951	20,4637	0,0108	22,8929	18,4020	1,3677	0,6726	100,6020	50,1040	42,3908	5,5452
ROSg(g)1	-	1-010	36,5080	0,0543	20,2235	0,0344	22,5700	18,5541	1,2863	0,6356	99,8662	49,8918	42,9983	5,2466
ROSg(g)1	-	1-011	36,0141	0,0679	20,3406	0,0279	22,8400	18,2305	1,2641	0,6605	99,4456	49,9976	42,8150	5,2252
ROSg(g)1	-	1-012	36,3728	0,0769	19,9231	0,0129	22,9963	18,1422	1,2544	0,6165	99,3951	50,8736	42,1802	5,1331
ROSg(g)1	-	1-013	36,1848	0,0758	20,0841	0,0000	23,0151	17,8173	1,2282	0,6374	99,0427	51,4229	41,6406	5,0521
ROSg(g)1	-	1-014	36,5408	0,0797	20,0397	0,0000	23,4111	17,8366	1,2521	0,5993	99,7593	51,8688	41,2769	5,0999
ROSg(g)1	-	1-015	36,5613	0,0583	20,0818	0,0043	22,8304	17,8859	1,2001	0,6014	99,2235	51,9662	41,3860	4,8875
ROSg(g)1	-	1-016	36,2160	0,0701	20,0614	0,0086	22,9115	18,2112	1,2165	0,5674	99,2627	50,7940	42,5296	5,0002
ROSg(g)1	-	1-017	36,1779	0,0469	20,1512	0,0386	23,1395	18,5163	1,2718	0,5525	99,8947	49,8213	43,3085	5,2355
ROSg(g)1	-	1-018	36,2168	0,0915	20,0160	0,0043	22,9165	18,6351	1,1850	0,5960	99,6612	49,8723	43,4993	4,8685
ROSg(g)1	-	1-019	36,2976	0,0677	19,9759	0,0043	22,7501	18,9624	1,1474	0,5473	99,7527	49,4942	44,1867	4,7058
ROSg(g)1	-	1-020	35,8939	0,0920	20,0897	0,0000	22,6757	18,8270	1,0953	0,5600	99,2336	49,4499	44,3414	4,5403
ROSg(g)1	-	1-021	36,1305	0,0582	20,1584	0,0258	22,4521	18,7853	1,2045	0,5404	99,3552	49,4507	43,9849	4,9638
ROSg(g)1	-	1-022	36,2243	0,0559	20,1670	0,0000	22,4772	19,0974	1,2168	0,6032	99,8418	48,6140	44,6021	5,0018
ROSg(g)1	-	1-023	36,0924	0,0683	19,8063	0,0000	22,6411	18,8582	1,1475	0,5813	99,1951	49,3510	44,1928	4,7329
ROSg(g)1	-	1-024	36,1437	0,0367	19,9591	0,0000	22,3082	18,8819	1,1421	0,6017	99,0734	49,2959	44,2147	4,7070
ROSg(g)1	-	1-025	36,2169	0,0485	20,0608	0,0000	22,7680	18,9236	1,1428	0,5663	99,7269	49,4150	44,2120	4,6993
ROSg(g)1	-	1-026	36,1164	0,0740	19,9397	0,0000	22,4053	19,0202	1,1127	0,5902	99,2585	49,1284	44,5376	4,5858
ROSg(g)1	-	1-027	36,1396	0,0609	19,8047	0,0000	22,3902	19,4319	1,1626	0,5738	99,5637	48,0264	45,4849	4,7897
ROSg(g)1	-	1-028	36,0780	0,0773	20,0247	0,0151	22,1597	19,5965	1,0771	0,6261	99,6545	47,7674	45,9327	4,4435
ROSg(g)1	-	1-029	36,2252	0,0655	20,1276	0,0302	21,6484	19,8020	1,0506	0,6281	99,5776	47,5898	46,2374	4,3176
ROSg(g)1	-	1-030	36,1038	0,0536	19,9758	0,0000	21,1468	20,2606	1,0279	0,4345	99,0030	46,9936	47,4788	4,2396
ROSg(g)1	-	1-031	35,7076	0,0631	19,9235	0,0108	20,8538	20,8106	1,0178	0,4653	98,8525	45,0637	49,2983	4,2436
ROSg(g)1	-	1-032	35,8637	0,0580	20,0495	0,0000	20,4236	21,1410	0,9597	0,4754	98,9709	44,7284	49,8686	3,9844
ROSg(g)1	-	1-033	36,0360	0,0637	19,9096	0,0000	20,4231	21,1878	0,9730	0,4548	99,0480	44,8953	49,7345	4,0198
ROSg(g)1	-	1-034	35,8073	0,0692	19,9700	0,0000	20,0159	22,0811	0,8981	0,5155	99,3571	42,5702	52,1559	3,7336
ROSg(g)1	-	1-035	35,8445	0,0569	20,1345	0,0022	20,3367	21,6435	0,9656	0,4824	99,4663	43,4662	51,0825	4,0111
ROSg(g)1	-	1-036	35,9674	0,0569	20,1074	0,0173	19,9464	21,8909	0,9436	0,4969	99,4268	43,1251	51,4900	3,9063
ROSg(g)1	-	1-037	36,1100	0,0613	20,1410	0,0000	20,2010	22,1180	0,8833	0,4850	99,9996	43,1065	51,8143	3,6420
ROSg(g)1	-	1-038	35,9316	0,0304	19,8625	0,0453	19,6284	22,4119	0,8441	0,4804	99,2346	42,2713	52,7972	3,4999
ROSg(g)1	-	1-039	36,0559	0,0540	19,9831	0,0022	19,7220	22,4220	0,8490	0,4760	99,5642	42,4676	52,6131	3,5063
ROSg(g)1	-	1-040	35,7200	0,0647	19,7420	0,0000	19,4332	22,5211	0,8069	0,4725	98,7604	41,8916	53,3300	3,3630
ROSg(g)1	-	1-041	35,4952	0,0681	19,8998	0,0281	19,4476	22,1779	0,7770	0,5241	98,4178	42,3159	52,8457	3,2586
ROSg(g)1	-	1-042	35,4417	0,0517	20,0000	0,0000	19,2573	22,8860	0,7964	0,5109	98,9440	40,4768	54,6342	3,3462
ROSg(g)1	-	1-043	35,6842	0,0411	19,7510	0,0000	19,0683	22,4233	0,8263	0,5045	98,2987	41,8594	53,1781	3,4490
ROSg(g)1	-	1-044	35,7791	0,0719	19,5944	0,0000	18,5348	23,5459	0,8182	0,5517	98,8960	39,2900	55,6564	3,4039
ROSg(g)1	-	1-045	35,8172	0,0983	19,9336	0,0065	18,1795	24,1331	0,8188	0,5221	99,5091	38,0882	56,9523	3,4009
ROSg(g)1	-	1-046	35,5145	0,0506	19,8853	0,0108	17,9277	23,7777	0,7341	0,5046	98,4053	38,7532	56,6479	3,0782
ROSg(g)1	-	1-047	35,7713	0,0579	19,8473	0,0022	17,6036	24,1762	0,7782	0,4879	98,7246	38,1257	57,1755	3,2392
ROSg(g)1	-	1-048	35,6499	0,0804	19,8067	0,0130	17,3084	24,2859	0,7793	0,4907	98,4143	37,6715	57,6030	3,2533
ROSg(g)1	-	1-049	35,7468	0,0747	19,9162	0,0065	16,3186	25,5934	0,7266	0,5337	98,9165	34,8303	60,5472	3,0254
ROSg(g)1	-	1-050	35,5331	0,0786	20,1244	0,0000	16,0507	25,5898	0,7725	0,4855	98,6346	34,4058	60,8971	3,2356
ROSg(g)1	-	1-051	35,5806	0,0606	19,7511	0,0000	16,1760	25,9366	0,7179	0,4875	98,7103	33,8662	61,6636	3,0040
ROSg(g)1	-	1-052	36,1038	0,0674	19,9712	0,0327	15,2936	26,2528	0,7295	0,4834	98,9344	34,0562	61,5033	3,0080
ROSg(g)1	-	1-053	35,5875	0,0814	19,7891	0,0218	15,4031	26,3636	0,7048	0,4846	98,4359	32,9570	62,6391	2,9473
ROSg(g)1	-	1-054	35,7831	0,1157	19,7990	0,0196	15,5064	26,4496	0,6275	0,5797	98,8806	33,2049	62,4556	2,6079
ROSg(g)1	-	1-055	35,3849	0,1436	19,7214	0,0000	15,0292	26,8413	0,6937	0,5403	98,3544	31,4012	64,0541	2,9137
ROSg(g)1	-	1-056	35,2444	0,0936	19,9158	0,0218	15,1547	27,0777	0,6709	0,5190	98,6979	30,6491	64,9442	2,8321
ROSg(g)1	-	1-057	34,8592	0,1294	20,0334	0,0000	15,0311	27,4130	0,6731	0,4998	98,6390	29,1753	66,4222	2,8705
ROSg(g)1	-	1-058	35,4186	0,1134	19,9328	0,0437	14,7430	27,0034	0,6566	0,5179	98,4294	31,2591	64,4210	2,7570
ROSg(g)1	-	1-059	35,3147	0,1278	19,9452	0,0153	14,7595	27,4625	0,6288	0,5303	98,7841	30,0598	65,6885	2,6472
ROSg(g)1	-	1-060	35,3998	0,1543	19,8748	0,0087	14,6611	27,1059	0,6715	0,5281	98,4042	30,9445	64,6438	2,8186
ROSg(g)1	-	1-061	35,1360	0,1413	19,7259	0,0065	14,5065	27,2412	0,6429	0,5024	97,9027	30,2823	65,4707	2,7195
ROSg(g)1	-	1-062	35,6105	0,0876	19,6430	0,0000	14,2439	26,9918	0,7111	0,4614	97,7493	31,5609	64,0820	2,9714
ROSg(g)1	-	1-063	34,7541	0,1345	19,3866	0,0000	14,4315	27,1757	0,6867	0,5152	97,0843	29,4407	66,0385	2,9370
ROSg(g)1	-	1-064	35,1777	0,1222	19,7941	0,0131	14,3958	27,4683	0,6100	0,4985	98,0797	29,9419	65,9654	2,5783
ROSg(g)1	-	1-065	35,3759	0,1071	19,6533	0,0000	14,3748	27,1916	0,6238	0,5048	97,8313	30,8950	64,9568	2,6228
ROSg(g)1	-	1-066	35,6157	0,0858	19,8444	0,0218	14,8094	27,2727	0,6803	0,4529	98,7830	31,0557	64,7419	2,8424
ROSg(g)1	-	1-067	35,6779	0,0736	20,0772	0,0000	14,5219	26,9034	0,7103	0,4595	98,4238	31,8884	63,7705	2,9633
ROSg(g)1	-	1-068	35,1123	0,1009	19,6225	0,0000	14,7528	27,0446	0,7087	0,4899	97,8317	30,4077	65,0982	3,0024
ROSg(g)1	-	1-069	35,6835	0,0948	19,6155	0,0305	14,8838	26,7037	0,6707	0,4929	98,1754	32,4676	63,2590	2,7964
ROSg(g)1	-	1-070	35,2736	0,0953	19,8193	0,0305	14,9762	27,0065	0,6946	0,4725	98,3685	30,9205	64,7175	2,9296
ROSg(g)1	-	1-071	35,1765	0,0998	19,9211	0,0196	14,8202	27,3294	0,6422	0,5064	98,5152	30,0796	65,6654	2,7158
ROSg(g)1	-	1-072	35,2115	0,1255	19,8536	0,0109	15,0780	27,0706	0,6442	0,4957	98,4900	30,8321	64,9435	2,7201
ROSg(g)1	-	1-073	35,6051	0,1477	19,8491	0,0044	14,6934	26,9411	0,6053	0,5053	98,3514	32,0673	63,8903	2,5265
ROSg(g)1	-	1-074	35,4592	0,1171	19,8036	0,0000	15,0802	27,3243	0,7095	0,4796	98,9735	30,4719	65,1070	2,9755
ROSg(g)1	-	1-075	35,2673	0,1290	19,9507	0,0087	14,8448	27,0592	0,7114	0,5025	98,4736	30,6698	64,8089	2,9989
ROSg(g)1	-	1-076	35,2316	0,1104	19,7377	0,0501	15,0189	27,1759	0,6983	0,4609	98,4838	30,4739	65,1800	2,9478
ROSg(g)1	-	1-077	35,7842	0,1033	20,0906	0,0000	14,6750	27,0894	0,6762	0,4874	98,9061	31,7518	63,9810	2,8109
ROSg(g)1	-	1-078	35,5922	0,0729	19,7401	0,0196	14,7433	27,0829	0,6608	0,4921	98,4039	31,4062	64,3512	2,7635

Sample code	Crystal	An. Pt.	SiO_2	TiO_2	Al_2O_3	Cr_2O_3	$FeO+Fe_2O_3$	MnO	MgO	CaO	Sum	Alm	Sps	Pyr
Rossaccio Beryl dike														
ROSb(g)1	-	1-001	36,2243	0,0174	20,5286	0,0261	17,2403	25,0364	0,3664	0,2687	99,7082	39,1788	58,5194	1,5073
ROSb(g)1	-	1-002	36,0402	0,0147	20,4123	0,0000	20,4621	20,9713	0,7903	0,4417	99,1326	46,1484	49,2709	3,2680
ROSb(g)1	-	1-003	36,1323	0,0316	20,4250	0,0216	20,0522	21,6682	0,7614	0,4097	99,5020	44,8859	50,7606	3,1394
ROSb(g)1	-	1-004	35,7682	0,0490	20,1619	0,0281	19,6050	22,6367	0,7604	0,4124	99,4217	42,0506	53,5493	3,1660
ROSb(g)1	-	1-005	35,6958	0,0507	19,9200	0,0281	19,3811	22,4837	0,7639	0,4843	98,8076	42,0678	53,2932	3,1869
ROSb(g)1	-	1-006	35,7320	0,0546	20,2085	0,0000	19,1519	22,8975	0,7332	0,4459	99,2236	41,3943	54,2147	3,0554
ROSb(g)1	-	1-007	35,7236	0,0648	19,9538	0,0087	18,9717	22,8507	0,7336	0,4203	98,7272	41,5790	54,1050	3,0572
ROSb(g)1	-	1-008	35,7242	0,0614	19,9376	0,0325	18,8819	22,6256	0,7021	0,4355	98,4008	42,1945	53,5749	2,9261
ROSb(g)1	-	1-009	35,5508	0,0580	19,8286	0,0022	18,4517	23,0785	0,6805	0,4459	98,0962	40,8902	54,9175	2,8501
ROSb(g)1	-	1-010	35,6822	0,0817	20,1066	0,0628	18,8674	22,8594	0,7048	0,4292	98,7941	41,6049	54,1690	2,9395
ROSb(g)1	-	1-011	35,3158	0,0394	19,8705	0,0411	18,6166	23,2026	0,7326	0,4590	98,2776	39,9170	55,6017	3,0899
ROSb(g)1	-	1-012	35,8234	0,0551	20,0828	0,0000	18,7455	23,5214	0,6598	0,4150	99,3030	40,4683	55,5494	2,7425
ROSb(g)1	-	1-013	35,6768	0,0653	20,0140	0,0108	18,7734	23,4821	0,7016	0,4289	99,1529	40,1138	55,6722	2,9276
ROSb(g)1	-	1-014	35,8363	0,0732	19,9938	0,0000	18,8513	23,2376	0,6514	0,4343	99,0779	41,1593	54,8386	2,7056
ROSb(g)1	-	1-015	35,9966	0,0631	19,9435	0,0000	18,7536	23,1557	0,6852	0,4149	99,0126	41,5189	54,4138	2,8339
ROSb(g)1	-	1-016	35,9174	0,0445	19,9488	0,0303	18,7189	23,1767	0,6383	0,4348	98,9097	41,4530	54,6044	2,6468
ROSb(g)1	-	1-017	35,6682	0,0551	20,1245	0,0000	19,0150	23,1749	0,7067	0,4379	99,1823	40,7669	54,9690	2,9502
ROSb(g)1	-	1-018	36,0817	0,0507	19,9505	0,0152	18,5598	23,2606	0,7159	0,4388	99,0732	41,1980	54,5457	2,9547
ROSb(g)1	-	1-019	35,4980	0,0737	20,1348	0,0000	18,9239	23,3614	0,6910	0,4201	99,1029	40,1818	55,6548	2,8974
ROSb(g)1	-	1-020	35,4275	0,0596	20,1243	0,0000	18,2217	23,7767	0,6101	0,4589	98,6788	39,2762	56,7737	2,5640
ROSb(g)1	-	1-021	35,8151	0,0624	20,2810	0,0000	17,8596	24,8478	0,4608	0,4608	99,7875	38,0213	58,6865	1,9155
ROSb(g)1	-	1-022	35,9177	0,0546	19,9954	0,0000	18,7924	23,3968	0,6720	0,4443	99,2732	40,7794	55,1108	2,7859
ROSb(g)1	-	1-023	35,6741	0,0473	20,1733	0,0000	18,7778	23,4652	0,6532	0,4559	99,2468	40,2477	55,6575	2,7269
ROSb(g)1	-	1-024	35,3314	0,0585	19,8841	0,0390	18,5974	23,4016	0,5861	0,4384	98,3365	40,1712	56,0311	2,4699
ROSb(g)1	-	1-025	35,6880	0,0574	19,9083	0,0217	18,6236	23,3946	0,6484	0,3188	98,6608	40,8822	55,4566	2,7052
ROSb(g)1	-	1-026	35,5690	0,0692	19,9669	0,0000	18,6933	23,2792	0,6816	0,4125	98,6717	40,5530	55,3537	2,8525
ROSb(g)1	-	1-027	35,7385	0,0445	19,9572	0,0260	18,6434	23,1408	0,7213	0,3941	98,6658	41,0212	54,7924	3,0059
ROSb(g)1	-	1-028	36,0140	0,0563	19,7163	0,0000	18,5186	23,4951	0,7038	0,4560	98,9601	40,5425	55,1926	2,9099
ROSb(g)1	-	1-029	35,6349	0,0772	20,1007	0,0000	18,5789	23,0216	0,7110	0,4254	98,5497	41,1226	54,6308	2,9696
ROSb(g)1	-	1-030	35,7079	0,0535	20,1216	0,0000	18,6410	23,1709	0,7068	0,3910	98,7927	40,9803	54,9003	2,9475
ROSb(g)1	-	1-031	35,6741	0,0895	19,9975	0,0108	18,8020	23,2381	0,7085	0,3747	98,8952	40,8517	55,0699	2,9551
ROSb(g)1	-	1-032	35,5921	0,0811	20,0218	0,0260	18,8677	22,9824	0,6992	0,4235	98,6938	41,2049	54,5988	2,9236
ROSb(g)1	-	1-033	35,9358	0,0490	19,8269	0,0000	18,8003	23,1563	0,7079	0,4180	98,8942	41,2981	54,5233	2,9336
ROSb(g)1	-	1-034	35,8270	0,0478	20,1342	0,0000	18,9786	23,2874	0,6911	0,3747	99,3408	41,0081	54,9997	2,8728
ROSb(g)1	-	1-035	35,6925	0,0715	19,9750	0,0087	19,0627	22,8606	0,7226	0,4460	98,8396	41,4818	54,1679	3,0135
ROSb(g)1	-	1-036	35,7940	0,0349	20,1154	0,0022	18,7444	23,1485	0,7332	0,3732	98,9458	41,0955	54,7368	3,0514
ROSb(g)1	-	1-037	35,8147	0,0620	20,0630	0,0000	18,9158	22,6290	0,7393	0,4534	98,6772	42,1250	53,4471	3,0733
ROSb(g)1	-	1-038	36,0000	0,0260	20,0576	0,0000	18,9585	22,3390	0,7274	0,4182	98,5267	43,2151	52,5304	3,0105
ROSb(g)1	-	1-039	35,5146	0,0017	20,0641	0,0325	19,0755	22,5058	0,7222	0,3733	98,2897	42,1693	53,6731	3,0314
ROSb(g)1	-	1-040	35,5015	0,0783	20,1958	0,0130	18,8045	22,7961	0,7711	0,4245	98,5848	41,1909	54,2974	3,2326
ROSb(g)1	-	1-041	35,5422	0,0563	20,2958	0,0000	18,4461	23,2231	0,6483	0,3910	98,6028	40,8298	55,2769	2,7160
ROSb(g)1	-	1-042	35,9563	0,0101	20,6305	0,0000	16,9505	24,9806	0,3936	0,3218	99,2434	38,5767	58,8330	1,6315
Val Garzelli upper dike														
VGa(g)1	2	1-001	36,8844	0,0057	20,9870	0,0150	25,3467	14,0136	1,7153	0,6239	99,5916	59,0792	32,1767	6,9320
VGa(g)1	2	1-002	36,7514	0,0211	20,9962	0,0107	25,7062	14,2445	1,6410	0,6079	99,9790	58,7600	32,8149	6,6536
VGa(g)1	2	1-003	36,7576	0,0273	21,0726	0,0215	25,2157	14,9438	1,4905	0,6505	100,1795	57,6476	34,4157	6,0416
VGa(g)1	2	1-004	36,6158	0,0602	21,0576	0,0129	24,8069	15,3395	1,3474	0,5518	99,7921	57,4686	35,4398	5,4790
VGa(g)1	2	1-005	36,9078	0,0749	20,9201	0,0150	24,4535	16,2579	1,2876	0,5682	100,4850	55,9064	37,2537	5,1929
VGa(g)1	2	1-006	36,5788	0,0760	20,7160	0,0000	24,6505	16,2957	1,2128	0,5073	100,0371	55,9066	37,6748	4,9350
VGa(g)1	2	1-007	36,5843	0,1043	20,5808	0,0000	24,4499	16,3329	1,1814	0,5113	99,7449	55,9688	37,7332	4,8038
VGa(g)1	2	1-008	36,8136	0,0675	20,8013	0,0129	24,6124	16,2615	1,1283	0,4501	100,1476	56,7663	37,3628	4,5627
VGa(g)1	2	1-009	36,8087	0,0386	20,8627	0,0107	24,8361	16,4427	1,1801	0,4270	100,6066	56,1760	37,8064	4,7757
VGa(g)1	2	1-010	36,6717	0,0725	20,5854	0,0086	24,9582	16,4027	1,1230	0,3759	100,1980	56,5160	37,8289	4,5584
VGa(g)1	2	1-011	36,5684	0,0584	20,7605	0,0000	24,4636	16,5214	1,0997	0,3878	99,8598	56,1662	38,2212	4,4777
VGa(g)1	2	1-012	36,2048	0,0459	20,9377	0,0000	23,8762	16,6353	1,0975	0,4740	99,2714	55,2030	38,8808	4,5147
VGa(g)1	2	1-013	36,7354	0,1042	20,5158	0,0000	24,4331	16,9415	1,0608	0,4454	100,2362	55,4294	38,9786	4,2957
VGa(g)1	2	1-014	36,4734	0,0510	20,9376	0,0193	23,9318	17,0482	1,0699	0,4565	99,9877	54,7434	39,5486	4,3684
VGa(g)1	2	1-015	36,3151	0,0799	20,8099	0,0108	23,3749	17,5396	0,9926	0,4787	99,6015	53,6807	40,8413	4,0680
VGa(g)1	2	1-016	36,5404	0,0532	20,8361	0,0000	23,7534	17,5506	0,9812	0,4353	100,1502	54,0887	40,6376	3,9987
VGa(g)1	2	1-017	36,4613	0,0741	20,6214	0,0021	23,4003	18,1646	1,0042	0,4691	100,1971	52,3918	42,1323	4,0995
VGa(g)1	2	1-018	36,5767	0,0436	20,9148	0,0323	22,6838	18,6764	0,9523	0,4823	100,3622	51,5006	43,2100	3,8778
VGa(g)1	2	1-019	36,4796	0,0860	20,5830	0,0000	23,0492	18,3653	0,9622	0,5045	100,0298	52,0296	42,5661	3,9251
VGa(g)1	2	1-020	36,4957	0,0407	20,5628	0,0000	22,5187	18,6991	0,9200	0,5032	99,7402	51,4080	43,3611	3,7548
VGa(g)1	2	1-021	36,3522	0,0566	20,6851	0,0238	21,5470	18,9581	0,9962	0,4808	99,0998	50,3835	44,1205	4,0805
VGa(g)1	2	1-022	36,1795	0,0866	20,8312	0,0302	21,4435	19,5693	1,0247	0,4536	99,6186	48,7128	45,7316	4,2146
VGa(g)1	2	1-023	36,1182	0,1189	20,6773	0,0000	21,2155	19,6819	1,0357	0,5843	99,4318	47,9649	46,0418	4,2642
VGa(g)1	2	1-024	36,1840	0,0956	20,9125	0,0735	20,7619	19,7707	0,9670	0,5044	99,2696	48,3454	46,1879	3,9761
VGa(g)1	2	1-025	36,3830	0,0837	20,6792	0,0043	20,6810	20,5618	1,0104	0,5025	99,9059	46,6043	47,7856	4,1329
VGa(g)1	2	1-026	36,1391	0,1210	20,7265	0,0259	20,9127	20,1653	0,9978	0,4858	99,5741	47,3144	47,1433	4,1057
VGa(g)1	2	1-027	35,4941	0,1408	20,2370	0,0000	20,8866	19,7474	0,9861	0,5487	98,0407	47,2358	46,9835	4,1293
VGa(g)1	2	1-028	36,3605	0,1313	20,6828	0,0000	20,7036	20,0809	1,0522	0,5612	99,5725	47,3975	46,6509	4,3023
VGa(g)1	2	1-029	36,3254	0,0690	20,7507	0,0000	20,9945	20,3080	1,0048	0,5400	99,9924	47,0069	47,2848	4,1177
VGa(g)1	2	1-030	36,2858	0,1201	20,8625	0,0000	20,5715	19,9736	0,9730	0,5298	99,3163	47,9442	46,5077	3,9875
Val Garzelli lower dike														
VGb(g)1	-	1-001	36,2370	0,0080	20,9347	0,0148	31,4714	10,0075	0,5933	0,4471	99,7138	72,8502	23,3876	2,4404
VGb(g)1	-	1-002	36,2253	0,0277	20,8424	0,0170	28,8473	13,5347	0,4663	0,3655	100,3262	65,3737	31,6280	1,9178
VGb(g)1	-	1-003	36,5263	0,0023	20,7447	0,0042	28,1260	13,9779	0,3997	0,3935	100,1746	64,8029	32,4116	1,6312
VGb(g)1	-	1-004	36,2433	0,0334	20,5599	0,0319	27,9868	14,5527	0,4724	0,4276	100,3080	62,8090	33,9860	1,9417
VGb(g)1	-	1-005	36,3766	0,0408	20,6568	0,0085	27,4201	14,6021	0,3966	0,4768	99,9783	63,0015	33,9713	1,6240
VGb(g)1	-	1-006	36,5746	0,0334	20,8233	0,0085	27,6174	14,3821	0,4231	0,3970	100,2594	63,8309	33,2835	1,7234
VGb(g)1	-	1-007	36,7580	0,0079	20,9202	0,0085	28,0903	14,1090	0,4446	0,4161	100,7546	64,4788	32,5057	1,8028
VGb(g)1	-	1-008	36,4221	0,0515	20,5246	0,0191	28,7063	13,4205	0,4692	0,4109	100,0242	65,6976	31,1765	1,9184
VGb(g)1	-	1-009	36,4332	0,0232	20,8071	0,0000	28,5531	13,5362	0,4744	0,3724	100,1996	65,5111	31,4541	1,9402
VGb(g)1	-	1-010	36,0318	0,0192	20,7361	0,0000	29,0217	13,3726	0,4814	0,4113	100,0741	65,3640	31,4225	1,9909
VGb(g)1	-	1-011	36,3186	0,0164	20,8265	0,0021	28,2134	13,7069	0,4344	0,3517	99,8700	65,2247	31,9557	1,7825
VGb(g)1	-	1-012	36,5767	0,0130	20,7143	0,0000	27,7291	14,2618	0,4371	0,3517	100,0837	64,1719	33,0171	1,7810
VGb(g)1	-	1-013	36,4639	0,0147	20,5842	0,0000	27,5004	14,3283	0,4939	0,3897	99,7751	63,5642	33,2725	2,0186
VGb(g)1	-	1-014	36,5237	0,0057	20,6471	0,0000	27,3961	14,3454	0,4099	0,4155	99,7434	63,8446	33,2638	1,6729
VGb(g)1	-	1-015	36,4365	0,0340	20,7284	0,0170	27,5604	14,4407	0,4234	0,3973	100,0377	63,5561	33,5453	1,7311
Val Del Dosso dike														
VDD(g)1	-	1-001	36,7037	0,0312	20,8944	0,0000	31,3972	10,0112	0,7029	0,4191	100,1597	72,8364	23,0879	2,8531
VDD(g)1	-	1-002	36,7061	0,0204	20,7654	0,0147	32,7253	9,7629	0,6666	0,3526	101,0140	73,7463	22,5187	2,7062
VDD(g)1	-	1-003	36,6324	0,0028	20,9220	0,0021	31,8391	11,0523	0,3894	0,2730	101,1131	72,0636	25,5533	1,5846
VDD(g)1	-	1-004	35,9137	0,0197	20,5640	0,0506	29,8816	12,9796	0,2351	0,1956	99,8399	67,8422	30,5990	0,9755
VDD(g)1	-	1-005	36,2471	0,0214	20,6344	0,0021	30,1924	12,8655	0,1766	0,1884	100,3279	68,6673	30,0501	0,7260
VDD(g)1	-	1-006	35,9253	0,0411	20,7632	0,0000	29,0194	13,9460	0,2219	0,1771	100,0940	65,7003	32,8519	0,9200
VDD(g)1	-	1-007	36,0553	0,0107	20,6901	0,0000	28,6268	14,0713	0,1561	0,1677	99,7780	65,8079	33,0486	0,6453
VDD(g)1	-	1-008	36,4220	0,0344	20,7266	0,0000	29,0687	14,2163	0,2056	0,1844	100,8580	65,5801	33,0369	0,8409
VDD(g)1	-	1-009	36,1643	0,0169	20,7252	0,0000	28,5456	14,6734	0,1381	0,2233	100,4868	64,4151	34,3545	0,5691
VDD(g)1	-	1-010	35,9069	0,0760	20,3310	0,0000	26,5475	15,8337	0,1917	0,2166	99,1034	61,2695	37,2905	0,7946

Sample code	Crystal	An. Pt.	SiO_2	TiO_2	Al_2O_3	Cr_2O_3	$FeO+Fe_2O_3$	MnO	MgO	CaO	Sum	Alm	Sps	Pyr
VDD(g)1	-	1-011	35,5673	0,0810	20,7479	0,0000	26,3686	16,4019	0,1586	0,2370	99,5623	59,6308	38,9929	0,6636
VDD(g)1	-	1-012	36,1008	0,0586	20,8048	0,0404	26,1940	16,6218	0,1820	0,2366	100,2390	59,5972	38,9508	0,7506
VDD(g)1	-	1-013	35,9436	0,0799	20,7754	0,0000	26,7088	16,6294	0,2150	0,2409	100,5930	59,2715	39,1214	0,8902
VDD(g)1	-	1-014	35,6815	0,0670	20,5964	0,0000	25,9722	16,7587	0,1580	0,2632	99,4970	58,8261	39,7255	0,6592
VDD(g)1	-	1-015	35,3665	0,0500	20,6888	0,0191	26,1070	16,7841	0,1436	0,1891	99,3482	58,6690	40,1541	0,6047
VDD(g)1	-	1-016	35,6384	0,0236	20,5032	0,0000	25,9143	17,1668	0,1621	0,2497	99,6581	57,7926	40,7793	0,6777
VDD(g)1	-	1-017	35,7333	0,0304	20,4329	0,0000	25,6271	17,0612	0,1661	0,2203	99,2713	58,2322	40,4151	0,6925
VDD(g)1	-	1-018	35,7316	0,0444	20,5004	0,0000	25,9561	16,9453	0,1677	0,2203	99,5658	58,5104	40,1306	0,6990
VDD(g)1	-	1-019	36,0603	0,0698	20,5156	0,0000	25,8696	16,6988	0,1852	0,2756	99,6749	59,2518	39,1660	0,7645
VDD(g)1	-	1-020	36,4060	0,0659	20,8810	0,0469	25,7499	17,0930	0,1567	0,2830	100,6824	58,8138	39,7136	0,6408
VDD(g)1	-	1-021	35,6727	0,0686	20,8097	0,0000	26,0975	17,2403	0,1713	0,3025	100,3626	57,5021	40,8758	0,7148
VDD(g)1	-	1-022	35,7121	0,0507	20,4936	0,0000	25,4519	16,6462	0,1914	0,2238	98,7697	59,0925	39,4386	0,7981
VDD(g)1	-	1-023	35,8655	0,0523	20,4488	0,0149	25,7963	16,9318	0,1898	0,2799	99,5793	58,4342	39,9425	0,7880
VDD(g)1	-	1-024	35,8553	0,0810	20,8841	0,0191	25,9415	16,9634	0,1479	0,2532	100,1455	58,6264	40,0044	0,6139
VDD(g)1	-	1-025	35,8982	0,0602	20,5445	0,0021	25,5335	17,1689	0,1670	0,2415	99,6159	58,1292	40,4583	0,6926
VDD(g)1	-	1-026	35,9181	0,0676	20,4783	0,0000	25,3992	16,9438	0,2040	0,2644	99,2754	58,4673	39,8996	0,8455
VDD(g)1	-	1-027	35,8195	0,0529	20,5701	0,0447	25,6118	16,9320	0,1532	0,2844	99,4686	58,5196	39,9937	0,6369
VDD(g)1	-	1-028	35,8822	0,0597	20,6209	0,0213	25,6525	17,1434	0,1895	0,2649	99,8344	58,0071	40,4166	0,7863
VDD(g)1	-	1-029	35,9715	0,0602	20,5220	0,0106	25,7904	16,8488	0,1619	0,2733	99,6387	58,8937	39,6232	0,6701
VDD(g)1	-	1-030	35,4071	0,0512	20,7428	0,0043	25,5468	17,0568	0,2087	0,2759	99,2936	57,5296	40,7587	0,8777
VDD(g)1	-	1-031	35,4270	0,0366	20,6093	0,0000	25,0091	17,1305	0,1845	0,2505	98,6475	57,5427	40,9245	0,7758
VDD(g)1	-	1-032	35,5744	0,0648	20,7450	0,0192	25,5212	16,8814	0,1565	0,2623	99,2248	58,4176	40,1385	0,6549
VDD(g)1	-	1-033	35,6874	0,0698	20,6267	0,0021	25,3824	16,8638	0,1724	0,2689	99,0735	58,5091	39,9657	0,7191
VDD(g)1	-	1-034	35,5433	0,0619	20,6343	0,0000	25,4629	17,4396	0,1810	0,2975	99,6205	56,8417	41,5045	0,7582
VDD(g)1	-	1-035	35,6463	0,0338	20,5363	0,0085	25,6576	17,1074	0,1868	0,2631	99,4398	57,8086	40,6205	0,7807
VDD(g)1	-	1-036	35,4029	0,0523	20,5789	0,0298	25,4491	17,1561	0,1894	0,2453	99,1038	57,4619	40,9999	0,7966
VDD(g)1	-	1-037	35,6169	0,0832	20,8202	0,0000	25,8333	17,2523	0,1820	0,2564	100,0443	57,5140	40,9556	0,7604
VDD(g)1	-	1-038	35,6957	0,0552	20,5432	0,0149	25,2737	17,0714	0,1786	0,2527	99,0854	58,0366	40,4607	0,7450
VDD(g)1	-	1-039	35,8961	0,0658	20,5197	0,0000	25,6161	17,0108	0,1666	0,2304	99,5055	58,5389	40,0834	0,6909
VDD(g)1	-	1-040	35,7025	0,0580	20,8474	0,0064	25,6732	17,1712	0,1620	0,2526	99,8733	57,8801	40,6871	0,6756
VDD(g)1	-	1-041	35,5585	0,0349	20,4687	0,0000	25,1463	17,0389	0,1840	0,2584	98,6897	57,8944	40,5567	0,7708
VDD(g)1	-	1-042	35,7534	0,0535	20,6451	0,0000	25,6586	17,1231	0,1957	0,2822	99,7116	57,8209	40,5193	0,8151
VDD(g)1	-	1-043	35,7704	0,0782	20,4890	0,0170	25,8977	16,9530	0,1621	0,2820	99,6494	58,4053	40,0769	0,6745
VDD(g)1	-	1-044	35,8464	0,0703	20,6488	0,0043	25,7013	17,0864	0,2040	0,2487	99,8102	58,0971	40,3135	0,8471
VDD(g)1	-	1-045	35,7096	0,0681	20,6182	0,0000	25,7318	16,9543	0,1684	0,2776	99,5280	58,3096	40,1566	0,7020
VDD(g)1	-	1-046	35,6976	0,0417	20,7471	0,0000	25,4983	17,3222	0,1869	0,3011	99,7949	57,2526	41,0646	0,7798
VDD(g)1	-	1-047	35,6258	0,0883	20,5929	0,0000	25,4113	17,1747	0,1703	0,2693	99,3326	57,7234	40,7569	0,7113
VDD(g)1	-	1-048	35,4549	0,0540	20,6637	0,0000	25,8213	16,9863	0,2071	0,2699	99,4572	57,7823	40,5332	0,8698
VDD(g)1	-	1-049	35,5040	0,0709	20,6311	0,0000	25,7521	16,6897	0,1896	0,2610	99,0984	58,6624	39,7562	0,7949
VDD(g)1	-	1-050	35,7591	0,0630	20,5322	0,0000	25,8273	17,0379	0,1781	0,2837	99,6813	58,1064	40,3032	0,7415
VDD(g)1	-	1-051	35,7518	0,0529	20,5100	0,0128	25,6335	16,8608	0,2201	0,3016	99,3435	58,2795	39,9009	0,9167
VDD(g)1	-	1-052	35,6152	0,0500	20,4804	0,0000	25,8628	17,2495	0,1968	0,2558	99,7105	57,4288	40,9796	0,8229
VDD(g)1	-	1-053	35,7745	0,0427	20,5508	0,0021	26,1248	17,1352	0,2204	0,2519	100,1024	57,7954	40,5332	0,9176
VDD(g)1	-	1-054	35,6760	0,0580	20,5649	0,0128	26,0511	17,0469	0,1975	0,2699	99,8771	57,9436	40,4225	0,8243
VDD(g)1	-	1-055	35,7561	0,0490	20,5964	0,0000	25,8538	16,8439	0,1807	0,2793	99,5592	58,5520	39,8593	0,7526
VDD(g)1	-	1-056	35,9540	0,0568	20,5765	0,0000	26,1654	17,0989	0,1807	0,2698	100,3021	58,2149	40,2337	0,7483
VDD(g)1	-	1-057	35,6960	0,0366	20,5115	0,0000	25,8117	16,5996	0,1351	0,2779	99,0684	59,2451	39,3576	0,5638
VDD(g)1	-	1-058	35,7835	0,0422	20,5725	0,0043	25,7963	16,6906	0,1715	0,2722	99,3331	58,9998	39,4720	0,7138
VDD(g)1	-	1-059	35,6203	0,0855	20,6539	0,0000	25,7713	17,0410	0,1883	0,2798	99,6401	57,9250	40,4482	0,7866
VDD(g)1	-	1-060	35,5156	0,0338	20,7114	0,0383	25,5833	16,9874	0,1630	0,2598	99,2926	58,0492	40,4839	0,6837
VDD(g)1	-	1-061	35,7949	0,0625	20,4559	0,0000	26,0735	16,4462	0,1663	0,2439	99,2432	59,7141	38,8651	0,6917
VDD(g)1	-	1-062	35,8801	0,0754	20,6792	0,0000	25,9437	17,2199	0,1915	0,2254	100,2152	57,9476	40,5860	0,7944
VDD(g)1	-	1-063	35,5794	0,0473	20,4700	0,0000	25,8168	16,8270	0,1653	0,2566	99,1624	58,5178	40,0183	0,6919
VDD(g)1	-	1-064	35,6263	0,0782	20,7441	0,0000	25,8783	16,9625	0,1809	0,2342	99,7045	58,2798	40,2613	0,7557
VDD(g)1	-	1-065	35,4058	0,0557	20,5481	0,0000	25,4758	16,9408	0,1847	0,2333	98,8442	58,0389	40,4791	0,7768
VDD(g)1	-	1-066	35,4659	0,0512	20,5614	0,0000	25,6553	17,0650	0,1816	0,2649	99,2453	57,7273	40,7107	0,7625
VDD(g)1	-	1-067	36,0200	0,0484	20,7748	0,0191	26,0144	16,8109	0,1719	0,2205	100,0800	59,1434	39,4906	0,7107
VDD(g)1	-	1-068	35,6711	0,0456	20,5327	0,0021	25,9731	17,0430	0,1409	0,2859	99,6944	58,1244	40,4294	0,5883
VDD(g)1	-	1-069	35,0379	0,0770	20,5643	0,0000	25,7736	16,8111	0,1702	0,2547	98,6888	57,9275	40,5719	0,7230
VDD(g)1	-	1-070	35,5367	0,0518	20,6302	0,0127	26,0392	16,8651	0,1627	0,2326	99,5310	58,4644	40,1533	0,6818
VDD(g)1	-	1-071	35,6511	0,0602	20,8180	0,0128	26,0006	16,9757	0,1790	0,2198	99,9172	58,3128	40,2799	0,7475
VDD(g)1	-	1-072	35,0383	0,0619	20,7851	0,0170	25,9484	16,9619	0,1871	0,2614	99,2611	57,4580	40,9487	0,7950
VDD(g)1	-	1-073	35,5382	0,0681	20,8316	0,0298	26,2228	16,7345	0,1984	0,2738	99,8972	58,5177	39,8269	0,8311
VDD(g)1	-	1-074	35,6698	0,0343	20,8250	0,0000	25,9779	17,0403	0,1530	0,2803	99,9806	58,0856	40,4341	0,6390
VDD(g)1	-	1-075	35,3958	0,0231	20,6455	0,0000	26,1331	16,5702	0,1596	0,2670	99,1943	58,8881	39,6322	0,6719
VDD(g)1	-	1-076	35,6298	0,0000	20,6529	0,0446	26,2160	16,5139	0,1606	0,2076	99,4254	59,4464	39,2574	0,6720
VDD(g)1	-	1-077	35,7848	0,0512	20,7098	0,0000	26,2476	16,6268	0,1753	0,2322	99,8277	59,2637	39,3123	0,7295
VDD(g)1	-	1-078	35,8542	0,0327	20,6332	0,0128	25,6997	16,4568	0,1873	0,2446	99,1213	59,6412	38,8501	0,7782
VDD(g)1	-	1-079	35,1087	0,0422	20,6693	0,0042	26,1528	16,6609	0,1679	0,2285	99,0345	58,4326	40,1584	0,7123
VDD(g)1	-	1-080	35,3312	0,0625	20,5440	0,0000	25,8447	16,7323	0,1958	0,2254	98,9359	58,4329	40,0594	0,8251
VDD(g)1	-	1-081	35,4702	0,0422	20,5311	0,0000	26,3735	16,5837	0,1889	0,2714	99,4610	58,8224	39,5653	0,7932
VDD(g)1	-	1-082	35,4453	0,0293	20,7212	0,0170	26,2719	16,4653	0,2022	0,2700	99,4222	59,0133	39,3211	0,8499
VDD(g)1	-	1-083	35,5950	0,0343	20,8861	0,0085	26,2854	16,6916	0,1851	0,2522	99,9382	58,7769	39,6898	0,7747
VDD(g)1	-	1-084	35,8719	0,0191	20,5531	0,0530	26,6981	16,1031	0,1985	0,2560	99,7528	60,4038	38,0072	0,8246
VDD(g)1	-	1-085	35,2146	0,0309	20,6509	0,0000	28,2016	15,0968	0,1744	0,2202	99,5894	62,3048	36,2878	0,7378
VDD(g)1	-	1-086	35,4839	0,0439	20,7518	0,0190	28,4692	14,5871	0,1902	0,2049	99,7500	63,7964	34,7871	0,7983
VDD(g)1	-	1-087	35,3579	0,0411	20,5604	0,0000	28,5621	14,3418	0,1799	0,1804	99,2236	64,3700	34,3260	0,7578
VDD(g)1	-	1-088	36,2994	0,0108	20,8863	0,0084	32,1709	9,7852	0,6769	0,3768	100,2147	73,2812	22,8275	2,7793
VDD(g)1	-	2-001	35,6233	0,0136	20,5802	0,0000	31,9811	9,7510	0,7883	0,3790	99,1165	72,3845	23,1780	3,2979
VDD(g)1	-	2-002	35,2122	0,0108	20,6094	0,0147	32,4673	9,5508	0,7114	0,3569	98,9335	72,9347	22,9684	3,0111
VDD(g)1	-	2-003	35,4117	0,0351	20,7373	0,0000	32,2043	9,6608	0,6658	0,3614	99,0764	73,0163	23,0902	2,8008
VDD(g)1	-	2-004	35,3467	0,0328	20,6423	0,0147	32,4764	9,7865	0,5644	0,3137	99,1775	73,2363	23,4348	2,3787
VDD(g)1	-	2-005	35,2710	0,0429	20,8120	0,0189	32,1364	10,0832	0,4913	0,2801	99,1358	72,8834	24,1918	2,0746
VDD(g)1	-	2-006	35,5037	0,0203	20,6393	0,0000	32,1668	10,5436	0,4687	0,2973	99,6397	71,9932	25,1428	1,9672
VDD(g)1	-	2-007	35,2989	0,0294	20,7975	0,0231	31,4957	10,8349	0,4188	0,2679	99,1662	71,4375	25,9823	1,7676
VDD(g)1	-	2-008	35,4459	0,0045	20,8881	0,0000	31,4028	11,3281	0,3377	0,2801	99,6872	70,6666	27,0667	1,4201
VDD(g)1	-	2-009	35,5141	0,0203	20,7595	0,0000	31,1517	11,6156	0,3571	0,2336	99,6519	70,1062	27,6910	1,4983
VDD(g)1	-	2-010	35,3635	0,0587	20,5927	0,0379	30,6870	11,8836	0,3557	0,2532	99,2323	69,3089	28,4273	1,4976
VDD(g)1	-	2-011	35,3908	0,0473	20,8521	0,0252	30,8449	12,5735	0,3163	0,2334	100,2835	67,9013	30,0618	1,3310
VDD(g)1	-	2-012	35,5072	0,0310	20,7143	0,0316	30,4269	12,3710	0,2423	0,2264	99,5507	68,8097	29,4909	1,0166
VDD(g)1	-	2-013	35,3140	0,0293	20,6721	0,0189	30,4192	12,8664	0,2351	0,1833	99,7383	67,6117	30,8407	0,9918
VDD(g)1	-	2-014	35,5081	0,0496	20,6685	0,0189	30,4248	12,9196	0,2225	0,2167	100,0287	67,6278	30,7858	0,9332
VDD(g)1	-	2-015	35,3142	0,0496	20,5080	0,0147	30,0515	12,8086	0,2288	0,1811	99,1565	67,7975	30,6887	0,9648
VDD(g)1	-	2-016	35,5614	0,0417	20,7085	0,0000	29,7369	13,0203	0,1883	0,1784	99,4355	67,6898	30,9845	0,7887
VDD(g)1	-	2-017	35,4315	0,0259	20,4909	0,0000	30,1112	12,9404	0,1939	0,1800	99,3738	67,7231	30,9175	0,8154
VDD(g)1	-	2-018	35,5453	0,0090	20,7115	0,0000	29,8053	12,9480	0,2065	0,2135	99,4391	67,6430	30,8477	0,8659
VDD(g)1	-	2-019	35,6411	0,0259	20,5938	0,0126	30,2422	13,0062	0,2059	0,1866	99,9143	67,6865	30,8921	0,8607
VDD(g)1	-	2-020	35,6430	0,0440	20,6106	0,0000	30,2159	12,9425	0,2170	0,1978	99,8708	67,7718	30,7274	0,9068
VDD(g)1	-	2-021	35,4538	0,0242	20,6844	0,0000	30,0337	12,8815	0,1896	0,1844	99,4516	67,8876	30,7585	0,7968
VDD(g)1	-	2-022	35,7416	0,0000	20,7753	0,0000	29,9218	13,2713	0,2097	0,1856	100,1053	67,1187	31,4503	0,8746
VDD(g)1	-	2-023	35,8663	0,0130	20,8603	0,0443	29,8412	13,3964	0,2151	0,2084	100,4450	66,8560	31,6277	0,8938

Sample code	Crystal	An. Pt.	SiO_2	TiO_2	Al_2O_3	Cr_2O_3	$FeO+Fe_2O_3$	MnO	MgO	CaO	Sum	Alm	Sps	Pyr
VDD(g)1	-	2-024	35,8755	0,0000	20,4783	0,0000	28,6144	14,0685	0,1560	0,2362	99,4289	65,4313	33,2151	0,6482
VDD(g)1	-	2-025	36,1409	0,0147	20,8056	0,0170	27,8201	15,1245	0,1788	0,2296	100,3312	63,1471	35,4352	0,7373
VDD(g)1	-	2-026	35,5968	0,0749	20,5665	0,0064	27,2370	15,5314	0,1740	0,2773	99,4643	61,5415	36,8976	0,7275
VDD(g)1	-	2-027	35,6659	0,0535	20,5331	0,0000	26,3253	16,2565	0,1798	0,2356	99,2497	59,9795	38,5629	0,7507
VDD(g)1	-	2-028	35,4837	0,0642	20,6467	0,0467	26,3300	16,1766	0,2001	0,2221	99,1701	59,9293	38,5614	0,8395
VDD(g)1	-	2-029	35,6166	0,0124	20,5307	0,0000	26,3634	16,3834	0,1287	0,2182	99,2534	59,8538	38,9514	0,5385
VDD(g)1	-	2-030	35,8614	0,0242	20,5069	0,0000	25,9739	16,6276	0,1589	0,2601	99,4130	59,3106	39,2525	0,6602
VDD(g)1	-	2-031	35,8101	0,0321	20,7781	0,0000	26,0738	16,6766	0,1966	0,2584	99,8257	58,9915	39,4180	0,8179
VDD(g)1	-	2-032	35,3292	0,0248	20,3839	0,0149	25,8961	16,7993	0,1504	0,3061	98,9047	58,1835	40,2544	0,6343
VDD(g)1	-	2-033	35,6110	0,0664	20,5385	0,0000	26,0360	16,7291	0,1609	0,3039	99,4458	58,6801	39,7342	0,6726
VDD(g)1	-	2-034	35,7748	0,0681	20,4860	0,0361	26,3747	16,5630	0,1946	0,3501	99,8474	58,9847	39,1585	0,8098
VDD(g)1	-	2-035	35,7767	0,0321	20,3925	0,0489	26,0212	16,3499	0,1786	0,2395	99,0394	59,8577	38,6818	0,7437
VDD(g)2	-	1-002	36,5391	0,0006	20,7136	0,0000	30,9587	11,4715	0,4875	0,2449	100,4159	70,7015	26,5915	1,9889
VDD(g)2	-	1-003	36,4706	0,0045	20,6203	0,0000	29,5582	13,3380	0,2310	0,1965	100,4191	67,5050	30,9737	0,9441
VDD(g)2	-	1-004	36,0538	0,0198	20,6269	0,0085	29,4302	13,3894	0,1810	0,1825	99,8921	67,2674	31,4424	0,7481
VDD(g)2	-	1-005	36,3394	0,0000	20,6538	0,0275	28,9054	13,3215	0,2023	0,2101	99,6600	67,5007	31,0499	0,8299
VDD(g)2	-	1-006	36,2163	0,0344	20,4615	0,0169	29,1761	13,6885	0,1978	0,1741	99,9656	66,6808	31,9909	0,8136
VDD(g)2	-	1-007	36,2534	0,0220	20,6518	0,0318	28,7493	13,9718	0,1910	0,1714	100,0425	66,0806	32,6280	0,7850
VDD(g)2	-	1-008	36,0968	0,0299	20,7299	0,0169	29,0358	13,9265	0,2003	0,2293	100,2654	65,8352	32,6579	0,8267
VDD(g)2	-	1-009	36,3474	0,0322	20,7173	0,0064	28,6973	13,9647	0,1723	0,2222	100,1598	66,1190	32,5203	0,7062
VDD(g)2	-	1-010	36,1272	0,0232	20,7166	0,0000	28,9735	13,7155	0,1890	0,1948	99,9398	66,5025	32,1405	0,7795
VDD(g)2	-	1-011	36,2891	0,0361	20,6507	0,0212	28,6764	14,3077	0,1752	0,1841	100,3405	65,3678	33,3698	0,7192
VDD(g)2	-	1-012	36,1544	0,0141	20,6906	0,0000	27,8041	14,5354	0,2077	0,2340	99,6403	64,4079	34,0427	0,8562
VDD(g)2	-	1-013	36,3882	0,0271	20,5925	0,0149	26,3076	16,3112	0,1804	0,2332	100,0551	60,6290	37,9461	0,7387
VDD(g)2	-	1-014	36,0847	0,0344	20,6154	0,0000	26,1787	16,0736	0,1882	0,1992	99,3742	60,9300	37,7020	0,7770
VDD(g)2	-	1-015	36,1087	0,0378	20,3744	0,0064	26,2741	16,5768	0,1831	0,2653	99,8266	59,6044	38,8537	0,7553
VDD(g)2	-	1-016	36,2280	0,0220	20,7915	0,0467	27,8619	14,6576	0,1803	0,2467	100,0347	64,2756	34,2535	0,7416
VDD(g)2	-	1-017	35,7221	0,0158	20,4450	0,0000	26,3879	15,7039	0,1956	0,3738	98,8441	60,8402	37,2230	0,8160
VDD(g)2	-	1-018	36,0845	0,0502	20,6607	0,0000	25,5172	17,1277	0,1883	0,2470	99,8756	58,3288	40,1614	0,7771
VDD(g)2	-	1-019	36,1283	0,0722	20,5074	0,0064	24,8586	17,4889	0,1517	0,2631	99,4766	57,6559	40,9400	0,6250
VDD(g)2	-	1-020	35,8330	0,0626	20,6897	0,0000	25,4519	17,2754	0,1289	0,2602	99,7017	57,9063	40,7812	0,5356
VDD(g)2	-	1-021	36,1201	0,0603	20,7610	0,0085	25,1962	17,5054	0,1678	0,2196	100,0389	57,6597	40,9981	0,6917
VDD(g)2	-	1-022	36,0526	0,0282	20,4989	0,0128	25,2589	17,1800	0,1453	0,2269	99,4036	58,3874	40,3382	0,6005
VDD(g)2	-	1-023	36,2991	0,0000	20,5743	0,0000	25,2129	17,0591	0,1419	0,1824	99,4697	59,0731	39,8057	0,5828
VDD(g)2	-	1-024	36,0096	0,0349	20,6500	0,0021	25,2073	17,5704	0,1672	0,2274	99,8689	57,3339	41,2983	0,6917
VDD(g)2	-	1-025	36,0433	0,0457	20,4343	0,0000	24,7524	17,3629	0,1703	0,1992	99,0081	57,9415	40,7633	0,7037
VDD(g)2	-	1-026	35,8832	0,0491	20,7583	0,0000	24,9125	17,4352	0,1763	0,2849	99,4995	57,3060	41,1125	0,7317
VDD(g)2	-	1-027	35,7770	0,0355	20,4905	0,0000	25,1421	17,3652	0,1620	0,2843	99,2566	57,3941	41,0806	0,6745
VDD(g)2	-	1-028	35,9892	0,0502	20,5871	0,0000	24,9630	17,6407	0,1612	0,2519	99,6433	57,1101	41,4738	0,6670
VDD(g)2	-	1-029	36,2496	0,0197	20,5524	0,0000	25,4982	17,3453	0,1933	0,2152	100,0737	58,0573	40,5122	0,7946
VDD(g)2	-	1-030	36,2103	0,0440	20,7275	0,0000	25,2401	17,2662	0,1554	0,1985	99,8420	58,4231	40,3509	0,6392
VDD(g)2	-	1-031	36,0063	0,0570	20,6171	0,0064	24,9172	17,3609	0,2188	0,2643	99,4480	57,5188	40,7908	0,9048
VDD(g)2	-	1-032	36,2819	0,0502	20,4923	0,0085	24,8985	17,5954	0,1755	0,2163	99,7186	57,6077	41,0339	0,7204
VDD(g)2	-	1-033	35,9149	0,0073	20,3426	0,0000	25,2996	17,6067	0,1627	0,2412	99,5750	57,0887	41,5166	0,6752
VDD(g)2	-	1-034	36,1072	0,0491	20,5226	0,0000	25,0604	17,2104	0,1521	0,2281	99,3299	58,3656	40,3309	0,6273
VDD(g)2	-	1-035	36,1580	0,0559	20,4149	0,0000	24,9435	17,3247	0,1897	0,2505	99,3372	57,9413	40,5361	0,7812
VDD(g)2	-	1-036	35,9864	0,0581	20,6025	0,0107	25,0347	17,3990	0,1727	0,2593	99,5234	57,6124	40,9019	0,7146
VDD(g)2	-	1-037	36,0371	0,0535	20,5878	0,0000	25,4352	17,4331	0,2123	0,2630	100,0220	57,4132	40,9284	0,8773
VDD(g)3	-	1-001	36,6688	0,0074	20,9153	0,0381	30,3446	10,8135	0,6586	0,3715	99,8178	71,2635	24,9740	2,6771
VDD(g)3	-	1-002	35,8324	0,0362	20,5672	0,0149	27,8839	14,0407	0,2086	0,2352	98,8191	65,2660	33,1641	0,8672
VDD(g)3	-	1-003	36,5704	0,0141	20,5157	0,0255	27,8374	14,9673	0,1812	0,2462	100,3578	63,8849	34,6556	0,7384
VDD(g)3	-	1-004	36,1469	0,1096	20,7961	0,0000	26,1909	16,2376	0,1706	0,2545	99,9062	60,5836	37,9618	0,7020
VDD(g)3	-	1-005	36,2160	0,0463	20,7271	0,0000	25,0627	16,9181	0,1870	0,3077	99,4649	58,7923	39,5293	0,7690
VDD(g)3	-	1-006	35,8959	0,0480	20,6611	0,0085	25,1068	16,9391	0,1973	0,2974	99,1541	58,3651	39,9295	0,8186
Upper Val Leggia dike														
VLGa(g)1	1	1	36,3493	0,0398	20,7954	0,0000	28,0980	13,2809	1,0405	0,2726	99,8765	64,0119	30,9214	4,2638
VLGa(g)1	1	2	35,4917	0,0568	20,5293	0,0000	25,2639	17,0536	0,2418	0,1819	98,8190	57,7879	40,6492	1,0144
VLGa(g)1	1	3	35,6797	0,0563	20,4323	0,0253	25,1940	17,1671	0,2916	0,1698	99,0161	57,5690	40,7048	1,2169
VLGa(g)1	1	4	36,0755	0,0220	21,0150	0,0000	27,4197	13,3923	1,1098	0,5294	99,5637	62,4155	31,4289	4,5840
VLGa(g)1	1	5	35,5553	0,0867	20,4024	0,0190	25,5942	17,2792	0,2757	0,1904	99,4029	57,1861	41,0874	1,1538
VLGa(g)1	1	6	36,0345	0,0600	20,4078	0,0000	28,4480	13,6031	0,5487	0,1331	99,2352	65,4030	31,9346	2,2672
VLGa(g)1	1	1-007	35,5620	0,0622	20,2285	0,0000	26,7942	14,7914	0,2747	0,1045	97,8175	63,3522	35,1834	1,1500
VLGa(g)1	1	1-008	35,3969	0,0575	20,2891	0,0042	27,4376	15,0477	0,2505	0,1138	98,5973	62,6389	35,9633	1,0537
VLGa(g)1	1	1-009	35,5370	0,0437	20,5927	0,0000	27,1562	15,0960	0,2684	0,1436	98,8376	62,4954	35,9472	1,1249
VLGa(g)1	1	1-010	35,7512	0,0547	20,3386	0,0000	27,0001	15,1078	0,2592	0,1190	98,6306	62,8125	35,7517	1,0796
VLGa(g)1	1	1-011	35,8123	0,1046	20,5536	0,0126	27,6501	15,7464	0,2395	0,1625	100,2816	61,3596	37,1605	0,9948
VLGa(g)1	1	1-012	35,6447	0,0385	20,5729	0,0000	27,1660	15,4708	0,2694	0,1385	99,3008	61,7257	36,7325	1,1258
VLGa(g)1	1	1-013	35,5502	0,0448	20,2122	0,0210	27,0550	15,3662	0,2408	0,1379	98,6281	61,9998	36,5762	1,0088
VLGa(g)1	1	1-014	35,7730	0,0691	20,6092	0,0147	27,0381	15,3139	0,2436	0,1358	99,1974	62,3738	36,2064	1,0137
VLGa(g)1	1	1-015	35,8106	0,0679	20,3475	0,0021	26,7394	15,7568	0,2348	0,1402	99,0993	61,3897	37,2154	0,9761
VLGa(g)1	1	1-016	35,9130	0,0385	20,5209	0,0000	26,7622	16,0914	0,2540	0,1352	99,7152	60,6227	37,9208	1,0535
VLGa(g)1	1	1-017	35,6936	0,0339	20,5252	0,0063	26,6232	15,9026	0,2322	0,1267	99,1437	60,9412	37,7097	0,9691
VLGa(g)1	1	1-018	35,6710	0,0800	20,5479	0,0000	26,6832	15,9653	0,2483	0,1610	99,3567	60,6357	37,8456	1,0359
VLGa(g)1	1	1-019	35,9143	0,0604	20,5340	0,0000	26,3748	16,0087	0,2626	0,1246	99,2794	60,8329	37,7072	1,0886
VLGa(g)1	1	1-020	35,6727	0,0684	20,5194	0,0105	26,2318	16,0917	0,2837	0,1464	99,0246	60,2243	38,1527	1,1839
VLGa(g)1	1	1-021	35,7350	0,0633	20,5262	0,0000	26,5520	15,9901	0,2359	0,1570	99,2595	60,6972	37,8499	0,9828
VLGa(g)1	1	1-022	35,4679	0,0351	20,5164	0,0316	26,1984	15,9205	0,2126	0,1492	98,5317	60,6655	37,9912	0,8929
VLGa(g)1	1	1-023	35,6375	0,0667	20,3601	0,0000	26,4063	15,7583	0,2567	0,1436	98,6292	61,0962	37,4004	1,0723
VLGa(g)1	1	1-024	35,3727	0,0500	20,4267	0,0000	26,1937	16,1039	0,2563	0,1234	98,5267	60,0276	38,5200	1,0790
VLGa(g)1	1	1-025	35,3896	0,0811	20,6682	0,0274	26,2537	16,2199	0,2613	0,1413	99,0425	59,7207	38,7534	1,0988
VLGa(g)1	1	1-026	35,4535	0,0909	20,4337	0,0443	26,1723	16,2054	0,2516	0,1739	98,8256	59,7785	38,6411	1,0559
VLGa(g)1	1	1-027	35,6870	0,0644	20,3501	0,0000	26,0467	16,3232	0,2899	0,1150	98,8763	59,7565	38,6893	1,2094
VLGa(g)1	1	1-028	35,6264	0,0972	20,4696	0,0021	26,3700	16,2740	0,2307	0,1396	99,2096	60,0061	38,6115	0,9634
VLGa(g)1	1	1-029	35,5832	0,0494	20,6673	0,0147	26,6636	16,3813	0,2503	0,1452	99,7550	59,5632	38,9525	1,0475
VLGa(g)1	1	1-030	35,3473	0,0690	20,4227	0,0168	26,4910	15,9814	0,2604	0,1537	98,7423	60,1992	38,2390	1,0966
VLGa(g)1	1	1-031	35,6762	0,0299	20,3525	0,0147	26,2143	16,2036	0,2615	0,1458	98,8985	60,0250	38,4454	1,0920
VLGa(g)1	1	1-032	35,6297	0,0598	20,4299	0,0274	26,2353	16,4437	0,2563	0,1261	99,2082	59,5089	39,0413	1,0710
VLGa(g)1	1	1-033	35,7876	0,0782	20,4430	0,0000	26,3748	16,2668	0,2189	0,1559	99,3252	60,1874	38,4363	0,9104
VLGa(g)1	1	1-034	35,5896	0,0816	20,4620	0,0042	26,1749	16,5441	0,2427	0,1328	99,2319	59,2802	39,3058	1,0149
VLGa(g)1	1	1-035	35,9096	0,0672	20,4943	0,0253	26,3137	16,6063	0,2256	0,1681	99,8101	59,4495	39,1144	0,9352
VLGa(g)1	1	1-036	35,5028	0,0817	20,4515	0,0000	25,9644	16,4362	0,2308	0,1576	98,8250	59,4131	39,1447	0,9675
VLGa(g)1	1	1-037	35,7309	0,0673	20,3214	0,0000	25,9898	16,2892	0,2201	0,1346	98,7533	60,1209	38,5590	0,9170
VLGa(g)1	1	1-038	35,6854	0,0626	20,4708	0,0147	26,3862	16,4792	0,2739	0,1659	99,5387	59,2975	39,0623	1,1427
VLGa(g)1	1	1-039	35,5048	0,0667	20,3499	0,0084	26,1803	16,5952	0,2982	0,1771	99,1806	58,6823	39,5337	1,2503
VLGa(g)1	1	1-040	35,6343	0,0896	20,4808	0,0211	26,0436	16,8865	0,2486	0,1581	99,5626	58,4252	40,0623	1,0381
VLGa(g)1	1	1-041	35,9082	0,0914	20,7004	0,0358	26,3446	16,7409	0,2585	0,1570	100,2368	59,0483	39,4130	1,0711
VLGa(g)1	1	1-042	35,5784	0,0482	20,5130	0,0000	26,2920	16,6087	0,2772	0,1160	99,4335	58,9912	39,4995	1,1603
VLGa(g)1	1	1-043	35,2536	0,0569	20,4312	0,0000	26,1714	16,5886	0,2461	0,1389	98,8867	58,7315	39,8075	1,0394
VLGa(g)1	1	1-044	35,3142	0,0827	20,4277	0,0000	26,0771	16,6980	0,2365	0,1429	98,9791	58,5912	39,9794	0,9966
VLGa(g)1	1	1-045	35,5453	0,0788	20,7175	0,0042	26,4454	16,7213	0,2567	0,1503	99,9195	58,6943	39,7786	1,0748
VLGa(g)1	1	1-046	35,4555	0,0909	20,6082	0,0000	26,3420	16,5815	0,2628	0,1581	99,4990	58,8847	39,5356	1,1028

Sample code	Crystal	An. Pt.	SiO_2	TiO_2	Al_2O_3	Cr_2O_3	$FeO+Fe_2O_3$	MnO	MgO	CaO	Sum	Alm	Sps	Pyr
VLGa(g)1	1	1-047	35,5241	0,0437	20,6690	0,0295	25,9829	16,9259	0,2867	0,1598	99,6216	57,9972	40,3192	1,2020
VLGa(g)1	1	1-048	35,9684	0,0472	20,5876	0,0000	26,1256	16,6822	0,2377	0,1699	99,8186	59,2648	39,2454	0,9842
VLGa(g)1	1	1-049	33,8376	0,0854	19,7055	0,0021	25,6851	16,7690	0,2630	0,1706	96,5183	56,4087	41,8957	1,1565
VLGa(g)1	1	1-050	34,1064	0,0923	19,6120	0,0105	25,5279	16,8376	0,2312	0,1522	96,5701	56,7845	41,7298	1,0085
VLGa(g)1	1	1-051	33,6873	0,0544	19,8448	0,0042	25,6993	16,9720	0,2411	0,1365	96,6396	55,8796	42,6211	1,0656
VLGa(g)1	1	1-052	33,6401	0,0728	19,5447	0,0168	25,4764	16,6223	0,2704	0,1382	95,7817	56,5800	41,7842	1,1963
VLGa(g)1	1	1-053	33,5133	0,0900	19,7634	0,0000	25,2301	16,6784	0,2346	0,1365	95,6463	56,4556	42,0674	1,0415
VLGa(g)1	1	1-054	33,6784	0,0482	19,5902	0,0000	25,2786	16,6530	0,2479	0,1433	95,6396	56,6116	41,8368	1,0961
VLGa(g)1	1	1-055	33,2278	0,0721	19,6604	0,0294	25,5867	16,7841	0,2461	0,1665	95,7731	55,6474	42,7143	1,1023
VLGa(g)1	1	1-056	32,9683	0,0384	19,6362	0,0126	25,1090	16,9472	0,2568	0,1549	95,1234	54,8351	43,5017	1,1602
VLGa(g)1	1	1-057	32,9506	0,0343	19,5390	0,0000	25,2616	16,9400	0,2688	0,1269	95,1212	54,8619	43,5106	1,2152
VLGa(g)1	1	1-058	35,3579	0,0609	20,5208	0,0274	25,3888	16,9602	0,2469	0,1637	98,7266	57,8891	40,5758	1,0396
VLGa(g)1	1	1-059	35,7356	0,0863	20,5877	0,0296	25,3792	17,2199	0,2850	0,1923	99,5156	57,4972	40,7405	1,1868
VLGa(g)1	1	1-060	35,5545	0,0851	20,5293	0,0000	25,0569	17,1200	0,2670	0,1913	98,8041	57,5959	40,7111	1,1175
VLGa(g)1	1	1-061	35,6957	0,0546	20,6462	0,0000	25,5258	16,9745	0,2265	0,1593	99,2826	58,3460	40,2316	0,9448
VLGa(g)1	1	1-062	35,3869	0,0609	20,4991	0,0084	25,4539	16,9822	0,2922	0,1419	98,8255	57,7463	40,5952	1,2294
VLGa(g)1	1	1-063	35,6084	0,0678	20,4911	0,0464	25,6340	16,9737	0,2749	0,1822	99,2785	57,9864	40,3169	1,1492
VLGa(g)1	1	1-064	35,7056	0,0632	20,2983	0,0190	25,7525	17,4647	0,2321	0,1619	99,6973	57,1726	41,3744	0,9678
VLGa(g)1	1	1-065	35,7857	0,0834	20,5384	0,0253	25,5634	16,8052	0,2546	0,1644	99,2204	58,7436	39,7062	1,0588
VLGa(g)1	1	1-066	35,3621	0,0557	20,4498	0,0422	25,5347	17,1122	0,3048	0,1424	99,0039	57,3465	40,9391	1,2834
VLGa(g)1	1	1-067	35,7833	0,0546	20,4773	0,0190	25,3083	17,1697	0,2712	0,2114	99,2948	57,6445	40,5947	1,1285
VLGa(g)1	1	1-068	35,6053	0,0477	20,5716	0,0359	25,5842	17,4003	0,2614	0,1564	99,6628	57,0851	41,3514	1,0934
VLGa(g)1	1	1-069	35,5740	0,0592	20,6089	0,0106	25,2984	17,0687	0,2878	0,1666	99,0742	57,7052	40,5891	1,2045
VLGa(g)1	1	1-070	35,4691	0,0661	20,6138	0,0190	25,7973	17,3747	0,2970	0,1514	99,7884	56,8640	41,4328	1,2465
VLGa(g)1	1	1-071	35,7447	0,0839	20,5336	0,0591	25,3356	17,3918	0,2255	0,1867	99,5609	57,3637	41,1388	0,9388
VLGa(g)1	1	1-072	35,4383	0,0759	20,4070	0,0232	25,5876	16,9678	0,2370	0,1614	98,8982	58,0283	40,4892	0,9954
VLGa(g)1	1	1-073	35,2717	0,0702	20,4614	0,0000	25,3487	16,8730	0,2572	0,1940	98,4762	57,8684	40,4577	1,0854
VLGa(g)1	1	1-074	35,3938	0,0535	20,3821	0,0380	25,3499	17,0810	0,2384	0,1872	98,7239	57,6011	40,8298	1,0030
VLGa(g)1	1	1-075	35,5543	0,0541	20,4311	0,0000	25,1803	17,0946	0,2701	0,1924	98,7769	57,6121	40,6776	1,1312
VLGa(g)1	1	1-076	35,6425	0,0679	20,5083	0,0275	25,0780	17,0662	0,2718	0,1919	98,8541	57,7909	40,4978	1,1352
VLGa(g)1	1	1-077	35,4881	0,0483	20,6795	0,0000	25,3229	17,2145	0,2707	0,1862	99,2102	57,2582	41,0443	1,1360
VLGa(g)1	1	1-078	35,5797	0,0816	20,6345	0,0000	25,2499	17,3853	0,2687	0,1895	99,3892	56,9906	41,3158	1,1239
VLGa(g)1	1	1-079	35,5987	0,0564	20,3404	0,0000	24,9612	17,2152	0,2428	0,1817	98,5964	57,5267	40,9115	1,0156
VLGa(g)1	1	1-080	37,2502	0,0600	21,3787	0,0000	25,1994	17,2743	0,2371	0,2227	101,6224	59,1813	39,2312	0,9477
VLGa(g)1	1	1-081	35,5681	0,0857	20,4814	0,0000	25,2356	17,4722	0,2759	0,1901	99,3090	56,7418	41,5323	1,1543
VLGa(g)1	1	1-082	35,3432	0,0656	20,4560	0,0000	25,4082	16,9777	0,2958	0,1649	98,7114	57,6244	40,6305	1,2459
VLGa(g)1	1	1-083	35,4151	0,0454	20,7599	0,0106	25,2705	17,4139	0,2641	0,1884	99,3679	56,7122	41,6077	1,1106
VLGa(g)1	1	1-084	35,3497	0,0546	20,5492	0,0274	25,3299	17,2314	0,2060	0,1642	98,9124	57,3954	41,2397	0,8677
VLGa(g)1	1	1-085	35,5843	0,1035	20,5057	0,0275	25,0735	17,2708	0,2421	0,1693	98,9767	57,4598	41,0195	1,0120
VLGa(g)1	1	1-086	35,5361	0,0650	20,4019	0,0233	25,1124	17,1855	0,3061	0,2009	98,8312	57,2074	40,9054	1,2823
VLGa(g)1	1	1-087	35,6646	0,0529	20,5687	0,0000	25,3699	17,1900	0,2492	0,1806	99,2759	57,6383	40,7793	1,0405
VLGa(g)1	1	1-088	35,5514	0,0604	20,3038	0,0000	25,2391	17,1719	0,2509	0,1610	98,7385	57,6052	40,8594	1,0507
VLGa(g)1	1	1-089	35,5820	0,0937	20,5633	0,0211	25,1460	17,7245	0,2859	0,2090	99,6255	56,0680	42,1085	1,1955
VLGa(g)1	1	1-090	35,6150	0,0540	20,8261	0,0063	25,6420	17,4081	0,2589	0,2041	100,0145	56,9511	41,3531	1,0825
VLGa(g)1	1	1-091	35,5936	0,0650	20,5475	0,0127	25,0153	17,0913	0,2574	0,1964	98,7792	57,7175	40,6155	1,0766
VLGa(g)1	1	1-092	35,6156	0,0518	20,3588	0,0127	25,1842	17,3280	0,2442	0,1958	98,9911	57,2265	41,1641	1,0210
VLGa(g)1	1	1-093	35,5546	0,0764	20,4024	0,0021	25,4930	17,3747	0,2743	0,1939	99,3714	56,9441	41,3243	1,1483
VLGa(g)1	1	1-094	35,4608	0,0701	20,3159	0,0127	25,0442	17,2533	0,2816	0,1772	98,6158	57,1339	41,1494	1,1821
VLGa(g)1	1	1-095	35,6552	0,0799	20,4947	0,0000	25,2995	17,4762	0,2321	0,1962	99,4338	56,9971	41,4455	0,9688
VLGa(g)1	1	1-096	35,5264	0,0724	20,4370	0,0000	25,2855	17,5512	0,2766	0,1873	99,3364	56,4964	41,7807	1,1589
VLGa(g)1	1	1-097	35,6320	0,0742	20,6900	0,0021	25,6449	17,5295	0,2582	0,2130	100,0439	56,6780	41,6040	1,0786
VLGa(g)1	1	1-098	35,5007	0,0673	20,5186	0,0169	25,3843	17,3436	0,3030	0,2210	99,3554	56,7426	41,3208	1,2706
VLGa(g)1	1	1-099	35,5554	0,0627	20,5135	0,0254	25,2141	17,2603	0,2913	0,2070	99,1297	57,0942	41,0631	1,2197
VLGa(g)1	1	1-100	35,4748	0,0897	20,3533	0,0000	25,2614	17,3407	0,2941	0,1884	99,0024	56,8741	41,3244	1,2336
VLGa(g)1	1	1-101	35,6474	0,0822	20,6287	0,0253	25,8365	17,3129	0,2907	0,1962	100,0199	57,1325	41,0652	1,2136
VLGa(g)1	1	1-102	35,3651	0,0443	20,3924	0,0000	25,0667	17,4878	0,2502	0,2002	98,8067	56,4960	41,8443	1,0537
VLGa(g)1	1	1-103	35,3906	0,0656	20,4045	0,0000	25,2393	17,0874	0,2437	0,1947	98,6258	57,5479	40,8383	1,0251
VLGa(g)1	1	1-104	35,5567	0,0650	20,3481	0,0000	25,3863	16,9930	0,2935	0,2041	98,8467	57,7332	40,4238	1,2288
VLGa(g)1	1	1-105	35,4602	0,0621	20,5327	0,0127	24,7843	17,2446	0,2369	0,2002	98,5337	57,2649	41,1363	0,9946
VLGa(g)1	1	1-106	35,6517	0,0604	20,6509	0,0169	25,6108	17,1849	0,2663	0,1868	99,6287	57,5518	40,7755	1,1121
VLGa(g)1	1	1-107	35,4933	0,0500	20,4187	0,0000	25,1621	17,2324	0,2947	0,2316	98,8828	56,9857	41,0794	1,2365
VLGa(g)1	1	1-108	35,4902	0,0759	20,5505	0,0000	25,1105	17,3463	0,2711	0,2048	99,0493	56,9139	41,3319	1,1369
VLGa(g)1	2	1	36,5252	0,0000	21,0371	0,0021	29,5996	11,2848	1,2139	0,4742	100,1369	67,4855	26,1690	4,9545
VLGa(g)1	2	2	35,9201	0,0509	21,0668	0,0000	30,2276	11,4043	0,7756	0,3906	99,8359	68,7577	26,8629	3,2155
VLGa(g)1	2	4	35,7010	0,0581	20,5115	0,0000	24,9438	17,1818	0,2658	0,2161	98,8781	57,5299	40,7138	1,1085
VLGa(g)1	3	1	36,2800	0,0099	20,9482	0,0000	28,9067	11,9249	1,3030	0,5432	99,9159	65,2086	27,8345	5,3530
VLGa(g)1	3	2	33,4435	0,0644	20,0223	0,0296	23,9806	16,4850	0,2294	0,2331	94,4879	56,5430	41,6902	1,0211
VLGa(g)1	3	1-003	35,9707	0,0388	20,7211	0,0000	28,4392	12,7711	1,0325	0,3465	99,3199	64,6453	30,0478	4,2756
VLGa(g)1	3	1-004	36,0109	0,0473	20,7678	0,0126	28,6878	13,4695	0,7852	0,1716	99,9527	64,5926	31,6500	3,2473
VLGa(g)1	3	1-005	35,8170	0,0767	20,5745	0,0063	28,5577	13,9164	0,6637	0,1399	99,7522	63,9675	32,8567	2,7580
VLGa(g)1	3	1-006	36,2270	0,0651	20,7007	0,0126	28,0732	14,7573	0,4923	0,1169	100,4451	63,1750	34,4566	2,0231
VLGa(g)1	3	1-007	35,8679	0,0519	20,5437	0,0168	27,8704	14,4895	0,4273	0,1225	99,3900	63,6814	34,1791	1,7740
VLGa(g)1	3	1-008	35,7857	0,0727	20,6514	0,0000	27,4387	14,6313	0,3800	0,1338	99,0936	63,4418	34,5776	1,5806
VLGa(g)1	3	1-009	35,9171	0,0363	20,9698	0,0042	27,5134	14,9804	0,3082	0,1146	99,8440	63,0800	35,3002	1,2782
VLGa(g)1	3	1-010	35,6971	0,0881	20,5820	0,0000	27,4068	14,9405	0,2737	0,1236	99,1118	63,1044	35,3844	1,1409
VLGa(g)1	3	1-011	35,4455	0,0645	20,5642	0,0000	27,6498	14,8821	0,2161	0,1061	98,9283	63,2585	35,5136	0,9076
VLGa(g)1	3	1-012	35,5615	0,0939	20,7272	0,0000	27,0841	15,1781	0,2612	0,1297	99,0357	62,4377	36,0795	1,0928
VLGa(g)1	3	1-013	35,6219	0,0599	20,6265	0,0105	27,0612	15,2672	0,2675	0,1167	99,0314	62,2755	36,2559	1,1181
VLGa(g)1	3	1-014	35,4576	0,0789	20,5337	0,0000	26,5767	15,4584	0,2793	0,1438	98,5284	61,5289	36,8650	1,1723
VLGa(g)1	3	1-015	35,5397	0,0593	20,6223	0,0000	26,8018	15,5138	0,2280	0,0921	98,8570	61,8404	36,9271	0,9552
VLGa(g)1	3	1-016	35,5681	0,0685	20,7666	0,0126	27,0471	15,4902	0,2517	0,1213	99,3261	61,7474	36,8343	1,0534
VLGa(g)1	3	1-017	35,5084	0,0593	20,4535	0,0253	26,5082	15,3077	0,2230	0,1292	98,2146	62,2070	36,4686	0,9351
VLGa(g)1	3	1-018	35,4705	0,0898	20,5991	0,0337	26,4574	15,6171	0,2870	0,1404	98,6950	61,1514	37,2213	1,2039
VLGa(g)1	3	1-019	35,7375	0,0663	20,6969	0,0000	26,5756	15,5485	0,2952	0,1410	99,0610	61,5485	36,7997	1,2297
VLGa(g)1	3	1-020	35,7634	0,0530	20,6303	0,0000	26,4297	15,5952	0,2440	0,1556	98,8712	61,6246	36,8938	1,0160
VLGa(g)1	3	1-021	35,8186	0,0766	20,5621	0,0000	26,4553	15,6606	0,2638	0,1286	98,9656	61,5466	36,9732	1,0962
VLGa(g)1	3	1-022	35,4578	0,0547	20,7674	0,0084	26,0937	16,0033	0,2582	0,1454	98,7889	60,2930	38,1838	1,0843
VLGa(g)1	3	1-023	35,6193	0,0627	20,6899	0,0000	26,4842	16,0732	0,2719	0,1593	99,3605	60,2145	38,1705	1,1365
VLGa(g)1	3	1-024	35,3292	0,0651	20,6382	0,0000	26,4902	15,6160	0,2458	0,1572	98,5417	61,1012	37,3869	1,0358
VLGa(g)1	3	1-025	35,6494	0,0760	20,5415	0,0042	26,4600	15,9448	0,2713	0,1628	99,1100	60,5558	37,8230	1,1327
VLGa(g)1	3	1-026	35,7595	0,0593	20,4460	0,0000	26,5796	16,2864	0,2807	0,1532	99,5647	59,8447	38,5281	1,1687
VLGa(g)1	3	1-027	35,9208	0,0628	20,6826	0,0190	26,3973	15,5784	0,2618	0,1523	99,0750	61,7760	36,6852	1,0851
VLGa(g)1	3	1-028	35,9431	0,0599	20,6452	0,0000	26,6009	16,1471	0,2447	0,1347	99,7756	60,5821	38,0032	1,0136
VLGa(g)1	3	1-029	35,3272	0,0714	20,7052	0,0253	26,0941	16,0473	0,3018	0,2038	98,7761	59,6947	38,4165	1,2716
VLGa(g)1	3	1-030	35,6261	0,0783	20,3350	0,0359	25,8832	16,1499	0,2511	0,1718	98,5313	60,1025	38,3327	1,0490
VLGa(g)1	3	1-031	35,6758	0,0927	20,6592	0,0000	26,0576	16,1170	0,2585	0,1600	99,0208	60,2525	38,1898	1,0781
VLGa(g)1	3	1-032	35,8706	0,0340	20,5070	0,0000	26,2902	16,3613	0,2381	0,1762	99,4774	59,8792	38,6060	0,9888
VLGa(g)1	3	1-033	35,7626	0,0725	20,4189	0,0000	26,2621	16,2998	0,2381	0,1627	99,2167	59,9765	38,5458	0,9910
VLGa(g)1	3	1-034	35,4673	0,0490	20,7346	0,0021	25,8863	16,1397	0,2644	0,1550	98,6984	59,9185	38,5036	1,1102
VLGa(g)1	3	1-035	35,7404	0,0737	20,4629	0,0000	26,4155	16,0776	0,2323	0,1824	99,1848	60,4437	38,0429	0,9674
VLGa(g)1	3	1-036	35,6205	0,0628	20,6731	0,0000	25,9409	16,3631	0,2731	0,1853	99,1188	59,4444	38,8575	1,1414

Sample code	Crystal	An. Pt.	SiO_2	TiO_2	Al_2O_3	Cr_2O_3	$FeO+Fe_2O_3$	MnO	MgO	CaO	Sum	Alm	Sps	Pyr
VLGa(g)1	3	1-037	35,3974	0,0663	20,7132	0,0021	25,9575	15,8402	0,2532	0,1472	98,3771	60,6405	37,8497	1,0649
VLGa(g)1	3	1-038	35,6400	0,0766	20,5496	0,0465	25,7082	16,4324	0,2222	0,1342	98,8097	59,6798	38,9894	0,9279
VLGa(g)1	3	1-039	35,9155	0,0530	20,7599	0,0000	26,0677	16,3704	0,2637	0,1656	99,5958	59,8493	38,5639	1,0933
VLGa(g)1	3	1-040	35,6184	0,0755	20,7409	0,0232	25,7446	16,2897	0,2719	0,1533	98,9175	59,7283	38,6751	1,1362
VLGa(g)1	3	1-041	35,9749	0,0594	20,6496	0,0063	25,7375	16,2501	0,2653	0,1483	99,0914	60,2486	38,2122	1,0980
VLGa(g)1	3	1-042	35,9844	0,0450	20,6260	0,0000	25,6403	16,2100	0,2173	0,1641	98,8871	60,4931	38,1194	0,8994
VLGa(g)1	3	1-043	35,8680	0,0593	20,5672	0,0000	25,6141	16,6830	0,2084	0,1398	99,1398	59,3708	39,3471	0,8651
VLGa(g)1	3	1-044	35,6076	0,0622	20,5559	0,0000	25,4714	16,4800	0,2709	0,1583	98,6063	59,2418	39,1498	1,1327
VLGa(g)1	3	1-045	35,5299	0,0507	20,7984	0,0000	25,5200	16,4626	0,2094	0,2044	98,7754	59,3032	39,2034	0,8777
VLGa(g)1	3	1-046	35,5362	0,0801	20,7009	0,0063	25,3109	16,2500	0,2597	0,1573	98,3014	59,7727	38,6662	1,0876
VLGa(g)1	3	1-047	35,4029	0,0806	20,7937	0,0000	25,4257	16,4743	0,2757	0,1892	98,6421	58,9226	39,3469	1,1589
VLGa(g)1	3	1-048	35,7001	0,0594	20,7036	0,0085	25,0604	16,5796	0,2655	0,1697	98,5468	59,0972	39,2868	1,1073
VLGa(g)1	3	1-049	35,4103	0,0432	20,4283	0,0127	24,9514	16,4738	0,2377	0,1758	97,7332	59,1001	39,3687	0,9998
VLGa(g)1	3	1-050	35,6355	0,0530	20,6433	0,0339	24,9666	16,8319	0,2462	0,1892	98,5996	58,4407	39,9622	1,0288
VLGa(g)1	3	1-051	35,6404	0,0674	20,6942	0,0000	25,1322	16,5785	0,2486	0,1887	98,5500	59,0519	39,3433	1,0384
VLGa(g)1	3	1-052	35,5550	0,0680	20,6483	0,0106	24,8812	16,5968	0,2555	0,2028	98,2182	58,8393	39,4807	1,0697
VLGa(g)1	3	1-053	35,3418	0,0617	20,6162	0,0000	24,8466	16,5275	0,2312	0,1769	97,8019	58,9325	39,5579	0,9740
VLGa(g)1	3	1-054	35,4763	0,0888	20,6094	0,0191	24,7334	16,5304	0,2597	0,1938	97,9109	58,9341	39,3925	1,0892
VLGa(g)1	3	1-055	35,5521	0,0818	20,6003	0,0000	25,4565	16,6868	0,2851	0,1695	98,8321	58,6102	39,6864	1,1934
VLGa(g)1	3	1-056	35,6572	0,0743	20,7461	0,0000	25,2288	16,7339	0,2501	0,1853	98,8757	58,7125	39,6876	1,0440
VLGa(g)1	3	1-057	35,6665	0,1147	20,6652	0,0000	25,1354	16,4954	0,2848	0,1893	98,5513	59,1667	39,0785	1,1875
VLGa(g)1	3	1-058	35,8438	0,0750	20,7394	0,0000	24,8131	16,7328	0,2767	0,2013	98,6821	58,7721	39,4781	1,1490
VLGa(g)1	3	1-059	35,4772	0,0765	20,5338	0,0021	25,5020	16,8940	0,2774	0,2127	98,9757	57,9265	40,2684	1,1638
VLGa(g)1	3	1-060	35,7025	0,0852	20,5857	0,0042	25,0043	17,2454	0,2850	0,1897	99,1020	57,4043	40,8395	1,1879
VLGa(g)1	3	1-061	36,3008	0,0755	21,2491	0,0000	25,1678	17,3896	0,2867	0,1741	100,6436	57,7998	40,5116	1,1756
VLGa(g)1	3	1-062	35,2906	0,0944	20,4255	0,0000	24,9550	17,0548	0,2425	0,1554	98,2182	57,6561	40,8507	1,0223
VLGa(g)1	3	1-063	35,3132	0,0656	20,6494	0,0000	25,1005	17,0821	0,2786	0,1767	98,6661	57,3751	40,9150	1,1745
VLGa(g)1	3	1-064	35,6151	0,0784	20,4622	0,0000	24,8000	16,8480	0,2476	0,1697	98,2210	58,4537	40,0019	1,0347
VLGa(g)1	3	1-065	35,1258	0,0714	20,3693	0,0000	24,5894	16,7199	0,2448	0,1875	97,3081	58,1357	40,2559	1,0374
VLGa(g)1	3	1-066	35,4759	0,0714	20,6546	0,0000	24,9474	16,9433	0,2532	0,1847	98,5305	57,9889	40,3918	1,0624
VLGa(g)1	3	1-067	35,7417	0,0374	20,5363	0,0000	24,8414	17,1642	0,2598	0,2291	98,8099	57,5874	40,6436	1,0828
VLGa(g)1	3	1-068	35,5446	0,0651	20,4006	0,0191	24,5400	16,9672	0,2739	0,1859	97,9964	57,9172	40,3760	1,1472
VLGa(g)1	3	1-069	36,1005	0,0564	20,6340	0,0148	25,4085	17,4801	0,2520	0,2272	100,1735	57,3227	40,9643	1,0394
VLGa(g)1	3	1-070	35,8454	0,0749	20,6383	0,0021	25,1870	17,2759	0,2760	0,2218	99,5214	57,4343	40,7578	1,1460
VLGa(g)1	3	1-071	35,8797	0,0656	20,7459	0,0106	25,6248	17,2945	0,2834	0,1734	100,0779	57,5364	40,7706	1,1759
VLGa(g)1	3	1-072	35,9918	0,0680	20,7476	0,0339	25,0926	17,1339	0,2635	0,2055	99,5368	58,0349	40,2644	1,0899
VLGa(g)1	3	1-073	36,1285	0,0576	20,9098	0,0000	25,2358	16,9080	0,2668	0,2084	99,7149	58,6912	39,5920	1,0996
VLGa(g)1	3	1-074	35,9218	0,0899	20,6748	0,0000	25,0966	16,9525	0,2777	0,1842	99,1975	58,4040	39,8973	1,1503
VLGa(g)1	3	1-075	35,8148	0,0334	20,6831	0,0064	24,8343	17,3617	0,2532	0,2032	99,1901	57,3085	41,0308	1,0532
VLGa(g)1	3	1-076	35,8401	0,0853	20,8916	0,0317	25,1924	16,9002	0,2394	0,1904	99,3711	58,5692	39,8686	0,9940
VLGa(g)1	3	1-077	35,8491	0,0662	20,2961	0,0148	24,9322	17,1175	0,2779	0,1707	98,7245	57,9492	40,3873	1,1540
VLGa(g)1	3	1-078	35,5109	0,0535	20,6323	0,0000	24,9455	17,1257	0,2611	0,1835	98,7125	57,5502	40,8019	1,0949
VLGa(g)1	3	1-079	35,8153	0,0605	20,5920	0,0000	24,8307	17,0305	0,2497	0,2016	98,7803	58,1350	40,2247	1,0380
VLGa(g)1	3	1-080	35,7562	0,0450	20,3650	0,0127	24,8049	16,5905	0,2634	0,2035	98,0412	59,0307	39,2629	1,0971
VLGa(g)1	3	1-081	35,9707	0,0646	20,6043	0,0021	24,9536	16,9762	0,2686	0,1877	99,0278	58,4100	39,9200	1,1117
VLGa(g)1	3	1-083	36,1421	0,0830	20,6654	0,0000	25,0235	16,9580	0,2614	0,2017	99,3351	58,6536	39,6732	1,0763
VLGa(g)1	3	1-084	35,9737	0,0761	20,5299	0,0000	24,6668	16,9441	0,3010	0,2204	98,7120	58,2676	39,8316	1,2454
VLGa(g)1	3	1-085	35,7896	0,0629	20,6687	0,0148	24,7094	16,8011	0,2686	0,2012	98,5163	58,5718	39,7093	1,1173
VLGa(g)1	3	1-086	36,1262	0,0478	20,8378	0,0275	24,9509	17,2743	0,2452	0,1893	99,6990	57,9678	40,4605	1,0108
VLGa(g)1	3	1-087	35,7072	0,0392	20,6012	0,0402	25,1125	17,0864	0,2406	0,2027	99,0300	57,8917	40,4969	1,0037
VLGa(g)1	3	1-088	35,6865	0,0559	20,4742	0,0042	25,1679	16,9700	0,2684	0,1836	98,8107	58,0994	40,2301	1,1199
VLGa(g)1	3	1-089	35,7108	0,0697	20,8289	0,0000	24,9584	16,8811	0,2689	0,1971	98,9149	58,3080	39,9806	1,1209
VLGa(g)1	3	1-090	35,6489	0,1082	20,6214	0,0042	25,1155	17,1772	0,2696	0,1874	99,1324	57,5938	40,7194	1,1248
VLGa(g)1	3	1-091	35,8475	0,0479	20,5662	0,0000	24,5499	17,1159	0,2432	0,2130	98,5836	57,9529	40,4008	1,0104
VLGa(g)1	3	1-092	35,8786	0,0847	20,7753	0,0212	25,2308	16,9308	0,2694	0,1786	99,3694	58,4517	39,8985	1,1174
VLGa(g)1	3	1-093	35,5432	0,0576	20,4970	0,0254	24,9241	16,8047	0,2385	0,2100	98,3005	58,3714	39,9973	0,9991
VLGa(g)1	3	1-094	35,6280	0,1060	20,6335	0,0000	24,7083	16,7989	0,2559	0,1792	98,3098	58,5462	39,8477	1,0684
VLGa(g)1	3	1-095	35,4164	0,0674	20,6971	0,0127	25,0674	16,7768	0,2278	0,2094	98,4750	58,3446	40,0653	0,9575
VLGa(g)1	3	1-096	35,7635	0,0761	20,6799	0,0106	24,8532	16,7927	0,2474	0,1680	98,5914	58,7605	39,7074	1,0296
VLGa(g)1	3	1-097	35,5223	0,0719	20,5972	0,0000	25,0594	17,0667	0,2963	0,1639	98,7777	57,6324	40,6324	1,2416
VLGa(g)1	3	1-099	35,8350	0,0709	20,6521	0,0106	24,5490	16,9785	0,2973	0,2237	98,6171	58,0261	40,0711	1,2350
VLGa(g)1	3	1-100	35,5462	0,0616	20,4709	0,0000	25,1365	17,0358	0,2720	0,2106	98,7336	57,6863	40,5405	1,1392
VLGa(g)1	3	1-101	35,3762	0,0881	20,5948	0,0000	25,0211	16,9472	0,2540	0,1831	98,4645	57,8777	40,5004	1,0684
VLGa(g)1	3	1-103	35,3927	0,0559	20,7224	0,0000	24,5317	16,8649	0,2429	0,1579	97,9684	58,1882	40,3125	1,0219
VLGa(g)1	3	1-104	35,6490	0,0697	20,7530	0,0000	24,8218	17,0902	0,2918	0,1904	98,8659	57,6643	40,5459	1,2185
VLGa(g)1	3	1-105	35,7410	0,0703	20,5175	0,0360	24,9668	16,9006	0,2611	0,1595	98,6528	58,4426	39,9925	1,0874
VLGa(g)1	3	1-106	35,3475	0,0869	20,7367	0,0000	24,9010	17,0528	0,2573	0,1864	98,5686	57,5661	40,7868	1,0831
VLGa(g)1	3	1-107	35,6049	0,0564	20,5762	0,0000	25,3766	17,0613	0,2593	0,1948	99,1295	57,7914	40,5387	1,0844
VLGa(g)1	3	1-108	35,3149	0,0755	20,5855	0,0000	25,0017	16,8197	0,2409	0,2168	98,2550	58,0519	40,2761	1,0153
VLGa(g)1	3	1-109	35,5673	0,0357	20,7765	0,0063	25,2153	16,9944	0,2633	0,1988	99,0576	57,8587	40,4401	1,1028
VLGa(g)1	3	1-110	35,7442	0,0830	20,5420	0,0318	24,7891	17,1203	0,2913	0,2028	98,8045	57,6824	40,4979	1,2128
VLGa(g)1	3	1-111	35,6163	0,0732	20,6329	0,0275	25,2230	16,6810	0,2177	0,1820	98,6536	58,9351	39,6084	0,9098
VLGa(g)1	3	1-112	35,6007	0,0807	20,5905	0,0000	25,0085	16,5701	0,2910	0,1769	98,3184	58,8959	39,3561	1,2165
VLGa(g)1	3	1-113	35,6919	0,0726	20,6831	0,0212	24,9232	16,8595	0,2419	0,1781	98,6715	58,5093	39,9481	1,0088
VLGa(g)1	3	1-115	35,6272	0,0530	20,6799	0,0423	24,9693	16,6805	0,3085	0,1720	98,5327	58,5819	39,6120	1,2894
VLGa(g)1	3	1-116	35,6965	0,0553	20,6291	0,0381	25,2067	16,7482	0,2782	0,1685	98,8206	58,6406	39,6937	1,1605
VLGa(g)1	3	1-117	35,4075	0,0743	20,6284	0,0000	24,5189	16,8830	0,2410	0,1741	97,9272	58,1378	40,3232	1,0131
VLGa(g)1	3	1-118	35,5747	0,0536	20,5223	0,0000	25,0163	16,8846	0,2252	0,1914	98,4681	58,3263	40,1553	0,9426
VLGa(g)1	3	1-119	35,5421	0,0915	20,6749	0,0000	25,2840	16,8143	0,3029	0,1291	98,8388	58,3509	39,9927	1,2680
VLGa(g)1	3	1-120	35,5196	0,0530	20,6084	0,0233	25,1671	16,5895	0,2056	0,1876	98,3541	59,0577	39,5151	0,8619
VLGa(g)1	3	1-121	35,5456	0,0421	20,6471	0,0000	25,1101	16,6376	0,2641	0,1837	98,4303	58,7303	39,6099	1,1066
VLGa(g)1	3	1-122	35,8254	0,0646	20,7802	0,0318	25,0006	16,6980	0,2849	0,1956	98,8811	58,8070	39,4248	1,1839
VLGa(g)1	3	1-123	35,4012	0,0558	20,4873	0,0021	25,3309	16,5468	0,2375	0,1723	98,2339	58,9375	39,5427	0,9989
VLGa(g)1	3	1-124	35,4843	0,0743	20,5979	0,0000	24,8289	16,7937	0,2479	0,1842	98,2112	58,3816	40,0232	1,0398
VLGa(g)1	3	1-125	35,5951	0,0761	20,6109	0,0000	24,9493	16,1605	0,2401	0,1574	97,7894	60,1300	38,3930	1,0040
VLGa(g)1	3	1-126	35,4985	0,0589	20,4630	0,0000	24,8110	15,9379	0,2467	0,1575	97,1735	60,5096	37,9808	1,0347
VLGa(g)1	3	1-127	35,5295	0,0997	20,5234	0,0021	24,8366	16,5574	0,2445	0,1680	97,9612	59,0819	39,3888	1,0237
VLGa(g)1	3	1-128	35,3480	0,0559	20,5735	0,0000	25,1253	16,2489	0,2620	0,1754	97,7890	59,4762	38,8891	1,1036
VLGa(g)1	3	1-129	35,5765	0,0542	20,3674	0,0000	25,1392	16,2245	0,2470	0,1747	97,7835	59,8577	38,5830	1,0338
VLGa(g)1	3	1-130	35,7004	0,0664	20,5993	0,0190	25,2443	16,0336	0,2586	0,1591	98,0807	60,4577	37,9871	1,0783
VLGa(g)1	3	1-131	35,6896	0,0439	20,6988	0,0000	25,0431	16,0703	0,2433	0,1631	97,9521	60,3919	38,1036	1,0153
VLGa(g)1	3	1-132	35,3403	0,1130	20,3858	0,0190	25,3547	16,0995	0,2478	0,1843	97,7444	59,9066	38,4932	1,0428
VLGa(g)1	3	1-133	35,7177	0,0565	20,5928	0,0000	25,7749	16,3221	0,2798	0,1820	98,9258	59,6283	38,6599	1,1664
VLGa(g)1	3	1-134	35,8004	0,0858	20,4632	0,0000	26,1881	16,5198	0,2518	0,1392	99,4483	59,5236	39,0139	1,0466
VLGa(g)1	3	1-135	35,8363	0,0594	20,6777	0,0042	25,4725	16,5072	0,2030	0,1781	98,9384	59,6580	38,9668	0,8434
VLGa(g)1	3	1-136	35,6636	0,0621	20,4984	0,0274	26,0542	16,6410	0,2729	0,1151	99,3347	59,0451	39,4703	1,1392
VLGa(g)1	3	1-137	35,6466	0,0743	20,6775	0,0000	25,8205	16,2821	0,2246	0,1635	98,8891	59,9440	38,6275	0,9378
VLGa(g)1	3	1-138	35,7400	0,0628	20,8388	0,0000	25,9897	16,0173	0,2770	0,1731	99,0987	60,4185	37,9093	1,1539
VLGa(g)1	3	1-139	35,4090	0,0916	20,4126	0,0000	25,7174	15,9903	0,2239	0,1679	98,0127	60,3767	38,1754	0,9408
VLGa(g)1	3	1-140	35,6352	0,0744	20,5082	0,0000	25,6854	15,7919	0,2828	0,1642	98,1421	60,8494	37,4765	1,1812
VLGa(g)1	3	1-141	35,7836	0,0945	20,3331	0,0000	25,6171	16,3440	0,2297	0,1758	98,5778	59,9098	38,6098	0,9550

Sample code	Crystal	An. Pt.	SiO_2	TiO_2	Al_2O_3	Cr_2O_3	$FeO+Fe_2O_3$	MnO	MgO	CaO	Sum	Alm	Sps	Pyr
VLGa(g)1	3	1-143	35,8116	0,0904	20,7428	0,0000	26,5842	16,4990	0,2517	0,1398	100,1195	59,5878	38,9489	1,0458
VLGa(g)1	3	1-144	35,8478	0,0767	20,6858	0,0000	25,9796	16,0156	0,2388	0,1461	98,9904	60,7921	37,7805	0,9915
VLGa(g)1	3	1-145	36,0781	0,0513	20,5742	0,0380	26,1138	15,8209	0,2425	0,1490	99,0678	61,4541	37,1029	1,0009
VLGa(g)1	3	1-146	35,7593	0,0680	20,5385	0,0106	26,0752	16,0218	0,2747	0,1624	98,9105	60,4751	37,8954	1,1436
VLGa(g)1	3	1-147	35,7130	0,0617	20,8351	0,0000	26,1127	15,9598	0,2277	0,1461	99,0561	60,8103	37,8026	0,9493
VLGa(g)1	3	1-148	35,7156	0,0715	20,5627	0,0338	26,0387	16,0496	0,2484	0,1607	98,8810	60,4786	38,0048	1,0353
VLGa(g)1	3	1-149	35,6431	0,0783	20,6398	0,0000	26,4983	16,1684	0,2475	0,1477	99,4231	60,1650	38,3583	1,0335
VLGa(g)1	3	1-150	35,6843	0,0697	20,5518	0,0000	26,3564	15,7657	0,2586	0,1365	98,8230	61,1454	37,3666	1,0788
VLGa(g)1	3	1-151	35,7856	0,0847	20,2965	0,0000	26,1748	15,6427	0,2117	0,1366	98,3326	61,7528	36,9586	0,8803
VLGa(g)1	3	1-152	35,6482	0,0662	20,4412	0,0000	26,6321	15,7924	0,2419	0,1196	98,9416	61,1603	37,4705	1,0102
VLGa(g)1	3	1-153	35,7879	0,0940	20,8299	0,0042	26,6763	15,4769	0,2004	0,1281	99,1977	62,2267	36,5574	0,8331
VLGa(g)1	3	1-154	35,8206	0,0577	20,6594	0,0021	26,2665	15,5500	0,2889	0,1400	98,7852	61,6563	36,7246	1,2009
VLGa(g)1	3	1-155	35,6813	0,0455	20,6453	0,0127	26,6302	15,6427	0,2653	0,1135	99,0365	61,4551	37,0971	1,1074
VLGa(g)1	3	1-156	35,8789	0,0622	20,5259	0,0000	27,2208	15,6043	0,2771	0,1330	99,7022	61,6640	36,7895	1,1498
VLGa(g)1	3	1-157	35,5746	0,0565	20,6517	0,0000	26,7022	15,3237	0,2115	0,1387	98,6589	62,2565	36,4410	0,8852
VLGa(g)1	3	1-158	35,6279	0,0720	20,3702	0,0084	26,7170	15,3507	0,2640	0,1096	98,5198	62,1292	36,4387	1,1030
VLGa(g)1	3	1-159	35,7820	0,0623	20,4710	0,0000	26,6833	14,9599	0,2307	0,1226	98,3118	63,3079	35,3656	0,9599
VLGa(g)1	3	1-160	35,8111	0,0582	20,6180	0,0316	27,0530	15,2375	0,2457	0,1242	99,1793	62,6116	35,9957	1,0216
VLGa(g)1	3	1-161	35,7930	0,0715	20,7222	0,0000	27,0145	15,3389	0,2263	0,1141	99,2805	62,4744	36,2434	0,9411
VLGa(g)1	3	1-162	36,8236	0,0688	21,3874	0,0000	27,1255	14,9790	0,2559	0,1244	100,7646	64,1982	34,4058	1,0345
VLGa(g)1	3	1-163	35,7472	0,0860	20,4662	0,0063	27,0135	14,5867	0,3304	0,1457	98,3820	63,6890	34,4997	1,3754
VLGa(g)1	3	1-164	35,6641	0,0410	20,5049	0,0084	27,0951	14,5036	0,3484	0,2087	98,3742	63,5030	34,4155	1,4551
VLGa(g)1	3	1-165	35,7368	0,0543	20,6353	0,0000	27,4757	14,3772	0,3610	0,2593	98,8996	63,6825	34,0367	1,5042
VLGa(g)1	3	1-166	35,8935	0,1017	20,7008	0,0000	27,2975	14,1563	0,5049	0,0996	98,7543	64,2762	33,3345	2,0925
VLGa(g)1	3	1-167	35,7993	0,0699	20,6530	0,0000	27,8226	13,4849	0,5742	0,1205	98,5244	65,3941	31,8582	2,3876
VLGa(g)1	3	1-168	35,9541	0,0834	20,7552	0,0000	28,0596	12,8269	0,8150	0,2379	98,7321	65,7541	30,1649	3,3733
VLGa(g)1	3	1-169	36,2143	0,0331	20,8619	0,0190	27,9399	12,6261	1,0515	0,4215	99,1673	64,9178	29,5104	4,3255
VLGa(g)1	3	1-170	36,1658	0,0000	20,7680	0,0000	27,6484	12,6473	1,0446	0,4956	98,7697	64,6059	29,6200	4,3059
Medium Val Leggia dike														
VLGm(g)1	-	1-001	37,0703	0,0688	20,5390	0,0240	18,6038	20,7910	1,4247	1,3226	99,8442	43,0230	47,4382	5,7214
VLGm(g)1	-	1-002	36,9425	0,0817	20,6058	0,0218	18,4173	21,3643	1,3253	1,1113	99,8700	42,5411	48,9019	5,3392
VLGm(g)1	-	1-003	36,8267	0,2356	19,9191	0,0000	18,2531	22,6193	1,3927	0,5571	99,8036	41,0016	51,7746	5,6107
VLGm(g)1	-	1-004	36,8895	0,1733	20,2322	0,0000	17,3621	23,4358	1,1891	0,5935	99,8755	39,8734	53,6204	4,7884
VLGm(g)1	-	1-005	36,5317	0,2177	20,1751	0,0131	17,2230	23,8128	1,2430	0,6003	99,8167	38,2329	54,9646	5,0497
VLGm(g)1	-	1-006	36,6446	0,2150	19,8365	0,0087	17,2558	23,4892	1,2615	0,6038	99,3151	39,0785	54,0544	5,1094
VLGm(g)1	-	1-007	36,8932	0,2318	20,0056	0,0000	17,7140	23,5396	1,2374	0,5463	100,1679	39,6558	53,7886	4,9765
VLGm(g)1	-	1-008	36,7947	0,2409	19,9557	0,0152	17,3505	23,7240	1,2514	0,5625	99,8949	38,9804	54,3443	5,0453
VLGm(g)1	-	1-009	36,5615	0,2178	19,8818	0,0000	17,3500	23,6574	1,2019	0,5493	99,4197	38,9571	54,5615	4,8788
VLGm(g)1	-	1-010	36,5009	0,2510	20,2281	0,0000	17,1026	23,9986	1,2266	0,5102	99,8180	38,1240	55,4022	4,9839
VLGm(g)1	-	1-011	36,5613	0,2414	20,1162	0,0000	17,0726	24,0124	1,1807	0,5058	99,6904	38,3808	55,3538	4,7904
VLGm(g)1	-	1-012	36,6356	0,2239	19,8874	0,0000	17,1315	23,9489	1,1255	0,5375	99,4903	38,7606	55,1157	4,5589
VLGm(g)1	-	1-013	36,7013	0,2307	19,8959	0,0240	17,1152	23,9537	1,1851	0,5598	99,6657	38,5614	55,0209	4,7911
VLGm(g)1	-	1-014	36,6910	0,2375	19,9827	0,0000	16,8908	23,9962	1,2225	0,5630	99,5837	38,2946	55,1263	4,9430
VLGm(g)1	-	1-015	36,8939	0,2253	19,8913	0,0109	17,4747	23,5272	1,3086	0,5557	99,8876	39,3638	53,7663	5,2635
VLGm(g)1	-	1-016	36,4341	0,2579	19,8242	0,0065	17,2424	23,6187	1,2529	0,5587	99,1954	38,6495	54,6169	5,0993
VLGm(g)1	-	1-017	36,7935	0,2621	19,8695	0,0480	17,2851	23,5501	1,3540	0,6688	99,8311	38,6815	53,9245	5,4568
VLGm(g)1	-	1-018	36,6909	0,2591	20,0851	0,0000	17,1097	23,7758	1,2463	0,5166	99,6835	38,8663	54,5960	5,0370
VLGm(g)1	-	1-019	36,5872	0,2631	20,1214	0,0196	16,9762	23,7377	1,2894	0,5696	99,5642	38,4577	54,6578	5,2255
VLGm(g)1	-	1-020	36,4995	0,3796	19,8651	0,0000	16,5670	24,4571	1,2787	0,7045	99,7515	36,4515	56,3143	5,1821
VLGm(g)1	-	1-021	36,9357	0,3078	20,0766	0,0000	17,2783	23,8221	1,2493	0,6431	100,3129	38,8470	54,2881	5,0109
VLGm(g)1	-	1-023	36,4713	0,3424	20,2249	0,0087	16,9662	23,8786	1,3069	0,7567	99,9557	37,4217	55,0664	5,3045
VLGm(g)1	-	1-024	35,7625	0,2964	19,9773	0,0000	16,8469	23,5776	1,2158	0,7163	98,3928	37,3351	55,4955	5,0367
VLGm(g)1	-	1-025	36,8120	0,2871	19,8734	0,0000	17,1943	24,5032	1,2702	0,7236	100,6638	36,7419	56,0503	5,1139
VLGm(g)1	-	1-026	36,7488	0,3061	20,0919	0,0065	16,8167	23,9039	1,2206	0,7782	99,8727	38,0727	54,7518	4,9207
VLGm(g)1	-	1-027	36,5943	0,4198	20,0194	0,0000	16,5939	24,6098	1,1707	0,7037	100,1116	36,7549	56,4740	4,7283
VLGm(g)1	-	1-028	36,8798	0,2478	20,3345	0,0000	16,4577	24,7929	1,1399	0,6818	100,5344	36,7901	56,6545	4,5846
VLGm(g)1	-	1-029	37,3265	0,2052	20,2988	0,0000	16,0003	24,5400	1,1530	0,6481	100,1719	38,1051	55,4562	4,5859
VLGm(g)1	-	1-030	36,9257	0,3263	19,9854	0,0000	15,8939	24,9565	1,0929	0,7102	99,8909	36,7024	56,8673	4,3831
VLGm(g)1	-	1-031	36,8288	0,3266	20,2102	0,0000	15,9812	24,7579	1,1622	0,7952	100,0621	36,4668	56,5619	4,6732
VLGm(g)1	-	1-032	36,4781	0,3303	19,7440	0,0000	15,9515	24,5232	1,1527	0,7096	98,8894	36,6945	56,5564	4,6789
VLGm(g)1	-	1-033	36,6227	0,3267	19,6635	0,0284	15,7606	25,0599	1,1315	0,7060	99,2993	35,8013	57,5718	4,5752
VLGm(g)1	-	1-034	36,6997	0,3278	19,7906	0,0372	15,8651	24,9847	1,1128	0,7055	99,5234	36,1858	57,2781	4,4901
VLGm(g)1	-	1-035	36,5461	0,3212	19,8309	0,0000	15,1885	24,9919	1,0480	0,7635	98,6901	35,9879	57,5416	4,2469
VLGm(g)1	-	1-036	36,4489	0,2690	19,7784	0,0000	15,2361	25,4143	1,1558	0,7280	99,0305	34,4387	58,7320	4,7011
VLGm(g)1	-	1-037	36,7103	0,2743	19,8376	0,0110	15,2004	25,4730	1,1074	0,7262	99,3402	34,9760	58,4444	4,4719
VLGm(g)1	-	1-038	36,7312	0,3532	19,4834	0,0022	15,3420	25,4094	1,0554	0,7788	99,1556	35,3198	58,1721	4,2527
VLGm(g)1	-	1-039	36,7729	0,3303	19,7119	0,0000	15,2630	25,3763	1,1062	0,7986	99,3592	35,1764	58,0579	4,4544
VLGm(g)1	-	1-040	36,6834	0,3629	19,8687	0,0000	15,0291	25,7643	1,1426	0,8001	99,6511	34,0220	59,0492	4,6091
VLGm(g)1	-	1-041	36,6706	0,2981	19,7546	0,0263	15,1975	25,3315	1,0630	0,8338	99,1754	35,1293	58,1541	4,2951
VLGm(g)1	-	1-042	36,7713	0,3702	19,5719	0,0263	14,8305	25,1480	1,1123	0,8169	98,6474	35,6706	57,4914	4,4755
VLGm(g)1	-	1-043	36,4633	0,3642	19,5613	0,0000	15,1148	25,2488	1,0781	0,8809	98,7114	34,8431	58,2129	4,3748
VLGm(g)1	-	1-044	36,7801	0,3484	19,7772	0,0592	14,7520	25,7813	1,1803	0,8398	99,5183	33,8694	58,9513	4,7501
VLGm(g)1	-	1-045	36,6219	0,3753	19,6661	0,0000	14,3710	25,3699	1,1019	0,8304	98,3365	34,9104	58,2275	4,4512
VLGm(g)1	-	1-046	36,7987	0,2631	19,9296	0,0307	14,2402	26,2755	1,0419	0,8376	99,4173	33,2206	60,1554	4,1983
VLGm(g)1	-	1-047	36,6768	0,4299	19,5465	0,0000	13,8382	25,5841	1,0672	0,9370	98,0797	34,4200	58,5668	4,2998
VLGm(g)1	-	1-048	36,4802	0,4133	19,7004	0,0330	13,6661	26,4477	1,0741	0,8674	98,6822	32,2339	60,8878	4,3522
VLGm(g)1	-	1-049	36,5505	0,3016	19,7655	0,0308	13,5864	27,1785	1,0690	0,8000	99,2823	30,7425	62,5936	4,3332
VLGm(g)1	-	1-050	36,4441	0,2882	19,9054	0,0000	13,2040	27,2285	0,9744	0,7797	98,8243	30,8510	62,9080	3,9623
VLGm(g)1	-	1-051	36,3758	0,4339	19,5990	0,0242	13,0595	27,1154	1,0648	0,8837	98,5563	30,5190	62,5762	4,3250
VLGm(g)1	-	1-052	35,8796	0,4830	19,6434	0,0000	12,8209	27,4567	1,0299	0,8251	98,1386	29,1577	64,1668	4,2362
VLGm(g)1	-	1-053	36,0016	0,4666	19,6549	0,0000	12,8515	27,0177	1,0350	0,8480	97,8753	30,3059	62,9504	4,2444
VLGm(g)1	-	1-054	35,6955	0,4765	19,2896	0,0088	12,5849	27,6400	1,0410	0,9349	97,6712	27,9835	64,9338	4,3043
VLGm(g)1	-	1-055	35,9370	0,5047	19,2598	0,0066	12,4128	26,9774	1,0668	0,9316	97,0967	29,9537	62,9187	4,3791
VLGm(g)1	-	1-056	35,9454	0,4899	19,2244	0,0000	12,6062	26,9417	1,0571	0,9275	97,1922	30,0836	62,8402	4,3396
VLGm(g)1	-	1-057	35,2501	0,4565	19,0936	0,0154	12,4806	26,9048	1,0266	0,9110	96,1386	28,9337	64,0242	4,2997
VLGm(g)1	-	1-058	36,1185	0,4538	19,4286	0,0000	12,5880	27,2305	1,0179	0,9376	97,7749	29,8232	63,2595	4,1620
VLGm(g)1	-	1-059	35,9953	0,5033	19,3473	0,0640	12,5455	26,6291	1,0309	0,9191	97,0345	31,0589	62,0086	4,2251
VLGm(g)1	-	1-060	36,3566	0,2865	19,5481	0,0000	12,3274	27,7033	0,9837	0,8414	98,0470	29,3648	64,1603	4,0098
VLGm(g)1	-	1-061	36,3318	0,3177	19,5975	0,0000	12,3613	27,0941	0,9597	0,7999	97,4620	30,9926	62,7517	3,9121
VLGm(g)1	-	1-062	36,0879	0,4094	19,6262	0,0242	12,6995	27,4477	0,9986	0,9105	98,2040	29,3531	63,8762	4,0902

Sample code	Crystal	An. Point	SiO_2	TiO_2	Al_2O_3	Cr_2O_3	$FeO+Fe_2O_3$	MgO	CaO	MnO	ZnO	Na_2O	K_2O	F
Codera Phosphate dike														
CODp(t)1	-	1-001	35,8041	0,1694	32,9836	0,0204	13,8036	1,7493	0,0781	0,6296	0,3738	2,0150	0,0728	0,2465
CODp(t)1	-	1-002	35,2390	0,1670	32,9159	0,0000	13,5532	1,8252	0,0925	0,6736	0,3702	2,0981	0,0628	0,4196
CODp(t)1	-	1-003	35,3297	0,3275	37,2066	0,0139	9,0284	1,4268	0,2049	1,2573	0,0938	2,2080	0,0454	0,7652
CODp(t)1	-	1-004	35,4503	0,1947	33,1249	0,0000	13,4007	1,9204	0,1069	0,6290	0,3516	2,0283	0,0636	0,1283
CODp(t)1	-	1-005	35,5732	0,1739	32,8440	0,0432	13,6642	1,8969	0,0907	0,6044	0,3385	2,0720	0,0738	0,4014
CODp(t)1	-	1-006	35,5291	0,1907	32,9998	0,0114	13,6632	1,9655	0,0775	0,6421	0,3458	2,0543	0,0601	0,1463
CODp(t)1	-	1-007	35,6249	0,1793	32,9075	0,0045	13,8589	1,9684	0,0769	0,6334	0,3513	2,0268	0,0588	0,4369
CODp(t)1	-	1-008	35,5844	0,1719	32,9612	0,0000	13,5642	2,0059	0,0751	0,7087	0,3346	2,0923	0,0673	0,2560
CODp(t)1	-	1-009	35,6425	0,1900	32,7333	0,0273	13,7088	2,1008	0,0757	0,6037	0,3607	2,0373	0,0477	0,1917
CODp(t)1	-	1-010	35,7388	0,1420	32,8410	0,0000	13,6058	2,0853	0,1134	0,5638	0,3664	2,0572	0,0566	0,2100
CODp(t)1	-	1-011	35,8745	0,1601	33,0650	0,0000	13,6317	2,1159	0,0698	0,6938	0,3794	2,0967	0,0296	0,3196
CODp(t)1	-	1-012	35,2811	0,1613	32,6801	0,0250	13,8933	2,1932	0,0787	0,5981	0,3739	2,1494	0,0600	0,1275
CODp(t)1	-	1-013	35,3120	0,1739	32,7202	0,0000	13,6574	2,2071	0,1092	0,5450	0,2861	2,0583	0,0632	0,4098
CODp(t)1	-	1-014	35,7149	0,1533	32,7826	0,0273	13,6105	2,2012	0,0782	0,5666	0,2955	2,1281	0,0367	0,3739
CODp(t)1	-	1-015	35,7548	0,1813	33,5681	0,0091	12,6698	2,1031	0,1261	0,6948	0,3313	2,2097	0,0482	0,3316
CODp(t)1	-	1-016	35,6649	0,1574	33,5990	0,0000	12,5214	2,0412	0,1154	0,6662	0,2863	2,0101	0,0334	0,2123
CODp(t)1	-	1-017	35,8795	0,1596	32,7797	0,0046	13,3889	2,1545	0,0639	0,5837	0,3758	2,1251	0,0500	0,3835
CODp(t)1	-	1-018	35,7395	0,1590	32,7912	0,0000	13,3797	2,2691	0,0937	0,5871	0,3816	2,1312	0,0507	0,4290
CODp(t)1	-	1-019	35,8133	0,1384	32,9487	0,0251	13,3258	2,1864	0,0722	0,5971	0,3386	2,1099	0,0485	0,4660
CODp(t)1	-	1-020	36,0865	0,1429	33,4058	0,0251	13,1580	2,1028	0,0998	0,5597	0,3499	2,0694	0,0242	0,3575
CODp(t)1	-	1-021	35,8974	0,1804	33,2339	0,0000	13,3160	2,0593	0,1129	0,5532	0,3741	2,0982	0,0653	0,4206
CODp(t)1	-	1-022	35,9554	0,1573	33,0529	0,0000	12,9582	2,1322	0,0926	0,6560	0,3911	2,1195	0,0400	0,0460
CODp(t)1	-	1-023	35,7320	0,1266	33,2375	0,0000	13,0509	2,1594	0,0878	0,5404	0,3686	2,1194	0,0435	0,1651
CODp(t)1	-	1-024	35,6496	0,1685	33,1513	0,0182	13,3454	2,1494	0,0872	0,5046	0,2881	2,0008	0,0497	0,1191
CODp(t)1	-	1-025	35,5759	0,1515	33,0330	0,0000	13,3923	2,0477	0,1015	0,5501	0,4022	2,0947	0,0274	0,1829
CODp(t)1	-	1-026	36,0575	0,1466	33,1434	0,0046	13,2048	2,1534	0,0884	0,5928	0,3387	2,0580	0,0396	0,3756
CODp(t)1	-	1-027	35,8287	0,1441	33,0686	0,0068	13,1380	2,0571	0,0962	0,6111	0,3106	2,0385	0,0435	0,3210
CODp(t)1	-	1-028	35,8040	0,1603	33,0330	0,0000	13,1654	2,0954	0,0878	0,5934	0,3777	2,1004	0,0579	0,4208
CODp(t)1	-	1-029	35,7694	0,1729	32,9569	0,0114	13,1972	2,0471	0,0908	0,6016	0,2975	2,0414	0,0411	0,0827
CODp(t)1	-	1-030	35,6804	0,1578	32,8288	0,0000	13,1716	2,1491	0,0723	0,6100	0,2844	2,1530	0,0629	0,4118
CODp(t)1	-	1-031	35,5960	0,1547	32,9870	0,0046	13,3051	2,0162	0,0717	0,6235	0,3049	2,0908	0,0657	0,2290
CODp(t)1	-	1-032	35,5868	0,1339	32,8695	0,0000	13,6384	2,1538	0,0621	0,5792	0,3217	2,0423	0,0403	0,1735
CODp(t)1	-	1-033	35,6878	0,1582	32,9444	0,0114	13,8300	2,1336	0,0764	0,6243	0,3441	2,0427	0,0566	0,2281
CODp(t)1	-	1-034	35,5719	0,1778	32,9195	0,0114	13,3075	2,1001	0,0878	0,5707	0,3199	2,1863	0,0692	0,6473
CODp(t)1	-	1-035	35,6204	0,1564	32,8200	0,0091	13,7088	2,0788	0,0740	0,6481	0,2618	2,0901	0,0455	0,2102
CODp(t)1	-	1-036	35,5963	0,1577	33,1616	0,0319	13,4557	1,8965	0,1092	0,6397	0,3983	2,0599	0,0472	0,3839
CODp(t)1	-	1-037	35,7488	0,2473	33,2998	0,0205	13,2868	1,9209	0,1063	0,6281	0,3554	2,0968	0,0397	0,2752
CODp(t)1	-	2-001	35,1059	0,2841	33,9951	0,0000	12,2360	1,4642	0,1163	1,2112	0,2052	2,1462	0,0603	0,6508
CODp(t)1	-	2-002	35,2872	0,1577	32,5930	0,0068	12,9497	2,3509	0,0770	0,5716	0,3750	2,2296	0,0462	0,4302
CODp(t)1	-	2-003	35,3247	0,1606	32,6768	0,0295	13,2844	2,3163	0,0888	0,5655	0,3543	2,1883	0,0463	0,3746
CODp(t)1	-	2-004	35,4164	0,1176	32,8362	0,0000	13,1222	2,3340	0,0853	0,5587	0,2966	2,2246	0,0512	0,3659
CODp(t)1	-	2-005	35,4864	0,1591	32,7439	0,0000	12,8612	2,2490	0,1075	0,5073	0,2874	2,2732	0,0548	0,0552
CODp(t)1	-	2-006	35,3185	0,1501	33,0068	0,0000	13,1089	2,3500	0,1247	0,5895	0,3396	2,1786	0,0311	0,4119
CODp(t)1	-	2-007	35,6218	0,1695	32,5750	0,0000	12,2745	2,2936	0,0871	0,5416	0,3228	2,1256	0,0398	0,3659
CODp(t)1	-	2-008	35,5074	0,1388	32,5573	0,0296	12,9625	2,2947	0,0817	0,5770	0,3749	2,1273	0,0786	0,3301
CODp(t)1	-	2-009	35,5111	0,1538	32,6893	0,0273	12,9994	2,2034	0,0984	0,5604	0,3954	2,1752	0,0408	0,2842
CODp(t)1	-	2-010	35,5047	0,1640	32,7768	0,0228	12,9115	2,3048	0,0836	0,5436	0,3863	2,2105	0,0501	0,3027
CODp(t)1	-	2-011	35,3868	0,1891	32,6898	0,0273	12,7713	2,3484	0,0973	0,6071	0,3285	2,1533	0,0636	0,1014
CODp(t)1	-	2-012	35,4970	0,1452	32,5071	0,0000	12,9425	2,2642	0,0633	0,5753	0,3415	2,1782	0,0593	0,1837
CODp(t)1	-	2-013	35,5519	0,1902	32,5754	0,0273	12,9228	2,2862	0,0925	0,6178	0,3583	2,2112	0,0568	0,1564
CODp(gt)1	-	1-001	35,8942	0,0892	33,8538	0,0000	12,3215	2,0922	0,0622	0,6241	0,3071	1,8062	0,0421	0,2220
CODp(gt)1	-	1-002	36,1537	0,0490	33,9155	0,0000	12,3648	2,1204	0,0293	0,5556	0,3483	1,8459	0,0431	0,2309
CODp(gt)1	-	1-003	35,9832	0,1017	33,9227	0,0091	12,4236	2,1544	0,0694	0,4912	0,2714	1,8563	0,0508	0,2492
CODp(gt)1	-	1-004	36,3333	0,1073	33,9774	0,0000	12,8331	2,1764	0,0526	0,5396	0,2339	1,9359	0,0559	0,2670
CODp(gt)1	-	1-005	36,1200	0,1043	33,7943	0,0275	12,4129	2,0973	0,0557	0,4752	0,3165	1,7557	0,0530	0,0833
CODp(gt)1	-	1-006	35,9536	0,0866	33,8396	0,0206	12,5851	2,0818	0,0544	0,5385	0,3482	1,7690	0,0215	0,0001
CODp(gt)1	-	1-007	36,1511	0,0961	34,1140	0,0229	12,5175	2,0948	0,0509	0,4864	0,3183	1,8203	0,0355	0,1386
CODp(gt)1	-	1-008	35,9717	0,0848	33,8772	0,0297	12,3989	2,0365	0,0712	0,4526	0,3483	1,8348	0,0569	0,1016
CODp(gt)1	-	1-009	36,0053	0,0672	34,1571	0,0366	12,6463	2,1191	0,0586	0,5276	0,2771	1,9070	0,0453	0,1015
CODp(gt)1	-	1-010	36,0138	0,0766	33,7338	0,0069	12,5511	2,1002	0,0497	0,5424	0,3089	1,8201	0,0435	0,2030
CODp(gt)1	-	1-011	36,1833	0,2144	32,9406	0,0000	13,0517	2,3839	0,1129	0,5085	0,3032	2,1910	0,0554	0,3941
CODp(gt)1	-	1-012	35,8843	0,1812	33,1423	0,0000	13,0079	2,2552	0,1094	0,4987	0,2826	2,1233	0,0520	0,2203
CODp(gt)1	-	1-013	35,7624	0,1750	33,1168	0,0000	12,9288	2,2468	0,1058	0,5050	0,3331	2,1069	0,0643	0,4124
CODp(gt)1	-	1-014	35,8018	0,2163	32,9951	0,0297	13,0298	2,1522	0,0849	0,4951	0,2807	2,1534	0,0184	0,0827
CODp(gt)1	-	1-015	36,0472	0,1950	32,9945	0,0000	13,0057	2,1090	0,1440	0,5206	0,2527	2,0104	0,0769	0,4223
CODp(gt)1	-	1-016	35,9449	0,1818	33,0584	0,0000	13,0210	2,0804	0,1141	0,5208	0,3294	2,0948	0,0580	0,4308
CODp(gt)1	-	1-017	35,6286	0,1798	33,4607	0,0160	13,1858	2,1266	0,1063	0,5153	0,3499	2,1065	0,0393	0,2382
CODp(gt)1	-	1-018	35,7055	0,1956	33,2025	0,0000	12,9621	2,0817	0,0968	0,5328	0,3181	2,1302	0,0711	0,3211
CODp(gt)1	-	1-019	35,6699	0,1975	33,1445	0,0000	12,9435	2,1026	0,0992	0,5390	0,3611	2,0434	0,0437	0,3669
CODp(gt)1	-	1-020	35,6018	0,1861	33,2625	0,0000	13,0549	2,1027	0,0986	0,6443	0,2676	2,1222	0,0471	0,4219
CODp(gt)1	-	1-021	35,7970	0,2049	33,2305	0,0388	12,8695	1,9864	0,1016	0,6593	0,3312	2,1409	0,0485	0,4503
CODp(gt)1	-	1-022	35,4983	0,1865	32,9247	0,0000	13,3675	1,9232	0,0788	0,6795	0,3983	2,1284	0,0500	0,3566
CODp(gt)1	-	2-001	35,0294	0,2076	34,0660	0,0000	13,2468	1,0720	0,0710	0,9968	0,4804	1,9740	0,0567	0,2026
CODp(gt)1	-	2-002	34,9233	0,2400	34,0263	0,0227	13,2391	1,0881	0,0858	1,0145	0,5419	2,0288	0,0535	0,3768
CODp(gt)1	-	2-003	35,0582	0,2061	33,9112	0,0000	13,6410	1,0404	0,0882	0,9599	0,5064	2,0308	0,0420	0,3663
CODp(gt)1	-	2-004	35,0447	0,2174	33,8116	0,0000	13,4263	1,0627	0,0507	0,9658	0,4915	2,0156	0,0419	0,4308
CODp(gt)1	-	2-005	34,8906	0,2173	34,1038	0,0045	13,7678	1,0433	0,0822	1,0221	0,3681	1,9793	0,0410	0,3391
CODp(gt)1	-	2-006	34,9938	0,1992	34,0071	0,0000	13,6781	0,9684	0,0947	1,0308	0,5903	1,9690	0,0626	0,4393
CODp(gt)1	-	2-007	35,1757	0,2118	34,2609	0,0000	13,5334	0,9695	0,0578	1,0548	0,4541	1,9761	0,0543	0,3033
CODp(gt)1	-	2-008	35,3567	0,1750	34,1822	0,0364	13,5109	0,9730	0,0733	0,9752	0,5513	2,0411	0,0659	0,3395
CODp(gt)1	-	2-009	35,0207	0,1980	33,9110	0,0000	13,6303	0,9665	0,0691	1,0453	0,4671	1,9537	0,0525	0,1103
CODp(gt)1	-	2-010	35,3366	0,2118	34,1380	0,0000	13,5171	0,9376	0,0852	1,0395	0,5437	2,0511	0,0413	0,3763
CODp(gt)1	-	3-001	35,9726	0,1423	37,9378	0,0000	7,8960	0,8840	0,2449	0,7710	0,0977	2,4251	0,0750	0,7018
CODp(gt)1	-	3-002	35,2330	0,2150	34,2629	0,0000	13,2119	0,9104	0,0668	1,0763	0,5121	1,8877	0,0588	0,2766
CODp(gt)1	-	3-003	35,2884	0,1794	34,5504	0,0137	13,3233	0,8827	0,0745	1,0153	0,5196	1,9155	0,0738	0,4138
CODp(gt)1	-	3-004	35,0111	0,2606	34,6755	0,0114	13,3103	0,9097	0,0477	1,0047	0,5195	1,8753	0,0391	0,4779
CODp(gt)1	-	3-005	35,3185	0,2519	34,3957	0,0000	13,2033	0,8960	0,0632	1,0503	0,5420	1,9193	0,0426	0,3134
CODp(gt)1	-	3-006	35,3046	0,2288	34,0327	0,0159	13,2318	0,9231	0,0680	0,9928	0,5719	2,0481	0,0603	0,2394
CODp(gt)1	-	3-007	35,1865	0,2250	34,3283	0,0000	13,3269	0,8724	0,0572	1,0443	0,4374	1,9269	0,0457	0,3315
CODp(gt)1	-	3-008	35,3728	0,2356	34,1074	0,0000	13,3454	0,9191	0,0519	1,0536	0,5195	1,9930	0,0432	0,3496
CODp(gt)1	-	3-009	35,4379	0,1981	34,5896	0,0000	13,4247	0,9495	0,0966	1,0644	0,5550	1,9444	0,0617	0,0738
CODp(gt)1	-	3-010	35,1524	0,2363	34,2181	0,0000	13,1667	1,0150	0,0668	0,9952	0,5103	1,9566	0,0631	0,5787
CODp(gt)1	-	3-011	35,0646	0,1875	34,2844	0,0000	13,3169	0,9226	0,0578	1,0248	0,4897	1,9807	0,0154	0,3309
CODp(gt)1	-	3-012	35,0545	0,2381	34,3811	0,0000	13,4209	0,9251	0,0793	0,9972	0,5195	1,9887	0,0513	0,3857
CODp(gt)1	-	3-013	35,0631	0,2081	34,1070	0,0227	13,3029	1,0030	0,1002	1,0222	0,5251	1,9490	0,0583	0,4685
CODp(gt)1	-	3-014	35,6505	0,1801	34,2271	0,0182	13,2665	0,8674	0,0650	0,9373	0,5925	1,8932	0,0404	0,1935
CODp(gt)1	-	3-015	35,4513	0,1501	34,3124	0,0228	12,9684	0,8777	0,0680	1,0131	0,5553	1,9284	0,0330	0,1479
CODp(gt)1	-	3-016	35,6196	0,1814	34,0454	0,0114	13,0331	0,9683	0,0436	1,0197	0,4263	1,9251	0,0449	0,2955
CODp(gt)1	-	3-017	35,3682	0,2835	33,7304	0,0274	12,9326	1,2498	0,1253	0,9906	0,3179	2,0038	0,0531	0,4433

Sample code	Crystal	An. Point	SiO_2	TiO_2	Al_2O_3	Cr_2O_3	$FeO+Fe_2O_3$	MgO	CaO	MnO	ZnO	Na_2O	K_2O	F
CODp(gt)1	-	3-018	35,4283	0,2715	33,8052	0,0068	13,3597	1,3392	0,1324	0,8642	0,2655	2,0119	0,0428	0,3863
CODp(gt)1	-	3-019	35,2962	0,2838	33,2624	0,0000	13,4970	1,4572	0,1228	0,9480	0,2075	2,1203	0,0441	0,7962
CODp(gt)1	-	3-020	35,4843	0,2927	33,3108	0,0000	13,1466	1,4207	0,1324	1,0199	0,2487	1,9892	0,0254	0,8454
CODp(gt)1	-	3-021	35,7230	0,2816	33,7984	0,0091	13,0687	1,3030	0,1271	1,0522	0,2712	2,0726	0,0257	0,6270
CODp(gt)1	-	3-022	35,4671	0,2503	33,1064	0,0661	13,0455	1,4885	0,1563	0,9832	0,2319	2,0493	0,0553	0,6266
CODp(gt)1	-	3-023	35,7365	0,2209	33,7007	0,0114	13,0044	1,3904	0,1522	1,0700	0,2730	2,0328	0,0621	0,5172
CODp(gt)1	-	3-024	35,6038	0,2252	33,3730	0,0000	13,1256	1,4892	0,1199	1,0024	0,2730	1,9608	0,0343	0,7446
CODp(gt)1	-	3-025	35,4204	0,2487	33,5566	0,0114	13,3985	1,3880	0,1442	1,1463	0,3047	2,1312	0,0446	0,6524
CODp(gt)1	-	3-026	36,3713	0,1533	37,8113	0,0210	7,6090	0,8038	0,2257	0,6635	0,1428	2,3164	0,0121	1,0470
CODp(gt)1	-	4-001	36,0973	0,1606	37,3932	0,0047	7,9491	0,9061	0,2574	0,9801	0,1728	2,2920	0,0301	0,7988
CODp(gt)1	-	4-002	34,8987	0,1964	34,8170	0,0137	12,7091	0,7015	0,0907	1,1661	0,6149	2,0506	0,0597	0,4711
CODp(gt)1	-	4-003	35,1979	0,2193	34,7460	0,0000	13,0509	0,7120	0,0697	1,2732	0,6782	1,9806	0,0532	0,3970
CODp(gt)1	-	4-004	35,0878	0,2146	34,4011	0,0023	12,7534	0,7664	0,0877	1,1321	0,6019	1,9620	0,0764	0,1760
CODp(gt)1	-	4-005	35,1356	0,2139	34,5045	0,0000	12,8642	0,7839	0,0704	1,0918	0,5944	1,8983	0,0656	0,5532
CODp(gt)1	-	4-006	34,8581	0,2074	34,5508	0,0068	13,2732	0,7830	0,0727	1,1524	0,6091	1,9110	0,0272	0,0462
CODp(gt)1	-	4-007	35,6358	0,2157	34,1311	0,0524	13,0162	0,7941	0,0328	1,1368	0,5084	1,9024	0,0560	0,5630
CODp(gt)1	-	4-008	35,1764	0,2327	34,1604	0,0000	12,9102	0,8550	0,0692	1,0705	0,5122	1,8817	0,0562	0,4522
CODp(gt)1	-	4-009	35,1258	0,2187	34,2302	0,0000	13,2844	0,8634	0,0697	1,1083	0,5512	1,9926	0,0643	0,4689
CODp(gt)1	-	4-010	35,0547	0,2654	33,9074	0,0000	12,9724	1,3324	0,1361	0,9066	0,2207	2,0585	0,0680	0,5434
Rossaccio Beryl dike														
ROSb(t)1	-	1	35,3895	0,2385	33,5929	0,0000	12,9439	1,7370	0,0766	0,7194	0,3141	2,2324	0,0520	0,5933
ROSb(t)1	-	2	36,1717	0,1264	34,0338	0,0000	13,5797	1,6163	0,0469	0,4724	0,3123	1,9752	0,0306	0,0638
ROSb(t)1	-	3	35,2637	0,2652	34,2100	0,0000	13,1341	1,9666	0,1207	0,6984	0,2886	2,1382	0,0543	0,6031
ROSb(t)1	-	3-001	35,7391	0,4419	33,7478	0,0387	13,1983	2,5892	0,1244	0,3642	0,2348	2,2098	0,0439	0,2015
ROSb(t)1	-	3-002	35,5504	0,1544	33,6608	0,0023	14,1368	1,2964	0,0891	0,5047	0,4149	2,0668	0,0328	0,2991
ROSb(t)1	-	3-003	35,7006	0,1819	33,7948	0,0181	14,0312	1,3994	0,0713	0,5275	0,4133	2,0783	0,0515	0,2726
ROSb(t)1	-	3-004	36,0116	0,1664	33,8548	0,0000	13,7461	1,3175	0,0642	0,6182	0,4097	2,0056	0,0469	0,4736
ROSb(t)1	-	3-005	35,8413	0,1458	34,0989	0,0045	14,0627	1,4000	0,0767	0,5981	0,3277	2,0218	0,0474	0,5356
ROSb(t)1	-	3-006	35,7335	0,1640	33,9456	0,0068	13,7406	1,4126	0,0850	0,4995	0,3650	2,1375	0,0298	0,5449
ROSb(t)1	-	3-007	35,8656	0,1583	33,7470	0,0589	13,6466	1,4154	0,0779	0,5463	0,3202	2,0736	0,0430	0,4100
ROSb(t)1	-	3-008	35,9367	0,1508	33,9734	0,0023	14,0584	1,4976	0,0749	0,5201	0,2719	2,0824	0,0556	0,5714
ROSb(t)1	-	3-009	35,7880	0,1528	33,8067	0,0113	13,7166	1,4867	0,0690	0,4971	0,3613	2,0102	0,0574	0,4366
ROSb(t)1	-	4-001	35,8139	0,1608	33,6646	0,0204	13,8739	1,5842	0,0803	0,5003	0,3313	2,1047	0,0625	0,2910
ROSb(t)1	-	4-002	36,0535	0,1590	33,6618	0,0000	13,7371	1,5799	0,0868	0,5098	0,3446	2,1285	0,0311	0,4547
ROSb(t)1	-	4-003	35,7645	0,1691	33,6396	0,0000	13,5514	1,5932	0,0952	0,5180	0,3111	2,0191	0,0529	0,3739
ROSb(t)1	-	4-004	35,8028	0,1883	33,7049	0,0000	13,7560	1,6146	0,0773	0,4950	0,2887	2,0468	0,0236	0,5181
ROSb(t)1	-	4-005	35,6719	0,1309	33,3959	0,0000	13,9470	1,7223	0,0845	0,4763	0,2812	2,0919	0,0677	0,2453
ROSb(t)1	-	4-006	35,8787	0,1465	33,4213	0,0000	13,8405	1,5984	0,0862	0,5433	0,3129	2,1412	0,0350	0,2730
ROSb(t)1	-	4-007	35,7532	0,1702	33,4392	0,0000	13,8660	1,6237	0,0696	0,4805	0,3110	2,0938	0,0412	0,5171
ROSb(t)1	-	5-001	36,0577	0,1484	33,7426	0,0295	13,7692	1,6175	0,1011	0,4571	0,4544	2,1392	0,0301	0,3364
ROSb(t)1	-	5-002	35,9298	0,1609	33,8137	0,0000	13,8084	1,6527	0,0750	0,5080	0,3632	2,0638	0,0338	0,0821
ROSb(t)1	-	5-003	35,9334	0,1291	33,6328	0,0000	13,8362	1,7058	0,0946	0,5248	0,2980	2,1197	0,0552	0,1822
ROSb(t)1	-	5-004	35,6979	0,1510	33,6725	0,0000	13,7202	1,7002	0,0886	0,3987	0,3018	2,0352	0,0346	0,4812
ROSb(t)1	-	5-005	36,1310	0,1428	33,7964	0,0227	13,8004	1,7535	0,0833	0,5970	0,3632	2,1588	0,0488	0,3643
ROSb(t)1	-	5-006	35,9097	0,1673	33,6674	0,0000	13,5293	1,7109	0,1053	0,4503	0,3707	2,0454	0,0366	0,3554
ROSb(t)1	-	6-001	35,6880	0,1821	33,5295	0,0000	13,9058	1,9164	0,0779	0,4505	0,2924	2,1375	0,0301	0,0728
ROSb(t)1	-	6-002	35,9156	0,0792	34,4768	0,0340	13,6688	1,6367	0,0595	0,5179	0,3260	1,9459	0,0276	0,3827
ROSb(t)1	-	6-003	36,1010	0,0942	33,9873	0,0431	13,5801	1,6345	0,0601	0,4538	0,3335	1,8567	0,0207	0,2920
ROSb(t)1	-	6-004	36,0376	0,0930	34,5260	0,0000	13,5295	1,6283	0,0584	0,4950	0,2944	1,8133	0,0324	0,3197
ROSb(t)1	-	6-005	36,0959	0,1118	34,3387	0,0250	13,2360	1,5546	0,0548	0,4932	0,2907	1,7698	0,0389	0,0001
ROSb(t)1	-	6-006	35,9724	0,0949	34,0251	0,0136	13,4166	1,5966	0,0613	0,4656	0,2888	1,8429	0,0464	0,3015
ROSb(t)1	-	6-007	36,1954	0,0936	34,2878	0,0000	13,5948	1,6102	0,0482	0,5135	0,2981	1,8300	0,0396	0,3924
ROSb(t)1	-	7-001	35,9786	0,1341	34,3465	0,0023	13,8140	1,5526	0,0667	0,4229	0,2683	1,8934	0,0297	0,2824
ROSb(t)1	-	7-002	35,9733	0,0718	34,1782	0,0000	13,4621	1,5208	0,0762	0,4136	0,3261	1,8488	0,0311	0,3739
ROSb(t)1	-	7-003	36,2731	0,0849	33,9098	0,0204	13,5051	1,6002	0,0679	0,5129	0,2627	1,7920	0,0438	0,2562
ROSb(t)1	-	7-004	36,1653	0,1218	34,0246	0,0000	13,4266	1,5996	0,0619	0,4361	0,3503	1,9765	0,0330	0,1919
ROSb(t)1	-	8-001	36,0358	0,0986	34,2325	0,0000	13,6853	1,5748	0,0315	0,4342	0,2497	1,9175	0,0203	0,3915
ROSb(t)1	-	8-002	36,2217	0,0912	34,0471	0,0091	13,3810	1,5540	0,0596	0,4285	0,3001	1,8535	0,0368	0,0916
ROSb(t)1	-	8-003	36,0090	0,1055	34,1120	0,0000	13,3108	1,6037	0,0673	0,5243	0,2907	1,9120	0,0371	0,4750
ROSb(t)1	-	8-004	35,8260	0,1349	34,4686	0,0045	13,3617	1,6006	0,0506	0,4492	0,2907	1,9299	0,0295	0,3380
ROSb(t)1	-	8-005	36,0369	0,0843	33,9460	0,0000	13,3222	1,5959	0,0566	0,4313	0,2758	1,8219	0,0343	0,0550
ROSb(t)1	-	8-006	36,1383	0,1211	34,4822	0,0136	13,5510	1,6003	0,0548	0,4182	0,2665	1,8124	0,0379	0,2376
ROSb(t)1	-	8-007	36,1050	0,0994	34,3934	0,0000	13,2833	1,5578	0,0852	0,4874	0,2834	1,8293	0,0520	0,3297
ROSb(t)1	-	8-008	36,2777	0,1099	33,9158	0,0000	13,5104	1,6284	0,0643	0,4925	0,3503	1,8541	0,0324	0,4470
ROSb(t)1	-	8-009	36,2489	0,1199	34,1722	0,0068	13,4544	1,6119	0,0554	0,4590	0,2739	1,8684	0,0323	0,2196
ROSb(t)1	-	8-010	36,2199	0,0849	34,3207	0,0136	13,3783	1,6046	0,0548	0,4646	0,2796	1,7580	0,0417	0,3658
ROSb(t)1	-	8-011	36,1604	0,0918	34,1020	0,0227	13,6391	1,5254	0,0488	0,3694	0,2795	1,7880	0,0338	0,4916
ROSb(t)1	-	8-012	35,9452	0,1055	34,0267	0,0159	13,5525	1,6027	0,0548	0,4893	0,2962	1,9153	0,0210	0,4465
Val Del Dosso dike														
VDD(t)1	-	1	35,0391	0,6802	32,8524	0,0000	13,3818	2,4621	0,1270	0,1524	0,1134	2,2410	0,0470	0,4453
VDD(t)1	-	2	35,6249	0,0523	34,6911	0,0000	13,9024	0,8569	0,0487	0,1841	0,0837	1,6986	0,0418	0,4350
VDD(t)1	-	3-001	34,8924	0,7333	33,1875	0,0182	13,1056	2,4055	0,1309	0,1159	0,1194	2,2089	0,0927	0,5195
VDD(t)1	-	3-002	34,9263	0,6292	32,9727	0,0000	13,6645	2,1554	0,1158	0,1255	0,1489	2,2416	0,0436	0,4985
VDD(t)1	-	3-003	35,0097	0,5934	33,1975	0,0113	13,7665	1,8585	0,0986	0,1679	0,0614	2,1296	0,0574	0,8951
VDD(t)1	-	3-004	34,9602	0,5609	33,2089	0,0000	14,2000	1,5287	0,0789	0,1509	0,2120	2,1584	0,0420	0,7117
VDD(t)1	-	3-005	35,2266	0,3557	33,2992	0,0294	14,0309	1,4759	0,0754	0,1566	0,1023	2,1322	0,0365	0,5602
VDD(t)1	-	3-006	35,1582	0,3082	33,5608	0,0068	14,1271	1,3298	0,0713	0,1943	0,2288	2,1328	0,0562	0,3884
VDD(t)1	-	3-007	34,7737	0,3057	33,6084	0,0000	14,2100	1,3131	0,0807	0,1516	0,0614	2,0452	0,0497	0,6306
VDD(t)1	-	3-008	35,9101	0,2723	33,3487	0,0251	12,6764	2,9174	0,1812	0,0903	0,0000	1,6576	0,0322	0,1470
VDD(t)1	-	3-009	34,9745	0,2595	34,0281	0,0000	14,3299	1,0344	0,0588	0,1872	0,1507	2,0550	0,0400	0,3969
VDD(t)1	-	3-010	35,3321	0,2522	33,7579	0,0000	14,0606	0,9787	0,0582	0,2664	0,1507	1,9388	0,0488	0,5519
VDD(t)1	-	3-011	35,0474	0,2584	33,7787	0,0000	14,1938	1,1620	0,0927	0,2132	0,0949	1,9372	0,0340	0,1812
VDD(t)1	-	3-012	35,0972	0,2191	33,8354	0,0000	14,3397	1,0281	0,0879	0,2009	0,1172	1,9545	0,0414	0,4332
VDD(t)1	-	3-013	34,8040	0,2569	33,6174	0,0000	14,4014	1,0490	0,0807	0,2600	0,0949	1,9941	0,0327	0,4689
VDD(t)1	-	3-014	35,3534	0,2198	33,8472	0,0249	14,1924	1,0143	0,0713	0,1827	0,1581	1,9994	0,0555	0,5148
VDD(t)1	-	3-015	35,1618	0,2167	33,9497	0,0000	13,9822	1,0915	0,0873	0,2654	0,2177	1,9886	0,0491	0,4615
VDD(t)1	-	3-016	35,3061	0,2068	33,9210	0,0068	13,9406	1,0117	0,0784	0,2578	0,1433	2,0246	0,0499	0,3446
VDD(t)1	-	3-017	35,0310	0,2018	33,8868	0,0181	14,0875	1,0135	0,0915	0,2202	0,0930	1,9043	0,0505	0,4344
VDD(t)1	-	3-018	35,4296	0,2124	34,0070	0,0068	14,0629	1,0409	0,0570	0,2532	0,1414	1,9065	0,0444	0,5610
VDD(t)1	-	3-019	35,4694	0,2338	33,8740	0,0000	13,8622	0,9879	0,0660	0,1682	0,0893	1,9464	0,0270	0,3720
VDD(t)1	-	3-020	35,1777	0,1613	33,6808	0,0226	14,0366	1,0062	0,0719	0,2647	0,1098	1,9768	0,0565	0,3894
VDD(t)1	-	3-021	34,9668	0,2385	33,6680	0,0000	14,0967	1,0526	0,0772	0,2489	0,0893	1,9879	0,0606	0,2718
VDD(t)1	-	3-022	35,4216	0,2162	33,7660	0,0000	13,9515	0,9745	0,0921	0,2409	0,1638	1,9224	0,0423	0,2904
VDD(t)1	-	3-023	34,4974	0,2440	33,8461	0,0090	14,2800	1,0053	0,0974	0,2944	0,1489	1,9666	0,0451	0,4155
VDD(t)1	-	3-024	35,3492	0,2162	34,0545	0,0000	14,2181	1,0334	0,0844	0,2441	0,1433	2,0346	0,0419	0,4252
VDD(t)1	-	3-025	34,5934	0,2129	33,8596	0,0000	14,2927	1,0110	0,0843	0,2411	0,2065	1,9516	0,0444	0,5496
VDD(t)1	-	3-026	34,9335	0,1701	33,8294	0,0023	14,1646	1,0336	0,0565	0,2004	0,0633	1,8800	0,0295	0,3257
VDD(t)1	-	3-027	35,0693	0,2035	33,7734	0,0023	14,3917	1,0613	0,0529	0,2962	0,1228	1,9733	0,0344	0,1991
VDD(t)1	-	3-028	35,1403	0,1694	33,6755	0,0023	14,1812	1,0425	0,1129	0,2280	0,1005	1,9641	0,0340	0,4070
VDD(t)1	-	3-029	35,1254	0,2006	33,7454	0,0090	14,0757	1,0319	0,0737	0,2841	0,1303	1,9803	0,0267	0,4706
VDD(t)1	-	3-030	35,5097	0,1789	33,8843	0,0000	14,0189	1,0429	0,0826	0,2400	0,0894	1,9529	0,0324	0,3628

Sample code	Crystal	An. Point	SiO_2	TiO_2	Al_2O_3	Cr_2O_3	$FeO+Fe_2O_3$	MgO	CaO	MnO	ZnO	Na_2O	K_2O	F
VDD(t)1	-	3-031	35,2372	0,1994	34,1159	0,0000	14,1024	1,1166	0,1052	0,2533	0,1080	1,9645	0,0499	0,5699
VDD(t)1	-	3-032	35,5403	0,0561	34,6887	0,0000	13,8759	0,8071	0,0345	0,1914	0,1173	1,6652	0,0321	0,4356
VDD(t)1	-	3-033	35,9395	0,0574	34,3198	0,0113	13,8912	0,8220	0,0470	0,2026	0,1527	1,6159	0,0423	0,0091
VDD(t)1	-	3-034	35,3556	0,0549	34,5539	0,0000	13,8961	0,8602	0,0298	0,2748	0,0670	1,7061	0,0403	0,1093
VDD(t)1	-	3-035	35,2398	0,0287	34,4040	0,0068	14,1116	0,8459	0,0434	0,2186	0,1080	1,6064	0,0528	0,0818
VDD(t)1	-	3-036	35,6584	0,0861	34,4357	0,0000	13,8508	0,8370	0,0286	0,2254	0,0969	1,6307	0,0328	0,3002
VDD(t)1	-	3-037	35,8332	0,0611	34,2974	0,0000	13,7360	0,8114	0,0310	0,1827	0,1527	1,7113	0,0366	0,1276
VDD(t)1	-	3-038	35,1589	0,0480	34,7402	0,0385	13,9306	0,8719	0,0571	0,2232	0,0912	1,6178	0,0384	0,3270
VDD(t)1	-	3-039	35,3513	0,0692	34,6639	0,0000	13,9205	0,8261	0,0327	0,2180	0,0875	1,6811	0,0456	0,0637
VDD(t)1	-	3-040	35,5212	0,0561	34,6486	0,0000	13,7336	0,8206	0,0518	0,2419	0,0428	1,6508	0,0314	0,4004
VDD(t)1	-	3-041	36,1128	0,0381	34,6219	0,0000	13,7599	0,8098	0,0417	0,2216	0,1155	1,6475	0,0435	0,1187
VDD(t)1	-	3-042	35,6124	0,0487	34,3369	0,0000	13,6381	0,7877	0,0458	0,2619	0,0987	1,6669	0,0359	0,3552
VDD(t)1	-	3-043	35,3169	0,0536	34,6814	0,0272	13,8972	0,8369	0,0482	0,2453	0,0987	1,6115	0,0317	0,3272
VDD(t)1	-	3-044	35,4575	0,0586	34,4936	0,0068	13,6840	0,8215	0,0262	0,2416	0,1229	1,6093	0,0549	0,2278
VDD(t)1	-	3-045	35,6793	0,0568	34,4060	0,0000	13,8317	0,8206	0,0440	0,2773	0,0894	1,6657	0,0370	0,3367
VDD(t)1	-	3-046	35,4739	0,0693	34,4619	0,0113	13,5013	0,8367	0,0333	0,2928	0,1602	1,6946	0,0192	0,1096
VDD(t)1	-	3-047	35,5435	0,0462	34,3437	0,0204	13,5718	0,8256	0,0631	0,2511	0,1416	1,6117	0,0392	0,3281
VDD(t)1	-	3-048	35,4488	0,0474	34,1361	0,0249	13,4006	0,8410	0,0548	0,2241	0,1360	1,7252	0,0471	0,2099
VDD(t)1	-	3-049	35,7251	0,0300	34,6186	0,0431	13,7133	0,8050	0,0405	0,2283	0,0261	1,6620	0,0679	0,2645
VDD(t)1	-	3-050	35,9126	0,0642	34,8112	0,0226	13,9367	0,8814	0,0423	0,2233	0,1583	1,7023	0,0285	0,1275
VDD(t)1	-	3-051	35,2855	0,0823	34,1949	0,0000	13,5264	0,8535	0,0274	0,2570	0,1788	1,6991	0,0192	0,4274
VDD(t)1	-	3-052	35,4397	0,0717	34,5130	0,0000	13,9394	0,8111	0,0405	0,2299	0,0708	1,6538	0,0513	0,1093
VDD(t)1	-	3-053	35,4089	0,0555	34,3850	0,0000	13,8907	0,8580	0,0351	0,2274	0,1211	1,6910	0,0186	0,0819
VDD(t)1	-	3-054	35,5488	0,0393	34,4360	0,0000	13,7528	0,8070	0,0458	0,2261	0,0969	1,6730	0,0386	0,1003
VDD(t)1	-	3-055	35,4932	0,0817	34,5271	0,0000	14,0320	0,8434	0,0494	0,2419	0,1360	1,7276	0,0218	0,1455
VDD(t)1	-	3-056	35,5550	0,0842	34,5404	0,0543	13,8418	0,8050	0,0393	0,2639	0,1062	1,6637	0,0248	0,2278
VDD(t)1	-	3-057	35,6780	0,0624	34,5859	0,0227	13,8286	0,8932	0,0631	0,2441	0,1304	1,6050	0,0242	0,4909
VDD(t)1	-	3-058	35,0998	0,0118	34,6390	0,0113	14,1340	0,8637	0,0351	0,2050	0,0969	1,5817	0,0421	0,3172
VDD(t)1	-	3-059	35,7207	0,0487	34,4944	0,0000	13,5542	0,8446	0,0471	0,2351	0,0820	1,6310	0,0288	0,1736
VDD(t)1	-	3-060	35,7233	0,0343	34,3807	0,0249	14,0068	0,8219	0,0571	0,2310	0,1062	1,6798	0,0214	0,3181
Upper Val Leggia dike														
VLGa(t)1	-	1-001	35,7806	0,4654	34,1654	0,0000	13,0051	1,3280	0,0470	0,1911	0,1303	1,8899	0,0416	0,0001
VLGa(t)1	-	1-002	36,5813	0,1097	35,2381	0,0366	11,8627	2,1699	0,0472	0,1985	0,0466	1,6703	0,0370	0,1018
VLGa(t)1	-	1-003	35,9213	0,3496	34,5724	0,0000	13,2003	1,0701	0,0537	0,1999	0,1832	1,3444	0,0413	0,0001
VLGa(t)1	-	1-004	35,5415	0,3599	34,4192	0,0046	13,4123	1,1796	0,0549	0,2420	0,1420	1,4072	0,0599	0,1102
VLGa(t)1	-	1-005	35,6542	0,3280	34,3475	0,0114	13,4416	1,1159	0,0728	0,2093	0,1420	1,3278	0,0335	0,0001
VLGa(t)1	-	1-006	35,8251	0,3971	34,5582	0,0091	13,2632	1,2263	0,0776	0,2503	0,0411	1,4359	0,0340	0,2577
VLGa(t)1	-	1-007	35,6094	0,3685	34,8395	0,0000	13,2370	1,3058	0,0538	0,2328	0,0767	1,4056	0,0675	0,0829
VLGa(t)1	-	1-008	35,4789	0,3627	34,6783	0,0205	13,1082	1,4445	0,0513	0,2556	0,0449	1,3849	0,0442	0,0738
VLGa(t)1	-	1-009	35,8102	0,4045	34,4048	0,0000	12,8341	1,4285	0,1063	0,2212	0,0841	1,4699	0,0572	0,2675
VLGa(t)1	-	1-010	35,8577	0,3713	34,8175	0,0274	12,7985	1,4895	0,0998	0,2452	0,1271	1,5362	0,0465	0,0924
VLGa(t)1	-	1-011	35,9443	0,3017	34,7333	0,0091	12,7328	1,5213	0,0771	0,2748	0,0935	1,4646	0,0235	0,0185
VLGa(t)1	-	1-012	35,7565	0,3263	34,5632	0,0091	12,7862	1,5829	0,0885	0,2520	0,1122	1,5270	0,0539	0,0554
VLGa(t)1	-	1-013	35,9593	0,2826	34,8004	0,0000	12,5427	1,7003	0,0987	0,2275	0,0954	1,4554	0,0306	0,2588
VLGa(t)1	-	1-014	35,7578	0,3298	34,7995	0,0206	12,3884	1,7104	0,1083	0,2053	0,0786	1,5429	0,0480	0,1667
VLGa(t)1	-	1-015	35,9970	0,3368	34,5582	0,0137	12,4038	1,8185	0,1149	0,2117	0,1011	1,5501	0,0323	0,0001
VLGa(t)1	-	1-016	35,8581	0,2827	34,6102	0,0160	12,3495	1,8044	0,1131	0,2124	0,1067	1,4898	0,0514	0,2406
VLGa(t)1	-	1-017	35,8802	0,2788	34,8210	0,0023	12,4186	1,9186	0,1184	0,2451	0,0786	1,5240	0,0498	0,0648
VLGa(t)1	-	1-018	35,9423	0,2947	34,8052	0,0000	12,3917	1,8633	0,1059	0,2138	0,0842	1,5817	0,0512	0,0741
VLGa(t)1	-	1-019	35,8443	0,3067	34,4975	0,0344	12,1925	2,0320	0,1251	0,2188	0,0468	1,6398	0,0558	0,1113
VLGa(t)1	-	1-020	36,0432	0,2256	34,5295	0,0092	12,1507	2,0245	0,0957	0,2554	0,0468	1,7427	0,0266	0,1852
VLGa(t)1	-	1-021	36,0674	0,2776	34,7351	0,0091	12,5887	1,9160	0,1107	0,2494	0,0767	1,6686	0,0345	0,1387
VLGa(t)1	-	1-022	36,0365	0,2743	34,8244	0,0000	12,6144	1,9405	0,1399	0,2133	0,1515	1,6871	0,0482	0,0923
VLGa(t)1	-	1-023	35,9744	0,2400	34,8994	0,0000	12,4032	1,9867	0,0999	0,2000	0,1142	1,6291	0,0293	0,2494
VLGa(t)1	-	1-024	36,0962	0,3061	34,6877	0,0344	12,3174	2,0351	0,1514	0,2538	0,0412	1,5833	0,0439	0,1670
VLGa(t)1	-	1-025	36,1850	0,3164	34,7555	0,0000	12,0042	2,0755	0,1012	0,2221	0,0824	1,5831	0,0268	0,0558
VLGa(t)1	-	1-026	35,8510	0,3612	34,6536	0,0000	11,9134	2,1794	0,1665	0,2084	0,1123	1,6933	0,0736	0,0093
VLGa(t)1	-	1-027	36,0655	0,2939	34,6187	0,0000	11,8348	2,2174	0,1438	0,1961	0,0824	1,7107	0,0545	0,1394
VLGa(t)1	-	1-028	36,0359	0,2965	34,4943	0,0253	11,6702	2,2793	0,1474	0,2138	0,0000	1,6531	0,0395	0,2606
VLGa(t)1	-	1-029	36,3043	0,1644	35,0644	0,0000	11,5866	1,9688	0,0702	0,2124	0,0731	1,4494	0,0400	0,0466
VLGa(t)1	-	1-030	36,1406	0,1548	35,0066	0,0000	11,9500	1,9616	0,0881	0,2013	0,1086	1,3237	0,0391	0,0001
VLGa(t)1	-	1-031	36,1354	0,1554	35,2655	0,0000	12,0243	2,0176	0,0779	0,2108	0,0618	1,4611	0,0454	0,1949
VLGa(t)1	-	1-032	36,4317	0,1711	35,1412	0,0000	12,0298	1,9933	0,0689	0,2278	0,1011	1,4308	0,0251	0,0001
VLGa(t)1	-	1-033	36,7965	0,0812	35,4886	0,0092	11,7608	1,9298	0,0660	0,1972	0,0824	1,4210	0,0278	0,0466
VLGa(t)1	-	1-034	36,5632	0,0982	35,4545	0,0046	11,6805	1,9127	0,0600	0,2456	0,1049	1,3329	0,0237	0,0001
VLGa(t)1	-	1-035	36,5362	0,1076	35,2690	0,0161	11,9093	1,9758	0,0641	0,1657	0,0431	1,4271	0,0207	0,1209
VLGa(t)1	-	1-036	36,7582	0,0976	35,1841	0,0000	11,7990	1,8787	0,0330	0,2277	0,0656	1,3675	0,0412	0,0187
VLGa(t)1	-	1-037	36,2243	0,0648	35,2876	0,0069	11,9446	1,9326	0,0617	0,1875	0,0431	1,3784	0,0101	0,1856
VLGa(t)1	-	1-038	36,4280	0,0869	35,3149	0,0000	11,7426	1,9759	0,0414	0,1911	0,0862	1,3581	0,0370	0,0001
VLGa(t)1	-	1-039	36,7145	0,0548	35,1807	0,0000	11,6551	1,9915	0,0588	0,1970	0,0337	1,4173	0,0284	0,1863
VLGa(t)1	-	1-040	36,3839	0,0617	35,4538	0,0344	11,9583	1,9309	0,0791	0,2027	0,0599	1,3136	0,0152	0,0001
VLGa(t)1	-	1-041	36,7788	0,0712	35,2254	0,0023	11,8724	1,9283	0,0564	0,2669	0,0525	1,3548	0,0152	0,1677
VLGa(t)1	-	1-042	36,5085	0,0837	35,4031	0,0000	12,0411	1,9712	0,0594	0,2424	0,0918	1,4536	0,0116	0,1486
VLGa(t)1	-	1-043	36,4160	0,0762	35,3530	0,0000	11,9927	1,9883	0,0456	0,2424	0,0693	1,4796	0,0423	0,0001
VLGa(t)1	-	1-044	36,5389	0,0737	35,2646	0,0046	11,7460	1,9777	0,0438	0,2114	0,0862	1,4309	0,0383	0,1024
VLGa(t)1	-	1-045	36,1219	0,0579	35,1930	0,0092	11,9855	1,9710	0,0845	0,2401	0,0506	1,4074	0,0459	0,2042
VLGa(t)1	-	1-046	36,3198	0,0774	35,2459	0,0000	12,0089	1,9697	0,0761	0,2109	0,0318	1,4499	0,0309	0,0001
VLGa(t)1	-	1-047	36,6237	0,0724	35,4159	0,0000	12,1341	2,0278	0,0612	0,2660	0,0843	1,3701	0,0261	0,0372
VLGa(t)1	-	1-048	36,5763	0,0699	35,4135	0,0000	11,9804	1,9820	0,0606	0,2396	0,1162	1,4120	0,0470	0,0001
VLGa(t)1	-	1-049	36,6192	0,0675	35,2952	0,0000	11,3899	1,9790	0,0708	0,2373	0,1256	1,4578	0,0246	0,1121
VLGa(t)1	-	1-050	36,2699	0,1083	35,2704	0,0275	11,9090	2,0466	0,0744	0,1707	0,1049	1,4826	0,0187	0,0744
VLGa(t)1	-	1-051	36,6873	0,0869	35,0976	0,0230	11,6907	2,0850	0,0762	0,2001	0,0993	1,3990	0,0399	0,0560
VLGa(t)1	-	1-052	36,6251	0,0649	35,2664	0,0161	11,7764	1,9588	0,0648	0,2319	0,1256	1,4094	0,0070	0,0001
VLGa(t)1	-	1-053	36,5183	0,1291	35,3206	0,0000	11,6673	2,0406	0,0792	0,2312	0,1349	1,5460	0,0264	0,1490
VLGa(t)1	-	1-054	36,4166	0,1279	35,2377	0,0000	11,7029	2,0496	0,0906	0,1492	0,0768	1,4462	0,0207	0,2696
VLGa(t)1	-	1-055	36,3009	0,1530	35,1154	0,0000	11,9621	2,0437	0,0953	0,2138	0,0881	1,4477	0,0502	0,0279
VLGa(t)1	-	1-056	36,4343	0,1670	35,2934	0,0000	11,7199	2,0402	0,0720	0,1973	0,0506	1,5429	0,0382	0,1490
VLGa(t)1	-	1-057	36,5341	0,1695	35,1086	0,0000	11,6766	1,9750	0,0828	0,2033	0,0956	1,4499	0,0447	0,0001
VLGa(t)1	-	1-058	36,2892	0,1542	35,4769	0,0000	12,0738	2,0495	0,0917	0,2469	0,1761	1,4284	0,0390	0,2690
VLGa(t)1	-	1-059	35,9492	0,1951	34,9668	0,0000	11,8696	2,0541	0,0713	0,2498	0,0731	1,4963	0,0092	0,0001
VLGa(t)1	-	1-060	36,2397	0,1619	35,2800	0,0000	11,7339	2,0879	0,0606	0,2054	0,0562	1,4391	0,0267	0,0001
VLGa(t)1	-	1-061	35,6667	0,3229	34,3968	0,0138	11,9583	2,3286	0,1480	0,1897	0,0450	1,7417	0,0655	0,1578
VLGa(t)1	-	1-062	35,9923	0,2708	34,6938	0,0000	11,7531	2,2790	0,1403	0,2082	0,0506	1,8481	0,0323	0,2044
VLGa(t)1	-	1-063	36,0472	0,3175	34,6510	0,0000	11,6488	2,2639	0,1259	0,1895	0,0169	1,6923	0,0238	0,1118
VLGa(t)1	-	1-064	36,0651	0,2788	35,0727	0,0000	11,9358	2,1229	0,1162	0,2565	0,0824	1,6315	0,0310	0,1209
VLGa(t)1	-	1-065	36,2336	0,2712	34,8002	0,0092	12,1329	1,9654	0,0869	0,1982	0,0656	1,7747	0,0419	0,1021
VLGa(t)1	-	1-066	35,8658	0,2707	34,9163	0,0207	11,9170	2,1187	0,1240	0,1805	0,1161	1,8079	0,0554	0,1207
VLGa(t)1	-	1-067	35,8857	0,2799	34,7337	0,0046	12,1447	2,0458	0,1192	0,2348	0,1517	1,7779	0,0684	0,0371
VLGa(t)1	-	1-068	36,0092	0,3013	34,7352	0,0000	12,1667	2,0286	0,1186	0,2553	0,0899	1,8031	0,0649	0,0464
VLGa(t)1	-	1-069	35,9209	0,3063	34,5920	0,0160	12,1157	1,9800	0,1108	0,2606	0,1030	1,7741	0,0382	0,1762
VLGa(t)1	-	1-070	35,9558	0,3278	34,9099	0,0023	12,0518	1,9336	0,0929	0,2137	0,0749	1,7411	0,0554	0,0279

Sample code	Crystal	An. Point	SiO_2	TiO_2	Al_2O_3	Cr_2O_3	$FeO+Fe_2O_3$	MgO	CaO	MnO	ZnO	Na_2O	K_2O	F
VLGa(t)1	-	1-071	35,9612	0,2432	35,0153	0,0160	12,3907	1,7743	0,0850	0,2552	0,0805	1,6603	0,0263	0,3789
VLGa(t)1	-	1-072	36,0150	0,3029	35,1021	0,0000	12,4935	1,7032	0,0963	0,2590	0,1554	1,6926	0,0399	0,1573
VLGa(t)1	-	1-073	35,8077	0,2900	34,7628	0,0000	12,9323	1,5213	0,0873	0,2122	0,1628	1,6614	0,0382	0,0369
VLGa(t)1	-	1-074	35,6110	0,4169	34,7407	0,0000	12,7388	1,6209	0,0903	0,1993	0,1273	1,6689	0,0304	0,4327
VLGa(t)1	-	1-075	35,7416	0,3319	34,5595	0,0274	12,8867	1,4744	0,0837	0,2735	0,1946	1,7400	0,0314	0,0830
VLGa(t)1	-	1-076	35,9285	0,3602	34,3888	0,0000	13,0177	1,3904	0,0777	0,2122	0,0749	1,6725	0,0438	0,1659
VLGa(t)1	-	1-077	35,5453	0,4215	34,5347	0,0023	13,1224	1,2993	0,0765	0,1455	0,1254	1,7224	0,0420	0,1839
VLGa(t)1	-	1-078	35,5177	0,4057	34,8173	0,0000	13,2400	1,2866	0,0675	0,2075	0,1366	1,6949	0,0643	0,0368
VLGa(t)1	-	1-079	36,0243	0,4204	34,2202	0,0342	13,5674	1,3259	0,0669	0,1951	0,1291	1,7415	0,0509	0,0276
VLGa(t)1	-	1-080	35,6943	0,4217	34,3456	0,0433	13,4783	1,3165	0,0555	0,1972	0,1852	1,7204	0,0528	0,0001
VLGa(t)1	-	1-081	35,7055	0,4919	34,6904	0,0114	13,4054	1,2217	0,0424	0,1979	0,1852	1,7381	0,0380	0,2570
VLGa(t)1	-	1-082	36,0503	0,5646	34,1439	0,0206	12,2713	1,8516	0,0580	0,1320	0,1891	1,7661	0,0452	0,1946
VLGa(t)1	-	1-083	36,2185	0,7450	34,1775	0,0046	11,5597	2,7680	0,1450	0,1196	0,0862	1,8579	0,0411	0,1867
VLGa(t)1	-	1-084	35,9937	0,7297	33,8794	0,0000	11,2501	3,0320	0,1468	0,0648	0,0881	1,8373	0,0194	0,3544
VLGa(t)1	-	1-085	36,6012	0,6362	34,7287	0,0000	11,1394	2,7095	0,1517	0,0903	0,1181	1,7330	0,0287	0,3741
VLGa(t)1	-	1R-001	36,1834	0,4107	34,9036	0,0000	13,6232	1,2581	0,0453	0,1868	0,2163	1,8660	0,0570	0,0641
VLGa(t)1	-	1R-002	35,9542	0,4702	34,8415	0,0000	13,4914	1,2731	0,0430	0,1826	0,1830	1,8655	0,0443	0,0827
VLGa(t)1	-	1R-003	35,7645	0,4163	34,5025	0,0137	13,5539	1,2554	0,0674	0,1994	0,1326	1,8259	0,0600	0,1101
VLGa(t)1	-	1R-004	35,6375	0,5359	34,6568	0,0000	13,6779	1,2705	0,0638	0,1738	0,1401	1,7972	0,0329	0,2932
VLGa(t)1	-	1R-005	35,3193	0,4933	34,3443	0,0273	13,1171	1,2683	0,0537	0,1874	0,2109	1,7701	0,0550	0,1838
VLGa(t)1	-	1R-006	34,7262	0,4373	33,7695	0,0046	12,9740	1,2196	0,0621	0,2401	0,1700	1,7480	0,0397	0,2390
VLGa(t)1	-	1R-007	34,6230	0,4639	33,4298	0,0159	12,7801	1,1946	0,0364	0,2360	0,1586	1,8605	0,0421	0,1658
VLGa(t)1	-	1R-008	34,9309	0,4697	33,6411	0,0000	13,2396	1,3256	0,0346	0,2055	0,1308	1,8346	0,0473	0,1010
VLGa(t)1	-	2R-001	35,8582	0,4782	34,2134	0,0091	12,9374	1,3027	0,0514	0,2073	0,1830	1,7753	0,0359	0,2860
VLGa(t)1	-	2R-002	36,0679	0,4393	34,2193	0,0000	13,1301	1,3378	0,0334	0,1936	0,2072	1,8371	0,0399	0,0830
VLGa(t)1	-	2R-003	35,8418	0,4441	34,2796	0,0000	13,2673	1,2858	0,0364	0,1907	0,1661	1,7593	0,0222	0,1473
VLGa(t)1	-	2R-004	35,6538	0,4718	34,2693	0,0478	13,3895	1,2824	0,0453	0,1617	0,1101	1,8492	0,0285	0,2022
VLGa(t)1	-	2R-005	35,8783	0,4201	34,3815	0,0091	13,2193	1,3805	0,0609	0,2075	0,1940	1,7258	0,0381	0,2759
VLGa(t)1	-	2R-006	35,7837	0,4063	34,5712	0,0000	13,1825	1,2804	0,0340	0,2124	0,1586	1,7939	0,0302	0,3034
VLGa(t)1	-	2R-007	35,6308	0,4378	34,3028	0,0114	13,0295	1,2099	0,0537	0,1664	0,1922	1,8078	0,0336	0,3860
VLGa(t)1	-	2R-008	35,7997	0,4198	34,5901	0,0274	13,1154	1,2336	0,0346	0,1777	0,1531	1,8888	0,0469	0,1106
VLGa(t)1	-	2R-009	36,0735	0,4729	34,4952	0,0000	13,3050	1,2385	0,0125	0,1580	0,2035	1,7830	0,0216	0,1932
VLGa(t)1	-	2R-010	35,8121	0,4110	34,2249	0,0000	13,0082	1,2799	0,0257	0,1583	0,1512	1,8508	0,0567	0,0645
VLGa(t)1	-	2R-011	35,8489	0,4788	34,5235	0,0160	13,0209	1,3066	0,0328	0,1774	0,2184	1,8950	0,0424	0,2947
VLGa(t)1	-	2R-012	35,8381	0,4631	34,3457	0,0000	13,0835	1,4134	0,0358	0,1647	0,1998	1,9008	0,0372	0,1474
VLGa(t)1	-	2R-013	35,8589	0,5828	34,4679	0,0046	12,2992	1,8666	0,0688	0,1340	0,1868	1,8615	0,0317	0,2872
VLGa(t)1	-	2R-014	36,0510	0,6008	34,0529	0,0115	11,7572	2,2587	0,0676	0,0971	0,1178	1,7920	0,0106	0,1864
VLGa(t)1	-	2R-015	35,9006	0,7179	34,2624	0,0000	11,8228	2,5399	0,1239	0,1176	0,0673	1,9116	0,0470	0,2237
VLGa(t)1	-	2R-016	35,8576	0,6538	34,2762	0,0000	11,3362	2,5815	0,1162	0,1191	0,0711	1,8885	0,0390	0,2337
VLGa(t)1	-	2R-017	35,8435	0,7008	34,1115	0,0000	11,4887	2,6712	0,1078	0,0788	0,1234	1,8750	0,0531	0,2798
VLGa(t)1	-	2R-018	35,9826	0,6482	34,1914	0,0000	11,4097	2,6169	0,1246	0,0661	0,0991	1,9636	0,0499	0,3357
VLGa(t)1	-	2R-019	36,0051	0,5962	34,2963	0,0000	11,2696	2,6859	0,1073	0,0417	0,0954	1,8994	0,0474	0,0842
VLGa(t)1	-	2R-020	35,8508	0,6713	33,9480	0,0000	11,1868	2,8164	0,1456	0,0548	0,0692	1,9870	0,0439	0,1590
VLGa(t)1	-	2R-021	35,9040	0,5976	34,1838	0,0161	11,0488	2,7722	0,1301	0,1022	0,0879	1,9550	0,0388	0,2060
VLGa(t)1	-	2R-022	36,1920	0,6146	34,0549	0,0000	10,8406	2,8839	0,1013	0,1050	0,1552	1,9401	0,0398	0,3930
VLGa(t)1	-	2R-023	35,8134	0,6001	34,1283	0,0092	10,8791	2,9257	0,1402	0,0686	0,1496	1,9704	0,0356	0,3272
VLGa(t)1	-	2R-024	35,5855	0,7308	33,7268	0,0000	10,9558	3,0080	0,1803	0,0962	0,0973	1,9286	0,0461	0,3370
VLGa(t)1	-	2R-025	35,3703	0,7412	33,6155	0,0231	10,6914	3,0452	0,1714	0,1047	0,0804	1,9945	0,0522	0,2815
VLGa(t)1	-	3R-001	35,7739	0,3403	34,8198	0,0000	13,1107	1,4608	0,0718	0,2505	0,1217	1,7861	0,0243	0,1934
Lower Val Leggia dike														
VLGb(t)1	1	1	35,1737	0,5115	34,2544	0,0000	14,3789	0,4821	0,0130	0,2202	0,5957	2,1180	0,0252	0,9231
VLGb(t)1	2	1	34,8709	0,5113	34,4299	0,0451	14,3089	0,3389	0,0225	0,2805	0,6244	2,2869	0,0604	0,7273
VLGb(t)1	2	2-001	34,7330	0,5016	34,0347	0,0406	14,0352	0,4017	0,0320	0,2659	0,5944	2,2619	0,0550	0,8991
VLGb(t)1	2	2-002	34,9068	0,4528	34,3353	0,0316	14,4661	0,3569	0,0278	0,2570	0,5888	2,0880	0,0207	1,0299
VLGb(t)1	2	2-003	35,4295	0,4444	34,2288	0,0113	14,1441	0,3052	0,0314	0,1774	0,6797	2,0938	0,0126	0,7017
VLGb(t)1	2	2-004	35,1927	0,4779	34,5615	0,0158	13,5745	0,3421	0,0000	0,2713	0,6149	2,1372	0,0298	0,7956
VLGb(t)1	2	2-005	35,4290	0,4637	34,1198	0,0000	14,0316	0,3376	0,0006	0,2750	0,5813	2,1234	0,0126	0,7302
VLGb(t)1	2	2-006	35,4887	0,4944	34,2581	0,0090	13,9113	0,3275	0,0000	0,3076	0,6484	2,1552	0,0441	1,0893
VLGb(t)1	2	2-007	34,8753	0,5053	34,4661	0,0000	14,2679	0,3414	0,0231	0,2456	0,5925	2,2484	0,0647	0,7996
VLGb(t)1	2	2-008	34,5488	0,5589	34,4567	0,0045	14,4280	0,3044	0,0225	0,2744	0,6184	2,1752	0,0404	1,0564
VLGb(t)1	2	2-009	34,7072	0,5224	34,4187	0,0090	14,4256	0,2914	0,0302	0,2319	0,5145	2,2713	0,0408	1,0741
VLGb(t)1	2	2-010	34,9162	0,4857	34,6663	0,0722	14,4214	0,3695	0,0077	0,2679	0,5498	2,1205	0,0425	1,2089
VLGb(t)1	2	3-001	34,9214	0,5667	34,3363	0,0000	14,2915	0,3331	0,0000	0,2509	0,5368	2,1560	0,0522	1,1298
VLGb(t)1	2	3-002	34,8216	0,5341	34,0133	0,0000	14,1929	0,3133	0,0279	0,2691	0,6077	2,2002	0,0570	0,6128
VLGb(t)1	2	3-003	34,6923	0,4729	34,4263	0,0113	14,1807	0,3060	0,0124	0,2257	0,6130	2,2071	0,0205	1,0216
VLGb(t)1	2	3-004	34,8022	0,4996	34,3128	0,0226	14,5021	0,2550	0,0207	0,2023	0,4999	2,2008	0,0487	1,0565
VLGb(t)1	2	3-005	34,8294	0,4964	34,2919	0,0000	14,3446	0,3089	0,0267	0,2878	0,5591	2,2623	0,0559	0,8350
VLGb(t)1	2	3-006	34,7170	0,5001	34,3698	0,0023	14,2668	0,2980	0,0142	0,2637	0,5554	2,1696	0,0307	1,2350
VLGb(t)1	2	3-007	34,8021	0,5363	34,3252	0,0000	14,7129	0,3253	0,0077	0,2335	0,6480	2,1388	0,0426	0,8588
VLGb(t)1	2	3-008	35,1141	0,4690	34,2465	0,0000	14,4165	0,3697	0,0018	0,3014	0,6073	2,1865	0,0411	1,0126
VLGb(t)1	2	3-009	35,0039	0,4311	34,3549	0,0045	14,4028	0,3492	0,0207	0,2451	0,7317	2,2256	0,0271	1,1079
VLGb(t)1	2	3-010	34,7636	0,4581	34,2345	0,0000	14,0634	0,3840	0,0142	0,2295	0,7059	2,2010	0,0354	0,9062
VLGb(t)1	2	4-001	34,8695	0,5034	34,2194	0,0000	14,3583	0,3812	0,0041	0,2683	0,6596	2,0950	0,0335	1,0573
VLGb(t)1	2	4-002	35,1175	0,4547	34,4494	0,0023	14,4542	0,4173	0,0249	0,2538	0,7484	2,2379	0,0579	0,8066
VLGb(t)1	2	4-003	34,8457	0,4860	34,2522	0,0000	14,2135	0,3901	0,0207	0,2274	0,6204	2,2450	0,0377	0,7813
VLGb(t)1	2	4-004	35,2354	0,4930	34,4823	0,0000	14,3416	0,3450	0,0184	0,2488	0,7396	2,2081	0,0383	0,7102
VLGb(t)1	2	4-005	35,0913	0,4884	34,5060	0,0271	14,0068	0,3588	0,0202	0,2070	0,6858	2,2573	0,0415	1,0686
VLGb(t)1	3	1-001	34,9062	0,5005	34,1360	0,0068	13,9098	0,6441	0,0042	0,2201	0,3310	2,2548	0,0434	1,0710
VLGb(t)1	3	1-002	34,8669	0,4787	33,8998	0,0000	14,2163	0,7163	0,0136	0,1531	0,3958	2,1847	0,0191	1,2432
VLGb(t)1	3	1-003	34,9800	0,5426	34,1434	0,0000	13,9318	0,6727	0,0160	0,1616	0,4609	2,1261	0,0195	0,9360
VLGb(t)1	3	1-004	35,2135	0,5036	34,1262	0,0136	14,1873	0,6089	0,0207	0,2423	0,4534	2,1855	0,0481	1,0066
VLGb(t)1	3	1-005	35,1471	0,5195	34,0364	0,0068	13,9915	0,6267	0,0243	0,2375	0,3829	2,3249	0,0521	1,0791
VLGb(t)1	3	1-006	35,0671	0,5359	34,3342	0,0000	13,9556	0,6122	0,0178	0,2645	0,4444	2,1499	0,0442	1,1163
VLGb(t)1	3	1-007	35,0576	0,5173	34,1954	0,0226	14,3806	0,5618	0,0142	0,2220	0,3848	2,1949	0,0351	0,9522
VLGb(t)1	3	1-008	34,9979	0,5434	34,3331	0,0000	14,3295	0,5150	0,0190	0,2454	0,4963	2,1748	0,0233	1,1565
VLGb(t)1	3	1-009	35,1928	0,4699	33,8409	0,0158	13,8099	0,5170	0,0000	0,2942	0,5541	2,1404	0,0310	1,0362
VLGb(t)1	3	1-010	35,2521	0,5070	34,2109	0,0158	14,2606	0,4846	0,0136	0,1885	0,5019	2,2431	0,0274	0,9076
VLGb(t)1	3	1-011	35,1448	0,5068	34,0704	0,0272	13,6066	0,4243	0,0059	0,3059	0,5039	2,2442	0,0309	0,9760
VLGb(t)1	3	2-001	35,5196	0,5047	34,0836	0,0113	14,0060	0,4389	0,0261	0,2879	0,5354	2,0985	0,0350	1,0366
VLGb(t)1	3	2-002	35,2302	0,4878	34,3385	0,0136	14,0883	0,3825	0,0030	0,2270	0,5020	2,0701	0,0446	1,1683
VLGb(t)1	3	2-003	35,2864	0,5082	34,0893	0,0203	14,0996	0,4194	0,0101	0,2283	0,6171	2,1774	0,0170	1,2998
VLGb(t)1	3	2-004	35,2519	0,4730	34,1394	0,0045	13,8292	0,3881	0,0071	0,2690	0,5763	2,1886	0,0476	1,1518
VLGb(t)1	3	2-005	35,3176	0,5147	34,6986	0,0000	13,5033	0,3610	0,0362	0,2479	0,5951	2,1786	0,0576	0,9321
VLGb(t)1	3	2-006	34,9438	0,5449	34,6168	0,0000	14,5235	0,3628	0,0113	0,2798	0,6187	2,1097	0,0442	0,8974
VLGb(t)1	3	2-007	35,0851	0,5179	34,7109	0,0068	14,3381	0,3296	0,0302	0,2621	0,6225	2,2300	0,0680	0,9342
VLGb(t)1	5	1-001	34,9706	0,5048	34,1589	0,0000	14,1682	0,3817	0,0124	0,2858	0,7322	2,1953	0,0384	0,8338
VLGb(t)1	5	1-002	35,0963	0,5234	33,9877	0,0068	14,1719	0,4076	0,0290	0,2618	0,6198	2,1892	0,0416	0,9513
VLGb(t)1	5	1-003	34,7278	0,4801	34,3119	0,0000	14,2086	0,3782	0,0118	0,2594	0,6553	2,2149	0,0393	0,6828
VLGb(t)1	5	1-004	35,3833	0,4643	34,3365	0,0090	13,9748	0,3701	0,0154	0,2476	0,7372	2,2415	0,0372	0,9346
VLGb(t)1	5	1-005	34,8920	0,5145	34,2451	0,0113	14,5187	0,3702	0,0249	0,2627	0,7090	2,2079	0,0478	0,8150
VLGb(t)1	5	1-006	35,0103	0,5167	34,1797	0,0406	14,2672	0,3836	0,0107	0,2300	0,7573	2,1844	0,0608	0,9944

Sample code	Crystal	An. Point	SiO_2	TiO_2	Al_2O_3	Cr_2O_3	$FeO+Fe_2O_3$	MgO	CaO	MnO	ZnO	Na_2O	K_2O	F
VLGb(t)1	5	1-007	34,9391	0,5089	34,2153	0,0023	13,9152	0,3875	0,0000	0,2556	0,7649	2,2110	0,0168	0,9786
VLGb(t)1	5	1-008	35,0897	0,5187	34,2278	0,0023	14,1831	0,3817	0,0000	0,2643	0,6572	2,3025	0,0360	0,7460
VLGb(t)1	5	1-009	34,7556	0,5324	34,3316	0,0339	14,0486	0,4032	0,0000	0,2304	0,7333	2,2543	0,0578	0,8798
VLGb(t)1	5	1-010	34,7755	0,4891	34,4488	0,0090	14,0835	0,3574	0,0261	0,2001	0,6573	2,3127	0,0677	0,7813
VLGb(t)1	5	1-011	35,1884	0,4880	34,3038	0,0000	13,9853	0,3764	0,0095	0,1802	0,7557	2,1915	0,0619	0,7017
VLGb(t)1	5	1-012	35,0511	0,4638	34,2143	0,0000	13,8324	0,3732	0,0154	0,2351	0,6927	2,2372	0,0443	0,8279
VLGb(t)1	5	1-013	34,7123	0,5107	34,1416	0,0090	14,0244	0,3409	0,0332	0,2311	0,7203	2,1425	0,0478	0,8979
VLGb(t)1	5	2	35,0769	0,4741	34,4257	0,0045	14,5820	0,4065	0,0290	0,2117	0,6735	2,2581	0,0314	0,5201
VLGb(t)1	5	3-001	34,7463	0,5244	34,2974	0,0135	13,9907	0,3924	0,0083	0,2305	0,7278	2,1842	0,0437	0,9247
VLGb(t)1	5	3-002	35,2221	0,4758	34,3633	0,0023	14,3761	0,3777	0,0166	0,1979	0,6739	2,1626	0,0278	0,9227
VLGb(t)1	5	3-003	35,1007	0,4576	34,3179	0,0158	14,1154	0,3863	0,0030	0,2299	0,6966	2,1699	0,0410	0,6123
VLGb(t)1	5	3-004	35,3829	0,5068	34,2125	0,0090	14,1408	0,3642	0,0130	0,1880	0,6966	2,1294	0,0397	0,9343
VLGb(t)1	5	3-005	34,9086	0,4906	34,2325	0,0000	14,2140	0,3884	0,0065	0,2374	0,7407	2,1603	0,0317	1,0206
VLGb(t)1	5	3-006	34,7271	0,4964	34,4326	0,0000	14,2949	0,3739	0,0095	0,2661	0,6612	2,2031	0,0388	1,0742
VLGb(t)1	5	3-007	34,9200	0,5007	34,2086	0,0000	14,3827	0,3753	0,0124	0,2353	0,6983	2,2292	0,0498	0,9668
VLGb(t)1	5	3-008	34,5728	0,4914	34,2158	0,0180	14,2634	0,3738	0,0314	0,2546	0,7001	2,1711	0,0454	0,7897
VLGb(t)1	5	4	35,0629	0,5095	33,8593	0,0000	14,2884	0,3760	0,0107	0,2085	0,7243	2,1316	0,0475	0,8343

Inclusions EMPA

Sample code	Fragment	An. Pt	Inclusion	SiO_2	P_2O_5	CaO	Y_2O_3	La_2O_3	Ce_2O_3	Pr_2O_3	Nd_2O_3	Sm_2O_3	Gd_2O_3	Tb_2O_3	Dy_2O_3	Ho_2O_3	Er_2O_3	Yb_2O_3	PbO	ThO_2	UO_2	Sum
CODg(th)1	1	1	Thorite	17,7956	1,9291	0,0000	2,8137	0,0000	0,0536	0,0199	0,0000	0,1241	0,4132	0,0000	0,3628	0,0534	0,2166	0,1980	0,3807	63,0744	14,6964	102,1315
CODg(th)1	1	2	Thorite	17,5705	2,1412	0,0000	3,2741	0,0000	0,0352	0,0000	0,1956	0,2955	0,4989	0,0000	0,5702	0,1028	0,2405	0,2062	0,2354	53,8473	21,8950	101,1084
CODg(th)1	2	1	Thorite	17,5108	2,0625	0,0000	2,8673	0,0000	0,0719	0,0000	0,0873	0,1072	0,3134	0,0326	0,4781	0,1705	0,2195	0,1835	0,3305	55,8370	21,1187	101,3908
CODg(th)1	2	2	Monazite	0,9695	28,2457	0,2541	0,9195	12,5663	30,8380	3,6231	12,3373	3,2822	0,0000	0,0000	0,3285	0,0000	0,0418	0,0000	0,1333	4,1476	0,2597	97,9466
CODg(th)1	2	3	Xenotime	0,5434	33,5047	0,0692	42,6605	0,5647	1,3377	0,1353	0,7357	0,7545	3,3916	0,4205	4,5780	1,1055	3,1668	3,8607	0,0877	1,6066	0,6140	99,1371
CODg(th)1	2	4	Thorite	18,8308	1,1028	0,0000	1,6459	0,0247	0,0000	0,0000	0,1114	0,1333	0,2587	0,0014	0,3488	0,0000	0,1129	0,1052	0,3590	55,1408	24,2287	102,4044
CODg(th)1	2	5	Monazite	1,0971	27,8108	0,3557	1,0093	12,1092	29,8471	3,4232	12,1654	3,1725	0,0000	0,0000	0,2789	0,0400	0,0572	0,0000	0,2098	5,6736	0,1701	97,4199
CODg(th)1	2	6	Xenotime	0,8003	32,7972	0,0471	41,7794	0,0721	0,2092	0,0351	0,7994	0,5629	3,2357	0,4452	4,5085	1,0682	3,2149	4,0199	0,0720	2,0644	1,6984	97,4299
CODg(th)1	2	7	Monazite	0,9154	28,0390	0,2766	0,9222	12,2800	31,2008	3,4810	13,0603	3,3378	0,0000	0,0000	0,3485	0,0162	0,0439	0,0000	0,1531	4,2451	0,1126	98,4325
CODg(th)1	2	8	Thorite	18,0126	1,4414	0,0030	2,1361	0,0590	0,1229	0,0000	0,0430	0,0910	0,3624	0,0391	0,3481	0,0317	0,1746	0,1599	0,4580	53,6628	24,6164	101,7620
CODg(th)1	2	9	Thorite	18,3200	1,1086	0,0000	1,7742	0,0806	0,0000	0,0000	0,1623	0,0352	0,2445	0,0000	0,2962	0,0456	0,1250	0,0685	0,3180	53,6459	25,8098	102,0344
CODg(th)1	2	10	Monazite	0,8460	28,6400	0,2889	0,9519	12,8369	30,8346	3,5164	12,3535	3,2458	0,0000	0,0000	0,4054	0,0000	0,0479	0,0000	0,1838	4,1278	0,1431	98,4220
CODg(th)1	2	11	Euxenite-(Y)	0,0000	0,0010	0,4310	14,5622	0,0185	0,1653	0,0121	0,3892	0,7305	1,9080	0,3388	3,0011	0,5465	1,5141	1,7511	0,0000	2,3746	20,1308	47,8748
CODg(th)1	3	1	Thorite	17,8524	1,9550	0,0115	2,8094	0,0651	0,0135	0,0244	0,0923	0,1532	0,4920	0,0000	0,4577	0,0478	0,2200	0,1753	0,2944	62,3561	15,4557	102,4758
CODg(th)1	3	2	Thorite	17,8941	1,9296	0,0000	2,8597	0,0536	0,0766	0,0000	0,1110	0,1253	0,4591	0,0000	0,5147	0,0740	0,2411	0,1974	0,4427	59,9117	17,5734	102,4640
CODg(th)1	3	3	Thorite	17,8348	1,9424	0,0000	2,7137	0,0000	0,0201	0,0000	0,1268	0,1783	0,4404	0,0000	0,5339	0,0188	0,2072	0,1588	0,3050	55,9625	21,6810	102,1237
CODg(th)1	3	4	Thorogummite	17,0061	1,5636	0,0424	2,4143	0,0020	0,0491	0,0237	0,0000	0,0855	0,3271	0,0000	0,4069	0,0540	0,1634	0,0950	0,3050	52,6751	24,1533	99,3665
CODg(th)1	3	5	Thorogummite	16,4056	1,6825	0,2841	2,4690	0,0000	0,1048	0,0000	0,1369	0,1518	0,4273	0,0000	0,4279	0,0938	0,1796	0,1282	0,3844	52,6070	22,0097	97,4926
CODg(th)1	3	6	Thorite	17,9675	1,8246	0,0000	2,7732	0,0000	0,1239	0,0000	0,2059	0,1683	0,4948	0,0256	0,4887	0,0539	0,2485	0,1333	0,3144	53,8991	23,1144	101,8361
CODg(th)1	3	7	Thorite	17,7808	2,0298	0,0000	3,2074	0,0000	0,0467	0,0000	0,0415	0,1656	0,4031	0,0109	0,5782	0,1890	0,2112	0,1570	0,3055	55,6751	21,1591	101,9609
CODg(th)1	3	8	Thorite	18,0336	2,2170	0,0000	3,3649	0,0000	0,0127	0,0000	0,1649	0,2042	0,5170	0,0623	0,5574	0,0502	0,2551	0,1860	0,4069	54,1853	22,4063	102,6238
CODg(th)1	3	9	Thorogummite	16,5452	1,3633	0,0000	2,2814	0,0000	0,0000	0,0034	0,0000	0,1207	0,4865	0,0474	0,4871	0,0758	0,2094	0,0903	0,3818	52,2380	21,9119	96,2422
CODg(th)1	3	10	Monazite	1,7712	26,8245	0,2110	1,1434	10,7128	28,4600	3,2584	12,3639	2,8286	0,0000	0,0000	0,3251	0,0000	0,0629	0,0000	0,1840	8,4126	1,3964	97,9548
CODg(th)1	3	11	Monazite	1,4043	26,7750	0,3217	1,1277	11,2801	28,4756	3,3701	12,1122	2,9331	0,0000	0,0000	0,3715	0,0000	0,0792	0,0000	0,1813	6,9868	0,8124	96,2310
CODg(th)1	3	12	Monazite	1,1448	27,6686	0,2930	0,9187	11,7474	30,0912	3,3886	12,7661	3,1339	0,0000	0,0000	0,3917	0,0464	0,0263	0,0000	0,2037	5,3132	0,1946	97,3282
CODg(th)1	3	13	Xenotime	2,9367	28,9366	0,0301	36,3316	0,0144	0,0000	0,0000	0,1548	0,8851	4,0437	0,4419	5,2362	1,0672	2,6872	2,3706	0,1848	10,3283	4,2157	99,8649
CODg(th)1	4	1	Thorite	17,8756	1,8096	0,0000	2,8065	0,0183	0,0000	0,0269	0,0520	0,0989	0,3732	0,0000	0,4142	0,0472	0,2115	0,1747	0,2590	63,6085	14,1711	101,9472
CODg(th)1	4	2	Thorite	17,8572	1,8621	0,0000	3,0928	0,0161	0,0592	0,0273	0,0051	0,1216	0,4413	0,0501	0,4127	0,0620	0,2699	0,2457	0,2331	63,3767	14,5366	102,6695
CODm(m)1	3	6	REE silicate	17,9622	2,1407	0,0059	3,6182	0,0442	0,1879	0,0466	0,2987	0,3571	0,7323	0,0000	0,8428	0,1362	0,2105	0,1100	0,2725	70,5389	5,7833	103,2880
CODm(m)1	3	7	REE silicate	18,2983	1,8074	0,0574	2,7895	0,2230	0,2588	0,1157	0,2966	0,2388	0,4084	0,0185	0,6742	0,1443	0,1597	0,0738	0,2202	73,0650	4,0905	102,9401
VCA(m)1Pa	-		?	0,3597	4,8884	0,0941	1,4167	2,4818	5,2573	1,0294	2,4456	1,2543	0,5399	0,0000	0,9263	0,0976	0,1336	0,0000	0,2681	55,9524	26,9771	104,1223
VCA(m)1Pa	-		?	1,0009	16,1118	0,2811	1,1678	9,6564	21,6564	2,3354	8,5445	2,4230	0,4466	0,0000	0,6859	0,0680	0,0933	0,0000	0,2047	18,7338	15,2027	98,6123
VCA(m)1Pb	1	1	Xenotime	1,3332	32,3366	0,1956	41,0291	0,0763	0,0264	0,0450	0,3384	0,6029	3,2678	0,4824	5,0606	1,1160	3,1237	3,3136	0,1696	0,7854	5,8712	99,1738
VCA(m)1Pb	1	2	Xenotime	1,1686	32,6842	0,1909	41,4115	0,0475	0,0950	0,0183	0,3378	0,7271	3,3546	0,5153	5,0597	1,0651	3,1719	3,3227	0,0728	0,6947	5,2368	99,1745
VCA(m)1Pb	1	3	Xenotime	1,1515	32,7072	0,1859	41,3031	0,0195	0,0018	0,0000	0,2770	0,6717	3,2402	0,4968	5,1287	1,0787	3,2119	3,3806	0,0680	0,7073	5,1760	98,8059
VCA(m)1Pb	1	4	Xenotime	1,3708	32,2564	0,2147	40,2974	0,0000	0,0912	0,0000	0,3627	0,7595	3,3011	0,4848	5,1751	1,0721	3,0624	3,3727	0,0697	0,8551	6,1699	98,9156
VCA(m)1Pb	1	5	Xenotime	0,2923	33,9794	0,2107	43,4010	0,0128	0,0967	0,0117	0,4404	0,6996	3,4638	0,4195	5,3727	1,1502	3,2651	3,6092	0,1698	0,5070	1,7559	98,8578
VCA(m)1Pb	1	6	Xenotime	0,3943	34,1191	0,2193	43,0251	0,0000	0,0296	0,0673	0,3702	0,6386	3,3790	0,4761	5,3623	1,2200	3,2570	3,4501	0,0212	0,2326	2,5431	98,8049
VCA(m)1Pb	1	7	Xenotime	1,2823	32,3314	0,2013	41,2129	0,0000	0,0576	0,0000	0,3881	0,6299	3,1617	0,4162	4,8822	1,1300	3,1564	3,2569	0,1471	0,8282	5,6833	98,7655
VCA(m)1Pb	1	8	Xenotime	1,5838	31,9780	0,1987	40,1970	0,0000	0,0449	0,0000	0,3633	0,6905	3,1097	0,4274	4,9987	1,0710	3,0700	3,2342	0,1593	1,0001	6,8677	98,9943
VCA(m)1Pb	1	9	Xenotime	1,6947	31,5890	0,2148	39,9141	0,0184	0,0861	0,0000	0,2761	0,6304	3,2284	0,3675	4,8961	1,1289	3,1343	3,2331	0,1306	1,0887	7,3596	98,9908
VCA(m)1Pb	1	10	Xenotime	1,0379	33,0754	0,1662	41,2793	0,0139	0,1237	0,0000	0,3422	0,6869	3,3247	0,4271	5,1074	1,1976	3,1725	3,3560	0,0638	0,6008	4,8044	98,7798
VCA(m)1Pb	2	1	?	17,9336	0,0000	0,0878	0,8459	0,0000	0,0000	0,0000	0,0305	0,0000	0,0913	0,0202	0,1062	0,0692	0,1410	0,1962	0,2739	1,2449	42,6309	63,6716
VCA(m)1Pb	2	2	?	3,1200	2,4012	0,0077	2,2321	0,0000	0,0000	0,0000	0,0000	0,0681	0,7162	0,1338	1,5684	0,3636	0,7857	1,0331	0,0000	0,0000	0,1085	12,5384
VCA(m)1Pb	2	3	Zircon	35,3028	0,0001	0,0078	0,3833	0,0000	0,0000	0,0000	0,0709	0,0000	0,0230	0,0385	0,0000	0,0000	0,0950	0,2231	0,0073	0,0126	0,8911	37,0555
VCA(m)1Pb	2	4	Xenotime	0,2225	34,4995	0,0585	44,6835	0,0294	0,0000	0,0552	0,2869	0,6348	3,5448	0,5669	5,5045	1,1906	3,3136	3,2290	0,0905	0,2051	0,8113	98,9266
VCA(m)1Pb	2	5	Xenotime	0,2248	34,7206	0,0190	44,9665	0,0000	0,0020	0,0316	0,2010	0,5229	3,4504	0,5307	5,6881	1,2141	3,3796	3,4831	0,0996	0,0492	0,6601	99,2433
VCA(m)1Pb	2	6	Xenotime	0,6917	33,5347	0,1348	43,1777	0,0119	0,0757	0,0000	0,3846	0,6279	3,4419	0,5374	5,2701	1,2226	3,2275	3,2900	0,1534	0,6139	3,1120	99,5078
VCA(m)1Pb	3	1	Zircon	34,7996	0,0001	0,0035	0,0942	0,0000	0,0000	0,0000	0,0000	0,0000	0,0181	0,1081	0,0000	0,0247	0,0429	0,0454	0,0570	0,0062	0,2249	35,4247
VCA(m)1Pb	3	2	Zircon	35,4850	0,0001	0,0075	0,2126	0,0143	0,0000	0,0000	0,0000	0,0000	0,0302	0,0773	0,0854	0,0273	0,0880	0,1601	0,0000	0,0129	0,4356	36,6363
VCA(m)1Pb	3	3	Xenotime	0,1606	34,7211	0,0517	45,1059	0,0000	0,0365	0,0099	0,2254	0,6091	3,6566	0,5984	5,7632	1,2707	3,3126	3,2652	0,0344	0,1756	0,6335	99,6304
VCA(m)1Pb	3	4	Xenotime	0,5552	34,2155	0,2300	42,4458	0,0106	0,0741	0,0000	0,3979	0,7607	3,4663	0,4353	5,3966	1,1669	3,2368	3,5202	0,1081	0,4184	3,1965	99,6349
VCA(m)1Pb	3	5	Uraninite	0,0210	0,2563	0,0000	0,2640	0,0049	0,0053	0,1029	0,0000	0,0768	0,2686	0,0000	0,1717	0,0935	0,1781	0,1709	0,6608	12,5610	86,6920	101,5278
VCA(m)1Pb	4	1	Xenotime	1,2445	32,3977	0,1959	41,8646	0,0000	0,0539	0,0141	0,4134	0,6645	3,1383	0,3808	5,2995	1,2188	3,0627	3,3638	0,1796	0,8269	5,5526	99,8716
VCA(m)1Pb	4	2	Xenotime	1,2756	31,9685	0,1976	40,6899	0,0000	0,0799	0,0327	0,4847	0,6664	3,1502	0,5048	5,1709	1,0460	3,0670	3,2525	0,1404	0,8252	5,7740	98,3263
VCA(m)1Pb	4	3	Xenotime	0,2677	34,1330	0,9287	42,7668	0,0000	0,0323	0,0471	0,3253	0,6441	3,3862	0,5563	5,3575	1,1756	3,3271	3,4352	0,1021	0,1437	1,9634	98,5921
VCA(m)1Pb	4	4	Xenotime	1,3631	30,5923	0,2148	39,6551	0,0000	0,1141	0,0742	0,3477	0,7234	3,2578	0,4237	4,9717	1,0975	3,1757	3,2588	0,1814	0,8639	6,0734	96,3886
VCA(m)1Pb	4	5	Xenotime	1,3422	32,0940	0,2000	40,1902	0,0000	0,1092	0,0746	0,3702	0,6187	3,1810	0,5179	5,1319	1,1350	2,9697	3,3158	0,2065	0,8412	6,0884	98,3865
VCA(m)1Pb	4	6	Xenotime	1,1214	32,5361	0,1912	41,3205	0,0088	0,0672	0,0000	0,3836	0,6920	3,3341	0,4380	4,9152	1,1545	3,1660	3,2952	0,1127	0,7113	5,2659	98,7137
VCA(m)1Pb	4	7	Xenotime	1,4120	32,1723	0,1950	40,5961	0,0000	0,0520	0,0000	0,3875	0,6844	3,2468	0,4576	5,0784	1,0856	3,0272	3,2569	0,1389	0,8298	6,2055	98,8260
VCA(m)1Pb	4	8	?	0,1489	9,4399	0,0839	13,4813	0,0173	0,0000	0,0000	0,0000	0,0347	0,5414	0,1110	1,0263	0,2098	0,5796	0,5793	0,1517	0,0520	0,1978	26,6549
VCA(m)1Pb	4	9	?	0,2147	13,0355	0,0339	17,9988	0,0000	0,0191	0,0188	0,0319	0,1504	0,7677	0,1715	1,1081	0,1918	0,7248	0,6306	0,1614	0,1864	0,5156	35,9610
VCA(m)1Pb	5	1	Xenotime	1,2278	32,7910	0,1960	41,6294	0,0532	0,1508	0,0238	0,3788	0,6879	3,2122	0,4692	5,0455	0,9997	3,0958	3,3915	0,1759	0,7449	5,2753	99,5487
VCA(m)1Pb	5	2	Xenotime	1,3310	32,4937	0,2041	41,1388	0,0149	0,0181	0,0000	0,3313	0,5515	3,1134	0,3958	5,0075	1,1831	3,0210	3,2747	0,0004	0,8242	6,2273	99,1308
VCA(m)1Pb	5	3	Xenotime	1,5323	32,2745	0,2125	40,9998	0,0547	0,0639	0,0000	0,4656	0,6268	3,0970	0,4129	4,9380	1,0819	2,9793	3,3407	0,1229	0,8811	7,0367	100,1206
VCA(m)1Pb	5	4	Xenotime	1,0406	32,8687	0,1604	41,9806	0,0000	0,0417	0,0958	0,3551	0,6052	3,2836	0,5739	5,1484	1,2385	3,2357	3,2976	0,1432	0,6227	4,7636	99,4553
VCA(m)1Pb	5	5	Xenotime	1,0736	32,9856	0,1917	41,7093	0,0103	0,0831	0,0589	0,4323	0,6022	3,3733	0,4733	5,0617	1,1432	3,1522	3,2589	0,0000	0,6227	4,7952	99,0275
VCA(m)1Pb	7	1	Xenotime	1,3031	32,5000	0,1966	40,9408	0,0000	0,0922	0,0935	0,3057	0,6347	3,1609	0,4515	5,0311	1,1085	3,1602	3,4170	0,0000	0,7771	5,8681	99,0410
VCA(m)1Pb	7	3	?	0,2073	19,5926	0,2080	23,5668	0,0067	0,0218	0,0000	0,0956	0,4097	1,9014	0,2927	3,2706	0,7448	1,9052	2,1923	0,6228	0,3109	45,0115	100,3607
VCA(m)1Pb	7	4	Xenotime	0,2695	30,2519	0,1385	39,2542	0,0000	0,0938	0,0844	0,2162	0,5656	3,1054	0,4753	5,0429	1,1798	2,9420	3,0640	0,2032	1,4220	6,7344	95,0431
VCA(m)1Pb	7	5	Xenotime	0,1136	35,0992	0,0276	45,5580	0,0210	0,0019	0,0000	0,3107	0,6966	3,5089	0,5549	5,5614	1,3271	3,3504	3,1873	0,0649	0,0635	0,4620	99,9090
VCA(m)1Pb	7	6	Xenotime	1,3686	32,2563	0,2068	40,4531	0,0198	0,0269	0,0000	0,4363	0,6478	3,0865	0,5167	5,0993	1,0824	3,0993	3,4333	0,1398	0,7996	6,1473	98,8198
VCA(m)1Pb	8	1	Xenotime	0,3565	34,9898	0,1155	45,6177	0,0073	0,0414	0,0000	0,1680	0,4499	3,2448	0,5759	5,3943	1,1570	3,1302	2,6000	0,1355	0,5194	1,4804	99,9836
VCA(m)1Pb	8	2	Xenotime	0,3100	34,6779	0,0979	45,4793	0,0000	0,0869	0,1292	0,2073	0,6545	3,6160	0,5709	5,6779	1,2121	3,0529	2,4927	0,0000	0,1362	1,4985	99,9002
VCA(m)1Pb	8	3	Xenotime	0,2896	34,9169	0,0720	44,2905	0,0000	0,0800	0,0385	0,2610	0,5964	3,4629	0,5251	5,4784	1,1674	3,2637	3,4741	0,0911	0,2828	1,2314	99,5218
VCA(m)1Pb	9	1	Xenotime	1,1927	32,7032	0,1802	41,1196	0,0000	0,0428	0,0245	0,3676	0,7027	3,2071	0,4907	5,0539	1,0806	3,2021	3,2961	0,1503	0,7688	5,4445	99,0274
VCA(m)1Pb	9	2	Xenotime	0,2628	34,6733	0,0634	44,1011	0,0262	0,0714	0,0000	0,2348	0,6758	3,5625	0,5624	5,6490	1,2252	3,3347	3,3425	0,1478	0,2268	1,1159	99,2756
VCA(m)1Pb	9	3	Xenotime	0,5106	34,0626	0,1206	43,6969	0,0193	0,0965	0,0126	0,3256	0,5957	3,3764	0,5104	5,4023	1,1604	3,2653	3,2460	0,0817	0,6061	2,0391	99,1281

Sample code	Fragment	An. Pt	SiO_2	P_2O_5	CaO	Y_2O_3	La_2O_3	Ce_2O_3	Pr_2O_3	Nd_2O_3	Sm_2O_3	Gd_2O_3	Tb_2O_3	Dy_2O_3	Ho_2O_3	Er_2O_3	Yb_2O_3	PbO	ThO_2	UO_2	Sum
Codera Garnet dike																					
CODg(m)1P	-	1	0,9627	29,0200	0,7942	2,6872	11,2130	27,9321	3,2782	11,4702	3,0825	0,3183	0,0000	0,7311	0,0792	0,1499	0,0092	0,1824	6,6102	0,5922	99,1126
CODg(m)1P	-	2	0,9000	28,7436	0,8683	2,7913	10,9454	27,6755	3,0697	11,2584	3,1466	0,3858	0,0000	0,8296	0,1339	0,1464	0,0271	0,1481	6,7081	0,5683	98,3461
CODg(m)1P	-	3	0,7857	28,9261	0,7908	2,4580	11,1457	28,6815	3,1717	11,5442	3,0112	0,3235	0,0000	0,7211	0,0480	0,1290	0,0250	0,1599	5,8820	0,4866	98,2900
CODg(m)1	7	1	0,7162	29,0117	0,8226	2,6858	11,1122	28,4838	3,3032	11,5874	3,2457	0,1772	0,0000	0,7339	0,0463	0,1876	0,0441	0,1849	5,9968	0,5371	98,8765
CODg(m)1	7	2	1,0164	29,2567	0,9097	2,7301	10,6023	27,3726	3,1377	11,3147	3,0331	0,3805	0,0000	0,7448	0,0625	0,1574	0,0077	0,1094	7,2421	0,5695	98,6472
CODg(m)1	7	3	0,7222	29,2234	0,7665	2,5714	10,9478	28,1513	3,3856	11,6868	3,3080	0,3055	0,0000	0,7331	0,0488	0,1412	0,0000	0,1341	5,7411	0,5160	98,3828
CODg(m)1	11	1	0,9056	28,9960	0,8755	2,5158	12,0278	28,6121	3,1777	11,2118	2,6244	0,2591	0,0000	0,6621	0,0976	0,1160	0,0276	0,1785	6,0476	0,5916	98,9268
CODg(m)1	11	2	0,8179	28,7871	0,7952	2,5183	11,4776	28,3286	3,3568	11,1628	2,8515	0,2017	0,0000	0,7587	0,0579	0,1572	0,0000	0,1781	6,0087	0,4750	97,9331
CODg(m)2	1	1	0,7870	29,3128	0,8006	3,1194	11,1053	28,1369	3,0944	11,6079	3,0776	0,3078	0,0000	0,8077	0,0856	0,1967	0,0338	0,1885	5,7049	0,5439	98,9108
CODg(m)2	1	2	1,3219	28,1555	1,0090	2,8170	10,7380	26,1637	3,0190	10,7853	2,5993	0,4210	0,0000	0,7216	0,0550	0,1625	0,0069	0,1428	9,2991	0,7985	98,2161
CODg(m)2	1	3	1,1824	28,6856	0,9766	3,3478	10,4186	26,2243	3,0630	10,5552	2,8954	0,5928	0,0000	0,9104	0,1428	0,1971	0,0150	0,1858	8,3892	0,8428	98,6248
CODg(m)2	1	4	0,8661	29,1837	0,9417	3,3494	10,9171	27,1988	3,0686	11,1027	2,9534	0,5022	0,0000	0,8899	0,1139	0,2160	0,0238	0,2160	6,7799	0,6895	99,0127
CODg(m)2	1	5	1,1969	28,4719	0,9741	2,7193	11,8352	27,7943	3,0525	10,8010	2,6707	0,3587	0,0000	0,8081	0,1007	0,1955	0,0323	0,1722	7,3000	0,6130	99,0964
CODg(m)2	1	6	0,9488	28,9033	0,9409	2,5926	12,1325	28,5979	3,1474	10,8974	2,6362	0,2702	0,0000	0,6017	0,0708	0,1853	0,0092	0,1917	6,3654	0,5904	99,0817
CODg(m)2	1	7	1,1265	28,7525	0,9077	2,6476	11,8739	28,0861	2,9694	10,9976	2,6922	0,3367	0,0000	0,7559	0,0625	0,1554	0,0202	0,0256	7,0871	0,6339	99,1308
CODg(m)2	3	1	0,9703	28,6499	0,7408	2,1207	11,3351	28,6474	3,2004	11,6113	3,1541	0,2967	0,0000	0,7815	0,0326	0,1365	0,0099	0,2069	5,9649	0,5349	98,3939
CODg(m)2	3	2	1,0767	28,4656	0,9829	2,7256	11,7135	28,0907	3,0939	10,7818	2,7191	0,2999	0,0000	0,7602	0,0772	0,1690	0,0330	0,1550	6,9732	0,6332	98,7505
CODg(m)2	3	3	0,9106	29,0084	0,9001	2,5300	11,0703	27,7401	3,1749	10,7787	3,0045	0,2891	0,0000	0,6866	0,1458	0,1345	0,0000	0,0732	6,8662	0,5748	97,8878
CODg(m)2	3	4	0,9671	29,0871	0,9405	3,6956	10,1169	26,1061	3,1042	11,0905	3,0935	0,5830	0,0000	0,9361	0,1592	0,1923	0,0187	0,2044	7,4395	0,8657	98,6004
CODg(m)2	3	5	1,2376	29,2200	0,9422	2,7815	11,3995	27,5941	3,2783	11,2450	2,8842	0,3381	0,0000	0,7543	0,1178	0,1532	0,0088	0,1781	6,5205	0,5923	99,2455
CODg(m)3P	-	1	1,3300	28,2400	0,9700	2,7100	10,8000	26,9500	3,0500	10,6800	2,7300	0,4400	0,0000	0,7100	0,0800	0,1600	0,0200	0,0100	8,2800	0,7100	97,8700
CODg(m)3P	-	2	1,4200	27,5700	1,0300	2,5400	11,3200	27,1200	2,9800	10,2800	2,5300	0,3500	0,0000	0,6500	0,1100	0,1900	0,0300	0,0000	8,4300	0,8200	97,3700
CODg(m)3P	-	3	0,9700	28,9100	0,9700	3,2800	10,8500	26,9600	3,0700	10,9300	2,8900	0,4400	0,0000	0,8400	0,0600	0,2000	0,0300	0,0000	6,9100	0,6700	97,9800
CODg(m)3P	-	4	0,8600	28,4400	1,0200	2,9100	10,8800	27,2600	3,1100	10,9300	2,9200	0,3400	0,0000	0,8100	0,1000	0,1500	0,0000	0,0000	6,7800	0,7000	97,2100
CODg(m)3P	-	5	0,7900	29,2200	0,9100	3,1600	11,0500	27,4400	3,1000	11,1100	2,9600	0,4800	0,0000	0,8700	0,1000	0,2300	0,0000	0,0000	5,8500	0,6300	97,9000
CODg(m)3P	-	6	1,0600	28,5700	1,1300	3,0700	10,4300	26,4300	3,0600	10,7600	2,9100	0,4100	0,0000	0,8200	0,1500	0,1700	0,0400	0,0000	8,0500	0,8700	97,9300
CODg(m)3P	-	7	0,7100	29,0700	1,0700	3,0800	11,7400	27,4900	3,0700	10,5800	2,7600	0,3800	0,0000	0,8600	0,1200	0,1900	0,0300	0,0000	6,3900	0,7800	98,3200
CODg(m)3P	-	8	0,9000	28,5900	1,1400	2,8900	10,7300	26,8300	3,0500	10,8100	2,9100	0,2800	0,0000	0,7800	0,0900	0,1800	0,0000	0,0000	7,5500	0,8400	97,5700
CODg(m)3P	-	9	0,7300	29,2100	0,9900	3,2000	11,7300	27,6100	2,9400	10,5200	2,6500	0,4400	0,0000	0,8800	0,1100	0,2100	0,0700	0,0000	6,0300	0,7900	98,1100
CODg(m)3P	-	10	1,2800	28,1700	1,0600	2,7100	10,7200	26,7600	3,0200	10,6900	2,6600	0,3800	0,0000	0,7300	0,0800	0,1600	0,0100	0,0000	8,9200	0,7700	98,1200
CODg(m)3P	-	11	0,7900	29,1300	0,9600	3,1300	10,9500	27,4900	3,2300	11,1200	2,9700	0,4400	0,0000	0,8800	0,0900	0,2000	0,0400	0,0000	6,2200	0,6800	98,3200
Codera Trubinasca dike																					
CODt(m)1P	-	1	0,2283	29,9620	3,3985	0,8150	7,1490	21,5598	2,5969	9,1905	5,2655	0,5095	0,0000	0,3559	0,0242	0,0383	0,0000	0,1540	6,8978	9,4462	97,5914
CODt(m)1P	-	2	0,2109	30,1712	3,5632	0,8347	7,4982	21,4258	2,8722	9,2522	5,3442	0,5510	0,0000	0,4719	0,0048	0,0153	0,0000	0,2653	6,7649	10,0481	99,2939
CODt(m)1P	-	3	0,2375	30,0336	2,6033	0,5047	9,3816	25,4594	2,8141	9,5924	4,7920	0,1512	0,0000	0,3135	0,0581	0,0529	0,0000	0,2270	6,2623	6,4194	98,9030
CODt(m)1	1	1	0,2223	30,0817	3,2909	0,6337	8,1533	22,9246	2,8070	9,0653	4,7107	0,2742	0,0000	0,3308	0,0430	0,0000	0,0000	0,2272	7,0522	8,7912	98,6081
CODt(m)1	1	2	0,2149	29,7897	3,0330	0,5888	7,9834	23,3295	2,8250	9,5627	5,0692	0,3211	0,0000	0,3504	0,0123	0,0286	0,0000	0,2663	7,2489	7,6753	98,2991
CODt(m)1	1	3	0,2272	29,8748	3,4175	0,6816	8,0921	21,7931	2,7479	9,1965	4,9594	0,3472	0,0000	0,2712	0,0487	0,0000	0,0000	0,2005	6,9816	9,7029	98,5422
Codera Mary Dike																					
CODm(m)1P	1	1	1,5283	27,4808	1,2390	3,1994	9,0071	26,1234	3,1557	11,1907	3,2201	0,0930	0,0000	0,5932	0,1116	0,1588	0,0690	0,1682	10,8030	0,5614	98,7027
CODm(m)1P	1	2	1,0417	28,1539	0,8527	2,5134	9,6845	28,4304	3,5496	11,8164	3,4498	0,0000	0,0000	0,5548	0,0558	0,1298	0,0139	0,2147	7,1329	0,2702	97,8645
CODm(m)1P	1	3	1,4645	27,3673	1,1718	3,1579	9,2378	26,0870	3,2727	11,0904	3,1720	0,0000	0,0000	0,5930	0,1137	0,1378	0,0493	0,0958	10,4086	0,4861	97,9057
CODm(m)1	2	1	1,1560	28,0474	1,0654	2,4729	10,4602	28,3721	3,5308	10,9461	3,0389	0,0000	0,0000	0,5114	0,0515	0,1472	0,0268	0,2711	7,8719	0,3866	98,3563
CODm(m)1	2	2	1,3699	27,7632	1,1169	2,7897	8,9521	26,6133	3,4216	11,4146	3,5214	0,0215	0,0000	0,5592	0,0334	0,1335	0,0227	0,0522	9,9295	0,4967	98,2114
CODm(m)1	3	1	2,6722	25,1898	0,3081	0,3442	10,0277	30,1707	3,7223	12,3871	2,7176	0,0000	0,0000	0,0091	0,0000	0,0151	0,0000	0,2024	11,2462	0,1371	99,1496
CODm(m)1	3	2	1,5696	27,4257	1,0368	2,8480	9,5732	26,9435	3,2619	11,6069	3,1240	0,0596	0,0000	0,5758	0,0000	0,1231	0,0848	0,1945	10,0224	0,3957	98,8455
CODm(m)1	3	3	1,4189	27,4572	1,0508	2,8436	9,3584	27,1984	3,2541	11,3259	3,1492	0,0000	0,0000	0,6634	0,0578	0,1028	0,0004	0,0664	9,9598	0,4611	98,3682
CODm(m)1	3	4	1,4182	27,8950	1,0704	2,6600	9,7658	27,3382	3,2755	11,1672	2,9618	0,0000	0,0000	0,4804	0,0537	0,1090	0,0531	0,1475	9,6016	0,4600	98,4574
CODm(m)1	3	5	1,4739	27,6235	1,0993	3,0805	9,5095	26,3702	3,2589	11,1933	3,0383	0,0574	0,0000	0,6637	0,0620	0,1680	0,0245	0,2256	10,0224	0,5119	98,3829
CODm(m)1	4	1	1,0088	28,5569	1,0303	2,3141	10,5295	29,0775	3,4501	11,2989	3,2589	0,0000	0,0000	0,4685	0,0604	0,0821	0,0162	0,1306	7,4475	0,3527	99,0830
CODm(m)1	4	2	1,3095	27,8746	0,9613	2,7725	9,5229	27,3598	3,4257	11,8196	3,3994	0,0000	0,0000	0,5780	0,0000	0,1573	0,0304	0,1119	8,8212	0,3771	98,5212
CODm(m)1	4	3	1,0918	28,0567	1,0990	2,2153	10,2057	28,6858	3,4646	11,1641	3,1215	0,0000	0,0000	0,4637	0,0300	0,0927	0,0044	0,1300	8,0130	0,3864	98,2247
CODm(m)1	4	4	1,1433	27,9833	0,8437	2,6896	9,7139	28,4109	3,4222	11,9756	3,4495	0,0000	0,0000	0,5832	0,0656	0,1330	0,0202	0,1469	7,6449	0,3602	98,5860
CODm(m)1	5	1	1,0697	28,0260	0,9299	2,3817	10,2607	28,6457	3,3784	11,3131	3,1186	0,0000	0,0000	0,5733	0,1078	0,1110	0,0128	0,1939	7,6721	0,3327	98,1274
CODm(m)1	5	2	1,3598	27,7005	0,9782	2,8682	9,3374	27,7956	3,3759	11,5684	3,3959	0,0000	0,0000	0,5828	0,0935	0,1084	0,0552	0,2218	9,1192	0,3459	98,9067
CODm(m)1	5	3	1,2373	27,6114	0,9494	2,8084	9,6127	27,5362	3,4040	11,4998	3,1951	0,0000	0,0000	0,5993	0,0630	0,1617	0,0187	0,1350	8,7128	0,4677	98,0125
CODm(m)1	5	4	1,1055	27,8211	1,0026	2,4213	10,6534	29,1400	3,2726	11,0370	3,0049	0,0000	0,0000	0,5149	0,1167	0,1337	0,0000	0,2887	7,5011	0,3013	98,3148
CODm(m)1	5	5	2,6977	25,2699	0,2018	0,1668	10,3518	30,8782	3,7853	12,5934	2,5958	0,0000	0,0000	0,0000	0,0000	0,0000	0,0000	0,1797	11,2584	0,0801	100,0589
C-Sample																					
CODm(m)1	C	1	0,8750	29,3141	1,0065	2,6345	11,8064	27,4797	3,1214	10,7250	2,6877	0,3225	0,0000	0,7734	0,1171	0,1993	0,0304	0,1104	6,4126	0,6687	98,2847
CODm(m)1	C	2	0,8607	29,0954	1,0192	2,6562	11,6481	28,2934	3,0239	10,9479	2,7755	0,3168	0,0000	0,7661	0,0293	0,1734	0,0194	0,2125	6,3423	0,6434	98,8235
CODm(m)1	C	3	0,8675	29,4526	1,0163	2,8211	11,7892	28,2598	3,2794	10,8991	2,8858	0,2523	0,0000	0,7937	0,1064	0,1920	0,0000	0,1563	6,4315	0,6435	99,8465
CODm(m)1	C	4	0,8672	29,4013	0,9668	2,6437	11,9024	28,2458	3,0019	10,8053	2,8130	0,2683	0,0000	0,7369	0,1024	0,1632	0,0000	0,1527	6,3511	0,6365	99,0585
CODm(m)1	C	5	0,8576	29,4348	0,9822	2,6255	11,7050	28,7481	3,1537	10,8900	2,7717	0,2247	0,0000	0,7829	0,0596	0,1584	0,0253	0,1659	6,4474	0,5965	99,6293
CODm(m)1	C	6	0,9108	29,6413	0,9771	2,6595	11,6266	28,1239	3,0463	10,9071	2,7907	0,3069	0,0000	0,8125	0,1152	0,1523	0,0213	0,1233	6,5232	0,6600	99,3980
CODm(m)1	C	7	0,8976	29,4203	1,0265	2,8228	11,6535	28,4901	3,0701	11,1394	2,6631	0,3471	0,0000	0,7166	0,0914	0,1491	0,0146	0,2182	6,6297	0,7231	100,0732
CODm(m)1	C	8	0,9476	29,1637	1,0200	2,8688	11,5956	28,0343	3,1281	10,9075	2,6970	0,2664	0,0000	0,6877	0,0636	0,2002	0,0000	0,2292	6,8955	0,7009	99,4061
CODm(m)1	C	9	0,8195	29,5788	0,9642	3,5002	10,8622	26,7927	3,1649	11,5151	3,1172	0,5320	0,0000	0,9682	0,1619	0,2228	0,0618	0,1636	6,4024	0,7461	99,5736
CODm(m)1	C	10	0,8723	29,6310	0,9676	3,6734	10,8197	26,7595	3,1594	11,6457	3,0786	0,4504	0,0000	0,8774	0,0919	0,2299	0,0176	0,1231	6,5874	0,7824	99,7673
CODm(m)1	C	12	0,8987	29,2532	0,9765	2,6583	11,8619	28,3928	3,1206	10,9508	2,8029	0,1999	0,0000	0,6605	0,0438	0,1405	0,0007	0,0978	6,4557	0,5884	99,1030
CODm(m)1	C	13	0,8979	29,5709	0,9880	2,6502	11,8622	28,5973	2,9644	10,5571	2,7401	0,3204	0,0000	0,6901	0,1318	0,1340	0,0000	0,3091	6,5129	0,6677	99,5941
CODm(m)1	C	15	0,8650	29,2263	0,9863	2,4744	11,8076	28,1594	3,0858	10,7786	2,7441	0,2921	0,0000	0,7208	0,0055	0,1437	0,0571	0,1816	6,5007	0,6126	98,6416
CODm(m)1	C	17	0,8858	29,0341	0,7783	2,2380	11,2506	28,2916	3,3731	11,7157	3,0162	0,2147	0,0000	0,5949	0,1482	0,1553	0,0000	0,1607	6,4360	0,3827	98,6759
CODm(m)1	C	18	0,9610	29,2720	1,0171	2,9972	11,6330	27,9351	3,1772	10,9403	2,7520	0,3238	0,0000	0,8464	0,1132	0,2156	0,0000	0,2351	6,8455	0,6926	99,9571
CODm(m)1	C	19	0,9589	29,1835	1,0436	2,7517	11,5833	27,9611	3,1815	10,6120	2,7813	0,3330	0,0000	0,7684	0,0787	0,1088	0,0000	0,2258	7,0905	0,7402	99,4023
CODm(m)1	C	20	0,8334	29,0748	0,9705	2,6519	11,9691	28,3910	3,1469	10,8473	2,7362	0,2113	0,0000	0,7505	0,1370	0,2008	0,0355	0,2226	6,2162	0,6340	99,0290
CODm(m)1	C	21	1,1146	28,6953	0,9054	2,3067	10,6152	27,4442	3,2166	11,7134	2,9493	0,2891	0,0000	0,6241	0,1075	0,0978	0,0000	0,1067	8,2373	0,5086	98,9318

Sample code	Fragment	An. Pt	SiO_2	P_2O_5	CaO	Y_2O_3	La_2O_3	Ce_2O_3	Pr_2O_3	Nd_2O_3	Sm_2O_3	Gd_2O_3	Tb_2O_3	Dy_2O_3	Ho_2O_3	Er_2O_3	Yb_2O_3	PbO	ThO_2	UO_2	Sum
Medium Leggia valley dike																					
VLGm(m)1P	2	1	1,2175	28,3075	0,3197	1,0669	8,1595	25,6827	3,6769	16,0738	7,0602	0,0938	0,0000	0,2428	0,0520	0,0417	0,0000	0,0954	5,3848	0,1594	97,6346
VLGm(m)1P	2	10	1,4934	28,1980	0,2571	1,2913	7,2732	24,1159	3,6578	16,4075	6,9774	0,3887	0,0000	0,4466	0,0049	0,0101	0,0000	0,1761	6,2105	0,4798	97,3883
VLGm(m)1P	2	2	1,2824	28,2034	0,3274	1,3221	8,3753	25,9452	3,7203	15,4676	6,8182	0,1998	0,0000	0,2789	0,0414	0,0196	0,0000	0,0000	5,3719	0,1975	97,5710
VLGm(m)1P	2	3	1,1622	28,5800	0,3098	1,2886	8,4811	25,5868	3,8716	15,5622	6,8910	0,2908	0,0000	0,2811	0,0618	0,0213	0,0000	0,1212	4,8698	0,2027	97,5820
VLGm(m)1P	2	4	1,3291	28,1984	0,2652	1,3892	7,6508	24,9482	3,7351	16,6035	6,8189	0,2629	0,0000	0,4442	0,0176	0,0201	0,0000	0,1732	5,3729	0,4373	97,6666
VLGm(m)1P	2	5	1,4896	27,8046	0,2963	1,4784	8,0689	24,7966	3,6954	16,5698	6,1978	0,3664	0,0000	0,4588	0,0440	0,0509	0,0000	0,1808	6,1719	0,4274	98,0976
VLGm(m)1P	2	6	1,5599	28,2138	0,3043	1,5097	7,9308	24,7069	3,7136	16,3520	6,1494	0,3133	0,0000	0,4358	0,0000	0,0510	0,0000	0,1833	6,3057	0,4540	98,1835
VLGm(m)1P	2	7	1,3265	28,2269	0,3014	1,3399	8,5924	25,4360	3,6732	16,1474	5,8717	0,2380	0,0000	0,4079	0,0622	0,0476	0,0000	0,1400	5,6990	0,4026	97,9127
VLGm(m)1P	2	8	0,6745	29,1628	0,2472	1,7067	10,1789	27,3892	3,8456	15,8680	5,3707	0,0749	0,0000	0,4657	0,0000	0,0502	0,0000	0,1837	2,2523	0,2122	97,6826
VLGm(m)1P	2	9	1,4585	28,0653	0,2815	1,7350	7,8827	24,5836	3,6045	16,1331	6,3430	0,4195	0,0000	0,4649	0,0736	0,0085	0,0000	0,0992	6,0960	0,4660	97,7149
VLGm(m)1	1	1	1,2839	28,5843	0,2696	1,3786	8,5979	26,3347	3,8128	16,7237	5,8848	0,0865	0,0000	0,3506	0,0334	0,0134	0,0000	0,1933	4,5531	0,3028	98,4034
VLGm(m)1	1	2	1,6356	27,9282	0,3106	1,2904	8,5385	25,7165	3,6236	15,5124	5,6107	0,0183	0,0000	0,2659	0,0499	0,0738	0,0000	0,1606	6,9481	0,4064	98,0895
VLGm(m)1	3	1	1,6306	27,3136	0,2629	1,2590	8,5602	25,5473	3,5975	16,0435	5,4865	0,0083	0,0000	0,3059	0,0544	0,0000	0,0000	0,1789	6,8059	0,4074	97,4619
VLGm(m)1	3	2	1,3098	28,3705	0,2483	1,0731	8,4037	26,1787	3,7530	16,4119	6,5770	0,0109	0,0000	0,2726	0,0000	0,0295	0,0000	0,1622	4,6878	0,3505	97,8395
VLGm(m)1	3	3	1,3810	27,9966	0,2011	0,5217	7,0383	24,4386	3,9161	16,5770	9,0854	0,3144	0,0000	0,0698	0,0437	0,0000	0,0000	0,1744	4,6051	0,3741	96,7373
VLGm(m)1	5	1	1,6235	27,9481	0,2431	1,1879	8,4927	26,0045	3,6699	15,8880	5,4612	0,1023	0,0000	0,3146	0,0618	0,0000	0,0000	0,0830	6,7567	0,3549	98,1922
VLGm(m)1	5	2	1,0803	28,5295	0,1781	0,7325	7,2810	25,0483	4,0168	17,2558	8,1056	0,2612	0,0000	0,2622	0,0097	0,0079	0,0000	0,1274	3,7803	0,2624	96,9390
VLGm(m)1	8	1	1,5548	27,7634	0,2815	1,1043	8,5605	25,7239	3,7302	15,8247	5,6650	0,0514	0,0000	0,3361	0,0000	0,0000	0,0000	0,1273	6,4843	0,4122	97,6196
VLGm(m)1	8	2	1,1891	28,6620	0,2367	1,0582	8,4210	25,6822	3,7343	16,4702	6,2956	0,1862	0,0000	0,2662	0,0055	0,0456	0,0000	0,1864	4,7869	0,2855	97,5116
VLGm(m)1	11	1	1,6704	27,8569	0,2256	0,6175	6,0527	23,7299	3,8938	16,2634	9,2774	0,3496	0,0000	0,1692	0,0187	0,0115	0,0000	0,1891	6,9707	0,4774	97,7738
VLGm(m)1	11	2	1,0398	28,4603	0,2396	0,7831	7,4079	25,7781	3,9683	17,6916	7,6171	0,2195	0,0000	0,1739	0,0524	0,0032	0,0000	0,2209	3,6796	0,2182	97,5535
VLGm(m)1	11	3	1,4843	27,9545	0,2428	0,7165	7,9181	25,9193	3,8533	16,4533	7,0444	0,1040	0,0000	0,1503	0,0000	0,0129	0,0000	0,1751	5,0891	0,3819	97,4998
VLGm(m)1	12	1	1,1622	28,6923	0,3728	1,5941	10,7041	27,1826	3,4894	14,0590	4,6980	0,3128	0,0000	0,4259	0,0004	0,0835	0,0000	0,1291	5,4791	0,1987	98,5840
VLGm(m)1	12	2	1,6256	27,8737	0,2309	0,9094	6,7839	23,8182	3,7069	16,8823	7,9697	0,5868	0,0000	0,2627	0,0390	0,0000	0,0000	0,1422	6,2903	0,5425	97,6641
VLGm(m)1	12	3	0,8047	29,0776	0,2807	1,2450	8,6557	25,8067	3,6668	16,6109	6,7916	0,3726	0,0000	0,4529	0,0000	0,0136	0,0000	0,1635	3,0408	0,2992	97,2823
VLGm(m)1	12	4	1,5800	27,9568	0,2418	0,9605	6,4497	23,6484	3,6323	16,9720	8,0690	0,6134	0,0000	0,2128	0,0143	0,0000	0,0000	0,2513	6,3510	0,4909	97,4442
VLGm(m)1	12	5	1,5472	27,9853	0,2406	1,0702	6,9995	23,9448	3,7402	16,7201	7,5896	0,5727	0,0000	0,3581	0,0010	0,0000	0,0000	0,1364	6,3006	0,4992	97,7055
VLGm(m)1	16	1	1,4343	28,2260	0,2950	1,4215	7,8882	25,0418	3,6301	16,1621	6,0797	0,3732	0,0000	0,4282	0,0000	0,0336	0,0000	0,0971	6,1072	0,4165	97,6345
VLGm(m)1	16	2	1,5293	27,6949	0,2345	0,8108	6,5200	23,1179	3,7838	17,0148	8,6845	0,5452	0,0000	0,2214	0,0599	0,0000	0,0000	0,0658	6,1984	0,4800	96,9612
VLGm(m)1	16	3	1,3997	28,2479	0,2462	1,3985	8,0590	24,8708	3,8409	16,7160	6,3634	0,3473	0,0000	0,3947	0,0000	0,0313	0,0000	0,1103	5,6539	0,3739	98,0538
VLGm(m)1	16	4	1,5000	27,6944	0,2731	1,2115	8,2831	25,3934	3,7791	15,5075	5,8046	0,0000	0,0000	0,3009	0,0122	0,0105	0,0000	0,0928	6,3899	0,3636	96,6166
VLGm(m)1	17	1	1,2752	28,4984	0,2674	1,4504	8,5190	26,4390	3,6111	16,2065	5,8960	0,2362	0,0000	0,2697	0,0000	0,0264	0,0000	0,0596	4,7020	0,2877	97,7446
VLGm(m)1	17	2	1,5442	28,1160	0,3131	1,2101	8,4646	25,9104	3,7051	15,6850	5,7008	0,0381	0,0000	0,3677	0,0260	0,0179	0,0000	0,1032	6,8082	0,4102	98,4206
VLGm(m)1	17	3	1,2146	28,4164	0,2630	1,2768	8,6316	25,7184	3,7705	16,6466	5,8657	0,1941	0,0000	0,2683	0,0588	0,0000	0,0000	0,1020	4,6805	0,2672	97,3745
VLGm(m)1	17	4	1,4899	28,1302	0,2779	1,2493	8,6485	25,3393	3,6159	15,8552	5,8907	0,1468	0,0000	0,3015	0,0309	0,0123	0,0000	0,1388	6,2212	0,3944	97,7428
VLGm(m)1	19	1	1,6654	27,9535	0,3027	1,1923	8,6285	25,5800	3,5369	15,7302	5,5243	0,0436	0,0000	0,3220	0,0279	0,0166	0,0000	0,1190	7,1901	0,4355	98,2685
VLGm(m)1	19	2	1,5058	28,4872	0,2866	1,1932	9,0582	26,2244	3,6736	15,9659	5,3480	0,0000	0,0000	0,3140	0,0350	0,0440	0,0000	0,1593	5,4531	0,3943	98,1426
VLGm(m)2P	-	1	1,4399	27,9371	0,1989	0,7696	6,0336	23,6826	3,7880	17,2169	9,6982	0,5531	0,0000	0,1825	0,0398	0,0000	0,0000	0,1885	5,0500	0,4525	97,2312
VLGm(m)2P	-	2	1,2910	27,9703	0,1851	0,6328	5,9769	23,1758	3,7190	16,6117	10,2380	0,6083	0,0000	0,1760	0,0000	0,0000	0,0000	0,2558	4,8835	0,3604	96,0846
VLGm(m)2P	-	3	1,1446	28,2589	0,1996	0,6629	6,0554	23,2117	3,8168	16,0679	10,5090	0,5745	0,0000	0,1518	0,0000	0,0000	0,0000	0,1438	4,3211	0,3402	95,4582
VLGm(m)2P	-	4	0,9590	28,7844	0,1921	0,6673	5,5333	22,9463	3,8580	16,7860	11,2594	0,6881	0,0000	0,1887	0,0000	0,0000	0,0000	0,1786	3,4103	0,2559	95,7074
VLGm(m)2	3	1	0,8829	29,0787	0,1729	0,9004	7,8755	25,9493	3,9963	17,4637	7,1818	0,2352	0,0000	0,1315	0,0447	0,0120	0,0000	0,2225	3,0866	0,2087	97,4427
VLGm(m)2	3	3	1,4877	27,9607	0,2601	1,2543	8,6084	25,8925	3,6787	16,3819	5,7413	0,0955	0,0000	0,3859	0,0595	0,0000	0,0000	0,1644	6,1381	0,3622	98,4712
VLGm(m)2	3	4	1,2564	28,2309	0,2838	1,2394	8,2357	25,8066	3,8818	16,4798	6,1366	0,2920	0,0000	0,4588	0,0563	0,0517	0,0000	0,1712	4,8515	0,3217	97,7542
VLGm(m)2	4	1	1,3800	27,5000	0,2900	1,0300	8,7700	25,8500	3,6000	15,4400	6,1000	0,0100	0,0000	0,2700	0,0000	0,0100	0,0000	0,0000	5,2200	0,2900	95,7600
VLGm(m)2	4	2	1,1700	28,0500	0,3100	1,2000	10,2200	28,0600	3,7200	15,0200	4,3200	0,0000	0,0000	0,2700	0,0100	0,0400	0,0000	0,0000	4,6600	0,1800	97,2300
VLGm(m)2	4	3	1,5300	27,1500	0,2500	0,8700	6,8000	23,7300	3,7300	16,3500	7,6900	0,5100	0,0000	0,3000	0,0300	0,0000	0,0000	0,0000	5,7500	0,4800	95,1700
VLGm(m)2	4	4	1,1000	28,3600	0,3100	1,2200	10,0800	27,8900	3,6900	15,2200	4,4500	0,0000	0,0000	0,2600	0,0300	0,0300	0,0000	0,0000	4,5500	0,1600	97,3500
VLGm(m)2	6	1	1,2801	28,4866	0,2616	1,3490	8,2096	25,1119	3,9017	16,7696	6,3701	0,2150	0,0000	0,3612	0,0115	0,0081	0,0000	0,1530	4,5618	0,3150	97,3658
VLGm(m)2	6	2	1,4718	28,0747	0,2506	1,2476	7,2559	24,2877	3,7817	16,5569	7,3720	0,5178	0,0000	0,3114	0,0229	0,0258	0,0000	0,0310	6,0903	0,5243	97,8224
VLGm(m)2	6	3	1,5190	28,2316	0,2734	1,2463	8,6493	25,8016	3,6832	16,2200	5,7537	0,1061	0,0000	0,2921	0,0281	0,0000	0,0000	0,2459	6,1231	0,3606	98,5340
VLGm(m)2	7	1	1,2580	28,3788	0,2399	1,2405	8,3453	25,5523	3,7334	16,2711	6,2447	0,1487	0,0000	0,3613	0,0000	0,0060	0,0000	0,0839	5,2037	0,3240	97,3916
VLGm(m)2	7	2	1,4933	27,7474	0,2033	0,8587	5,3471	21,8497	3,7273	16,5631	10,6533	0,9093	0,0000	0,2002	0,0490	0,0163	0,0000	0,1491	5,7941	0,4650	96,0262
VLGm(m)2	8	1	1,0500	28,1000	0,2900	1,2400	9,2900	27,2900	3,7800	15,4200	5,2200	0,0000	0,0000	0,2900	0,0100	0,0400	0,0000	0,0000	4,2000	0,1600	96,3800
VLGm(m)2	8	2	1,6800	27,2500	0,2600	0,6000	6,2100	23,2600	3,7500	15,8300	8,9300	0,4700	0,0000	0,2000	0,0000	0,0000	0,0000	0,0000	6,4400	0,5000	95,3800
VLGm(m)2	8	3	1,5100	27,1800	0,2200	0,5700	6,5000	23,8800	3,8100	16,3400	8,5900	0,3100	0,0000	0,1500	0,0000	0,0000	0,0000	0,0000	5,5600	0,4300	95,0500
VLGm(m)2	8	4	1,4185	27,9881	0,2258	0,8375	7,3876	24,2691	3,7723	16,1320	7,9004	0,3222	0,0000	0,2553	0,0000	0,0034	0,0000	0,1975	5,9395	0,3841	97,0333
VLGm(m)2	9	1	1,1254	28,7061	0,2829	1,2935	9,0246	26,0422	3,7563	15,5026	6,8269	0,0912	0,0000	0,2258	0,0917	0,0060	0,0000	0,1261	4,6179	0,1755	97,8947
VLGm(m)2	9	2	0,9660	28,9118	0,2198	1,1218	7,5730	25,2183	3,8493	16,5675	8,4217	0,2557	0,0000	0,2273	0,0634	0,0646	0,0000	0,0884	3,6387	0,1539	97,3412
VLGm(m)2	9	3	1,4585	28,0114	0,2386	0,6688	5,8347	23,1351	3,7119	16,1983	10,4828	0,3431	0,0000	0,0967	0,0000	0,0000	0,0000	0,2118	5,6387	0,4146	96,4450
VLGm(m)2	11	1	1,4967	28,2592	0,2418	0,9540	6,9159	24,3724	3,6219	16,7803	7,7019	0,3548	0,0000	0,3331	0,0319	0,0364	0,0000	0,0743	6,0372	0,4295	97,6413
VLGm(m)2	11	2	1,4904	27,7844	0,2199	0,9109	7,0514	23,8803	4,0576	16,9059	8,0041	0,4282	0,0000	0,3239	0,0000	0,0088	0,0000	0,1649	5,9169	0,4529	97,6005
VLGm(m)2	12	1	1,2900	27,4400	0,2600	0,9300	7,9800	25,3600	3,7700	16,0400	6,4900	0,1900	0,0000	0,3900	0,0200	0,0200	0,0000	0,0000	4,9500	0,3300	95,4600
VLGm(m)2	12	2	0,9800	28,3200	0,2600	1,3800	10,8900	28,7700	3,7100	14,8400	3,8100	0,0000	0,0000	0,2900	0,0400	0,0700	0,0000	0,0000	3,6200	0,1300	97,1100
VLGm(m)2	12	3	1,4097	27,9320	0,2594	1,2262	8,3990	25,4633	3,7916	15,9345	6,2559	0,1679	0,0000	0,3351	0,0237	0,0524	0,0000	0,1409	5,8164	0,3522	97,5602
VLGm(m)2	12	4	1,0368	29,4895	0,2947	1,2809	10,7672	28,7116	3,6370	15,4302	4,0617	0,0000	0,0000	0,2832	0,0133	0,0375	0,0000	0,1454	4,3460	0,2040	99,7390
VLGm(m)2	14	1	1,1113	28,7441	0,1941	0,8919	6,9534	24,4955	3,8228	17,2217	7,9624	0,3841	0,0000	0,2165	0,0000	0,0000	0,0000	0,2428	4,1833	0,2463	96,6702
VLGm(m)2	14	2	1,1909	28,0391	0,1876	0,6613	6,2707	23,4478	3,7449	16,9985	9,9821	0,5170	0,0000	0,1583	0,0176	0,0096	0,0000	0,1643	4,3551	0,3509	96,0957
Cama valley dike																					
VCA(m)1Pa	-	1	0,6299	29,1018	2,4121	3,1884	10,3604	23,0430	2,5329	9,0687	2,6774	0,6019	0,0000	0,8790	0,0714	0,1439	0,0332	0,3257	11,8212	2,0851	98,9760
VCA(m)1Pa	-	2	0,7447	29,2219	2,1803	2,7209	10,7415	24,0935	2,7315	9,5808	2,7414	0,5575	0,0000	0,6865	0,1218	0,1019	0,0029	0,2135	11,9539	1,4831	99,8776
VCA(m)1Pa	-	3	0,5782	29,0885	2,0725	2,6960	11,8422	25,1606	2,6476	9,2670	2,4096	0,4202	0,0000	0,7775	0,1025	0,0933	0,0000	0,1072	10,0484	1,4991	98,8104
VCA(m)1Pa	-	4	0,5295	29,2218	1,9563	2,3579	11,9695	25,4434	2,7284	9,6702	2,4879	0,5190	0,0000	0,5818	0,1474	0,1401	0,0176	0,1587	9,9191	1,3389	99,1875
VCA(m)1Pb	10	1	0,5872	29,5929	2,1950	2,6476	10,8052	23,9952	2,8361	9,7259	2,7052	0,5322	0,0000	0,7885	0,1081	0,1467	0,0000	0,1563	11,2047	1,6947	99,7215
VCA(m)1Pb	10	2	0,5160	29,6441	2,1197	2,5326	11,6945	25,0456	2,6829	9,4336	2,4195	0,3640	0,0000	0,7320	0,0769	0,1212	0,0000	0,1766	10,2929	1,6548	99,5069
VCA(m)1Pb	10	3	0,4962	29,4386	2,1133	2,3384	11,9303	25,2894	2,7593	9,3879	2,6453	0,3392	0,0000	0,6828	0,0873	0,0986	0,0281	0,2086	9,8759	1,6532	99,3724
VCA(m)1Pb	10	4	0,4848	29,6931	2,0892	2,4373	12,1216	25,1945	2,6887	9,3912	2,5964	0,4708	0,0000	0,7025	0,0454	0,1017	0,0153	0,1427	10,0120	1,6006	99,7878
VCA(m)1Pb	10	5	0,5018	29,8337	2,0665	2,4648	11,7946	25,1749	2,7931	9,3493	2,6220	0,3879	0,0000	0,6660	0,0701	0,0963	0,0000	0,2593	9,9919	1,5374	99,6096
VCA(m)1Pb	10	6	0,5904	29,1423	2,2478	2,8056	10,9066	24,1488	2,5051	9,2885	2,7139	0,5702	0,0000	0,8552	0,0804	0,1208	0,0000	0,2331	11,4590	1,7129	99,3806

Sample	Fragment	An. Pt.	Mineral	Pb207/Pb206	1σ	Pb206/U238	1σ	Pb207/U235	1σ	Pb208/Th232	1σ	Pb206/U238	1σ	Pb207/U235	1σ	Pb208/Th232	1σ	% conc. 206/238-207/235	% conc. 206/238-208/232
CODERA AREA																			
CODg(th)1	2	16	Thorite	0,0434	0,0009	0,0054	0,0001	0,0324	0,0006	0,0017	0,00002	34,8	0,7	32,4	0,6	34,1	0,5	7%	2%
CODg(th)1	2	17	Thorite	0,0461	0,0009	0,0053	0,0001	0,0338	0,0007	0,0017	0,00002	34,2	0,7	33,8	0,7	34,3	0,5	1%	0%
CODg(th)1	2	18	Thorite	0,0429	0,0009	0,0052	0,0001	0,0304	0,0006	0,0017	0,00002	33,1	0,7	30,4	0,6	33,7	0,5	8%	-2%
CODg(th)1	2	19	Thorite	0,0437	0,0009	0,0049	0,0001	0,0296	0,0006	0,0016	0,00002	31,5	0,6	29,6	0,6	32,7	0,5	6%	-4%
CODg(th)1	3	20	Thorite	0,0443	0,0009	0,0048	0,0001	0,0294	0,0006	0,0016	0,00002	31,0	0,6	29,5	0,6	32,5	0,5	5%	-5%
CODg(th)1	3	21	Thorite	0,0419	0,0009	0,0049	0,0001	0,0283	0,0006	0,0016	0,00002	31,4	0,6	28,3	0,6	32,1	0,5	10%	-2%
CODg(th)1	3	22	Thorite	0,0430	0,0009	0,0052	0,0001	0,0305	0,0006	0,0016	0,00002	33,1	0,7	30,5	0,6	32,9	0,5	8%	1%
CODg(th)1	3	23	Thorite	0,0433	0,0009	0,0053	0,0001	0,0316	0,0006	0,0017	0,00002	34,0	0,7	31,6	0,6	34,1	0,5	7%	0%
CODg(th)1	4	24	Thorite	0,0421	0,0009	0,0051	0,0001	0,0297	0,0006	0,0017	0,00002	32,9	0,7	29,7	0,6	33,5	0,5	10%	-2%
CODg(th)1	4	25	Thorite	0,0436	0,0009	0,0048	0,0001	0,0290	0,0006	0,0016	0,00002	31,0	0,6	29,0	0,6	32,1	0,5	6%	-4%
CODg(m)1P	-	30	Monazite	0,0476	0,0016	0,0050	0,0001	0,0328	0,0011	0,0013	0,00002	32,2	0,6	32,8	1,1	26,1	0,4	-2%	19%
CODg(m)1P	-	31	Monazite	0,0823	0,0022	0,0055	0,0001	0,0620	0,0016	0,0014	0,00002	35,2	0,7	61,1	1,6	27,3	0,4	-74%	22%
CODg(m)1P	-	32	Monazite	0,0466	0,0019	0,0053	0,0001	0,0338	0,0014	0,0013	0,00002	33,8	0,7	33,7	1,4	25,7	0,4	0%	24%
CODg(m)1	7	33	Monazite	0,0399	0,0014	0,0053	0,0001	0,0291	0,0010	0,0013	0,00002	34,0	0,7	29,1	1,0	25,9	0,4	14%	24%
CODg(m)1	7	34	Monazite	0,0479	0,0014	0,0050	0,0001	0,0329	0,0009	0,0013	0,00002	32,0	0,6	32,8	0,9	26,3	0,4	-3%	18%
CODg(m)1	7	35	Monazite	0,0381	0,0013	0,0051	0,0001	0,0267	0,0009	0,0014	0,00002	32,7	0,6	26,8	0,9	28,1	0,4	18%	14%
CODg(m)2	1	36	Monazite	0,0486	0,0014	0,0052	0,0001	0,0351	0,0010	0,0012	0,00002	33,7	0,7	35,0	1,0	25,0	0,4	-4%	26%
CODg(m)2	1	37	Monazite	0,0483	0,0014	0,0052	0,0001	0,0347	0,0010	0,0013	0,00002	33,5	0,7	34,6	1,0	26,3	0,4	-3%	22%
CODg(m)2	1	38	Monazite	0,0485	0,0014	0,0051	0,0001	0,0340	0,0010	0,0013	0,00002	32,7	0,7	33,9	1,0	25,9	0,4	-4%	21%
CODg(m)2	3	39	Monazite	0,0470	0,0014	0,0050	0,0001	0,0323	0,0009	0,0013	0,00002	32,1	0,6	32,3	0,9	26,5	0,4	-1%	18%
CODg(m)2	3	40	Monazite	0,0467	0,0015	0,0052	0,0001	0,0334	0,0011	0,0013	0,00002	33,4	0,7	33,4	1,1	25,9	0,4	0%	23%
CODg(m)2	3	41	Monazite	0,0543	0,0015	0,0051	0,0001	0,0378	0,0011	0,0013	0,00002	32,5	0,6	37,7	1,0	25,5	0,4	-16%	22%
CODg(m)3P	-	4	Monazite	0,0479	0,0013	0,0049	0,0001	0,0321	0,0007	0,0014	0,00002	31,3	0,5	32,1	0,7	28,7	0,5	-3%	8%
CODg(m)3P	-	5	Monazite	0,0497	0,0013	0,0050	0,0001	0,0340	0,0008	0,0014	0,00002	31,9	0,5	33,9	0,8	28,7	0,5	-6%	10%
CODg(m)3P	-	6	Monazite	0,0437	0,0012	0,0053	0,0001	0,0319	0,0008	0,0014	0,00002	34,1	0,6	31,9	0,8	27,9	0,5	6%	18%
CODg(m)3P	-	7	Monazite	0,0522	0,0015	0,0051	0,0001	0,0367	0,0009	0,0014	0,00002	32,8	0,5	36,6	0,9	27,7	0,5	-12%	16%
CODt(m)1P	-	42	Monazite	0,0387	0,0008	0,0050	0,0001	0,0267	0,0006	0,0013	0,00002	32,2	0,6	26,7	0,6	25,9	0,4	17%	20%
CODt(m)1P	-	43	Monazite	0,0412	0,0009	0,0050	0,0001	0,0280	0,0006	0,0013	0,00002	31,8	0,6	28,1	0,6	25,7	0,4	12%	19%
CODt(m)1P	-	44	Monazite	0,0383	0,0008	0,0052	0,0001	0,0275	0,0006	0,0013	0,00002	33,5	0,7	27,5	0,6	26,9	0,4	18%	20%
CODt(m)1	1	45	Monazite	0,0420	0,0009	0,0051	0,0001	0,0295	0,0006	0,0013	0,00002	32,8	0,7	29,5	0,6	25,9	0,4	10%	21%
CODt(m)1	1	46	Monazite	0,0419	0,0009	0,0052	0,0001	0,0301	0,0006	0,0014	0,00002	33,6	0,7	30,1	0,6	28,3	0,4	10%	16%
CODt(m)1	1	47	Monazite	0,0397	0,0008	0,0051	0,0001	0,0280	0,0006	0,0013	0,00002	32,9	0,7	28,0	0,6	26,3	0,4	15%	20%
CODm(m)1P	1	5	Monazite	0,0483	0,0014	0,0059	0,0001	0,0391	0,0011	0,0013	0,00001	37,7	0,7	38,9	1,1	26,9	0,3	-3%	29%
CODm(m)1P	1	6	Monazite	0,0460	0,0013	0,0057	0,0001	0,0363	0,0010	0,0014	0,00002	36,8	0,7	36,2	1,0	28,1	0,4	2%	24%
CODm(m)1P	1	7	Monazite	0,0465	0,0014	0,0060	0,0001	0,0381	0,0011	0,0014	0,00002	38,2	0,8	38,0	1,1	28,7	0,4	1%	25%
CODm(m)1	3	8	Monazite	0,0488	0,0014	0,0060	0,0001	0,0402	0,0011	0,0014	0,00002	38,3	0,8	40,0	1,1	27,3	0,4	-4%	29%
CODm(m)1	3	9	Monazite	0,0429	0,0014	0,0058	0,0001	0,0343	0,0011	0,0013	0,00002	37,2	0,7	34,2	1,1	26,9	0,4	8%	28%
CODm(m)1	3	10	Monazite	0,0504	0,0015	0,0059	0,0001	0,0406	0,0012	0,0013	0,00001	37,6	0,7	40,4	1,1	26,7	0,3	-8%	29%
CODm(m)1	3	11	Monazite	0,0493	0,0015	0,0059	0,0001	0,0398	0,0012	0,0013	0,00001	37,7	0,7	39,7	1,2	26,7	0,3	-5%	29%
CODm(m)1	4	12	Monazite	0,0460	0,0020	0,0060	0,0001	0,0377	0,0016	0,0013	0,00002	38,2	0,8	37,6	1,6	26,5	0,4	2%	31%
CODm(m)1	4	13	Monazite	0,0505	0,0017	0,0059	0,0001	0,0413	0,0013	0,0013	0,00002	38,2	0,8	41,1	1,3	26,7	0,4	-8%	30%
CODm(m)1	4	14	Monazite	0,0511	0,0017	0,0058	0,0001	0,0409	0,0013	0,0013	0,00002	37,3	0,7	40,7	1,3	26,7	0,4	-9%	29%
CODm(m)1	4	15	Monazite	0,0507	0,0018	0,0056	0,0001	0,0392	0,0014	0,0013	0,00001	36,0	0,7	39,0	1,4	25,5	0,3	-8%	29%
CODm(m)1	C	15	Monazite	0,0484	0,0014	0,0050	0,0001	0,0336	0,0008	0,0013	0,00002	32,4	0,5	33,6	0,8	25,9	0,5	-4%	20%
CODm(m)1	C	16	Monazite	0,0503	0,0014	0,0050	0,0001	0,0343	0,0009	0,0013	0,00002	31,8	0,5	34,2	0,9	26,3	0,5	-7%	18%
CODm(m)1	C	17	Monazite	0,0521	0,0014	0,0049	0,0001	0,0354	0,0009	0,0013	0,00002	31,7	0,5	35,3	0,9	26,1	0,5	-11%	18%
CODm(m)1	C	18	Monazite	0,0521	0,0014	0,0049	0,0001	0,0352	0,0009	0,0013	0,00002	31,6	0,5	35,2	0,9	26,1	0,5	-11%	17%
BODENGO AREA																			
VLGm(m)1P	2	8	Monazite	0,0833	0,0039	0,0034	0,0001	0,0387	0,0017	0,0010	0,00001	21,7	0,4	38,5	1,7	20,4	0,3	-78%	6%
VLGm(m)1P	2	9	Monazite	0,0480	0,0016	0,0045	0,0001	0,0297	0,0009	0,0011	0,00001	28,9	0,5	29,7	0,9	22,4	0,3	-3%	22%
VLGm(m)1P	2	10	Monazite	0,0483	0,0016	0,0045	0,0001	0,0299	0,0009	0,0010	0,00001	28,9	0,5	29,9	0,9	20,2	0,3	-3%	30%
VLGm(m)1P	2	11	Monazite	0,0520	0,0016	0,0044	0,0001	0,0315	0,0009	0,0011	0,00001	28,2	0,5	31,5	0,9	22,0	0,3	-11%	22%
VLGm(m)1	11	31	Monazite	0,0492	0,0020	0,0047	0,0001	0,0315	0,0012	0,0010	0,00002	29,9	0,6	31,5	1,2	21,0	0,5	-5%	30%
VLGm(m)1	11	32	Monazite	0,0548	0,0019	0,0047	0,0001	0,0352	0,0011	0,0010	0,00001	30,0	0,5	35,1	1,1	20,6	0,3	-17%	31%
VLGm(m)1	11	33	Monazite	0,0555	0,0021	0,0046	0,0001	0,0351	0,0012	0,0010	0,00001	29,5	0,5	35,1	1,2	19,8	0,3	-19%	33%
VLGm(m)1	12	34	Monazite	0,0651	0,0023	0,0041	0,0001	0,0369	0,0012	0,0011	0,00002	26,4	0,5	36,8	1,2	23,0	0,5	-39%	13%
VLGm(m)1	12	35	Monazite	0,0552	0,0017	0,0042	0,0001	0,0317	0,0009	0,0010	0,00001	26,9	0,5	31,7	0,9	20,4	0,3	-18%	24%
VLGm(m)1	12	36	Monazite	*0,3119*	*0,0076*	*0,0107*	*0,0002*	*0,4599*	*0,0095*	*0,0012*	*0,00002*	*68,7*	*1,3*	*384,2*	*7,9*	*24,6*	*0,5*	*-459%*	*64%*
VLGm(m)1	16	37	Monazite	0,0499	0,0018	0,0048	0,0001	0,0328	0,0011	0,0010	0,00001	30,7	0,5	32,7	1,1	20,0	0,3	-7%	35%
VLGm(m)1	16	39	Monazite	*0,2885*	*0,0067*	*0,0065*	*0,0001*	*0,2575*	*0,0051*	*0,0013*	*0,00002*	*41,6*	*0,8*	*232,7*	*4,6*	*25,2*	*0,5*	*-459%*	*39%*
VLGm(m)1	16	40	Monazite	0,0507	0,0017	0,0045	0,0001	0,0315	0,0010	0,0010	0,00002	29,0	0,5	31,5	1,0	20,8	0,5	-9%	28%
VLGm(m)1	17	41	Monazite	0,0510	0,0017	0,0048	0,0001	0,0336	0,0011	0,0010	0,00001	30,7	0,5	33,5	1,1	20,0	0,3	-9%	35%
VLGm(m)1	17	42	Monazite	0,0569	0,0022	0,0048	0,0001	0,0372	0,0013	0,0010	0,00002	30,5	0,6	37,1	1,3	20,4	0,5	-21%	33%
VLGm(m)1	17	43	Monazite	0,0532	0,0025	0,0047	0,0001	0,0340	0,0015	0,0011	0,00002	29,9	0,6	33,9	1,5	21,4	0,5	-14%	28%
VLGm(m)2P	-	44	Monazite	0,0510	0,0019	0,0044	0,0001	0,0307	0,0011	0,0010	0,00002	28,0	0,5	30,7	1,1	20,2	0,5	-9%	28%
VLGm(m)2P	-	46	Monazite	0,0448	0,0019	0,0045	0,0001	0,0277	0,0011	0,0010	0,00002	28,9	0,5	27,7	1,1	19,2	0,4	4%	34%
VLGm(m)2P	-	47	Monazite	0,0620	0,0040	0,0043	0,0001	0,0365	0,0023	0,0010	0,00002	27,5	0,6	36,4	2,3	20,4	0,5	-32%	26%
VLGm(m)2	4	12	Monazite	0,0514	0,0024	0,0036	0,0001	0,0253	0,0011	0,0011	0,00001	23,0	0,4	25,3	1,1	21,4	0,3	-10%	7%
VLGm(m)2	4	13	Monazite	0,0402	0,0014	0,0045	0,0001	0,0248	0,0008	0,0010	0,00001	28,8	0,5	24,9	0,8	20,6	0,3	14%	28%
VLGm(m)2	4	14	Monazite	0,0872	0,0029	0,0047	0,0001	0,0569	0,0017	0,0011	0,00001	30,5	0,5	56,2	1,7	21,2	0,3	-84%	30%
VLGm(m)2	8	19	Monazite	0,0381	0,0018	0,0070	0,0001	0,0366	0,0017	0,0011	0,00001	44,7	0,8	36,5	1,7	21,8	0,3	18%	51%
VLGm(m)2	8	20	Monazite	0,0412	0,0014	0,0046	0,0001	0,0262	0,0008	0,0010	0,00001	29,6	0,5	26,2	0,8	20,8	0,3	11%	30%
VLGm(m)2	8	21	Monazite	0,0459	0,0017	0,0044	0,0001	0,0281	0,0009	0,0010	0,00001	28,5	0,5	28,1	0,9	20,6	0,3	1%	28%
VLGm(m)2	8	22	Monazite	0,0449	0,0017	0,0045	0,0001	0,0276	0,0010	0,0011	0,00001	28,7	0,5	27,6	1,0	21,8	0,3	4%	24%
VLGm(m)2	12	27	Monazite	0,0595	0,0026	0,0060	0,0001	0,0490	0,0020	0,0010	0,00001	38,4	0,7	48,6	2,0	21,0	0,3	-26%	45%
VLGm(m)2	12	28	Monazite	0,0599	0,0020	0,0046	0,0001	0,0376	0,0011	0,0011	0,00001	29,3	0,5	37,4	1,1	21,2	0,3	-28%	28%
VLGm(m)2	12	29	Monazite	0,0554	0,0018	0,0046	0,0001	0,0353	0,0011	0,0010	0,00001	29,7	0,5	35,2	1,1	20,6	0,3	-18%	31%
VLGm(m)2	12	30	Monazite	0,1092	0,0055	0,0058	0,0001	0,0873	0,0040	0,0010	0,00001	37,3	0,8	84,9	3,9	20,0	0,3	-128%	46%
VCA(m)1Pa	-	48	Monazite	0,0444	0,0011	0,0039	0,0001	0,0241	0,0006	0,0010	0,00001	25,3	0,5	24,1	0,6	20,2	0,2	5%	20%
VCA(m)1Pa	-	49	Monazite	0,0492	0,0012	0,0040	0,0001	0,0269	0,0007	0,0010	0,00001	25,5	0,5	26,9	0,7	20,4	0,2	-5%	20%
VCA(m)1Pa	-	50	Monazite	0,0469	0,0012	0,0041	0,0001	0,0265	0,0006	0,0010	0,00001	26,3	0,5	26,5	0,7	20,6	0,2	-1%	22%
VCA(m)1Pb	10	4	Monazite	0,0448	0,0008	0,0040	0,0001	0,0247	0,0004	0,0010	0,00001	25,8	0,3	24,8	0,4	20,2	0,2	4%	22%
VCA(m)1Pb	10	5	Monazite	0,0592	0,0010	0,0040	0,0001	0,0324	0,0006	0,0010	0,00001	25,5	0,3	32,4	0,6	20,8	0,2	-27%	19%
VCA(m)1Pb	10	6	Monazite	0,0459	0,0009	0,0039	0,0001	0,0249	0,0005	0,0010	0,00001	25,3	0,3	25,0	0,5	20,4	0,2	1%	20%
VCA(m)1Pb	10	7	Monazite	0,0571	0,0018	0,0036	0,0001	0,0287	0,0009	0,0010	0,00001	23,4	0,3	28,7	0,9	20,2	0,2	-23%	14%
VCA(m)1Pb	1	8	Xenotime	0,0442	0,0006	0,0035	0,0001	0,0213	0,0003	0,0023	0,00004	22,5	0,3	21,4	0,3			5%	
VCA(m)1Pb	1	9	Xenotime	0,0474	0,0007	0,0035	0,0000	0,0227	0,0003	0,0023	0,00004	22,3	0,3	22,8	0,3			-2%	
VCA(m)1Pb	5	10	Xenotime	0,0431	0,0006	0,0036	0,0001	0,0213	0,0003	0,0022	0,00004	23,1	0,3	21,4	0,3			7%	
VCA(m)1Pb	5	11	Xenotime	0,0448	0,0007	0,0035	0,0001	0,0216	0,0003	0,0027	0,00004	22,5	0,3	21,6	0,3			4%	

ACKNOWLEDGEMENTS

Since I am not good at acknowledging,
here are posted some photos that will do it for me.

Thanks also to:

A. Guastoni
A. M. Fioretti
S. Castelli

The 3rd floor team

HIGHLY ALCOHOLICS PADUAN GEOLOGISTS
HAPG
2013

And, of course,

Mum, dad and sis